UNIVERSITÀ degli STUDI di CATANIA

DIPARTIMENTO DI SCIENZE BIOMEDICHE E BIOTECNOLOGICHE

DOTTORATO IN "BASIC AND APPLIED BIOMEDICAL SCIENCES"

XXXV CICLO

LAZZARO LORENZO MATTIA

Ceftobiprole activity against *Enterococcus faecalis*: resistance development, interaction with multiple low-reactive Penicillin-Binding-Proteins (PBPs) and PBP4 alterations

TESI DI DOTTORATO

Coordinatore:
Prof.ssa Stefania Stefani

Tutor:
Prof.ssa Floriana Campanile

Triennio 2019/ 2022

TABLE OF CONTENTS

CHAPTER I

STUDY OF *STAPHYLOCOCCUS AUREUS*/OSTEOBLAST INTERACTION AND MOLECULAR CROSSTALK DURING ADAPTION IN PERSISTENT INFECTIONS

During my first PhD year, I continued the research project object of my Master degree thesis, focused on the study of *Staphylococcus aureus/*osteoblast interaction and the molecular "crosstalk" during adaption in persistent infections. This project was successfully concluded at the end of the year, with all results published.

1. INTRODUCTION

Staphylococcus aureus and specifically methicillin-resistant *S. aureus* (MRSA), is one of the main human pathogen causing severe and chronic infections, such as osteomyelitis **(Lowy, 1998)** and prosthetic join infections, implicating a high plethora of virulence factors in the pathogenesis of bone infection, which enable *S. aureus* cells to adhere and invade host tissue and evade immune defences. MRSA have been reported as the principal pathogens involved in these infections **(Campanile et al. 2015),** especially those belonging to clonal complex 5 **(Peng et al., 2019),** and associated with the staphylococcal chromosomal cassette (SCC*mec*) I and III **(Hussain et al., 2009).**

A specific class of proteins, known as "Microbial Surface components recognizing Adhesive Matrix Molecules" (MSCRAMMs), interact with and bind the host extracellular matrix (ECM) and plasma proteins, playing a crucial role in the osteomyelitis development. Among these, the collagen binding surface protein (Cna), mediate bacterial adherence to collagenous tissue, playing an important role in the orthopaedic implant related infections. This protein works in tandem with the bone sialoprotein binding protein (Bbp), involved in the pathogenesis of osteomyelitis **(Post et al. 2014).**

The coordinate expression of many virulence determinants is regulated by global regulatory elements, such as the Staphylococcal Accessory Regulator (sar *locus* and mainly SarA) **(Fig. 1)**, and the Accessory Global Regulator (agr *locus*), which comprises two divergent transcripts, RNAII and RNAIII encoding *agr*ACDB and the delta haemolysin gene (hld), respectively.

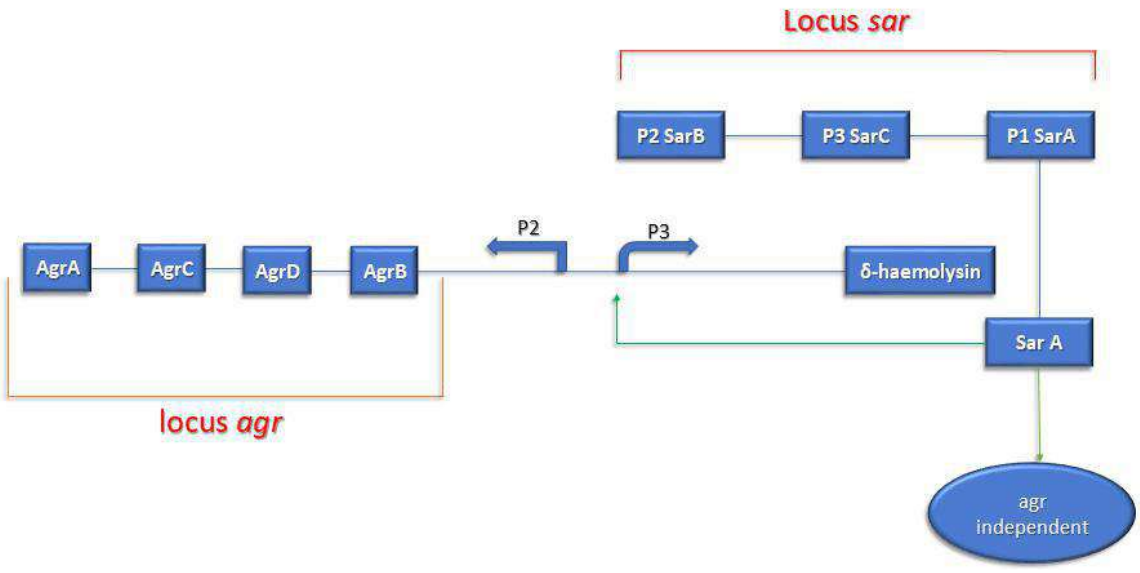

Figure 1 *agr/sarA interaction of the regulation virulence genes in S. aureus: sarA is over-expressed during the exponential phase.*

The *agr locus* upregulates the expression of toxins and secreted virulence factors, during the acute phase of infections, whereas *agr* needs to be silenced during chronic infections. Downregulation of *agr* enable the bacteria to silently persist within the intracellular location, without provoking the host immune response and without killing the host cells (**Tuchscherr et al. 2010).** In contrast, the expression of the alternative Sigma factor B (SigB) plays a crucial role during persistence. These regulatory elements, in turn, control the transcription of a wide variety of unlinked genes, many of which have been implicated in pathogenesis.

Sar A protein binds to several target gene promoters, including those of *agr, hla, spa,* and *fnbA,* modulating target gene transcription both by *agr*-dependent and *agr*-independent pathways **(Manna et al. 2004).** Contrary to *agr, sarA* up-regulates the expression of many cell wall proteins (i.e. fibronectin binding protein A) and selected exoproteins (i.e. α- and β-hemolysins), while repressing the transcription of the protein A gene (*spa*) **(Cheung et al. 1997).**

Two other genes, belonging to the Sar A protein family, are involved in the regulation of virulence genes:

1) *sarS,* whose expression is repressed by *sar*A and *agr*, which is a repressor of *hla* and *etb,* and a positive regulator of *spa;*
2) *rot* (repressor of toxin), which is a repressor of enterotoxin B *(seb)* and alpha-toxin *(hla),* itself repressed by the *agr* effector RNAIII and SarA **(Jenul & Horswill, 2018). (Fig. 2)**

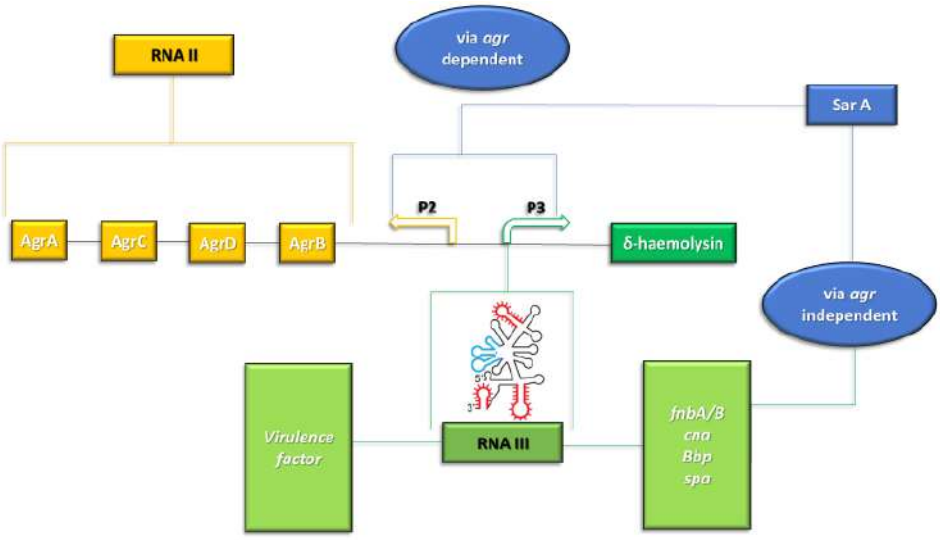

Figure 2 *Virulence genes under the control of agr locus and sarA regulators.*

S. aureus directly interacts with osteoblasts, following three different events:

- **Adhesion:** First*, S. aureus* cells interact with and bind the "bone-extracellular matrix" (BEM) components *via* multiple adhesins, the MCRAMMs, that recognize adhesive matrix-molecules. Among these, the collagen adhesin (Cna) and the bone sialoprotein binding protein (Bbp), the fibronectin binding protein A and B (FnBPA/B) **(Josse et al. 2015),** the fibrinogen-binding protein clumping factors A and B (ClfA/B), the SdrE, a serine-aspartate (SD) protein that anchors the cell wall

interacting with complement factor H and facilities colonization through adherence to the cell surface or extracellular matrix (ECM) components **(Herr & Thorman, 2017);**

- **Invasion:** *S. aureus* osteoblast invasion plays a crucial role in the initiation and maintenance of the inflammatory immune responses **(Sinha & Fraunholz, 2010).** The ability of fibronectin to link cell surface integrin α5β1 is considered the most common pathway for the internalization of *S. aureus* in osteoblasts;
- **Internalization:** *S. aureus* cells internalized in osteoblasts via a process that involves actin microfilaments, microtubules, and so on. This event is a key stage in the spreading of the infections, that allows *S. aureus* to persist inside osteoblasts, protected from the immune system, and gives to *S. aureus* the opportunity to sustain the infection **(Josse et al. 2015).** Following the internalization stage, osteoblasts secrete inflammatory factors, such as cytokines, chemokines, and growth factor, that can activate and recruit immune cells from the innate or adaptive immune system. Osteoblasts release viable staphylococci, which are then able to reinfect and internalize in new osteoblasts, representing the ones responsible for prolonged and persistent infections **(Garzoni & Kelley, 2009; Josse, Velard, & Gangloff, 2015).**

As extensively reported in the literature, most of the internalization experiments were conducted using the MG-63 cell line, derived from a juxtacortical osteosarcoma designed in the distal diaphysis of the left femur of a 14-year-old-male (ATCC® CRL-1427™; Standards Development Organization, LGC Standards S.r.l.). These cells show multiple advantages with respect to human and animal-derived primary cells, used not only in drug and biomaterial testing, but also in bone biology investigations. Primary cells, reproduce the behaviour of the original cellular niche, resulting in a preclinical model closed to clinical conditions, but the phenotypic and genotypic differences of these cells, isolated from different patients, make it difficult to study the disease under examination. Their limit is that after a certain number of cell divisions, these cells have a limited lifespan, due to a block in the cell division and, consequently, it becomes problematic to grow and maintain continuous cultures.

The MG-63 cells showed the ability to overcome the limits imposed by cells primarily derived from the bone, being easy to maintain, possessing a relative stable phenotype and, when cultured, appearing as rapidly proliferating aggregates. Finally, they possess the ability of infinite proliferation typical of malignant cells, such as MG-63 cells, providing to be a valid *in vitro* model for the study of bacterial infection mechanisms, such as the *S. aureus* internalization **(Stracquadanio et al.; 2021).**

pathogens

MDPI

Review

Staphylococcus aureus Internalization in Osteoblast Cells: Mechanisms, Interactions and Biochemical Processes. What Did We Learn from Experimental Models?

Stefano Stracquadanio [1,*,†], Nicolò Musso [1,†], Angelita Costantino [2,3], Lorenzo Mattia Lazzaro [1], Stefania Stefani [1] and Dafne Bongiorno [1]

1 Medical Molecular Microbiology and Antibiotic Resistance Laboratory (MMARLab), Department of Biomedical and Biotechnological Sciences (BIOMETEC), University of Catania, 95125 Catania, Italy; nmusso@unict.it (N.M.); lazzclml@gmail.com (L.M.L.); stefanis@unict.it (S.S.); dbongio@unict.it (D.B.)
2 Department of Drug and Health Sciences, University of Catania, 95125 Catania, Italy; angelita25costantino@gmail.com
3 Interuniversity Consortium for Biotechnology, Area di Ricerca, Padriciano, 34149 Trieste, Italy
* Correspondence: s.stracquadanio@hotmail.it; Tel.: +393-284-752-223
† Consider that the first two should be regarded as joint First Authors.

Abstract: Bacterial internalization is a strategy that non-intracellular microorganisms use to escape the host immune system and survive inside the human body. Among bacterial species, *Staphylococcus aureus* showed the ability to interact with and infect osteoblasts, causing osteomyelitis as well as bone and joint infection, while also becoming increasingly resistant to antibiotic therapy and a reservoir of bacteria that can make the infection difficult to cure. Despite being a serious issue in orthopedic surgery, little is known about the mechanisms that allow bacteria to enter and survive inside the osteoblasts, due to the lack of consistent experimental models. In this review, we describe the current knowledge about *S. aureus* internalization mechanisms and various aspects of the interaction between bacteria and osteoblasts (e.g., best experimental conditions, bacteria-induced damages and immune system response), focusing on studies performed using the MG-63 osteoblastic cell line, the best traditional (2D) model for the study of this phenomenon to date. At the same time, as it has been widely demonstrated that 2D culture systems are not completely indicative of the dynamic environment in vivo, and more recent 3D models—representative of bone infection—have also been investigated.

Keywords: human osteoblast; MG-63; *Staphylococcus aureus*; internalization mechanisms; bone tissue engineering; 3D bone infection model

Citation: Stracquadanio, S.; Musso, N.; Costantino, A.; Lazzaro, L.M.; Stefani, S.; Bongiorno, D. *Staphylococcus aureus* Internalization in Osteoblast Cells: Mechanisms, Interactions and Biochemical Processes. What Did We Learn from Experimental Models?. *Pathogens* **2021**, *10*, 239. https://doi.org/10.3390/pathogens10020239

Academic Editor: Bryan Heit

Received: 29 January 2021
Accepted: 17 February 2021
Published: 19 February 2021

1. Background

During the first steps of growth, remodeling and recovery of the bone, different cell types co-exist and cooperate to form the extracellular bone matrix (EBM) [1,2]. Among these, osteoblasts are the cells that form the bone and, together with osteoclasts, preserve its physiological homeostasis [3].

Pathological conditions, such as bacterial infections, are responsible for altered osteoblast activity. In detail, surgical procedures, especially in the presence of medical (orthopedic) devices, are responsible for an increased susceptibility of osteoblasts to osteomyelitis [4–7] and, in this context, *Staphylococcus aureus* represents a frequent intra- and extracellular pathogen [8].

The host–pathogen interaction between osteoblasts and *S. aureus* occurs through the recognition of pathogen-associated molecular patterns (PAMPs) by the pattern recognition receptors (PRRs) exposed on the extracellular surface of the osteoblasts. The consequent production of chemokines and cytokines is responsible for the recruitment and subsequent

activation of innate and adaptive immune cells, typical of the cellular inflammatory response [9]. At the same time, the overstimulation of osteoblasts by *S. aureus* causes an increase in osteoclastogenesis with consequent osteoblast death, as well as an alteration of bone homeostasis (Figure 1) [10,11].

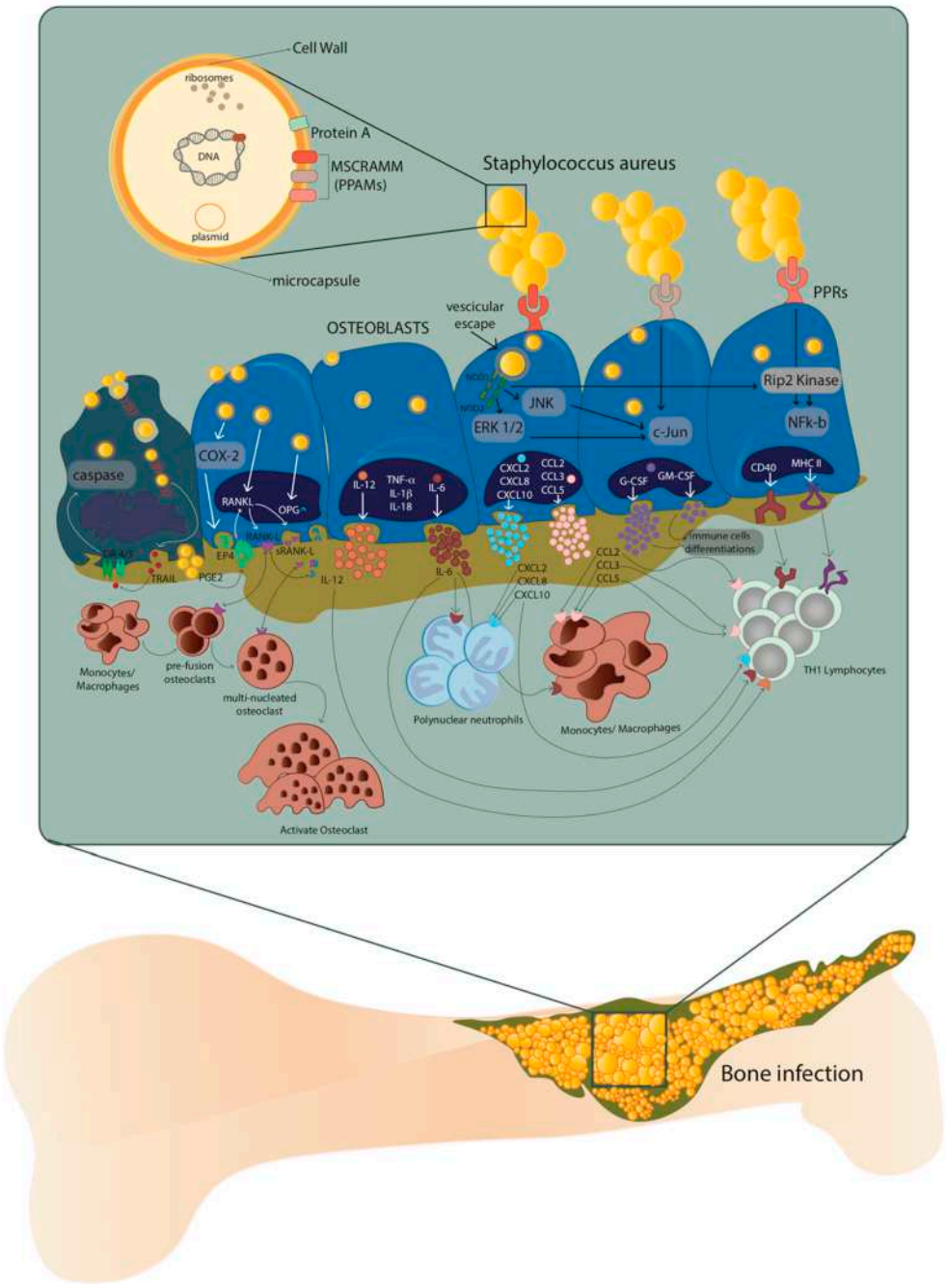

Figure 1. Host–pathogen interaction between osteoblasts and *Staphylococcus aureus*. After internalization, *S. aureus* escapes from the vesicle and interacts with extracellular receptors TLR2 and TNFR-1, as well as with intracellular receptors TLR9 and NODs through α5β1 integrin and actin filaments of the osteoblasts. This interaction increases the expression of cytokines IL-1β, IL-18, TNF-α, the production and release of IL-6, IL-12 and the expression and release of chemokines CXCL2, CXCL8, CXCL10, CCL2, CCL3, CCL5 and growth factors G-CSF and GM-CSF. At the same time, the expression and production of CD40 and MHC II increase. Illustration by A. Costantino (co-author).

The presence of proteins and glycans—such as type I collagen, bone sialoprotein, osteopontin and fibronectin—make the EBM a perfect niche for *S. aureus* that binds these EBM components through multiple adhesins known as microbial surface components which recognize adhesive matrix molecules (MSCRAMMs) [8,12]. Indeed, the *S. aureus* attachment to the EBM represents a key step in the onset of osteomyelitis, where type I collagen represents approximately 90–95% of the organic fraction of the EBM directly interacting with this pathogen (Figure 1).

Recently, it was demonstrated that the ability of *S. aureus* to internalize inside osteoblasts is a key strategy to protect itself and maintain the infection. On the contrary, osteoblasts respond to *S. aureus* internalization by secreting inflammatory factors—such as cytokines, chemokines and growth factors—which, in turn, activate and recruit immune cells from the innate or adaptive immune systems (Figure 1) [13].

The excessive formation and activation of osteoclasts is caused by an increase in RANK-L expression and production through the COX-2/PGE2 pathway. This leads to severe bone resorption as well as to decreased production of osteoprotegerin (OPG). Finally, through the release of membrane-damaging virulence factors such as phenol-soluble modulins (PSMs), *S. aureus* can cause osteoblast necrosis and apoptosis through intrinsic and extrinsic caspase pathways. These processes can lead to the release of intracellular *S. aureus*, which can re-infect other osteoblasts.

Consequently, the ability of *S. aureus* to survive in osteoblasts after internalization also results in effective escape from the antibiotic therapy, which cannot penetrate inside the cells [14,15].

The hypothesis that increasing our understanding of the immune response, as well as intensifying the host's defenses, could be a valuable avenue for developing new anti-infectious strategies dates back several years [16].

The use of murine or human in vitro culture models—including primary cells, induced osteoblasts from pluripotent stem cells and immortalized and malignant cell lines—has allowed a better understanding of osteoblast cell biology during infection processes [17].

To date, the progress of research in the field of orthopedic engineering, as well as the development of new therapies and biomaterials, increases the importance of these in vitro models. At the same time, a deeper knowledge of their phenotypic and genotypic status and their differences in relation to primary human osteoblast cells is needed, especially in order to choose the most appropriate experimental model.

In this regard, the results obtained from in vitro infections of osteoblasts grown as two-dimensional (2D) monolayers provided important information on the molecular mechanisms underlying bacterium–host cell interactions. Despite this, these models do not reproduce the dynamic aspects of this interaction, such as the organization of osteoblasts in healthy bone to provide strength and resistance and therefore to respond better to bacterial infections [18,19]. To overcome these limitations, animal models of osteomyelitis were considered the gold standard for the study of bone infections, but the different responses to bacteria between the mouse model and other animal models made the use of these models not exhaustive [20–23]. From here, more relevant in vitro models that physiologically mimic the human bone microenvironment have been developed and will be discussed in the last section of this review.

S. aureus vs. Mycobacterium tuberculosis

Before delving into different aspects of *S. aureus* internalization, a comparison between the behavior of *S. aureus* and that of an obligate intracellular bacterium, such as *Mycobacterium tuberculosis*—the etiological agent of tuberculosis (TBC)—could be useful.

While *M. tuberculosis* needs to replicate within human cells to disseminate to other individuals and cause disease, internalization of *S. aureus* by osteoblasts is a key element in the spread of the infection, as it allows *S. aureus* to persist inside osteoblasts protected from the immune system and it gives *S. aureus* the opportunity to sustain the infection [3], but it is not necessary for its replication.

M. tuberculosis spreads from person to person almost exclusively by aerosolized particles that can be trapped in the upper airway or oropharynx. Once in the lower respiratory tract, *M. tuberculosis* is primarily phagocytosed by macrophages and dendritic cells, but neutrophils are also infected [24]. Although *M. tuberculosis* usually infects macrophages, it was also found in non-myelocytic cells of TBC patient. As *M. tuberculosis* internalization in non-phagocytic cells is an actin-dependent process involving heparin-binding hemagglutinin, toll-like receptors (TLRs), surfactant proteins and complement and scavenger receptors [25], *S. aureus* internalization involves some cytoskeletal elements too, particularly actin microfilaments. It has been demonstrated that the internalization process of *S. aureus* can occur with dead bacteria but not with dead osteoblasts, suggesting that the internalization process is more of an active cellular mechanism than an active bacterial mechanism [26].

After *M. tuberculosis* or *S. aureus* internalization, infected cells trigger a local inflammatory response that attracts immune cells to the site of infection. Osteoblasts infected by *S. aureus* secrete inflammatory factors like cytokines, chemokines and growth factors, all of which can activate and recruit immune cells from the innate or adaptive immune systems [27], while *M. tuberculosis* promotes the buildup of cellular aggregates forming the granulomas, that represent a complex environment constituted by macrophages, multinucleated giant cells, epithelioid and foamy cells, granulocytes and lymphocytes [25].

We only reported the main common characteristics regarding the internalization process of both *M. tuberculosis* and *S. aureus*, as *M. tuberculosis* internalization in phagocytic cells needs more tricks to allow the bacteria to escape the phagosomal threat.

2. MG-63 Osteoblast-Like Cell Line as an Effective In Vitro Model to Investigate Host–Pathogen Mechanisms during *S. aureus* Infection

Although preclinical models are known to offer an essential prescreening method for testing new biomaterials useful in the treatment of orthopedic disorders, the increasingly restrictive regulations for the use of in vivo models and the ever-increasing demand for primary cells from healthy or sick donors have led to the development of "continuous" osteoblast cell models. Among these, human- and animal-derived primary cells [28–32], immortalized cell lines [33,34], malignant cells [35–37], and induced pluripotent stem cells (iPSs) are used not only in drug and biomaterial testing, but also in bone biology investigations.

Certainly, primary cells, deriving directly from patients, better reproduce the behavior of the original cellular niche, resulting in a preclinical model closer to clinical conditions. Over the years, however, researchers and physicians have realized that the phenotypic and often genotypic differences of these cells isolated from different patients make it difficult to study the disease under examination and consequently to establish the best therapeutic strategy.

An improvement in the knowledge of bone biology and, in particular, osteoblast cells has been achieved through the development of stabilized osteoblast cell lines as models for in vitro investigation of cell differentiation, cytokines and hormone regulation, matrix protein synthesis and secretion and molecular mechanisms of bone diseases. At the same time, these models were found to be useful for the evaluation of the cytocompatibility and osteogenicity of new biomaterials [17].

There is no evidence indicating the superiority of one model over the others; therefore, an evaluation of their respective advantages and disadvantages, on the basis of studies to be conducted, is important.

Primary cultures represent an in vitro model that uses cells directly obtained from tissue biopsies (~1 cm^3) or organ dissections. These cells have the unique characteristic of maintaining their genetic, morphological and functional features. This makes them the best representative indicators of normal cell phenotype and early-stage disease progression, and as such they are commonly used as in vitro tools for preclinical and investigative biological research and toxicological studies, besides reducing the number of animals required for preclinical toxicology studies at an initial stage, making them cost-saving.

Even though primary human osteoblasts tend to preserve their differentiated phenotype in vitro, after a certain number of cell divisions, these cells have a limited lifespan and will stop dividing (or senesce) and may be more difficult to grow and maintain than a continuous (immortalized) cell line. Induced variability in primary cells obtained from donors and in subculture practices is one of the main challenges faced by researchers studying cell signaling pathways [17].

Specifically, it has been shown that the age of the donor influences the proliferative capacity of isolated cells, whose proliferation times are doubled if derived from patients over the age of 65 [38,39].

Furthermore, bone aging, defined as a change in the degree and distribution of bone mineralization, is also age-dependent. This is reflected in the physiology of isolated osteoblast cells, characterized not only by slower proliferation, but also by phenotypic modification [40,41]. Likewise, the expression of genes and the synthesis of proteins associated with the osteoblast phenotype are also influenced by the age of the donor, as well as by the anatomical site of isolation. For example, it is now known that FGFβ and IGFII gene expression is downregulated in osteoblast cells isolated from the mandible, and the synthesis of type I collagen and osteonectin shows higher expression in cells isolated from fetal to 20-year-old bone donors, while a 65% decrease in collagen levels was observed in cells from donors older than 20 years [42].

Moreover, when these cells are extracted ex vivo and transferred to a culture environment, they may lose their structural and functional characteristics. In this regard, cells having completely different morphology in vivo at the tissue level may show similar morphology in the culture environment [43,44].

Thus, donor age, site of isolation and the gender differences that we have discussed so far are just some of the factors that can influence the behavior of primary human osteoblast cells and, in turn, confer different times of phenotypic modification in vitro. As a result, in the absence of a homogenous target of patients/donors, obtaining cultures of osteoblasts suitable for the study of basic applied biology or particular mechanisms, such as infection, is not efficient.

The ease of obtaining results in experiments and their repeatability, as well as the ease of maintenance, the unlimited number of cells without the need for isolation and the relative phenotypic stability of immortalized or continuous MG-63 cell lines has allowed researchers, in some respects, to overcome the limits imposed by cells primarily derived from the bone (HObs). Although these cell models differ in some respects from primary osteoblast cells, Czekanska et al. showed that MG-63 cells show some distinct similarities to HObs [45].

According to Billiau et al., the MG-63 cell line is derived from a juxtacortical osteosarcoma diagnosed in the distal diaphysis of the left femur of a 14-year-old male [35]. When cultured, these cells appear as rapidly proliferating aggregates without exhibiting contact inhibition [46].

The similarity between MG-63 and HObs was already studied several years ago, when Franceschi et al. observed the response of these cells to 1,25-dihydroxyvitamin D3 (1,25 (OH) 2D3) as an effect on cell morphology and on the phenotype comparable to normal osteoblasts [47].

More recent studies have shown that the cell growth kinetics of MG-63 were comparable to that of HObs as the exponential growth phase was observed from day 2 to day 6, followed by a plateau phase from day 6 to day 10 [45]. This result is confirmed by the ability of infinite proliferation typical of malignant cells, such as MG-63 cells, where the lack of intrinsic cell cycle control contributes to tumor progression.

Czekanska et al. also observed that the activity of alkaline phosphatase, an enzyme identifying mature osteoblasts, was lower in MG-63 cells than in primary cells [45]. This result confirmed the different degree of differentiation of MG-63 towards a more immature phenotype, compared to HObs.

The expression analysis of key osteoblast-specific genes [45] showed that the transcription factor Runx2—which regulates gene expression of the all-important bone matrix proteins (including ALP, OC, BSP and type I collagen)—is expressed more in MG-63 than in HObs, except on day 2 [48,49].

As previously introduced, type I collagen is essential for the function of osteoblast cells [50] and is overexpressed in the phase preceding matrix mineralization [51,52], in order to allow the formation of fibrils and a subsequent physiological maturation of the matrix. On the contrary, MG-63 cells show a low expression of type I collagen as well as of osteocalcin [45]. Consequently, the reported studies highlight the limitations of these cells as a model for the phenotypic development of osteoblasts as well as for the evaluation of the mineralization of the matrix and the properties of new biomaterials [45].

On the other hand, the MG-63 cell line proved to be a valid in vitro model for the study of bacterial infection mechanisms, especially during *S. aureus* internalization [14,53–57]. In 2010, Schroder and Tschopp demonstrated that the innate immune response against pathogens involves the activation of an inflammatory pathway known as the inflammasome activation pathway [58]. Inflammasomes are multiprotein signaling complexes that are assembled following the recognition of stress/pathogenic signals; among these, caspase-1 is the most involved [59]. Upon stimulation by pathogens, caspase-1 binds to an adapter molecule known as apoptosis- associated speck-like protein (ASC) [60]. This binding leads to the autocatalytic cleavage of caspase-1, the processing of pro-IL-1β and pro-IL-18 and the secretion of mature IL-1β and IL-18, triggering in some cases even an inflammatory form of cell death (pyroptosis) [61]). Recent studies have shown that this also applies to *S. aureus* and MG-63 cells [62,63].

Finally, in previously published works, we demonstrated that internalization, using MG-63 cells, is a pathophysiological pathway of some methicillin-resistant *S. aureus* (MRSA) which depends on the total number of cells infected and not on the number of bacterial cells that enter each osteoblast. Furthermore, even if our strains were not homogeneous in terms of genetic backgrounds and virulence factors, ST22-IVh and ST239-III *S. aureus* showed higher intracellular persistence in host cells, making them more prone to developing chronic and recurrent infections, and the different genetic background was also accompanied by a different modulation of inflammatory phenomena, metabolism and antioxidant machinery [64,65].

Take home message: We can conclude that although primary cell lines, and in particular HObs, have the advantage of maintaining their genetic, morphological and physiological features, they also have a limited life span and are difficult to grow and maintain in continuous cultures. MG-63, in our experience, is also a valid in vitro model for the study of *S. aureus* internalization and persistence, both as regards the mechanisms underlying the ability of *S. aureus* to adhere, invade and persist within osteoblasts and the host cell response to infection.

3. Multiplicity of Infection (MOI) and Invasiveness of Different Bacterial Strains

In the presence of prosthetic devices, complete eradication of bacterial infection is often a challenging task. Internalization in non-professional phagocytes is an important pathogenic mechanism actuated by bacteria to elude host defenses and medical therapies. The efficiency of invasion differs across bacterial species and adjustments to the titer of the microbial *inocula* used in the assay are often needed to enumerate intracellular bacteria.

There is a precise relation between the inoculum, in terms of multiplicity of infection (MOI), and the internalized bacteria. Furthermore, there is a relationship between MOI, internalized bacterium ratio and medical therapies [66,67].

Intracellular invasion occurs through a variety of pathogenic species. Some bacteria are obligate intracellular pathogens, while other only become intracellular to escape the host immune system. Among these, the following genera are the most representative: *Mycobacterium; Escherichia; Salmonella; Listeria; Shigella; Legionella; Chlamydia; Yersinia; Streptococcus; Staphylococcus* and *Enterococcus* (in particular *E. faecalis*). *S. aureus* is the

only one capable of causing the onset of clinically relevant pathogenic mechanisms and consistently invades osteoblast cells [68].

Different MOIs have been adopted depending on the bacterial species tested. For example, an MOI of 100:1 (bacteria:host cells) is the inoculum titer most frequently used to test *S. aureus*. The inoculum level increases to 500:1 for *S. epidermidis* [55,69] and 1000:1 for *S. lugdunensis* [70]. The different MOIs used showed rapid and efficient internalization of *S. aureus* at low inoculum levels and inefficient internalization of other species at high inoculum levels.

Two other parameters are used to express the potential of invasiveness of bacterial strains: (i) the number of internalized bacteria (NIB) at an established MOI, expressed in term of Colony-Forming Units (CFUs) per number of eukaryotic cells, influenced by the MOI used; and (ii) the percentage of internalized bacteria (PIB), which represents the percent fraction of the inoculum taken up by eukaryotic cells; this value is not affected by the MOI and can be used to express the degree of invasiveness of prokaryotic cells into eukaryotic cells.

Examining the correlation between MOI values and PIB values, it emerged that—over a broad range of inoculum levels—the MOI did not appear to affect PIB values [71]. PIB values can be used to compare strain invasiveness without fearing major effects resulting from varying MOIs.

However, a new parameter was proposed to express the invasiveness of bacterial strains: the internalization minimal inoculum (IMI), corresponding to the lowest MOI required for the internalization of a single bacterium. This value is inversely related to invasiveness and corresponds to the lowest concentration at which internalization occurs under the test condition used. Internalization at a 1:1 MOI inoculum (l1M) corresponds to the number of bacteria internalized when hypothetically exposing each eukaryotic cell to a single bacterium (i.e., using a 1:1 MOI). Its value is proportional to the degree of invasiveness of the strain given by the log10 of the IMI value (LIMI), obtained from the regression curve of log MOI vs. log (CFU).

In conclusion, the most used parameters to express the intracellular invasiveness of bacterial strains are the NIB and PIB values. PIB values can be used across a broad range of MOIs without fearing the influence of the inoculum size. Ultimately, PIB values do not depend on the MOI, whereas NIB values are strongly MOI-dependent.

Therefore, we can speculate that the internalization process can be influenced by several factors, such as: (i) bacterial sedimentation rate, influenced by the microbe size, shape and tendency to agglomerate and by the viscosity of the medium; (ii) composition of the culture medium; (iii) cell line used in the assay, considering its histological origin, phagocytic activity (professional or non-professional phagocytic cells in primary or secondary cultures), level of expression of integrins capable of interacting with adhesins; (iv) bacterial strain type (bacterial species and genes encoding for invasiveness).

As already mentioned, different MOIs have been used in several studies depending on the strains tested. These include e.g., *S. aureus*, *S. epidermidis* and *S. lugdunensis*, opportunistic pathogens causing implant-related infections.

These species can survive antibiotic therapies through different mechanisms related to genetic determinants, biofilm production and penetration into eukaryotic cells as the main causes of chronic infections. Furthermore, eukaryotic cells are impermeable to many antibiotics, such as rifampin, that are able to pass through the prokaryotic cell membrane [72,73].

Many staphylococcal species, other than *S. aureus*, are emerging as opportunistic pathogens capable of causing serious and persistent implant-associated infections. According to some authors, *S. epidermidis* is the foremost isolated staphylococcal species responsible for orthopedic infections and is able to internalize into osteoblasts, whilst others report *S. epidermidis* as the second staphylococcal species isolated during orthopedic infections (Khalil et al. 2007; Valour et al. 2013), but its antimicrobial resistance profile is

usually not as severe as that of *S. aureus*. *S. lugdunensis* is an emergent pathogen responsible for periprosthetic infections [74].

The invasive potential of different bacterial species and their ability to internalize into the MG-63 cell line was evaluated using a method based on microtiter plates, where they were challenged with osteoblasts.

Campocia et al., in 2016, used different MOIs for each *Staphylococcus* species tested. The MOI value was always recorded in order to know the inoculum levels actually reached: MOI 560:1 for *S. epidermidis* and MOI 1844:1 for *S. lugdunensis*.

S. epidermidis has an extremely low rate of internalization, not comparable with that observed for *S. aureus*. Furthermore, the bacterial survival rate appeared rather marginal. Most *S. epidermidis* tested with MOI 500:1 showed a relatively low internalization (<50 CFUs), while other strains showed high internalization (>50 CFUs).

Some groups of bacteria appear homogeneous in terms of CFUs internalized regardless of the inoculum level, while others exhibit some heterogeneity in spite of similar inoculum levels. *S. lugdunensis* showed very low levels of internalization regardless of the level of inoculum, even though it was tested with a relatively high MOI (1000:1).

The species considered exhibited marginal rates of internalization compared to *S. aureus*, since *S. aureus* showed a higher rate of internalization at a lower MOI (100:1).

S. aureus requires a very low inoculum to reach a high internalization rate, whereas *S. epidermidis* cell invasiveness remains low and marginal. This finding suggests that the active mechanisms of invasion exhibited by *S. aureus* are either absent or much less efficient in *S. epidermidis*. Similarly, the clinical isolates of *S. lugdunensis* showed a low level of internalization (Figure 2) [70].

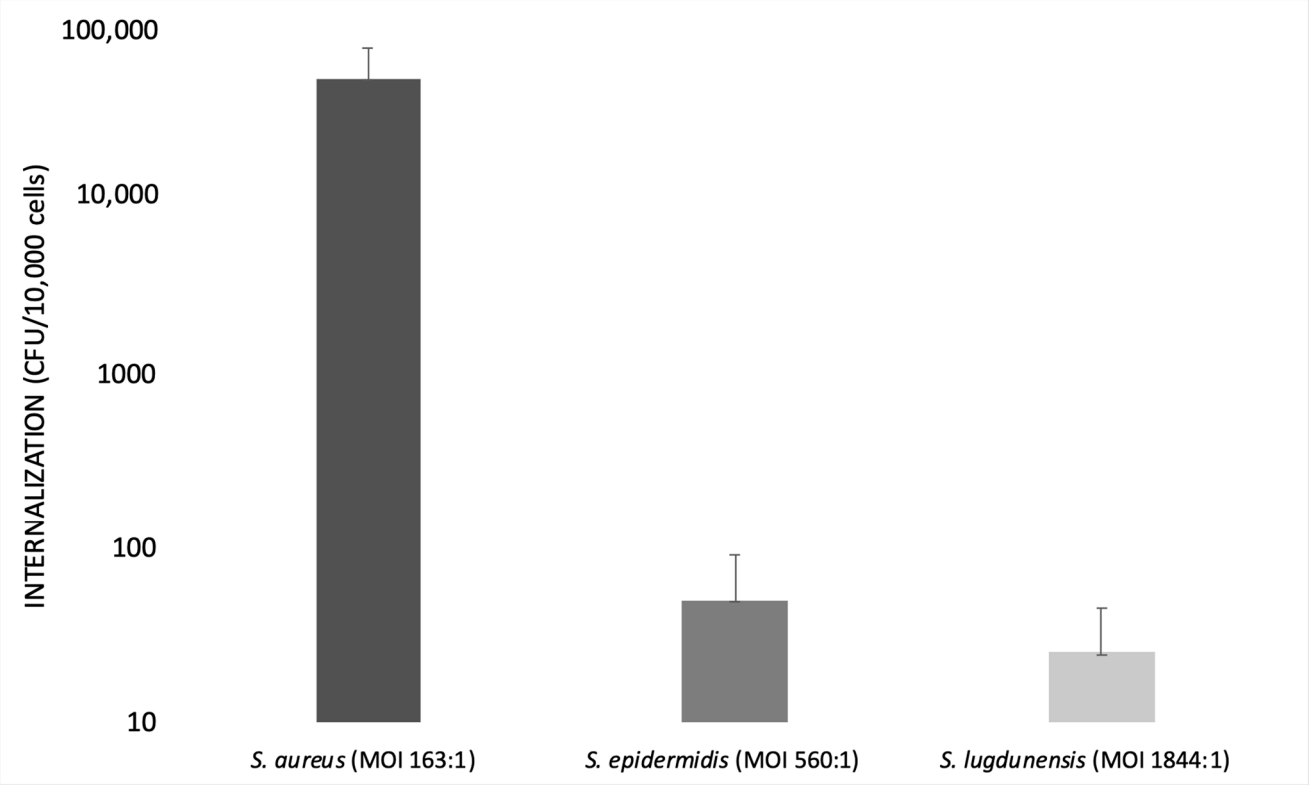

Figure 2. Bar graph illustrating the internalization of *S. aureus*, *S. epidermidis* and *S. lugdunensis* at different multiplicities of infection (MOIs) on a logarithmic scale (modified from Campocia et al., 2016).

To confirm the use of diverse MOIs in the internalization process, studies performed by Valour et al. (2013) compared the different behavior of *S. aureus* and *S. epidermidis* during internalization. As previously shown, *S. epidermidis* has a low rate of internalization, being

an innocuous commensal of the human skin and mucous membranes, but it is considered a leading opportunistic pathogen [70].

The contrast between the low incidence of *S. epidermidis* orthopedic device infection and the highly prevalent *S. epidermidis* carriage suggests that *S. epidermidis* bone and joint infections may either correspond to accidental events due to colonizing strains or to a specific, more virulent sub-population of commensal isolates.

Two predominant mechanisms have been proposed to be involved in orthopedic device infections, i.e., bacterial invasion and persistence in non-professional phagocytes, such as osteoblasts [75]; and the bacterial ability to form biofilm [76,77].

To verify the ability of internalization of *S. epidermidis* into the MG-63 cell line, an invasion assay of *S. epidermidis* was carried out using an MOI of 500:1 for *S. epidermidis* and an MOI of 100:1 for *S. aureus* (used as a control strain).

The results of this assay demonstrated that the number of internalized bacteria was MOI-dependent. There was a difference in bone cell invasion rates between *S. epidermidis* and *S. aureus* strains. *S. epidermidis* showed a lower rate of internalization. This could be due to several factors, such as the "cell line effect"—i.e., the use of the MG-63 cell line—and the acquisition of some phenotypic characteristics that may not reflect the in vivo reality [78].

To exclude a bias due to a "cell line effect", the low internalization rate of *S. epidermidis* was confirmed using primary bone cells. For this reason, all assays were repeated using primary human osteoblasts [69].

Fibronectin-binding protein-like molecules are absent in *S. epidermidis*, therefore, the process of invasion is different from that of *S. aureus*.

Finally, the internalization of *S. epidermidis* in human osteoblasts is not a common pathophysiological mechanism in orthopedic device infections, contrary to what was observed in other clinical situations or with other strains (e.g., *S. aureus*).

MOI Values Were Selected Depending on the Strain Used and Several other Factors

In general, the best choice is to use as few bacteria as possible to reduce cell damage, as important strain-dependent differences may be missed if extended incubation periods or large inocula are used [79].

Hamza et al. (2014) performed an infection experiment using rat osteoblasts and *S. aureus* at different MOIs over different incubation times. They found that intracellular CFUs increased from MOI 100 to MOI 500 and that MOIs greater than 500 did not result in an increase in intracellular CFUs. Osteoblast viability did not change significantly in an MOI range of 100–1000. As a result, high intracellular CFUs and high osteoblast viability were reached at MOI 500 [80].

In the study carried out by Bongiorno et al. (2020), the frequency of internalization was evaluated in a cell culture model of infection using *S. aureus* and MG-63 osteoblasts at an MOI of 100:1. In order to assess this MOI, they first tested MG-63 infection with *S. aureus* ATCC 12598 at the following MOIs: 12:1, 50:1, 100:1 and 200:1. It was observed that, at MOI 12 and 50, the ability of *S. aureus* to internalize into non-specialized cells, such as the osteoblasts, was very limited, while with an MOI of 200, MG-63 cultured cells showed phenomena of cytotoxicity [64].

Take home message: Taken together, this information suggests that researchers should choose the right MOI carefully when designing an internalization experiment, strictly depending on the bacterial species (sometimes even the clone) and the cell line. Higher is not always better. It is critical to know if the bacteria are obligate or opportunistic intracellular species and if the cells are professional phagocytes. Furthermore, internalization experiments should consider other, less used, parameters, i.e., number of internalized bacteria (NIB), percentage of internalized bacteria (PIB) and internalization minimal inoculum (IMI), as these can help researchers to better describe and compare their results.

4. Interaction between *S. aureus* and MG-63 Osteoblast Cells

S. aureus is capable of inducing DNA damage in several host cells, such as osteoblast-like MG-63 cells. The pathogens develop multiple strategies to promote infections [81], interfering with survival pathways [82] and suppressing the immune response of the host, thus facilitating the establishment of chronic infections and promoting host cell transformations [83].

4.1. DNA Damage

Bacteria can damage the host DNA directly and indirectly, e.g., through the production of reactive oxygen species (ROSs). *S. aureus* induces disease especially during chronic infections and the chronification of *S. aureus* infection leads to a phenotypical adaption from a highly virulent to a less virulent form called "small colony variant" (SCV), characterized by increased intracellular persistence, diminished ability of immune system stimulation and lower ability to induce low levels of cytokines release [84].

S. aureus versatility during infection is due to the production of many factors, the most notable being: (i) pore-forming toxins; (ii) exfoliative toxins, involved in tissue disintegration; (iii) adhesins, involved in tissue colonization; (iv) ROS, that can lead to the formation of deleterious oxidative host DNA lesions (promoting the oxidation of guanidine-forming 7,8-dihydro-8-oxoguanine or 8-oxoG); (v) cyclomodulins, which alter the host cell cycle to promote infections.

Deplanche et al. (2019) demonstrated that *S. aureus* induces ROS-mediated DNA damage, followed by DNA repair, and identified "phenol-soluble modulin" (PSM alpha) and lipoproteins (Lpls) as the effectors of this phenomenon. Consequently, 8-oxoG is more expressed in the infected cells.

H2AX is a protein used as a marker of DNA damage. In particular, Deplance et al. demonstrated that *S. aureus* induces dose-dependent H2AX phosphorylation (γH2AX) in osteoblast-like MG-63 cells, in the presence of double-strand break (DSB) damage without apoptosis.

In response to the bacterial agent activity, host cells promote the formation of highly cytotoxic ROS as a defense mechanism against bacteria.

The role of ROS in causing DNA damage was investigated by incubating host cells with N-acetyl-cysteine (NAC), a ROS inhibitor. The incubation of host cells with NAC for 1 h, 6 h and 20 h before infection with *S. aureus* prevented the induction of DNA damage, showing that ROS are involved in *S. aureus*-induced DNA damage [85].

8-oxoG DNA lesions are the most common type of lesions that can generate DNA double-strand breaks when occurring during DNA replication and are thus deleterious [86]. Eukaryotic cell DNA damage may reversibly arrest cell cycle progression to allow DNA repair [87,88]. In addition to DNA damage, cell cycle arrest may be associated with the actin state organization [89,90].

S. aureus triggers ROS-mediated DNA damage, thus affecting the genomic integrity and/or regulating gene transcriptional activation. The induced DNA damage depends on the balance between the levels of the expression of PSMα and Lpls and on bacterial adaptation during chronification, linked to the maintenance of the host genome integrity.

Furthermore, previous studies have proven that the *S. aureus* virulence factors PSMs and Lpls had properties similar to cyclomodulins since they induce G2/M transition delay in infected cells [91,92]. The consequences of *S. aureus*-induced G2/M delay were investigated: the G2 cellular phase is advantageous for bacterial intracellular replication and is associated with a decreased production of antibacterial peptides that may contribute to the persistence of the infection [91,93].

4.2. Virulence Factors

As already known, persistent infections are associated with a wide plethora of virulence factors regulated by the "accessory gene regulator" (*agr* system).

Valour et al. (2015-b) showed that Methicillin-sensitive *Staphylococcus aureus* (MSSA) internalization rates inside osteoblasts were significantly higher in chronic bone and joint infection (BJI) isolates than in acute BJI isolates, and that no difference existed between the two groups in terms of cytotoxicity. Similarly, no differences in the ability of both groups to convert to the SCV phenotype were observed, and biofilm formation was not different between acute and chronic BJI isolates either.

Delta-toxin-negative strains tend to be more represented in chronic BJI and the absence of delta-toxin expression was associated with higher internalization rates. In the same study, the lack of a relationship between BJI chronicity and bacterial genetic backgrounds or virulence factors, as well as an association between osteoblast invasion and *agr* deficiency, were reported. Moreover, acute infections are usually associated with a functional *agr* system. *agr* dysfunction appears to occur during infection and in the presence of persistent bacteremia. Furthermore, infection chronicity appeared to be the main factor associated with *agr* dysfunction. A strong relation between *agr* dysfunction and the bacterial phenotypic mechanism associated with BJI chronicity—including enhanced biofilm formation and increased osteoblastic invasion with reduced infection-induced cytotoxicity—was revealed. The loss of *agr* function that occurs during certain infections seems to be linked with BJI chronicity through the promotion of an intraosteoblastic *S. aureus* reservoir caused by a limitation of intracellular staphylococcal cell damage and through enhanced biofilm formation [16].

Finally, the *agr* system controls the expression of PSM-encoding genes (PSMα 1 to 4, PSMβ 1 and 2 and δ-toxin, sometimes referred to as PSMγ) [94,95]. PSM stimulates the production of inflammatory cytokines [96] and has a role in IL-1β production by infected MG-63 cells. This was demonstrated by analyzing a Wild Type (WT) strain of *S. aureus* and an *S. aureus* LAC Δpsmαβhld mutant for their ability to stimulate the release of IL-1 β. The level of IL-1 β was lower in the supernatant of WT MG-63 cells exposed to the LAC Δpsmαβhld mutant compared to the level observed in the supernatant of WT MG-63 cells exposed to wild-type LAC (Figure 3).

4.3. Immune System

After pathogen invasion, the immune system (IS) recruits an inflammasome, an immune signaling platform that activates proteases, such as caspase-1, that proteolytically matures and promotes the secretion of mature IL-1β and IL-18.

The innate immune response against microbes involves an inflammatory pathway known as the activation of inflammasomes. Caspase-1 is synthesized in cells as a 45 kDa inactive precursor that is cleaved to reach its mature form consisting of two subunits of 20 and 10 kDa after inflammasome activation [97]. After stimulation by pathogens, inflammasome assembly leads to the autocatalytic cleavage of caspase-1, the processing of pro-IL-1β and pro-IL-18 and the secretion of mature IL-1β and IL-18.

It was reported that the expression of inflammasome-associated proteins was significantly higher in infected bones than in uninfected ones, as found in patients with osteomyelitis. In an *S. aureus*-induced murine osteomyelitis model, a higher expression of these proteins was reported [98].

Lima Leite et al. (2020) used the MG-63 cell line as a model of infection with an *S. aureus* strain and a CASP1−/− mutant MG-63 cell line (obtained by using the CRISPR-Cas9 editing system) to evaluate the role of caspase-1 after the invasion process. To test caspase-1 activation, MG-63 cells were incubated with bacterial lipopolysaccharides (LPS) and adenosine triphosphate (ATP), two inflammasome activators. Western blot analysis showed that incubating MG-63 cells with the activators resulted in the activation of caspase-1, while the ELISA test revealed a production of low levels of IL-1 β after 2 h and a higher production after 6 h (Figure 4).

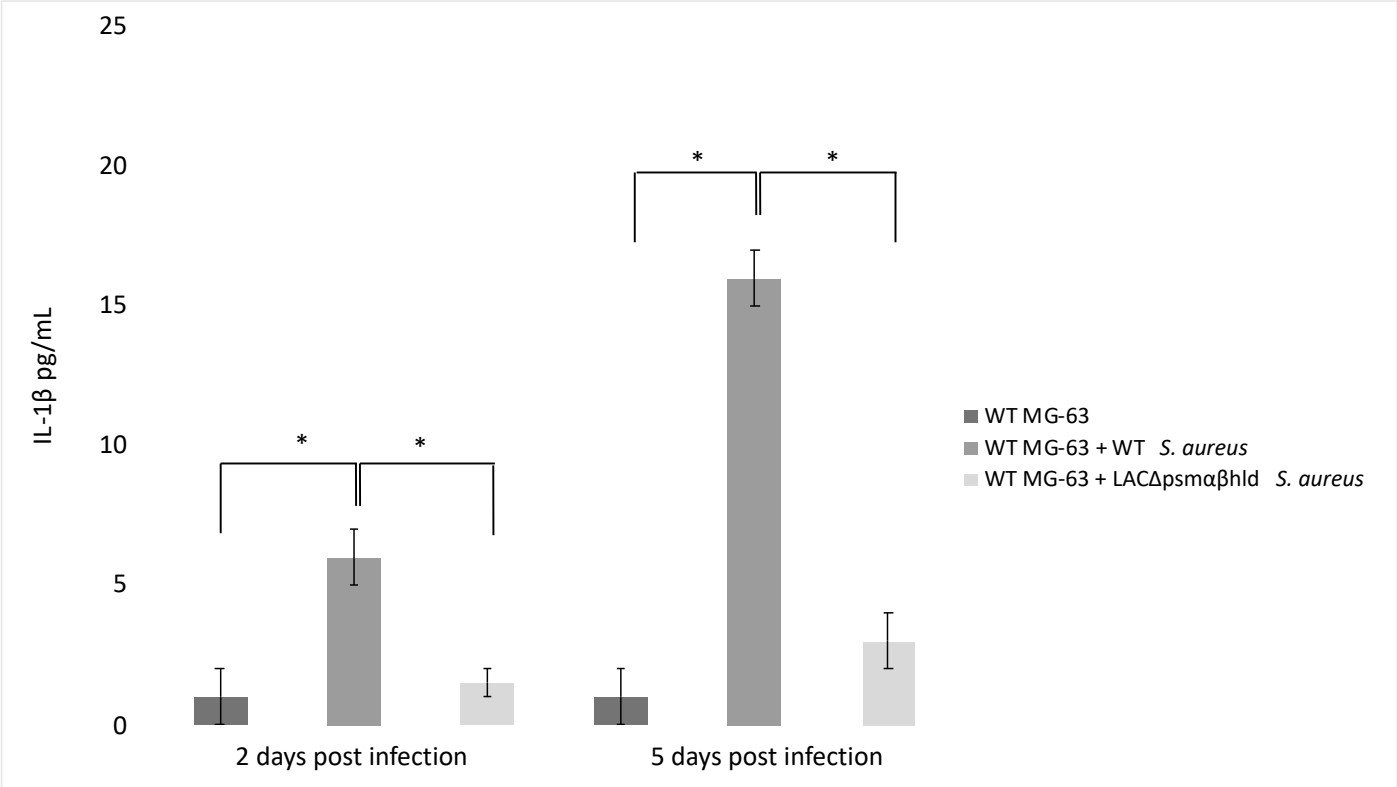

Figure 3. *S. aureus* phenol-soluble modulin (PSM) stimulates IL-1β release from infected osteoblast-like MG-63 cells. MG-63 cells were exposed to wild-type *S. aureus* (USA 300) and its isogenic mutant LAC Δpsmαβhld (*S. aureus* strain lacking PSMα, PSMβ and δ-toxin) at MOI 50:1. IL-1β levels were determined by ELISA 2 and 5 days postinfection. The differences were assessed by the analysis of variance (ANOVA). p Values < 0.05 (*) were considered to be significant (modified from Lima Leite et al., 2020).

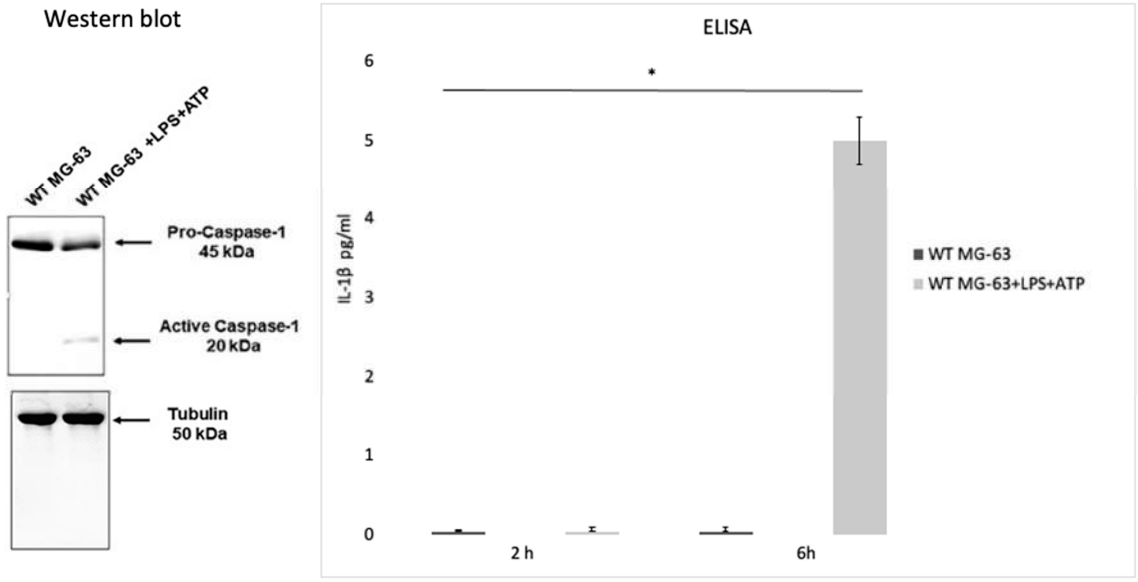

Figure 4. Caspase activation in the MG-63 cell line. Western blot analysis confirmed that the wild type MG-63 cells incubated with lipopolysaccharides and adenosine triphosphate (LPS+ATP) produce active caspase-1. An ELISA was performed to confirm IL-1β production in the WT MG63 cell line and in WT MG-63+LPS+ATP at 2 h and 6 h. The differences were assessed by the analysis of variance (ANOVA). p Values < 0.05 (*) were considered to be significant (from and modified from Lima Leite et al., 2020).

Inflammasome recruited and activated pro-caspase-1, which promoted IL-1β and IL-18 maturation. Six hours after the beginning of the infection with a 50:1 MOI, the number of *S. aureus* CFUs recovered from mutant cells was significantly higher than those recovered from WT MG-63 cells. WT MG-63 cells and CASP1−/− mutant MG-63 clones expressed apoptosis-associated speck-like protein, while only WT MG-63 produced IL-1β after exposure to inflammasome [62].

To evaluate the role of *S. aureus* as an inflammasome activator, IL-1β production in WT and CASP1−/− mutant MG-63 cells was measured. In the latter case, a lack of IL-1β was recorded (in contrast to what was observed in WT MG-63 cells). During these experiments, several *S. aureus* strains were used. All strains induced IL-1β release, showing that this mechanism is strain-independent. Moreover, IL-1β was not detected in the supernatant of MG-63 cells exposed to killed bacteria, suggesting that factors associated with viable bacteria are involved in inflammasome activation.

S. aureus clearance by osteoblast-like MG-63 cells depends on caspase-1. Indeed, the number of viable bacteria recovered from infected cells was significantly larger in CASP1−/− mutant MG-63 than in WT MG-63. This evidence suggest that the lack of caspase-1 impairs the ability of osteoblast-like cells to limit *S. aureus* growth. A drastic increase in the proliferation of internalized bacteria in osteoblastic mutant cells has already been highlighted [62] (Figure 5).

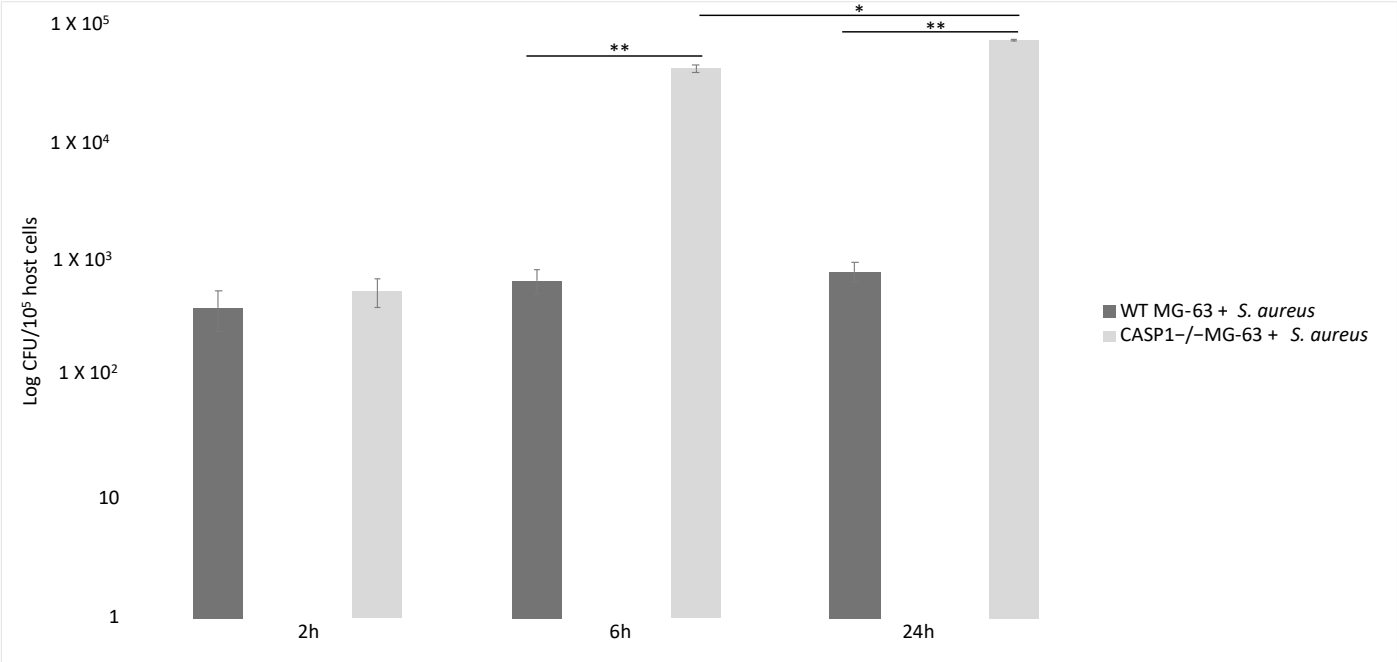

Figure 5. Involvement of caspase-1 in bacterial clearance in WT MG-63 and in CASP1−/− mutant MG-63 at different time points. *S. aureus* MOI 50:1. Tukey's Honestly Significant Difference test was applied for comparison of means between the groups. $p < 0.01$ (**) for the comparison of the number of internalized bacteria in CASP1−/−MG-63 cells with those in WT MG-63 cells, and p values < 0.05 (*) for the comparison of the number of internalized bacteria in CASP1−/−MG-63 cells 6 and 24 h post-infection were considered to be significant (modified from Lima Leite et al., 2020).

In fact, a correlation exists between the lack of caspase-1 activation and a failure in limiting *S. aureus* replication inside phagocytic cells [99,100]. Furthermore, it was demonstrated by Dinarello et al. (2012) that human osteoblast-like MG-63 cells induce an immune response against *S. aureus* through inflammasome activation and the processing of IL-1β, the main inflammatory cytokine. Finally, CASP1−/− mutant MG-63 cells' inability to limit the intracellular replication of *S. aureus* was reported. This work points out that active caspase-1 prevents exacerbated intracellular replication of *S. aureus*. Osteoblasts

therefore are not passive bystanders, but active players in host defenses against *S. aureus* infection [63].

As mentioned above, *S. aureus* is capable of inducing the production of cytokines and chemokines by binding to extracellular or intracellular receptors. In this way, *S. aureus* induces inflammatory cell recruitment, leading to bone loss [3]. Cultured osteoblasts infected with bacteria secrete immune modulators of the inflammatory response, cytokines and chemokines, which trigger bone inflammation and destruction [65,101,102].

To counteract internalization in osteoblasts and the resulting inflammatory process, serratia-peptidase (SPEP)—a metalloprotease produced by *Serratia marcescens* already used as an anti-inflammatory agent—was used [103]. This molecule modulates adhesin expression, enhances antibiotic efficacy toward biofilm-forming bacteria and interferes with *S. aureus* adhesion to abiotic surfaces [104,105].

Selan et al. (2017) showed the effect of SPEP during the internalization process of *S. aureus* in the MG-63 cell-line, using an MOI of 30:1.

The internalization efficiencies of SPEP-pretreated bacteria and untreated bacteria were compared. SPEP-pretreated *S. aureus* exhibited significantly reduced efficiency of internalization. MG-63 cells incubated in the absence of bacteria and with/without SPEP treatment showed that MG-63 proliferation remains unaffected, while when bacteria were pretreated with SPEP, a slight, statistically non-significant decrease in proliferation was recorded for all *S. aureus*. The authors highlighted that the production of chemokines was significantly diminished following treatment with the anti-inflammatory molecule. Chemokine levels in the supernatant derived from MG-63 cells infected with *S. aureus* and pretreated with SPEP were slightly lower than in the supernatant derived from MG-63 cells infected with untreated bacteria. This is a consequence of the reduced internalization of SPEP-pretreated bacteria: lower internalization leads to less stimulation and lower production of the pro-inflammatory chemokine MCP-1 [106].

Take home message: *S. aureus* interaction with MG-63 is widely studied and, in particular, three aspects are of fundamental importance: DNA damage or mutation, the production of virulence factors and the immune system response. *S. aureus* can damage the host DNA by inducing ROS production and can modify its DNA to adapt to the intracellular environmental (SCV). Moreover, persistent infection is modulated by the *agr* locus responsible for the virulence factors and implicated in the establishment of chronic and persistent infections. After pathogen invasion, host cells prompt the IS to produce the inflammasome and activate an immune signaling platform.

5. Antimicrobial Activity against Intraosteoblastic Pathogens

S. aureus can invade osteoblastic cells, which evade the immune response of the host and become a reservoir of bacteria, somewhat protected from the activity of many antimicrobial molecules.

Valour et al. (2015-a) evaluated the efficacy of antimicrobial therapy in *S. aureus* BJI. They evaluated the intraosteoblastic activity of the main antimicrobial agents used for staphylococcal BJI in an in vitro model of osteoblast infection. An infection assay with an MOI of 100:1 was employed, incubating all cells with three different concentrations for each antibiotic.

Inside the bones, vancomycin and daptomycin reach concentrations that cannot significantly prevent bacteria intracellular growth, while an intracellular bacteriostatic effect was observed using ceftaroline and teicoplanin. A significant intracellular bactericidal effect was observed for fosfomycin, linezolid, tigecycline, oxacillin, rifampin, ofloxacin and clindamycin. At the minimum concentration, only rifampin, ofloxacin and fosfomycin were bactericidal. At the maximum concentration, all aforementioned antibiotics were bactericidal, with the exception of vancomycin and daptomycin. Furthermore, at an intracellular concentration, the number of SCVs significantly decreased in the osteoblasts treated with ofloxacin, rifampin and daptomycin. In addition, oxacillin, ceftaroline, line-

zolid, fosfomycine and tigecycline reduced the proportion of intracellular SCVs, but only at their maximum concentration.

Considering that intraosteoblastic *S. aureus* constitutes a bacterial reservoir leading to chronicity and relapse, targeting intracellular bacteria might be a major therapeutic issue in antimicrobial therapy for BJI [16,107].

Vancomycin intracellular efficacy is lower than that of teicoplanin, probably due to its slow uptake and accumulation in the cell. Conversely, rifampin and fluoroquinolones have a fast intracellular uptake. Previously published studies showed that the intracellular activity of antistaphylococcal drugs depends on the exposure time and extracellular concentration of the molecule tested, which emphasizes the importance of using a therapeutic bone concentration. When using systemic therapeutic concentrations, only ofloxacin was able to limit the intracellular emergence of SCVs.

A combination of levofloxacin and rifampin is the elective treatment for acute staphylococcal BJI managed with debridement, antibiotics and implant retention (DAIR) [108,109]. This regime is bactericidal and highly active against biofilm-embedded staphylococci and has good bioavailability and bone diffusion [110].

Meléndez-Carmona et al. (2019) evaluated the effects of rifampin and levofloxacin, alone and in combination, against the process of MSSA internalization in MG-63 cells using an MOI of 100:1. Both antibiotics showed a significant CFU decrease (a log10 of CFU) compared to bacterial CFUs within untreated cells, whereas the combination did not show higher activity compared to levofloxacin monotherapy. Rifampin, alone and in combination with levofloxacin, showed a significant increase in the percentage of SCVs and a significant reduction in the number of intracellular CFUs in comparison with untreated osteoblast cells [111].

Dupieux et al. (2017) demonstrated that, when using *S. aureus* strains to infect osteoblasts, daptomycin did not reduce MSSA number and was poorly active against MRSA. Instead, oxacillin and ceftaroline revealed significant intracellular activity, although oxacillin is not usually active against MRSA. In this paper, two different molecular combinations were used, in particular: daptomycin/oxacillin was more active against intracellular MSSA and MRSA compared with daptomycin and oxacillin alone; and daptomycin/ceftaroline was less efficient than ceftaroline alone. It seems that in acid intracellular conditions, oxacillin was able to enhance daptomycin activity versus *S. aureus* [112].

Abad et al. (2019) demonstrated that linezolid and tedizolid, in intracellular conditions, were able to slightly reduce the inoculum of *S. aureus* and this reduction was strain-dependent, not MIC-dependent (Minimum Inhibitory Concentration dependent), but improved cell viability. These two oxazolidinones alone are not useful versus *S. aureus* strains associated with chronic forms of BJI due to their weak intracellular activity, but they are able to reduce infection-related cytotoxicity, suggesting a role in modulating the intracellular expression of staphylococcal virulence factors [113].

Take home message: Overall, the use of antimicrobials to fight bone and joint infections (BJIs) seems to be more an art than a science, due to the different ability of antibiotics to enter osteoblastic cells, resulting in varying therapy efficacy as well as in the possible failure of molecules which are commonly effective against staphylococcal infections (e.g., vancomycin). In many cases, a combination of two molecules is the right choice to eradicate the infection, but even single molecules that cannot enter cells (e.g., oxazolidinones) can provide important effects by inhibiting, to some extent, the consequences of an infection.

6. Biomimetic 3D In Vitro Models to Investigate Osteomyelitis

In the previous sections, we have seen how conventional models, in particular the use of immortalized cultures such as the MG63 cell line, make a valuable contribution to understanding the mechanisms of host–pathogen interactions, especially those concerning the internalization of *S. aureus* in osteoblasts. Using these models, it was possible to recreate some aspects of osteomyelitis, such as the formation of biofilms or the interaction of bacteria with one or more of the host organism's cell types [114], but they are far from resembling

bone tissue and from reproducing fibrous encapsulation- or osteomyelitis-induced bone abscesses with a necrotic core.

Nevertheless, it has been widely demonstrated that *S. aureus* can reach the bone or metal implant surface by binding to extracellular matrix (ECM) proteins via microbial surface components that recognize adhesive matrix molecules such as collagen-binding protein and bone protein-binding sialoprotein [115]. Among the numerous survival strategies used, *S. aureus* can proliferate and form microcolonies known as staphylococcal abscess communities (SACs) [116], responsible for an abscess structure with surrounding fibrin deposits which make the bacterial core inaccessible to the host's immune cells [117]. Furthermore, Flemming et al. recently analyzed the different causes of antibiotic resistance in *S. aureus* when residing in biofilms [118].

The in vivo mouse models currently in use seemed to be able to give a greater contribution to these studies [22], but have several flaws, for example, planktonic bacteria are inoculated directly into the bone, without taking into account that the origin of osteomyelitis is often derived from a biofilm that bacteria have formed at the site of infection. In addition, there is an incompatibility between the results obtained in mice and those observed in patients [23].

In this regard, the opportunity of developing a sophisticated 3D in vitro model able to recreate the dynamic changes in osteomyelitis infection is of great interest.

Raic et al. developed a 3D in vitro model of biofilm-induced osteomyelitis to study the effects of postoperative osteomyelitis-inducing bacteria on the bone marrow [119], as the analysis of this tissue allows the study of the early stages of the infection, which is not clinically apparent and therefore difficult to treat [1,120,121]. Their system is the first biomimetic human in vitro osteomyelitis model to allow understanding of the early stages of disease progression and to overcome the limitations of other model systems, for example: (a) results of animal models are often not transferable to human beings [20,122], while their bone marrow model does not pose the problem of interspecies-related differences, as it is composed of human cells; (b) in vitro models are for the most part performed on conventional 2D tissue culture plates that are not able to mimic the natural 3D conditions, potentially generating in vitro artifacts; (c) to mimic biofilm-triggered osteomyelitis [23,123], especially in animal studies, planktonic bacteria are used and this does not reflect the in vivo situation; contrary to that, biofilms of planktonic bacteria are used in this model to mimic biofilm-triggered osteomyelitis. In detail, postoperative osteomyelitis was reproduced by developing a new 3D protein scaffold with a macroporous architecture that resembles the trabecular bone. In order to mimic the cellular compartment of the stem cell niche, human hematopoietic stem and progenitor cells (HSPCs) and mesenchymal stromal cells (MSCs) were seeded within this scaffold.

A very important component for the development of these models is the choice of the material to be used. In 2010, Pagedar et al. showed that the level of biofilm formation of *S. aureus* depends on the hydrophilicity of the surface [124]. In fact, the model developed by Raic in titanium (a material used in the clinic) showed the formation of biofilms containing active metabolic bacteria different from the conventional plastic plates used for in vitro cell cultures [119].

As demonstrated by Meng et al. in 2014, followed by studies by Ravi et al., cells exhibit different behaviors in terms of differentiation, protein expression or cell survival rate when grown in a 2D or 3D system [125,126]. Similarly, these cells will react differently to bacterial factors when placed in a 2D or 3D environment. This suggests the importance of carefully selecting not only the materials, but also the bacteria that are relevant for in vitro functional modeling of osteomyelitis. Moreover, the use of these 3D models may provide a better understanding of the molecular interactions and cellular responses to osteomyelitis, which are crucial for the development of new therapies for the treatment of this debilitating disease. In this regard, Kavanagh et al. developed a three-dimensional (3D) bone infection model to examine the processes of *S. aureus* bone colonization and infection [127]. To simulate the infection process, the scaffold, produced using an EDAC

(1-Ethyl-3-(3-Dimethylaminopropyl)carbodiimide) cross-linked glycosaminoglycan collagen biomaterial, was inoculated with a co-culture of osteoblasts and *S. aureus*. Thanks to this model, it was possible to observe the ability of osteoblasts to counteract bone loss and bone destruction by increasing the levels of mineralization of the weakened bone. This discovery is groundbreaking and is only observable in a 3D environment. Indeed, in stark contrast to what has just been described, the same authors had previously shown that in 2D cell culture conditions, *S. aureus* protein A mediates attachment to osteoblasts, but following this link, there was a loss of proliferation and the inhibition of mineralization in osteoblasts [9,11,128]. The development of a physiologically more relevant collagen-based scaffold not only has given a new insight into this pathological phenomenon, but is in line with the characteristic signs of osteomyelitis observed clinically. The images of the two models described above are shown in Figure 6. For a more exhaustive discussion of 3D host–pathogen infection models compared to conventional systems, also refer to Hofstee et al. [114] and Barila et al. [129].

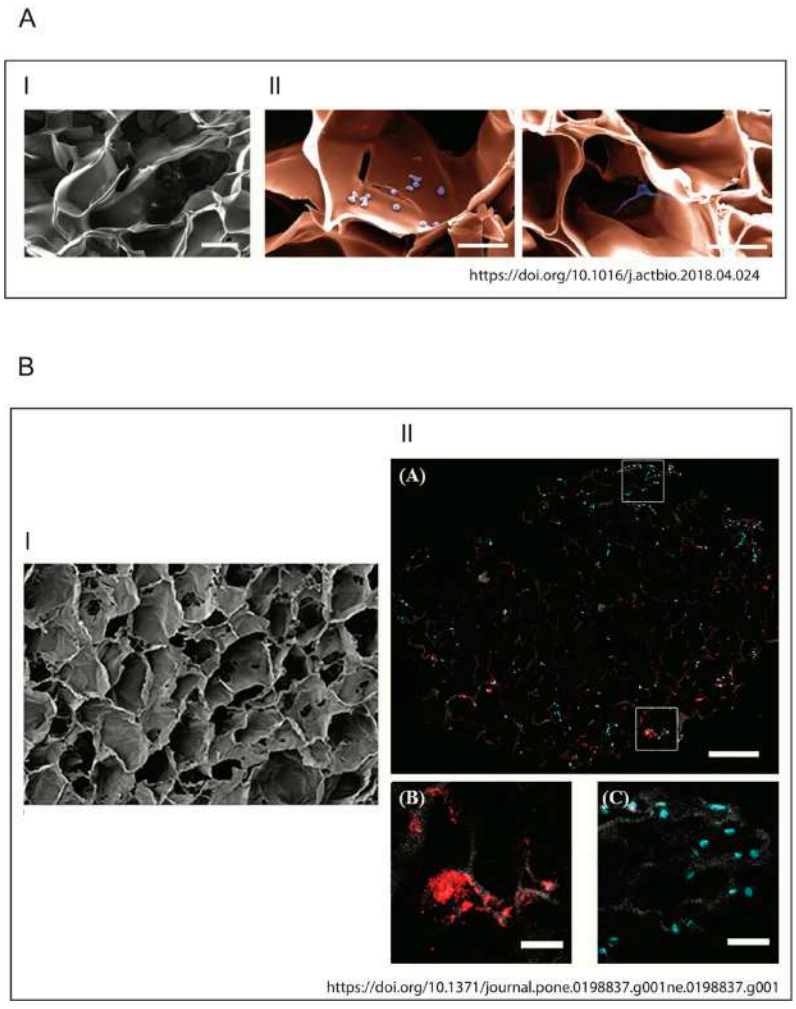

Figure 6. Illustrations of biomimetic 3D in vitro models. (**A**) Architecture and biocompatibility of the 3D protein scaffold. (I) Pseudocolored SEM picture of a cross section of the applied macroporous 3D protein scaffold. The image shows the porous structure inside the scaffold. Scale bar: 100 mm. (II) SEM image of 3D protein scaffold seeded with the HSPC (left) and MSC (right) cell lines. The cells (violet) are located inside of the pores of the scaffold (orange) and adhere to the scaffold material. Scale bar: 50 mm (Raic et al./Acta Biomaterialia 73 (2018) 250–262). (**B**) Pore architecture of scaffolds seeded with osteoblasts and infected by *S. aureus***.** (I) SEM of 3D scaffold only (100×, Scale bare 100 μM); (II) qualitative assessment of cellular and bacterial co-infiltration of the collagen scaffold (from Kavanagh et al., 2018).

Take home message: In conclusion, osteomyelitis infection is characterized by a complex and dynamic environment that cannot be fully understood using a conventional model. Thus, physiologically more relevant collagen-based scaffolds represent an innovative and valuable tool to investigate the ability of osteoblasts to counteract bone loss and bone destruction by increasing the levels of mineralization of weakened bone in a similar way to what happens in patients.

7. Conclusions

For over half a century, the study of the mechanisms that govern osteomyelitis has remained the weak point of orthopedic surgery. Despite many advances in understanding the pathophysiological consequences of bone infection, standards of care treatments have not undergone major changes and some aspects of intracellular persistence in chronic osteomyelitis have not yet been well elucidated [130].

As demonstrated in several publications, biofilm-forming *S. aureus* is the most common pathogen in implant-associated infections, as well as the main cause of reinfection, due to its high resistance to the immune response and antibiotic treatments [131–134]. Our knowledge about the ability of *S. aureus* to infect not only bone-forming cells (osteoblasts) but also the cells responsible for bone resorption (osteoclasts) [135] derives from the use of conventional in vivo and in vitro 2D models. In particular, in this review, we have analyzed how the use of a standardized in vitro model, such as immortalized MG-63 cell cultures, provides valuable help in understanding the mechanisms of internalization and interaction of *S. aureus* and osteoblasts. Despite being different from primary osteoblasts in some respects, these cells allow us to standardize studies aiming to obtain further information to predict the capability of staphylococcal clones—often associated with recurrent and chronic infections—to invade, internalize and persist within the human cells, as well as to confirm the active role of osteoblasts in the host defense against *S. aureus* infections. At the same time, these models have recently been defined as physiologically limited systems and unable to mimic the complex dynamic environment in which cells are found in the human body [18,19,136]. To make up for this, 3D models (scaffolds) consisting of engineered biomaterials capable of reproducing bone tissue have been developed and it was demonstrated that they can provide information otherwise not obtainable through traditional models. It is clear that conventional 2D in vitro models represent a valid model for studying some of the aspects that occur during bacterial infection (for example, the use of MG-63 cells for the internalization mechanisms of *S. aureus*) in detail. Conversely, 3D bone scaffolds ensure a dynamic and global view of the pathological phenomenon of interest (for example, tissue–host–pathogen interactions).

Author Contributions: Conceptualization, N.M., D.B., S.S. (Stefano Stracquadanio) and S.S. (Stefania Stefani); writing/original draft preparation, L.M.L. and A.C.; writing/review and editing, S.S. (Stefano Stracquadanio), N.M., D.B. and S.S. (Stefania Stefani); funding acquisition, D.B. and S.S. (Stefania Stefani). All authors have read and agreed to the published version of the manuscript.

Funding: The authors received no financial support for the authorship, and/or publication of this article.

Institutional Review Board Statement: Not applicable.

Informed Consent Statement: Not applicable.

Data Availability Statement: No new data were created or analyzed in this study. Data sharing is not applicable to this article.

Acknowledgments: We wish to thank Floriana Campanile for her support and suggestions and Pharmatranslated for the language revision process.

Conflicts of Interest: The authors declare no conflict of interest.

References

1. Lew, D.P.; Waldvogel, F.A. Osteomyelitis. *Lancet* **2004**, *364*, 369–379. [CrossRef]
2. Hudson, M.C.; Ramp, W.K.; Nicholson, N.C.; Williams, A.S.; Nousiainen, M.T. Internalization of *Staphylococcus aureus* by cultured osteoblasts. *Microb. Pathog.* **1995**, *19*, 409–419. [CrossRef]
3. Josse, J.; Velard, F.; Gangloff, S.C. *Staphylococcus aureus* vs. Osteoblast: Relationship and Consequences in Osteomyelitis. *Front. Cell Infect. Microbiol.* **2015**, *5*, 85. [CrossRef]
4. Montanaro, L.; Speziale, P.; Campoccia, D.; Ravaioli, S.; Cangini, I.; Pietrocola, G.; Giannini, S.; Arciola, C.R. Scenery of *Staphylococcus* implant infections in orthopedics. *Future Microbiol.* **2011**, *6*, 1329–1349. [CrossRef] [PubMed]
5. Kim, P.H.; Leopold, S.S. Inbrief: Gustilo-Anderson classification. [corrected]. *Clin. Orthop. Relat. Res.* **2012**, *470*, 3270–3274. [CrossRef]
6. Hogan, A.; Heppert, V.G.; Suda, A.J. Osteomyelitis. *Arch. Orthop. Trauma Surg.* **2013**, *133*, 11831196. [CrossRef]
7. Shi, S.; Zhang, X. Interaction of *Staphylococcus aureus* with osteoblasts (Review). *Exp. Ther. Med.* **2012**, *3*, 367–370. [CrossRef]
8. Heilmann, C. *Adhesion Mechanisms of Staphylococci. Advances in Experimental Medicine and Biology*; Linke, D., Goldman, A., Eds.; Springer: Dordrecht, The Netherlands, 2011; Volume 715, pp. 105–123.
9. Claro, T.; Widaa, A.; O'Seaghdha, M.; Miajlovic, H.; Foster, T.J.; O'Brien, F.J.; Kerrigan, S.V. *Staphylococcus aureus* protein A binds to osteoblasts and triggers signals that weaken bone in osteomyelitis. *PLoS ONE* **2011**, *6*, e18748. [CrossRef]
10. Tucker, K.A.; Reilly, S.S.; Leslie, C.S.; Hudson, M.C. Intracellular *Staphylococcus aureus* induces apoptosis in mouse osteoblasts. *Fems Microbiol. Lett.* **2000**, *186*, 151–156. [CrossRef] [PubMed]
11. Widaa, A.; Claro, T.; Foster, T.J.; O'Brien, F.J.; Kerrigan, S.W. *Staphylococcus aureus* protein a plays a critical role in mediating bone destruction and bone loss in osteomyelitis. *PLoS ONE* **2012**, *7*, e40586. [CrossRef]
12. Wen, Q.; Gu, F.; Sui, Z.; Su, Z.; Yu, T. The Process of Osteoblastic Infection by *Staphylococcus aureus*. *Rev. Int. J. Med. Sci.* **2020**, *17*, 1327–1332. [CrossRef]
13. Turner, M.D.; Nedjai, B.; Hurst, T.; Pennington, D.J. Cytokines and chemokines: At the crossroads of cell signalling and inflammatory disease. *Bio-Chim. Biophys. Acta* **2014**, *1843*, 2563–2582. [CrossRef] [PubMed]
14. Valour, F.; Trouillet-Assant, S.; Riffard, N.; Tasse, J.; Flammier, S.; Rasigade, J.P.; Chidiac, C.; Vandenesch, F.; Ferry, T.; Laurent, F. Antimicrobial activity against intraosteoblastic *Staphylococcus aureus*. *Antimicrob. Agents Chemother.* **2015**, *59*, 2029–2036. [CrossRef]
15. Spellberg, B.; Lipsky, B.A. Systemic antibiotic therapy for chronic osteomyelitis in adults. *Clin. Infect. Dis.* **2012**, *54*, 393–407. [CrossRef] [PubMed]
16. Valour, F.; Rasigade, J.P.; Trouillet-Assant, S.; Gagnaire, J.; Bouaziz, A.; Karsenty, J.; Lacour, C.; Bes, M.; Lustig, S.; Bénet, T.; et al. Delta-toxin production deficiency in *Staphylococcus aureus*: A diagnostic marker of bone and joint infection chronicity linked with osteoblast invasion and biofilm formation. *Clin. Microbiol. Infect.* **2015**, *21*, 568.e1–568.e11. [CrossRef]
17. Czekanska, E.M.; Stoddart, M.J.; Richards, R.G.; Hayes, J.S. In search of an osteoblast cell model for in vitro research. *Eur. Cells Mater.* **2012**, *24*, 1–17. [CrossRef]
18. Baker, B.M.; Chen, C.S. Deconstructing the third dimension: How 3D culture microenvironments alter cellular cues. *J. Cell Sci.* **2012**, *125 Pt 13*, 3015–3024. [CrossRef]
19. Fitzgerald, K.A.; Malhotra, M.; Curtin, C.M.; O' Brien, F.J.; O' Driscoll, C.M. Life in 3D is never flat: 3D models to optimize drug delivery. *J. Control. Release* **2015**, *215*, 39–54. [CrossRef] [PubMed]
20. Mestas, J.; Hughes, C.C.W. Of Mice and Not Men: Differences between Mouse and Human Immunology. *J. Immunol.* **2004**, *172*, 2731–2738. [CrossRef] [PubMed]
21. Patel, M.; Rojavin, Y.; Jamali, A.A.; Wasielewski, S.J.; Salgado, C.J. Animal Models for the Study of Osteomyelitis. *Semin. Plast. Surg.* **2009**, *23*, 148–154. [CrossRef] [PubMed]
22. Reizner, W.; Hunter, J.G.; O' Malley, N.T.; Southgate, R.D.; Schwarz, E.M.; Kates, S.L. A systematic review of animal models for *Staphylococcus aureus* osteomyelitis. *Eur. Cells Mater.* **2014**, *27*, 196–212. [CrossRef]
23. Shanks, N.; Greek, R.; Greek, J. Are animal models predictive for humans? *Philos. Ethics Hum. Med.* **2009**, *4*, 2. [CrossRef]
24. Eum, S.Y.; Kong, J.H.; Hong, M.S.; Lee, Y.J.; Kim, J.H.; Hwang, S.H.; Cho, S.N.; Via, L.E.; Barry, C.E., 3rd. Neutrophils are the predominant infected phagocytic cells in the airways of patients with active pulmonary TB. *Chest* **2010**, *137*, 122–128. [CrossRef]
25. Lerner, T.R.; Borel, S.; Gutierrez, M.G. The innate immune response in human tuberculosis. *Cell Microbiol.* **2015**, *17*, 1277–1285. [CrossRef]
26. Jevon, M.; Guo, C.; Ma, B.; Mordan, N.; Nair, S.P.; Harris, M.; Henderson, B.; Bentley, G.; Meghji, S. Mechanisms of internalization of *Staphylococcus aureus* by cultured human osteoblasts. *Infect. Immun.* **1999**, *67*, 2677–2681. [CrossRef] [PubMed]
27. Horn, J.; Stelzner, K.; Rudel, T.; Fraunholz, M. Inside job: *Staphylococcus aureus* host-pathogen interactions. *Int. J. Med. Microbiol.* **2018**, *308*, 607–624. [CrossRef]
28. Abe, Y.; Aida, Y.; Abe, T.; Hirofuji, T.; Anan, H.; Maeda, K. Development of mineralized nodules in fetal rat mandibular osteogenic precursor cells: Requirement for dexame-thasone but not for beta-glycerophosphate. *Calcif. Tissue Int.* **2000**, *66*, 66–69. [CrossRef] [PubMed]
29. Bellows, C.G.; Aubin, J.E.; Heersche, J.N.; Antosz, M.E. Mineralized bone nodules formed in vitro from enzymatically released rat calvaria cell populations. *Calcif. Tissue Int.* **1986**, *38*, 143–154. [CrossRef]

30. Cao, X.Y.; Yin, M.Z.; Zhang, L.N.; Li, S.P.; Cao, Y. Establishment of a new model for culturing rabbit osteoblasts in vitro. *Biomed. Mater.* **2006**, *1*, L16–L19. [CrossRef] [PubMed]
31. Ecarot-Charrier, B.; Glorieux, F.H.; van der Rest, M.; Pereira, G. Osteoblasts isolated from mouse calvaria initiate matrix mineralization in culture. *J. Cell Biol.* **1983**, *96*, 639–643. [CrossRef]
32. Collignon, H.; Davicco, M.J.; Barlet, J.P. Isolation of cells from ovine fetal long bone and characterization of their osteoblastic activities during in vitro mineralization. *Arch. Physiol. Biochem.* **1997**, *105*, 158–166. [CrossRef] [PubMed]
33. Wang, D.; Christensen, K.; Chawla, K.; Xiao, G.; Krebsbach, P.H.; Franceschi, R.T. Isolation and characterization of MC3T3-E1 preosteoblast; subclones with distinct in vitro and in vivo differentiation/mineralization potential. *J. Bone Miner. Res.* **1999**, *14*, 893–903. [CrossRef] [PubMed]
34. Harris, S.A.; Enger, R.J.; Riggs, B.L.; Spelsberg, T.C. Development and characterization of a conditionally immortalized human fetal osteoblastic cell line. *J. Bone Miner. Res.* **1995**, *10*, 178–186. [CrossRef]
35. Billiau, A.; Edy, V.G.; Heremans, H.; Van, D.J.; Desmyter, J.; Georgiades, J.A.; De, S.P. Human interferon: Mass production in a newly established cell line, MG-63. *Antimicrob. Agents Chemother.* **1977**, *12*, 11–15. [CrossRef] [PubMed]
36. Rodan, S.B.; Imai, Y.; Thiede, M.A.; Wesolowski, G.; Thompson, D.; Bar-Shavit, Z.; Shull, S.; Mann, K.; Rodan, G.A. Characterization of a human osteosarcoma cell line (Saos-2) with osteoblastic properties. *Cancer Res.* **1987**, *47*, 4961–4966. [PubMed]
37. Ponten, J.; Saksela, E. Two established in vitro cell lines from human mesenchymal tumors. *Int. J. Cancer* **1967**, *2*, 434–447. [CrossRef] [PubMed]
38. Voegele, T.J.; Voegele-Kadletz, M.; Esposito, V.; Macfelda, K.; Oberndorfer, U.; Vecsei, V.; Schabus, R. The effect of different isolation techniques on human osteoblast-like cell growth. *Anticancer Res.* **2000**, *20*, 3575–3581. [PubMed]
39. Jonsson, K.B.; Frost, A.; Nilsson, O.; Ljunghall, S.; Ljunggren, O. Three isolation techniques for primary culture of human osteoblast-like cells: A comparison. *Acta Orthop. Scand.* **1999**, *70*, 365–373. [CrossRef] [PubMed]
40. Bonjour, J.P.; Theintz, G.; Buchs, B.; Slosman, D.; Rizzoli, R. Critical years and stages of puberty for spinal and femoral bone mass accumulation during adolescence. *J. Clin. Endocrinol. Metab.* **1991**, *73*, 555–563. [CrossRef]
41. Bergot, C.; Wu, Y.; Jolivet, E.; Zhou, L.Q.; Laredo, J.D.; Bousson, V. The degree and distribution of cortical bone mineralization in the human femoral shaft change with age and sex in a microradiographic study. *Bone* **2009**, *45*, 435–442. [CrossRef] [PubMed]
42. Fedarko, N.S.; Vetter, U.K.; Weinstein, S.; Robey, P.G. Age-related changes in hyaluronan, proteoglycan, collagen, and osteonectin synthesis by human bone cells. *J. Cell Physiol.* **1992**, *151*, 215–227. [CrossRef]
43. Kasperk, C.; Wergedal, J.; Strong, D.; Farley, J.; Wangerin, K.; Gropp, H.; Ziegler, R.; Baylink, D.J. Human bone cell phenotypes differ depending on their skeletal site of origin. *J. Clin. Endocrinol. Metab.* **1995**, *80*, 2511–2517.
44. Martinez, M.E.; Del Campo, M.T.; Medina, S.; Sanchez, M.; Sanchez-Cabezudo, M.J.; Esbrit, P.; Martinez, P.; Moreno, I.; Rodrigo, A.; Garces, M.V.; et al. Influence of skeletal site of origin and donor age on osteoblastic cell growth and differentiation. *Calcif. Tissue Int.* **1999**, *64*, 280–286. [CrossRef] [PubMed]
45. Czekanska, E.M.; Stoddart, M.J.; Ralphs, J.R.; Richards, R.G.; Hayes, J.S. A phenotypic comparison of osteoblast cell lines versus human primary osteoblasts for *Biomaterials* testing. *J. Biomed. Mater. Res. A* **2014**, *102*, 2636–2643. [CrossRef]
46. Heremans, H.; Billiau, A.; Cassiman, J.J.; Mulier, J.C.; de Somer, P. In vitro cultivation of human tumor tissues. II. Morphological and virological characterization of three cell lines. *Oncology* **1978**, *35*, 246–252. [CrossRef]
47. Franceschi, R.T.; Romano, P.R.; Park, K.Y. Regulation of type I collagen synthesis by 1,25-dihydroxyvitamin D3 in human osteosarcoma cells. *J. Biol. Chem.* **1988**, *263*, 18938–18945. [CrossRef]
48. Schinke, T.; Karsenty, G. *Transcriptional Control of Osteoblast Differentiation and Function. Principles of Bone Biology*; Academic Press: London, UK, 2002; pp. 83–92.
49. Ducy, P.; Zhang, R.; Geoffroy, V.; Ridall, A.L.; Karsenty, G. Osf2/Cbfa1: A transcriptional activator of osteoblast differentiation. *Cell* **1997**, *89*, 747–754. [CrossRef]
50. Wenstrup, R.J.; Witte, D.P.; Florer, J.B. Abnormal differentiation in MC3T3-E1 preosteoblasts expressing a dominant-negative type I collagen mutation. *Connect. Tissue Res.* **1996**, *35*, 249–257. [CrossRef] [PubMed]
51. Ryoo, H.M.; Hoffmann, H.M.; Beumer, T.; Frenkel, B.; Towler, D.A.; Stein, G.S.; Stein, J.L.; van Wijnen, A.J.; Lian, J.B. Stage-specific expression of Dlx-5 during osteoblast differentiation: Involvement in regulation of osteocalcin gene expression. *Mol. Endocrinol.* **1997**, *11*, 1681–1694. [CrossRef] [PubMed]
52. Kirkham, G.; Cartmell, S. Genes and Proteins Involved in the Regulation of Osteogenesis. *Top. Tissue Eng.* **2007**, *3*, 3270–3274.
53. Ahmed, S.; Meghji, S.; Williams, R.J.; Henderson, B.; Brock, J.H.; Nair, S.P. *Staphylococcus aureus* fibronectin binding proteins are essential for Internalization by osteoblasts but do not account for differences in intracellular levels of bacteria. *Infect. Immun.* **2001**, *69*, 2872–2877. [CrossRef] [PubMed]
54. Nair, S.P.; Bischoff, M.; Senn, M.M.; Berger Bächi, B. The sigma B regulon influences internalization of *Staphylococcus aureus* by osteoblasts. *Infect. Immun.* **2003**, *71*, 4167–4170. [CrossRef]
55. Khalil, H.; Williams, R.J.; Stenbeck, G.; Henderson, B.; Meghji, S.; Nair, S.P. Invasion of bone cells by *Staphylococcus epidermidis*. *Microbes Infect.* **2007**, *9*, 460–465. [CrossRef] [PubMed]
56. Testoni, F.; Montanaro, L.; Poggi, A.; Visai, L.; Campoccia, D.; Arciola, C.R. Internalization by osteoblasts of two *Staphylococcus aureus* clinical Isolates differing in their adhesin gene pattern. *Int. J. Artif. Organs* **2011**, *34*, 789–798. [CrossRef] [PubMed]
57. Jauregui, C.E.; Mansell, J.P.; Jepson, M.A.; Jenkinson, H.F. Differential interactions of *Streptococcus gordonii* and *Staphylococcus aureus* with cultured osteoblasts. *Mol. Oral Microbiol.* **2013**, *28*, 250–266. [CrossRef]

58. Schroder, K.; Tschopp, J. The inflammasomes. *Cell* **2010**, *140*, 821–832. [CrossRef]
59. Lamkanfi, M.; Dixit, V.M. The Inflammasomes. *PLoS Pathog.* **2009**, *5*, e1000510. [CrossRef]
60. Mariathasan, S.; Newton, K.; Monack, D.M.; Vucic, D.; French, D.M.; Lee, W.P.; Roose-Girma, M.; Erickson, S.; Dixit, V.M. Differential activation of the inflammasome by caspase-1 adaptors ASC and Ipaf. *Nature* **2004**, *430*, 213–218. [CrossRef]
61. Strowig, T.; Henao-Mejia, J.; Elinav, E.; Flavell, R. Inflammasomes in health and disease. *Nature* **2012**, *481*, 278–286. [CrossRef]
62. Lima Leite, E.; Gautron, A.; Deplanche, M.; Nicolas, A.; Ossemond, J.; Nguyen, M.T.; do Carmo, F.L.R.; Gilot, D.; Azevedo, V.; Götz, F.; et al. Involvement of caspase-1 in inflammasomes activation and bacterial clearance in *S. aureus*-infected osteoblast-like MG-63 cells. *Cell Microbiol.* **2020**, *22*, e13204. [CrossRef]
63. Dinarello, C.A.; Simon, A.; van der Meer, J.W.M. Treating inflammation by blocking interleukin-1 in a broad spectrum of diseases. *Nat. Rev. Drug Discov.* **2012**, *11*, 633–652. [CrossRef]
64. Bongiorno, D.; Musso, N.; Lazzaro, L.M.; Mongelli, G.; Stefani, S.; Campanile, F. Detection of methicillin-resistant *Staphylococcus aureus* persistence in osteoblasts using imaging flow cytometry. *MicrobiologyOpen* **2020**, *9*, e1017. [CrossRef]
65. Musso, N.; Caruso, G.; Bongiorno, D.; Grasso, M.; Bivona, D.A.; Campanile, F.; Caraci, F.; Stefani, S. Different Modulatory Effects of Four Methicillin-Resistant *Staphylococcus aureus* Clones on MG-63 Osteoblast-Like Cells. *Biomolecules* **2021**, *11*, 72. [CrossRef]
66. Bhavsar, A.P.; Guttman, J.A.; Finlay, B.B. Manipulation of host-cell pathways by bacterial pathogens. *Nature* **2007**, *449*, 827–834. [CrossRef] [PubMed]
67. Ellington, J.K.; Harris, M.; Hudson, M.C.; Vishin, S.; Webb, L.X.; Sherertz, R. Intracellular *Staphylococcus aureus* and antibiotic resistance: Implications for treatment of staphylococcal osteomyelitis. *J. Orthop. Res.* **2006**, *24*, 87–93. [CrossRef]
68. Maali, Y.; Martins-Simões, P.; Valour, F.; Bouvard, D.; Rasigade, J.P.; Bes, M.; Haenni, M.; Ferry, T.; Laurent, F.; Trouillet-Assant, S. Pathophysiological mechanisms of *Staphylococcus* non-*aureus* bone and joint infection: Interspecies homogeneity and specific behavior of *S. pseudintermedius*. *Front. Microbiol.* **2016**, *7*, 1063. [CrossRef] [PubMed]
69. Valour, F.; Trouillet-Assant, S.; Rasigade, J.P.; Lustig, S.; Chanard, E.; Meugnier, H.; Tigaud, S.; Vandenesch, F.; Etienne, J.; Ferry, T.; et al. *Staphylococcus epidermidis* in orthopedic device infections: The role of bacterial internalization in human osteoblasts and biofilm formation. *PLoS ONE* **2013**, *8*, e67240. [CrossRef]
70. Campoccia, D.; Testoni, F.; Ravaioli, S.; Cangini, I.; Maso, A.; Speziale, P.; Montanaro, L.; Visai, L.; Arciola, C.R. Orthopedic implant infections: Incompetence of *Staphylococcus epidermidis*, *Staphylococcus lugdunensis*, and *Enterococcus faecalis* to invade osteoblasts. *J. Biomed. Mater. Res. A* **2016**, *104*, 788–801. [CrossRef] [PubMed]
71. Campoccia, D.; Montanaro, L.; Ravaioli, S.; Cangini, I.; Testoni, F.; Visai, L.; Arciola, C.R. New Parameters to Quantitatively Express the Invasiveness of Bacterial Strains from Implant-Related Orthopaedic Infections into Osteoblast Cells. *Materials* **2018**, *11*, 550. [CrossRef]
72. Stewart, P.S.; Costerton, J.W. Antibiotic resistance of bacteria in biofilms. *Lancet* **2001**, *358*, 135–138. [CrossRef]
73. Arciola, C.R.; Campoccia, D.; Speziale, P.; Montanaro, L.; Costerton, J.W. Biofilm formation in Staphylococcus implant infections. A review of molecular mechanisms and implications for biofilm-resistant materials. *Biomaterials* **2012**, *33*, 5967–5982. [CrossRef] [PubMed]
74. Arciola, C.R.; Campoccia, D.; Baldassarri, L.; Pirini, V.; Huebner, J.; Montanaro, L. The role of *Enterococcus faecalis* in orthopedic peri-implant infections demonstrated by automated ribotyping and cluster analysis. *Biomaterials* **2007**, *28*, 3987–3995. [CrossRef]
75. Ellington, J.K.; Reilly, S.S.; Ramp, W.K.; Smeltzer, M.S.; Kellam, J.F.; Hudson, M.C. Mechanisms of *Staphylococcus aureus* invasion of cultured osteoblasts. *Microb. Pathog.* **1999**, *26*, 317–323. [CrossRef] [PubMed]
76. Costerton, J.W.; Stewart, P.S.; Greenberg, E.P. Bacterial biofilms: A common cause of persistent infections. *Science* **1999**, *284*, 1318–1322. [CrossRef] [PubMed]
77. Brady, R.A.; Leid, J.G.; Calhoun, J.H.; Costerton, J.W.; Shirtliff, M.E. Osteomyelitis and the role of biofilms in chronic infection. *FEMS Immunol. Med. Microbiol.* **2008**, *52*, 13–22. [CrossRef]
78. Pautke, C.; Schieker, M.; Tischer, T.; Kolk, A.; Neth, P.; Mutschler, W.; Milz, S. Characterization of osteosarcoma cell lines MG- 63, Saos-2 and U-2 OS in comparison to human osteoblasts. *Anticancer Res.* **2004**, *24*, 3743–3748.
79. Edwards, A.M.; Massey, R.C. How does *Staphylococcus aureus* escape the bloodstream? *Trends Microbiol.* **2011**, *19*, 184–190. [CrossRef]
80. Hamza, T.; Li, B. Differential responses of osteoblasts and macrophages upon *Staphylococcus aureus* infection. *BMC Microbiol.* **2014**, *14*, 207. [CrossRef]
81. Chumduri, C.; Gurumurthy, R.K.; Zietlow, R.; Meyer, T.F. Subversion of host genome integrity by bacterial pathogens. *Nat. Rev. Mol. Cell Biol.* **2016**, *17*, 659–673. [CrossRef]
82. Alto, N.M.; Orth, K. Subversion of cell signaling by pathogens. *Cold Spring Harb. Perspect. Biol.* **2012**, *4*, a006114. [CrossRef]
83. Johnson, K.S.; Ottemann, K.M. Colonization, localization, and inflammation: The roles of *H. pylori* chemotaxis in vivo. *Curr. Opin. Microbiol.* **2017**, *70*, 365–373. [CrossRef] [PubMed]
84. Trouillet-Assant, S.; Lelièvre, L.; Martins-Simões, P.; Gonzaga, L.; Tasse, J.; Valour, F.; Rasigade, J.P.; Vandenesch, F.; Muniz Guedes, R.L.; Ribeiro de Vasconcelos, A.T.; et al. Adaptive processes of *Staphylococcus aureus* isolates during the progression from acute to chronic bone and joint infections in patients. *Cell Microbiol.* **2016**, *18*, 1405–1414. [CrossRef] [PubMed]
85. Deplanche, M.; Mouhali, N.; Nguyen, M.T.; Cauty, C.; Ezan, F.; Diot, A.; Raulin, L.; Dutertre, S.; Langouet, S.; Legembre, P.; et al. *Staphylococcus aureus* induces DNA damage in host cell. *Sci. Rep.* **2019**, *9*, 7694. [CrossRef] [PubMed]

86. van Loon, B.; Markkanen, E.; Hübscher, U. Oxygen as a friend and enemy: How to combat the mutational potential of 8-oxo-guanine. *DNA Repair* **2010**, *9*, 604–616. [CrossRef]
87. Reinhardt, H.C.; Yaffe, M.B. Kinases that control the cell cycle in response to DNA damage: Chk1, Chk2, and MK2. *Curr. Opin. Cell Biol.* **2009**, *21*, 245–255. [CrossRef]
88. Smith, J.L.; Bayles, D.O. The contribution of cytolethal distending toxin to bacterial pathogenesis. *Crit. Rev. Microbiol.* **2006**, *32*, 227–248. [CrossRef]
89. Meng, X.; Leslie, P.; Zhang, Y.; Dong, J. Stem cells in a three-dimensional scaffold environment. *SpringerPlus* **2014**, *3*, 80. [CrossRef]
90. Rupes, I.; Webb, B.A.; Mak, A.; Young, P.G. G2/M arrest caused by actin disruption is a manifestation of the cell size checkpoint in fission yeast. *Mol. Biol. Cell.* **2001**, *12*, 3892–3903. [CrossRef]
91. Deplanche, M.; Filho, R.A.; Alekseeva, L.; Ladier, E.; Jardin, J.; Henry, G.; Azevedo, V.; Miyoshi, A.; Beraud, L.; Laurent, F.; et al. Phenol-soluble modulin α induces G2/M phase transition delay in eukaryotic HeLa cells. *FASEB J.* **2015**, *29*, 1950–1959. [CrossRef]
92. Nguyen, M.T.; Deplanche, M.; Nega, M.; Le Loir, Y.; Peisl, L.; Götz, F.; Berkova, N. *Staphylococcus aureus* Lpl Lipoproteins Delay G2/M Phase Transition in HeLa Cells. *Front. Cell Infect. Microbiol.* **2016**, *6*, 201. [CrossRef]
93. Alekseeva, L.; Rault, L.; Almeida, S.; Legembre, P.; Edmond, V.; Azevedo, V.; Miyoshi, A.; Even, S.; Taieb, F.; Arlot-Bonnemains, Y.; et al. *Staphylococcus aureus*-induced G2/M phase transition delay in host epithelial cells increases bacterial infective efficiency. *PLoS ONE* **2013**, *8*, e63279. [CrossRef]
94. Otto, M. Basis of virulence in community-associated methicillinresistant *Staphylococcus aureus*. *Annu. Rev. Microbiol.* **2010**, *64*, 143–162. [CrossRef]
95. Queck, S.Y.; Jameson-Lee, M.; Villaruz, A.E.; Bach, T.H.L.; Khan, B.A.; Sturdevant, D.E.; Otto, M. RNAIII-independent target gene control by the agr quorum-sensing system: Insight into the evolution of virulence regulation in *Staphylococcus aureus*. *Mol. Cell.* **2008**, *32*, 150–158. [CrossRef]
96. Syed, A.K.; Reed, T.J.; Clark, K.L.; Boles, B.R.; Kahlenberg, J.M. *Staphylococcus aureus* phenol-soluble modulins stimulate the release of proinflammatory cytokines from keratinocytes and are required for induction of skin inflammation. *Infect. Immun.* **2015**, *83*, 3428–3437. [CrossRef] [PubMed]
97. Lamkanfi, M.; Dixit, V.M. Mechanisms and functions of inflammasomes. *Cell* **2014**, *157*, 1013–1022. [CrossRef]
98. Zhu, X.; Zhang, K.; Lu, K.; Shi, T.; Shen, S.; Chen, X.; Dong, J.; Gong, W.; Bao, Z.; Shi, Y.; et al. Inhibition of pyroptosis attenuates-induced bone injury in traumatic osteomyelitis. *Ann. Transl. Med.* **2019**, *7*, 170. [CrossRef]
99. Cohen, T.S.; Boland, M.L.; Boland, B.B.; Takahashi, V.; Tovchigrechko, A.; Lee, Y.; Sellman, B.R.S. *S. aureus* evades macrophage killing through NLRP3-dependent effects on mitochondrial trafficking. *Cell Rep.* **2018**, *22*, 2431–2441. [CrossRef] [PubMed]
100. Sokolovska, A.; Becker, C.E.; Ip, W.K.E.; Rathinam, V.A.K.; Brudner, M.; Paquette, N.; Stuart, L.M. Activation of caspase-1 by the NLRP3 inflammasome regulates the NADPH oxidase NOX2 to control phagosome function. *Nat. Immunol.* **2013**, *14*, 543–553. [CrossRef] [PubMed]
101. Miyamoto, K.; Ninomiya, K.; Sonoda, K.H.; Miyauchi, Y.; Hoshi, H.; Iwasaki, R.; Miyamoto, H.; Yoshida, S.; Sato, Y.; Morioka, H.; et al. MCP-1 expressed by osteoclasts stimulates osteoclastogenesis in an autocrine/paracrine manner. *Biochem. Biophys. Res. Commun.* **2009**, *383*, 373–377. [CrossRef]
102. Bost, K.L.; Bento, J.L.; Petty, C.C.; Schrum, L.W.; Hudson, M.C.; Marriott, I. Monocyte chemoattractant protein-1 expression by osteoblasts following infection with *Staphylococcus aureus* or Salmonella. *J. Interferon Cytokine Res.* **2001**, *21*, 297–304. [CrossRef] [PubMed]
103. Bhagat, S.; Agarwal, M.; Roy, V. Serratiopeptidase: A systematic review of the existing evidence. *Int. J. Surg.* **2013**, *11*, 209–217. [CrossRef]
104. Papa, R.; Artini, M.; Cellini, A.; Tilotta, M.; Galano, E.; Pucci, P.; Amoresano, A.; Selan, L. A new anti-infective strategy to reduce the spreading of antibiotic resistance by the action on adhesion-mediated virulence factors in *Staphylococcus aureus*. *Microb. Pathog.* **2013**, *63*, 44–53. [CrossRef] [PubMed]
105. Selan, L.; Papa, R.; Tilotta, M.; Vrenna, G.; Carpentieri, A.; Amoresano, A.; Pucci, P.; Artini, M. Serratiopeptidase: A well-known metalloprotease with a new non-proteolytic activity against *S. aureus* biofilm. *BMC Microbiol.* **2015**, *15*, 207. [CrossRef]
106. Selan, L.; Papa, R.; Ermocida, A.; Cellini, A.; Ettorre, E.; Vrenna, G.; Campoccia, D.; Montanaro, L.; Arciola, C.R.; Artini, M. Serratiopeptidase reduces the invasion of osteoblasts by *Staphylococcus aureus*. *Int. J. Immunopathol. Pharm.* **2017**, *30*, 423–428. [CrossRef]
107. Rasigade, J.P.; Trouillet-Assant, S.; Ferry, T.; Diep, B.A.; Sapin, A.; Lhoste, Y.; Ranfaing, J.; Badiou, C.; Benito, Y.; Bes, M.; et al. PSMs of hypervirulent *Staphylococcus aureus* act as intracellular toxins that kill infected osteoblasts. *PLoS ONE* **2013**, *8*, e63176. [CrossRef]
108. Ariza, J.; Cobo, J.; Baraia-Etxaburu, J.; Benito, N.; Bori, G.; Cabo, J.; Corona, P.; Esteban, J.; Horcajada, J.P.; Lora-Tamayo, J.; et al. Executive summary of management of prosthetic joint infections. Clinical practice guidelines by the Spanish Society of Infectious Diseases and Clinical Microbiology (SEIMC). *Enferm. Infecc. Microbiol. Clin.* **2017**, *35*, 189–195. [CrossRef] [PubMed]
109. Osmon, D.R.; Berbari, E.F.; Berendt, A.R.; Lew, D.; Zimmerli, W.; Steckelberg, J.M.; Rao, N.; Hanssen, A.; Wilson, W.R. Diagnosis and management of prosthetic joint infection: Clinical practice guidelines by the Infectious Diseases Society of America. *Clin. Infect. Dis.* **2013**, *56*, e1–e25. [CrossRef]

110. Muller-Serieys, C.; Saleh Mghir, A.; Massias, L.; Fantin, B. Bactericidal activity of the combination of levofloxacin with rifampin in experimental prosthetic knee infection in rabbits due to methicillin-susceptible *Staphylococcus aureus*. *Antimicrob. Agents Chemother.* **2009**, *53*, 2145–2148. [CrossRef] [PubMed]
111. Meléndez-Carmona, M.Á.; Muñoz-Gallego, I.; Viedma, E.; Lora-Tamayo, J.; Chaves, F. Intraosteoblastic activity of levofloxacin and rifampin alone and in combination against clinical isolates of methicillin-susceptible *Staphylococcus aureus* causing prosthetic joint infection. *Int. J. Antimicrob. Agents* **2019**, *54*, 356–360. [CrossRef]
112. Dupieux, C.; Trouillet-Assant, S.; Camus, C.; Abad, L.; Bes, M.; Benito, Y.; Chidiac, C.; Lustig, S.; Ferry, T.; Valour, F.; et al. Intraosteoblastic activity of daptomycin in combination with oxacillin and ceftaroline against MSSA and MRSA. *J. Antimicrob. Chemother.* **2017**, *72*, 3353–3356. [CrossRef]
113. Abad, L.; Tafani, V.; Tasse, J.; Josse, J.; Chidiac, C.; Lustig, S.; Ferry, T.; Diot, A.; Laurent, F.; Valour, F. Evaluation of the ability of linezolid and tedizolid to eradicate intraosteoblastic and biofilm-embedded *Staphylococcus aureus* in the bone and joint infection setting. *J. Antimicrob. Chemother.* **2019**, *74*, 625–632. [CrossRef]
114. Hofstee, M.I.; Muthukrishnan, G.; Atkins, G.J.; Riool, M.; Thompson, K.; Morgenstern, M.; Stoddart, M.J.; Richards, R.G.; Zaat, S.; Moriarty, T.F. Current Concepts of Osteomyelitis: From Pathologic Mechanisms to Advanced Research Methods. *Am. J. Pathol.* **2020**, *190*, 1151–1163. [CrossRef]
115. Hudson, M.C.; Ramp, W.K.; Frankenburg, K.P. *Staphylococcus aureus* adhesion to bone matrix and bone-associated biomaterials. *Fems Mmicrobiol. Lett.* **1999**, *173*, 279–284. [CrossRef]
116. Brandt, S.L.; Putnam, N.E.; Cassat, J.E.; Serezani, C.H. Innate immunity to *Staphylococcus aureus*: Evolving paradigms in soft tissue and invasive infections. *J. Immunol.* **2018**, *200*, 3871–3880. [CrossRef] [PubMed]
117. Thomer, L.; Schneewind, O.; Missiakas, D. Pathogenesis of *Staphylococcus aureus* bloodstream infections. *Annu. Rev. Pathol.* **2016**, *11*, 343–364. [CrossRef]
118. Flemming, H.C.; Wingender, J.; Szewzyk, U.; Steinberg, P.; Rice, S.A.; Kjelleberg, S. Biofilms: An emergent form of bacterial life. *Nat. Rev. Microbiol.* **2016**, *14*, 563–575. [CrossRef]
119. Raic, A.; Riedel, S.; Kemmling, E.; Bieback, K.; Overhage, J.; Lee-Thedieck, C. Biomimetic 3D in vitro model of biofilm triggered osteomyelitis for investigating hematopoiesis during bone marrow infections. *Acta Biomater.* **2018**, *73*, 250–262. [CrossRef] [PubMed]
120. Agarwal, S. Osteolysis—basic science, incidence and diagnosis. *Curr. Orthop.* **2004**, *18*, 220–231. [CrossRef]
121. Pineda, C.; Espinosa, R.; Pena, A. Radiographic imaging in osteomyelitis: The role of plain radiography, Computed Tomography, Ultrasonography, Magnetic Resonance Imaging, and Scintigraphy. *Semin. Plast. Surg.* **2009**, *23*, 80–89. [CrossRef]
122. Knight, A. Systematic reviews of animal experiments demonstrate poor human clinical and toxicological utility. *Altern. Lab. Anim.* **2007**, *35*, 641–659. [CrossRef] [PubMed]
123. Williams, D.L.; Haymond, B.S.; Woodbury, K.L.; Beck, J.P.; Moore, D.E.; Epperson, R.T.; Bloebaum, R.D. Experimental model of biofilm implant-related osteomyelitis to test combination *Biomaterials* using biofilms as initial inocula. *J. Biomed. Mater. Res.* **2012**, *100*, 1888–1900. [CrossRef]
124. Pagedar, A.; Singh, J.; Batish, V.K. Surface hydrophobicity, nutritional contents affect *Staphylococcus aureus* biofilms and temperature influences its survival in preformed biofilms. *J. Basic Microbiol.* **2010**, *50* (Suppl. 1), S98–S106. [CrossRef] [PubMed]
125. Heng, Y.W.; Koh, C.G. Actin cytoskeleton dynamics and the cell division cycle. *Int. J. Biochem. Cell Biol.* **2010**, *42*, 1622–1633. [CrossRef]
126. Ravi, M.; Paramesh, V.; Kaviya, S.R.; Anuradha, E.; Solomon, F.D.P. 3D cell culture systems: Advantages and applications. *J. Cell. Physiol.* **2015**, *230*, 16–26. [CrossRef] [PubMed]
127. Kavanagh, N.; O' Brien, F.J.; Kerrigan, S.W. *Staphylococcus aureus* protein A causes osteoblasts to hyper-mineralise in a 3D extra-cellular matrix environment. *PLoS ONE* **2018**, *13*, e0198837. [CrossRef]
128. Claro, T.; Widaa, A.; McDonnell, C.; Foster, T.J.; O'Brien, F.J.; Kerrigan, S.W. *Staphylococcus aureus* protein A binding to osteoblast tumor necrosis factor receptor 1 results in activation of nuclear factor kappa B and release of interleukin-6 in bone infection. *Microbiology* **2013**, *159 Pt 1*, 147–154. [CrossRef]
129. Barrila, J.; Crabbé, A.; Yang, J.; Franco, K.; Nydam, S.D.; Forsyth, R.J.; Davis, R.R.; Gangaraju, S.; Ott, C.M.; Coyne, C.B.; et al. Modeling host-pathogen interactions in the context of the microenvironment: Threedimensional cell culture comes of age. *Infect. Immun.* **2018**, *86*, e00282-18. [CrossRef] [PubMed]
130. Masters, E.A.; Trombetta, R.P.; de Mesy Bentley, K.L.; Boyce, B.F.; Gill, A.L.; Gill, S.R.; Nishitani, K.; Ishikawa, M.; Morita, Y.; Ito, H.; et al. Evolving concepts in bone infection: Redefining "biofilm", "acute vs. chronic osteomyelitis", "the immune proteome" and "local antibiotic therapy". *Bone Res.* **2019**, *7*, 20. [CrossRef]
131. Darouiche, R.O. Treatment of infections associated with surgical implants. *N. Engl. J. Med.* **2004**, *350*, 1422–1429. [CrossRef]
132. Keren, I.; Kaldalu, N.; Spoering, A.; Wang, Y.; Lewis, K. Persister cells and tolerance to antimicrobials. *Fems Microbiol. Lett.* **2004**, *230*, 13–18. [CrossRef]
133. Yun, C.H.; Mengwasser, K.E.; Toms, A.V.; Woo, M.S.; Greulich, H.; Wong, K.K.; Meyerson, M.; Eck, M.J. The T790M mutation in EGFR kinase causes drug resistance by increasing the affinity for ATP. *Proc. Natl. Acad. Sci. USA* **2008**, *105*, 2070–2075. [CrossRef] [PubMed]
134. Zimmerli, W.; Trampuz, A.; Ochsner, P.E. Prosthetic-joint infections. *N. Engl. J. Med.* **2004**, *351*, 1645–1654. [CrossRef] [PubMed]

135. De Mesy Bentley, K.L.; MacDonald, A.; Schwarz, E.M.; Oh, I. Chronic osteomyelitis with *Staphylococcus aureus* deformation in submicron canaliculi of osteocytes: A case report. *JBJS Case Connect.* **2018**, *8*, e8. [CrossRef]
136. Imamura, Y.; Mukohara, T.; Shimono, Y.; Funakoshi, Y.; Chayahara, N.; Toyoda, M.; Kiyota, N.; Takao, S.; Kono, S.; Nakatsura, T.; et al. Comparison of 2D- and 3D-culture models as drug-testing platforms in breast cancer. *Oncol. Rep.* **2015**, *33*, 1837–1843. [CrossRef] [PubMed]

2. AIM OF THE WORK

The main goals of this project were: i) to understand the role of *S. aureus* in the host/pathogen interactions, with a focus on its intracellular survival within human osteoblasts after the infection and internalization processes, at different time periods; ii) to evaluate how *S. aureus* cells change their behaviour during their persistence within human cells; iii) to evaluate the molecular crosstalk between *S. aureus* cells and human osteoblasts during adaptation in persistent infections.

This project can be subdivided into two parts **(Table 1).**

Part I: Assessment of the internalization ability of methicillin-resistant *Staphylococcus aureus* clinical isolates in human osteoblasts MG-63	Part II: Study of the metabolic activity by cellular vitality assay and expression studies of diverse marker during osteoblast infections.
***Ex-vivo* infection**	**Vitality assay (MTT)**
Flow cytometric assay	**Expression level of transcription by RTq-PCR**

Table 1 *Schematic representation of project*

Part I: Assessment of the internalization ability of methicillin-resistant *Staphylococcus aureus* clinical isolates in human osteoblasts MG-63

The first part focuses on estimating the frequency of internalization and the persistence of a selected sample of MDR-MRSA clinical isolates with different molecular backgrounds, within the human osteoblast cell line MG63 at different time periods, compared to the ATCC12598 *S. aureus* control strain (ST30-t076, originally isolated from septic arthritis) by an *ex-vivo* model of infection and a novel flow cytometric assay, the imaging flow cytometry (IFC). The study sample consisted of 15 invasive MRSA isolates, belonging to different genetic background classes: ST239-SCC*mec* III, ST5-SCC*mec* II, ST8-SCC*mec* IV, ST228-SCC*mec* I, and ST22-SCC*mec* IVh. The invasive isolate ATCC12598 (Cowan ST30-t076; ATCC® Standards Development Organization, LGC Standards S.r.l.) was used as control strain for invasion and persistence assays and for the statistical analysis of the results obtained by the *in-vitro* cell culture methods and IFC assays. Infection experiments were performed on the human osteosarcoma cell line MG-63 (ATCC® CRL-1427™; Standards Development Organization, LGC Standards S.r.l.). The internalization frequency was evaluated in a cell culture model of infection (*ex vivo)* in MG-63 osteoblasts at a multiplicity of infection (MOI) of 100:1. MG-63 culture were infected for 2 and 24 h in antibiotic-free conditions. Estimation of intracellular bacteria was determined 3h post-infection (p.i.) to assess the bacterial internalization processes, and 24h p.i. to assess persistence, by osmotic MG-63 cell lysis, serial dilution plating of the lysate on blood agar plates, incubation at 37°C overnight and CFU/ml counting. All samples were examined by fluorescence and confocal microscopy to obtain images of internalized bacterial cells. **(Fig.3)**

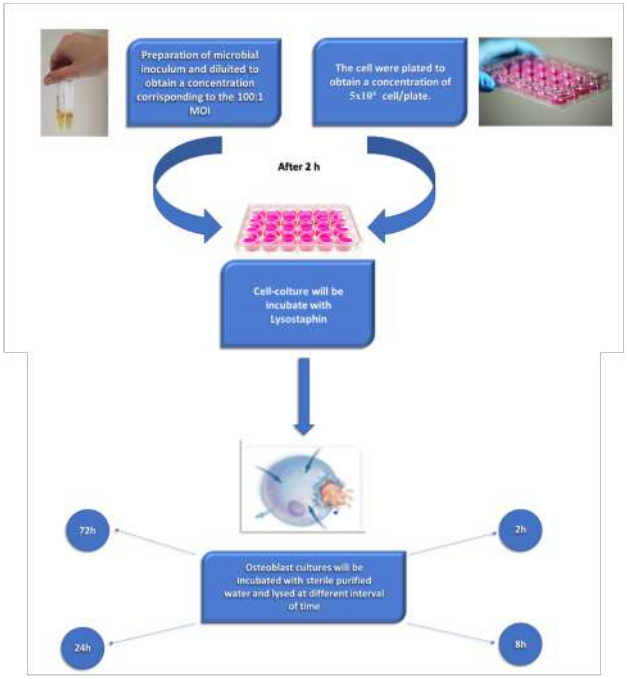

Figure 3 *Workflow for the detection of intracellular bacteria by the ex-vivo Imaging Flow Cytometric assay.*

To overcome the limitations of the *ex-vivo* model, the internalization frequency was evaluated by flow cytometric assay, using a FlowSight® Imaging Flow Cytometer, that acquire up to 12 images simultaneously of each cell and analyzed by IDEAS® (Image Data Exploration and Analysis Software).The internalized bacteria were calculated counting the fluorescence spots inside MG-63 cells considering 10000 events. **(Fig.4)**

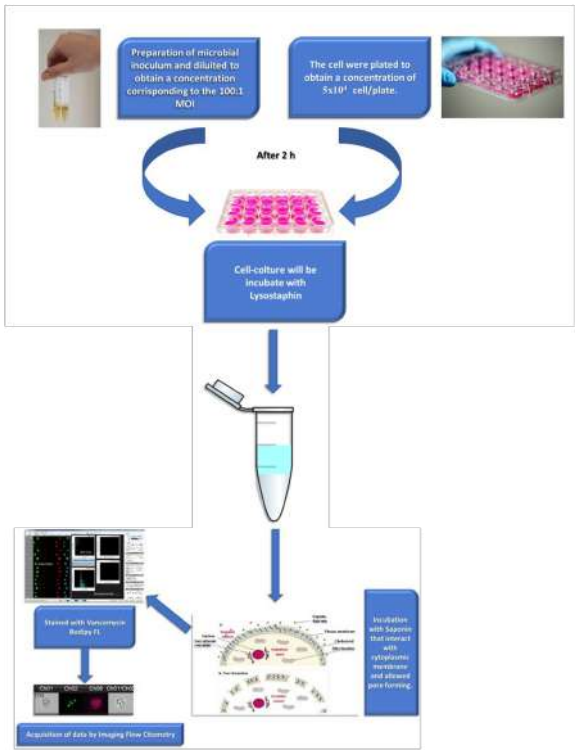

Figure 4 *Workflow for the detection of intracellular bacteria by Flow cytometric assay.*

The analysis of data obtained by the *in-vitro* culture method showed different invasion rates among the MRSA clones in study: ST239-SCC*mec* III showed the best ability to internalize (0.36-0.43 CFU/cell); lower internalization rates were analysed among other clones: ST5-SCC*mec* II rifampicin resistant (RIF-R) (0.23-0.32 CFU/cell); ST8-SCC*mec* IV-RIF-R (0.45-0.55 CFU/cell); ST228-SCC*mec* I-RIF-R (0.057-0.025 CFU/cell); ST22-SCC*mec* IVh-RIF-R (0.22-0.31 CFU/cell). ATCC12598 (ST30-t076) internalization rate were 0.20 CFU/cell respectively, according to bibliographic data.

In this first *in-vitro* analysis, we demonstrated that the ability to invade osteoblasts is correlated to the genetic background: ST239, ST8, ST5 and ST22 showed higher internalization efficiency; conversely, ST228 did not exhibit significant rates of internalization.

The analysis of the data obtained by the *ex-vivo* Imaging Flow Cytometric assay showed a statistical difference of persistence among the MRSA clones. ATCC 12598 ST30-t076, the invasive isolate used as control strain for invasion and persistence assays, persisted inside 51% of MG-63 for 24h p.i., and the same ability to persist was detected in ST239-SCC*mec* III (47.82%) and ST22-SCC*mec* IVh (50.55%) clones. The other clones analyzed, ST5-SCC*mec* II (26.59%), ST228-SCC*mec* I (20.25%), ST8-SCC*mec* IV (19.52%), were less able to persist inside MG-63 cells. These statistically relevant results obtained by Imaging flow cytometry assays allowed us to establish that the intracellular rates did not depend to the number of bacterial cells that manage to enter/replicate inside a single MG-63 osteoblast, but to the total number of cells that were infected. Also by the ex-vivo assay, ST22-IVh and ST239-III clones showed higher intracellular persistence in host cells, making them more prone to develop chronic and recurrent infections.

Comparing the data obtained by the cell culture method with those of the IFC assay, we obtained greater reproducibility rates and several intracellular bacteria, with the advantage of analyzing live host cells. The combination of these techniques allowed us to understand how the interaction between host and clinical pathogens varies among the diverse genetic backgrounds.

These novel findings provided an insight into host-pathogen successful interaction of specific MRSA clones and could contribute to the development of a new knowledge-based-approach for treatment of chronic infections.

Received: 30 November 2019 | Revised: 1 February 2020 | Accepted: 10 February 2020

DOI: 10.1002/mbo3.1017

ORIGINAL ARTICLE

MicrobiologyOpen Open Access WILEY

Detection of methicillin-resistant *Staphylococcus aureus* persistence in osteoblasts using imaging flow cytometry

Dafne Bongiorno[1] | Nicolò Musso[2] | Lorenzo Mattia Lazzaro[1] | Gino Mongelli[1] | Stefania Stefani[1,2] | Floriana Campanile[1]

[1]Department of Biomedical and Biotechnological Sciences (BIOMETEC), Medical Molecular Microbiology and Antibiotic Resistance Laboratory (MMAR*Lab*), University of Catania, Catania, Italy

[2]Bio-nanotech Research and Innovation Tower (BRIT), University of Catania, Catania, Italy

Correspondence
Dafne Bongiorno, Department of Biomedical and Biotechnological Sciences (MMARL), University of Catania, Via Santa Sofia, 97, 95123 Catania, Italy.
Email: d.bongiorno@unict.it

Abstract

Methicillin-resistant *S. aureus* has been reported as the main pathogen involved in chronic infections, osteomyelitis, and prosthetic joint infections. The host/pathogen interaction is dynamic and requires several changes to promote bacterial survival. Here, we focused on the internalization and persistence behavior of well-characterized *Staphylococcus aureus* invasive strains belonging to the main ST-MRSA-SCC*mec* clones. To overcome the limitations of the cell culture method, we comparatively analyzed the ability of internalization within human MG-63 osteoblasts with imaging flow cytometry (IFC). After evaluation by cell culture assay, the MRSA clones in the study were all able to readily internalize at 3h postinfection, the persistence of intracellular bacteria was evaluated at 24h both by routine cell culture and IFC assay, after vancomycin-BODIPY staining. A statistical difference of persistence was found in ST5-SCC*mec*II (26.59%), ST228-SCC*mec*I (20.25%), ST8-SCC*mec*IV (19.52%), ST239-SCC*mec*III (47.82%), and ST22-SCC*mec*IVh (50.55%) showing the same ability to internalize as ATCC12598 (51%), the invasive isolate used as control strain for invasion and persistence assays. We demonstrated that the intracellular persistence process depends on the total number of infected cells. Comparing our data obtained by IFC with those of the cell culture assay, we obtained greater reproducibility rates and a number of intracellular bacteria, with the advantage of analyzing live host cells. Moreover, with some limitations related to the lack of whole-genome sequencing analysis, we validated the different proclivities to persist in the main Italian HA-MRSA invasive isolates and our results highlighted the heterogeneity of the different clones to persist during cell infection.

KEYWORDS

genetic background, imaging flow cytometry, internalization, methicillin-resistant *S. aureus*, osteoblast

Bongiorno and Musso equally contributed to this work.

1 | INTRODUCTION

Staphylococcus aureus is one of the most adaptable human pathogens and is able to infect many organs and damage tissues, causing severe infections. One of the most interesting strategies is associated with its persistence, through changes from the aggressive wild-type phenotype to small colony variant (SCV) forms, more adaptive long-term persistent cells. In these dynamic changes, it becomes refractory to prolonged antimicrobial treatment required for chronic infections, recurrent osteomyelitis (OM), and prosthetic joint infections (PJIs); Tuchscherr & Löffler, 2016). In particular, PJIs can have a dramatic impact on the quality of life of a patient, often requiring surgical intervention and prosthesis removal (Moore et al., 2017; Purrello et al., 2016; Stefani et al., 2012).

Even if the prevalence of methicillin-resistant *S. aureus* (MRSA) in these infections is lower than that of MSSA, these human pathogens are still problematic because they are often associated with antimicrobial resistance, leading to high rates of hospitalization and mortality as well as the burden of associated costs (Gould et al., 2011).

In the assessment of the interaction between *S. aureus* isolates and osteoblasts during PJIs and OM, three events are crucial: adhesion, invasion, and the postinvasion process or internalization. Adhesion of *S. aureus* to host structures is a prerequisite for colonization and disease development and relies on the expression of a large number of cell surface proteins (adhesins) of the microbial surface component recognizing adhesive matrix molecules (MSCRAMM) and of the secretable expanded repertoire adhesive molecules (SERAM) classes. *S. aureus* osteoblast invasion plays a crucial role in the initiation and maintenance of inflammatory immune responses (Sinha & Fraunholz, 2010). Recent studies have demonstrated that *S. aureus* is able to internalize in the osteoblast cytoplasm, and this localization can represent a reservoir of bacteria for chronic disease (Horn, Stelzner, Rudel, & Fraunholz, 2018).

During postinvasion events, *S. aureus* is internalized in osteoblasts via a process that involves actin microfilaments, microtubules, receptor-mediated endocytosis, and activation of signal transduction cascades. Osteoblasts release viable staphylococci, which are then able to reinfect and internalize in new osteoblasts, representing the potential key for prolonged and persistent infections (Garzoni & Kelley, 2009; Josse, Velard, & Gangloff, 2015). Many papers have reported *S. aureus* internalization in osteoblasts considering diverse aspects related to the mechanism of pathogenicity (Jevon et al., 1999), the induction of various responses from the osteoblasts (Josse et al., 2016), and their impact on the interaction between osteoclasts and osteoblasts (Josse et al., 2015).

Furthermore, different cell culture models have been used to study the frequency of internalization of *Staphylococcus* spp. in osteoblasts. These assays involve the use of gentamicin or lysostaphin to eliminate the external and adherent bacterial cells, and the quantification of live bacteria is performed by host cell lysis and plate counting (Jevon et al., 1999; Valour et al., 2013; Wright & Friedland, 2004). As reported in many papers, this method is time-consuming and lacks reproducibility (Trouillet et al., 2011).

Taking into consideration the disadvantages of the cell culture gold standard assay and the heterogeneity of the main Italian *S. aureus* invasive isolates recently described in 2015 (Campanile et al., 2015), we aimed to (a) provide a novel method of detection of intracellular *S. aureus* by analyzing live host cells through imaging flow cytometry (IFC) to strengthen the conventional cell culture method and (b) confirm the reliability and reproducibility of this method validating the different proclivities to persist during cell infection (at 24 hr p.i.) of the main HA-MRSA invasive isolates responsible for bone infections and PJIs, belonging to different epidemic clones.

2 | MATERIAL AND METHODS

2.1 | Strains included in the study

The study sample consisted of 15 invasive MRSA isolates already molecularly characterized by standard genotyping methods internationally recognized as defining MRSA clones, and belonging to ST239-SCC*mec*III, ST5-SCC*mec*II, ST8-SCC*mec*IV, ST228-SCC*mec*I, and ST22-SCC*mec*IVh, three strains for each clone. These strains were selected from a large collection of 640 MRSA strains isolated during an Italian national survey that was carried out in 2012. All the strains were phenotypically and molecularly characterized (Table A1) as previously reported (Bongiorno, Mongelli, Stefani, & Campanile, 2018; Campanile et al., 2015). The invasive isolate ATCC12598 (Cowan ST30-t076; ATCC® Standards Development Organization, LGC Standards S.r.l.) was used as control strain for invasion and persistence assays and for the statistical analysis of the results obtained with the cell culture method and IFC (McPherson et al., 2008).

2.2 | Eukaryotic cell culture preparation

Infection experiments were performed on the human osteosarcoma cell line MG-63 (ATCC® CRL-1427™; Standards Development Organization, LGC Standards S.r.l.). During the expansion period, the cells were grown in 75 cm^2 flasks with modified Eagle's medium (MEM), HEPES, GlutaMAX™ Supplement (cat. No. 42360024, containing 1 g/L D-glucose, GIBCO™; Thermo Fisher Scientific Monza, Italy), supplemented with 10% FBS (fetal bovine serum; cat. No. 16000044, GIBCO™; Thermo Fisher Scientific) and 100 U/ml of penicillin/streptomycin (cat. No. 15070063 GIBCO™; Thermo Fisher Scientific). The cell culture was incubated at 37°C in a humidified atmosphere with 5% CO_2 and 95% air. The medium was changed twice per week. Twenty-four hours before infection 3×10^5 cells were multi-well plated on MEM medium, supplemented with 10% FBS without penicillin/streptomycin and washed twice with 500 µl MEM per well, before the infection step. A single 24-well plate was used for the cell culture method using osmotic lysis, while a single 6-well plate was used for cytofluorimetric analysis. All experiments were performed in triplicate.

2.3 | Evaluation of the frequency of internalization and intracellular persistence in the cell culture model using MG-63 osmotic lysis

The internalization frequency was evaluated in a cell culture model of infection in MG-63 osteoblasts at a multiplicity of infection (MOI) of 100:1, as previously reported (Campoccia et al., 2018). Moreover, to assess the final MOI, we previously tested MG-63 infection with ATCC12598 at 12, 50, 100, and 200 MOI, observing that with 12 and 50 MOI the ability to internalize in nonspecialized cells such as osteoblasts for *S. aureus* was very low, instead, with 200 MOI, MG-63 cultured cells showed phenomena of cytotoxicity.

Bacterial isolates were grown in Brain Heart Infusion broth (BHI; cat. No. CM1135; Oxoid Limited, Thermo Fisher Scientific Inc) at 37°C overnight. The bacterial concentration was evaluated by optical density (OD) at 600 nm. Bacterial suspensions were prepared using MEM supplemented with 10% FBS. MG-63 cultures were infected for 2 and 24 hr in antibiotic-free conditions; extracellular bacterial lysis was carried out for 1 hr at 37°C with 100 mg/ml lysostaphin (cat. No. L7386-15MG; Sigma-Aldrich, Merck KGaA; Figure A1). In addition, before and after lysostaphin treatment, the infected cell cultures were washed with PBS, and the culture medium was changed before the 24-hr incubation.

Estimation of intracellular bacteria was determined 3 hr p.i. to assess the bacterial internalization processes and 24 hr p.i. to assess persistence, by osmotic MG-63 cell lysis, serial dilution plating of the lysate on blood agar plates, incubation at 37°C overnight and CFU/ml counting. The proportion of internalized bacteria/MG-63 cells was calculated considering the MOI, the number of MG-63 cells, and the number of CFUs counted after cell lysis.

2.4 | Evaluation of the bacterial intracellular persistence frequency by imaging cytofluorimetric analysis

Infected cells, prepared as previously described at an MOI of 100:1, were first washed with 1× phosphate-buffered saline (PBS; cat. No. P5493; Sigma-Aldrich, Merck), followed by an incubation step of 3–5 min at 37°C with 0.05% trypsin-EDTA solution (cat. No. T4049; Sigma-Aldrich, Merck), and the cellular suspension was reversibly permeabilized with saponin 0.1% (cat. No. 55,255; Sigma-Aldrich, Merck) in PBS. Saponin interacts with membrane cholesterol, selectively removing it and leaving holes in the membrane. This transient permeabilization does not require cell fixing. After 15 min in saponin, the bacterial cells were labeled with 0.08 μg/ml BODIPY™ FL vancomycin (VBFL; cat. No. V34850; Invitrogen™), the membrane-impermeable green-fluorochrome vancomycin analogue that specifically binds the cell-wall peptidoglycan of Gram-positive bacteria and does not penetrate intact cells. The suspensions were then washed three times with PBS to remove the transient permeabilization and checked under the microscope to be sure that the cells had maintained their cell integrity. The labeled cellular suspension was analyzed by a FlowSight® Imaging Flow Cytometer (Amnis® FlowSight® Millipore, Merck), which quantitatively detects brightfield, darkfield, and fluorescent images with high sensitivity. This instrument acquires up to 12 images simultaneously of each cell or object including brightfield, scatter, and multiple fluorescent images at rates of up to 5,000 objects per second with high photonic sensitivity. Detailed analysis of intensity, location, and colocation of probes is achieved by IDEAS® (Image Data Exploration and Analysis Software), which offers powerful tools for statistically robust analysis of images, as well as standard flow cytometry graphing tools and statistics for hundreds of morphological features in addition to intensity. Acquisition analysis was driven by the powerful INSPIRE® and IDEAS® packages, using the main function of the INSPIRE® program during the acquisition and the IDEAS® Spot Counting analysis during results generation (Amnis, EMD Millipore).

The spots recovered in cytofluorometry imaging (total spots and full cells) were examined in a representative sample of 10,000 events, and we then theoretically normalized the result on a sample of plated cells (300,000 cells/well) and compared the total spots recovered with the whole theoretically internalized sample.

2.5 | Statistical model

Statistical analysis and the relative graphs were made using GraphPad Prism 5 (GraphPad Software Inc.). Statistical significance was assessed using Student's *t* test, both for cell culture methods and cytofluorimetric analyses. The significance threshold was set at p-value ≤ .05 (significant), p-value ≤ .01 (highly significant), and p-value ≤ .001 (extremely significant). In the cell culture assays, the colonies and the spots were counted and the data were plotted and represented as the mean ± standard deviation (*SD*) of the percentage of recovered internalized bacteria with respect to inoculated bacteria versus ATCC12598, obtained in at least two independent experiments performed in triplicate. In the flow cytometric assays, the number of single-cell events analyzed was never less than 9,980 cells out of 10,000 events at the outset.

3 | RESULTS

3.1 | Evaluation of the invasion of different MRSA genetic backgrounds in MG-63 human osteoblasts in the cell culture model

The invasiveness of different MRSA genetic backgrounds was evaluated by the cell culture infection model, using 15 invasive HA-MRSA strains belonging to the five different epidemic clones included in the study (ST239-SCC*mec*III, ST5-SCC*mec*II, ST8-SCC*mec*IV, ST228-SCC*mec*I, and ST22-SCC*mec*IVh, 3 strains for each clone) at 3 hr postinfection (p.i.). The rates of infection (CFU/infected MG-63) and ±*SD* recovered at 3 hr were **ATCC12598-ST30** $3.2 \times 10^6 \pm 3.7 \times 10^5$; **ST239-SCC*mec*III** $2.7 \times 10^6 \pm 2.8 \times 10^4$; **ST5-SCC*mec*II** $3.3 \times 10^6 \pm 5.8 \times 10^5$; **ST8-SCC*mec*IV** $2.4 \times 10^6 \pm 1.4 \times 10^5$; **ST228-SCC*mec*I** $2.8 \times 10^6 \pm 6.3 \times 10^5$; and **ST22-SCC*mec*IVh** $4.3 \times 10^6 \pm 6.8 \times 10^5$.

Three hours after the infection process, no substantial differences in the number of intracellular bacteria were observed, indicating that all analyzed strains had an internalization rate similar to one of the invasive strain ATCC12598 (Figure A2 and Table A2).

3.2 | Evaluation of the bacterial intracellular persistence frequency by imaging flow cytometric analysis—IFC

3.2.1 | Construction of the analysis template on ATCC12598

The frequencies of intracellular bacterial cells within MG-63 osteoblasts were evaluated after selective VBFL-bacterial labeling by the novel imaging flow cytometric approach using the new generation Amnis® FlowSight® Imaging Flow Cytometer.

We acquired 10,000 events for each sample and as quality control, the stained and not stained bacterial suspension to exclude autofluorescence; a negative control of infected, but not permeabilized cells, was also acquired to guarantee the exclusively intracellular localization of green spots. For each experiment, a sample of unmarked cells was acquired to exclude cellular autofluorescence or false-negative results.

The acquisition analysis was driven by INSPIRE® and IDEAS® packages. The size of every single event was established during the acquisition phase employing the scatter plot set utilizing the diameter as a parameter. This portion was referred to as a single-cell event. This first filter step was necessary to eliminate debris and cell aggregates. The 488 nm and 642 nm lasers were set to an intensity power of 30 mW for all experiments. Extracellular bacteria were efficiently disrupted by lysostaphin treatment, confirmed by the absence of fluorescence outside the MG-63 cells, in all the experiments conducted for all the samples included in the study (Figure 1).

Using IDEAS, population statistics and imaging were completely integrated; all results obtained were subdivided into two consequential steps: (a) The first analysis was performed on scatter plots using the Size Scatter in order to separate cells by size and fluorescence intensity, obtaining two large groups: labeled and unlabeled cells. On these two groups, the percentage of internalized bacteria were calculated; and (b) the second analysis was performed on a labeled cell subgroup, using the "spot counting" tool, that sets the fluorescence channel and acquires at least 20 individual events within the high and low spot categories. Evaluation of internalized bacteria by spot counting, according to the subcategories, the software identifies "N" subgroups divided by an increasing number of spots, and each subgroup was analyzed for mean fluorescence intensity (Figure 2).

3.2.2 | Analysis of the sample

Figure 3a shows the percentage of full versus empty MG-63 cells, with respect to the control strain. ATCC12598 persisted inside 51% of MG-63 at 24 hr p.i., and the same ability to persist was found in clones ST239 (47.82%) and ST22 (50.55%). The other clones analyzed were less able to persist inside MG-63, and in particular, ST5 26.59% (p = .038), ST228 20.25% (p = .0120), and ST8 19.52% (p = .0054; Table A3). Detailed data for every single strain included in the sample are reported in Figure A3 and Table A4.

These results of the internalization described above derive from Figure 3b in which we defined clones with 0 spots, 1 to 5, and over 6 spots. For the first category, 0 spots inside MG-63 cells (empty cells), the sample can be divided into two major groups, the first group included strains belonging to ST5, ST228, and ST8 and showed a percentage of empty cells ranging from 78.8% to 80% (in particular, ST5: 78.80 ± 2.46%; ST8: 79.80 ± 2.46; ST228: 80 ± 7.65%); and the second group included strains belonging to ST239, ST22, and ATCC12598 and showed about 51.5% of empty cells (in particular, ST239: 52.17 ± 7.65; ST22: 51.11 ± 5.76; ATCC12598: 51.92 ± 1.15). For the second category, 1 to 5 spots inside MG-63 cells, we found the same two groups, the first one (ST5, ST228, and ST8) showed a percentage of about 19.5% cells (in particular, ST5: 19.87 ± 2.05%; ST8: 19.49 ± 3.76; ST228: 19.35 ± 7.42%) and the second one showed a percentage ranging from 41.9% to 45% (in particular, ST239: 42.33 ± 3.4; ST22: 45.12 ± 4.16; ATCC12598: 41.97 ± 0.36). The third category, MG-63 with more than six spots inside, were less represented: 0.64 ± 0.33% for ST228, 0.71 ± 3.76% for ST8, and 1.33 ± 2.05% for ST5. Moreover, in this case, ST22 (3.77 ± 1.6%) and ST239 (5.8 ± 2.2%) showed values similar to ATCC12598 (6.11 ± 0.78%).

3.3 | Evaluation of the intracellular persistence of different MRSA genetic backgrounds in MG-63 human osteoblasts in the cell culture model

After assessing the internalization process, the proclivity to persist inside MG-63 was examined at 24 hr p.i., as reported in Figure 4a.

Although not statistically significant, the levels of intracellular bacteria changed at 24h after the infection process; in particular, ST239 (p = .99), ST8 (p = 1), and ST22 (p = .5585) showed a greater ability to persist within MG-63 osteoblasts, with respect to ST5 (p = .169) and ST228 (p = .4881) versus the ATCC12598 invasive control strain (Table A5).

3.4 | Cell culture methods versus imaging flow cytometric analysis

The rate of persistence at 24 hr was evaluated comparing the data obtained with the conventional cell culture method and data obtained with IFC and was carried out considering the number of intracellular spots per bacteria cell, as shown in Figure 4b, for each MRSA genetic background. Statistical analysis was conducted versus ATCC12598, and the percentage of internalization ± *SD*, p-values, and 95% confidence intervals are reported in Table A6.

Comparing the data set obtained with the two techniques, the rate of persistence of clones of ST239 and ST22 in MG-63 cells was

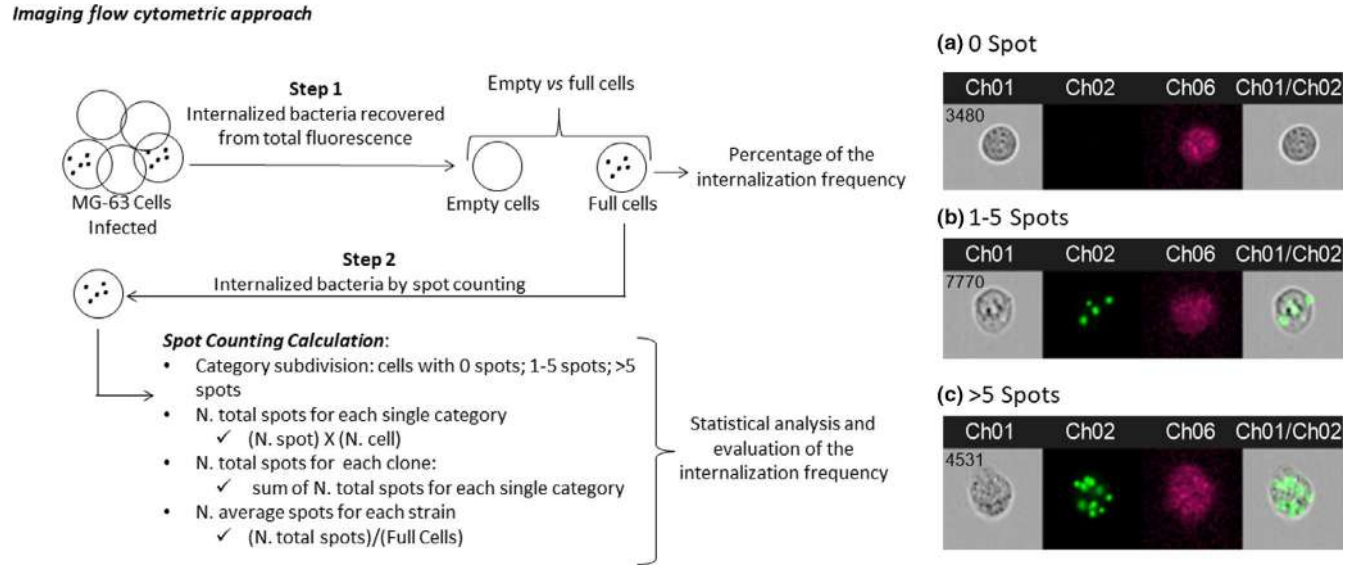

FIGURE 1 Images obtained by FlowSight® Imaging Flow Cytometer (Amnis® FlowSight® Millipore, Merck KgaA, Darmstadt, Germany), acquiring 10,000 events per sample: (a) MG-63, without spots inside the cell; (b) a single MG-63 cell with four spots inside (each spot was considered as a single bacterial cell); and (c) a single MG-63 cell with >5 spots. CH1 brightfield; CH2 band nM 505–560; CH6 Side Scatter (SSC) 785 nM; CH1/CH2 merge brightfield and 505–560 nM band

similar to that of ATCC12598; clones ST5 and ST228 were less able to persist. The only exception was clone ST8 that showed a result comparable to ATCC12598 by the cell culture method; however, this result was not confirmed by IFC.

The overall trend in all clones of the two techniques was the same; moreover, the IFC method was more sensitive as demonstrated by the *SD* values that were lower with respect to the conventional culture method.

4 | DISCUSSION AND CONCLUSIONS

Staphylococcus aureus is considered an extracellular pathogen; moreover, strains belonging to different genetic backgrounds have been known to develop an aptitude to invade and survive in phagocytic and nonphagocytic cells, and this ability can play a significant role in related diseases. Host cell invasion contributes to protecting *S. aureus* from antibiotics and the immune response and establishes a latent reservoir of bacteria that can be responsible, in particular in osteomyelitis, for the pathogenesis of this chronic and recurrent infection (Tuchscherr et al., 2011).

Staphylococcus aureus/host cell interaction is strongly conditioned by both host cell type and *S. aureus* isolate; in fact, the ability to internalize and survive in osteoblasts exhibits strain-dependent differences (Strobel et al., 2016).

In our study, different clinical MRSA strains, from invasive infections and belonging to the main worldwide HA-MRSA genetic backgrounds, were compared for their persistence ability. Our results highlighted the heterogeneity of the different clones to persist during cell infection.

The results obtained by the cell culture method demonstrated that initially (3 hr p.i.) all clones were internalized in MG-63 human osteoblasts, supporting the fact that a variety of genetic backgrounds are capable of invading host cells, but were able to differentially resist over 24 hr p.i. as demonstrated by the variable slight increase or decrease in CFU recovery; these results also suggest that osteoblasts could represent intracellular persistence niches in which *S. aureus* strains persist intracellularly and possibly replicate for a longer infection time. Our observation was supported by a previous study in which the ability of *S. aureus* to survive intracellularly for up to 7 days in osteoblasts was demonstrated (Hamza & Li, 2014).

Using the cell culture assay, we found a wide standard deviation among the different experiments for the same isolates, resulting from a large number of factors that can influence this experiment. Moreover, comparing the internalization rate of the different clones with the standard strain, no statistical significance in the ability to internalize and survive within osteoblasts was found.

The data from routine cell culture assays were improved with those obtained by the more sensitive and reliable IFC method that, together with specialized analytic software, combines the statistical power and fluorescence sensitivity of standard flow cytometry with the spatial resolution and quantitative morphology of digital microscopy, to accurately address cell counting and internalization scoring in intracellular infections (Haridas, Ranjbar, Vorobjev, Goldfeld, & Barteneva, 2017).

Fully integrated IFC and statistical analyses, with the same conditions of internalization (24 hr), allowed us to better standardize the experiments: This method was more sensitive, allowing the acquisition of a very high number of events, and was reproducible for every single sample. Our results indicated that, despite the bacterial invasion rates reflected in the trend of the cell culture data, IFC assays detected important differences that would otherwise have been undetectable.

All isolates belonging to ST5-II, ST8-IV, and ST228-I showed a statistically significant lower aptitude to intracellularly subsist

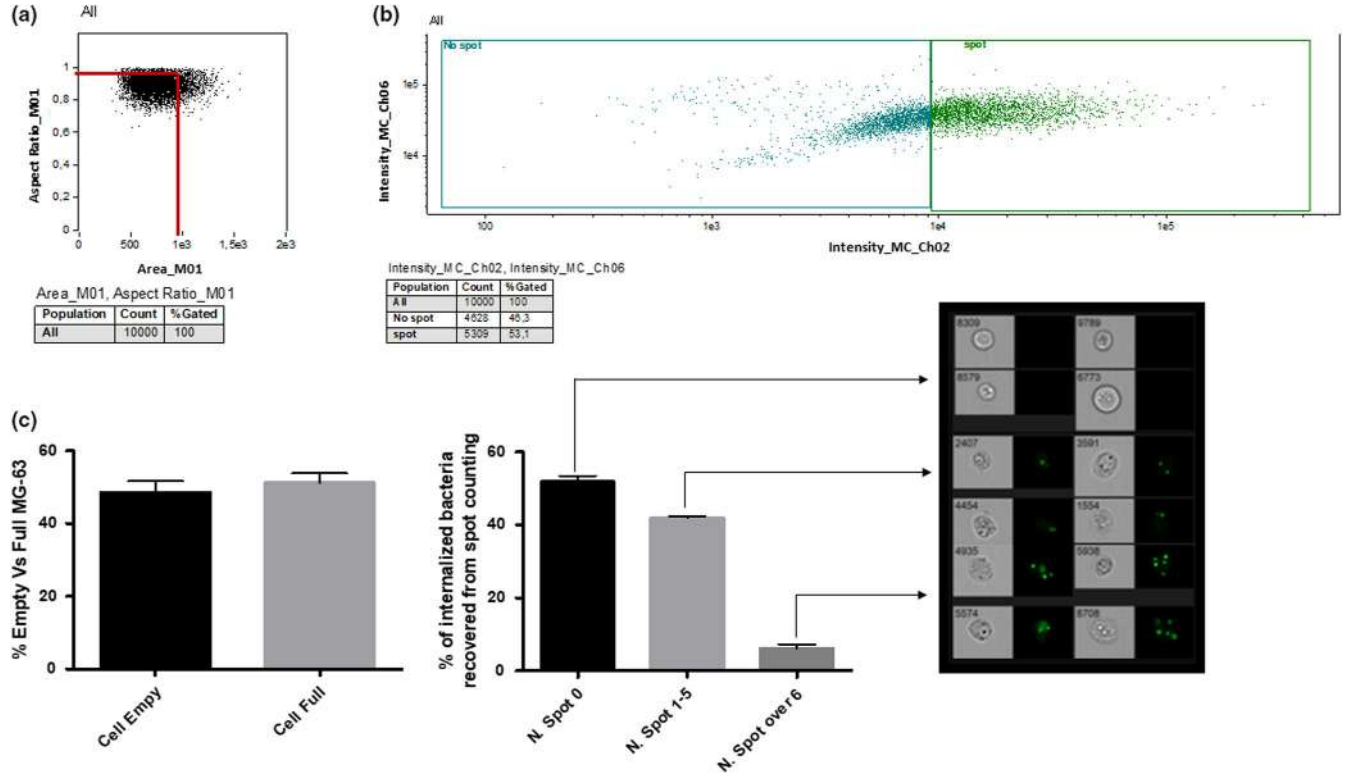

FIGURE 2 The layout used for the analysis of internalized *S. aureus* during acquisition using IFC. The layout was created for the analysis of ATCC12598 after 24 hr postinternalization in MG-63 and then applied to every single analysis for all internalization events: (a) Elimination of all events that had a noncircular shape (surface tension is responsible for the shape of liquid droplets. Although easily deformed, droplets of water tend to be pulled into a spherical shape by the cohesive forces of the surface layer. The spherical shape minimizes the necessary "wall tension" of the surface layer according to La Place's law. The cortical tension pulls the cell into a spherical shape, similar to surface tension pulling a water drop into a sphere), identifiable by the ratio between the area and the diameter, the ideal ratio of a spherical cell between width and length is 1, the graph identifies most of the events considered as "single cells" around this value. This step allowed us to acquire 10,000 events representing individual cells, eliminating debris and aggregates that would have distorted the subsequent analysis; (b) Comparison of the fluorescence intensity of the channel (in this example Ch02) corresponding to the labeled cells versus size scatter signal (Ch06). In this step, we have the creation of a cellular cloud characterized by size-shape and fluorescence quantity that divided the total amount of cells into two large groups that only differ in the amount of fluorescence. This raw analysis step precedes the more precise spot counting step; (c) Final analysis using IDEAS software that was able (after setting parameters such as Spot Low cells and High Spot cells) to identify empty and full cells (shown in the first graph), and divide the event categories by the number of "fluorescent spots." For each identified category, it was possible to evaluate the amount of fluorescence and the average fluorescence. The software organized every single gallery (deriving from a category of "number of spots" of the spot counting) based on various parameters. Each gallery was evaluated for minima and maxima fluorescence intensity, evaluating the relative accuracy of the number of spots corresponding to the category assigned by the Spot Counting

(demonstrated by both the total number of spots and the number of infected cells). All ST239-III and ST22-IVh isolates had intracellular frequencies equal to or greater than those of the reference ATCC12598 strain, suggesting their possible role as invasive and persistent clones responsible for chronic and recurrent infections.

Statistically relevant results obtained by imaging flow cytometry assays allowed us to understand that the intracellular rates did not depend on the number of bacterial cells that manage to enter/replicate inside a single MG-63 osteoblast, but on the total number of cells that were infected. The ability to internalize and persist inside osteoblasts seems, therefore, not only related to the clone but to other factors that deserve to be investigated.

Furthermore, our observations have been supported by the increase, in the last ten years, of strains belonging to ST239 and ST22 associated with bacteremia and PJIs (Coombs, Daley, Lee, Pang, 2019; Jain, Chowdhury, Datta, Chowdhury, & Mukhopadhyay, 2019; Peng et al., 2019) and probably associated with prophage-mediated virulence determinants (*sas*X), crucial for colonization, immune evasion, and host cell invasion (Bakthavatchalam, Triplicane Dwarakanathan, Munusamy, Jennifer, & Veeraraghavan, 2019).

This study presents some limitations that should be mentioned: whole-genome sequencing analysis, for detecting different genetic variants and gene-expression studies, and for determining whether a particular gene or set of genes is responsible for the specific internalization behavior, was not performed. The pathogenic and molecular characteristics that enhance the aptitude to internalize in, escape from, or persist within host cells undoubtedly reside in the differential expression of regulatory and virulence genes (Horn et al., 2018; Josse et al., 2015).

The current study contributes to our understanding of the differential interaction between osteoblasts and invasive MRSA strains

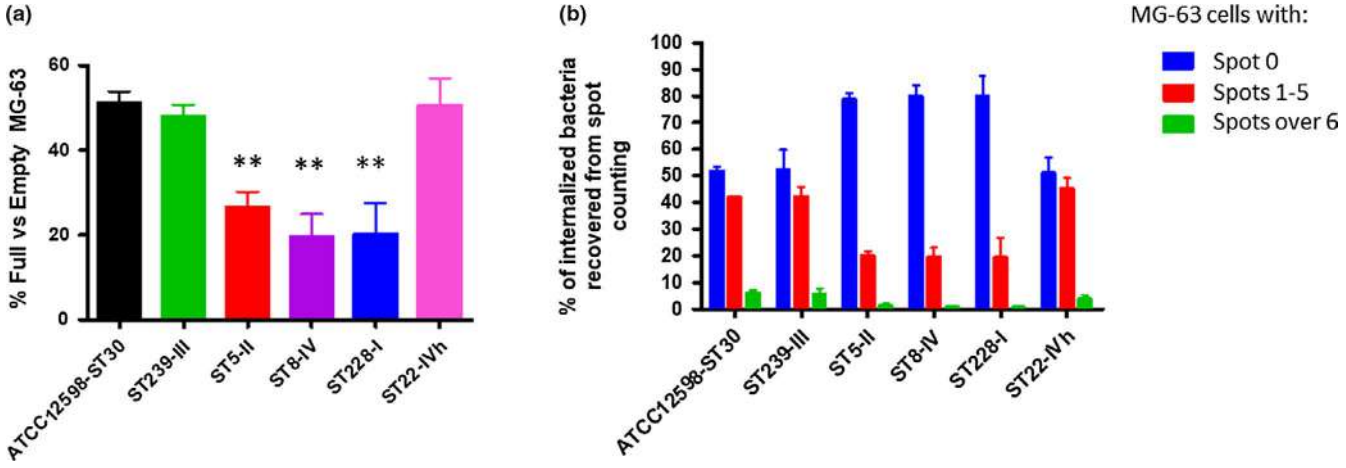

FIGURE 3 (a) Evaluation of the internalization frequency by IFC. After 24 hr p.i. at an MOI of 100:1, external and adherent bacteria were removed by lysostaphin treatment. The MG-63 cells infected with the different strains were stained with the membrane-impermeable fluorochrome VBFL and analyzed on a flow cytometer (Amnis FlowSight Millipore), acquiring 10,000 events per sample. The graph reports the percentage of spots for cell ± *SD* for each strain for three different experiments. Statistical significative *p*-value ≤ .05 *; highly significative ≤.01**; extremely significative ≤.001***. (b) Invasion rate of MRSA strains from different genetic backgrounds. After 2 hr of infection at an MOI of 100:1, external and adherent bacteria were removed by lysostaphin treatment for 1 hr. The infected MG-63 cells were lysed at 24 hr postinfection after a lysostaphin treatment for 1 hr. The MG-63 cells infected with the different strains were osmotically lysed, and the number of intracellular bacteria was determined by plating serial dilutions of the lysates on blood agar plates and counting the colonies grown after overnight incubation. The graph reports the mean ± *SD* for each clone for three different experiments

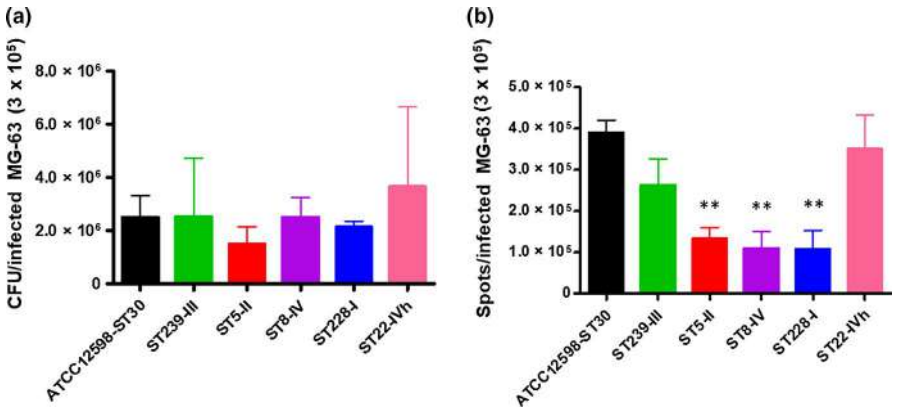

FIGURE 4 Evaluation of the persistence frequency by IFC evaluation, after 24 hr p.i. at an MOI of 100:1, external and adherent bacteria were removed by lysostaphin treatment. The MG-63 cells infected with the different strains were stained with the membrane-impermeable fluorochrome VBFL and analyzed on a flow cytometer (Amnis FlowSight Millipore), acquiring 10,000 events per sample. (a) The graph shows the distribution of spots corresponding to the category assigned by the Spot Counting, for each clone. (b) The graph shows the percentage of full versus empty cells, recovered from spot counting. The graph reports the percentage of spots for cell ± *SD* for each strain for three different experiments. Statistical significative *p*-value ≤ .05*; highly significative ≤ .01**; extremely significative ≤ .001***

belonging to different genetic backgrounds. By means of an imaging flow cytometry-based approach, we demonstrated that internalization is a pathophysiological pathway of some MRSA depending on the total number of cells infected and not on the bacterial cells that enter each osteoblast. Furthermore, even if our strains were not homogeneous in terms of genetic backgrounds and virulence factors, ST22-IVh and ST239-III showed higher intracellular persistence in host cells, making them more prone to developing chronic and recurrent infections. We believe that our study provides additional information useful to predict the proclivity of some staphylococcal clones associated with recurrent and chronic infections, to invade, internalize, and persist within human cells, with respect to others.

ACKNOWLEDGMENTS

Some of the results of this study were presented at the 29th ECCMID (O0927) and the 44th Italian Society of Microbiology (SIM) congress (P127). We would like to thank professor V. Cardile and A. Graziano, and the BRIT laboratory at the University of Catania (Italy) for valuable technical assistance and laboratories and in particular to S. Grimaldi. The manuscript was partially supported by a research grant project number PRIN2017SFBFER form Minister of Research (MIUR), Italy; a research grant for a private company; a research grant entitled "Identification of cancer driver genes for novel diagnostics and therapeutic strategies—Piano per la ricerca 2016-2018—Linea di intervento 2—University of Catania, Dept. of Biomedical

and Biotechnological Sciences." We also wish to thank the Scientific Bureau of the University of Catania for language support.

CONFLICT OF INTERESTS

None declared.

AUTHOR CONTRIBUTIONS

Dafne Bongiorno equally contributed to conceptualization, data curation, formal analysis, methodology, validation, writing–original draft, and writing–review and editing; Nicolò Musso equally contributed to conceptualization, data curation, formal analysis, methodology, software, validation, and writing–original draft; Lorenzo Lazzaro equally contributed to methodology and made supporting role in validation; Gino Mongelli equally contributed to investigation and methodology, and made supporting role in validation; Stefania Stefani equally contributed to funding acquisition, resources, supervision, validation, and writing–review and editing; Floriana Campanile equally contributed to conceptualization, funding acquisition, project administration, supervision, writing–original draft, and writing–review and editing.

ETHICS STATEMENT

None required.

DATA AVAILABILITY STATEMENT

All data are provided in full in the results section of this paper and in the Appendices 1 and 2.

ORCID

Dafne Bongiorno https://orcid.org/0000-0002-8672-0484
Nicolò Musso https://orcid.org/0000-0003-2451-1158
Gino Mongelli https://orcid.org/0000-0003-0976-2936
Stefania Stefani https://orcid.org/0000-0003-1594-7427
Floriana Campanile https://orcid.org/0000-0002-8405-5425

REFERENCES

Bakthavatchalam, Y. D., Triplicane Dwarakanathan, H., Munusamy, E., Jennifer, L., & Veeraraghavan, B. (2019). A distinct geographic variant of *sas*X in methicillin-resistant *Staphylococcus aureus* ST239 and ST368 lineage from South India. *Microbial Drug Resistance*, *25*, 413–420.

Bongiorno, D., Mongelli, G., Stefani, S., & Campanile, F. (2018). Burden of rifampicin- and methicillin-resistant *Staphylococcus aureus* in Italy. *Microbial Drug Resistance*, *24*, 732–738.

Campanile, F., Bongiorno, D., Perez, M., Mongelli, G., Sessa, L., Benvenuto, S., … Stefani, S. (2015). Epidemiology of *Staphylococcus aureus* in Italy: First nationwide survey. *Journal of Global Antimicrobial Resistance*, *3*, 247–254.

Campoccia, D., Montanaro, L., Ravaioli, S., Cangini, I., Testoni, F., Visai, L., & Arciola, C. R. (2018). New parameters to quantitatively express the invasiveness of bacterial strains from implant-related orthopaedic infections into osteoblast cells. *Materials*, *11*, 550. https://doi.org/10.3390/ma11040550

Coombs, G. W., Daley, D. A., Lee, Y. T., & Pang, S. (2019). Australian Group on Antimicrobial Resistance (AGAR) Australian *Staphylococcus aureus* Sepsis Outcome Programme (ASSOP) Annual Report 2017. *Communicable Diseases Intelligence*, *16*, 43. https://doi.org/10.33321/cdi.2019.43.43

Garzoni, C., & Kelley, W. L. (2009). *Staphylococcus aureus*: New evidence for intracellular persistence. *Trends in Microbiology*, *17*, 59–65. https://doi.org/10.1016/j.tim.2008.11.005

Gould, I. M., Gauda, R., Esposito, S., Gudiol, F., Mazzei, T., & Garau, J. (2011). Management of serious methicillin-resistant *Staphylococcus aureus* infection: What are the limits? *International Journal of Antimicrobial Agents*, *37*, 202–209.

Hamza, T., & Li, B. (2014). Differential responses of osteoblasts and macrophages upon *Staphylococcus aureus* infection. *BMC Microbiology*, *14*, 207. https://doi.org/10.1186/s12866-014-0207-5

Haridas, V., Ranjbar, S., Vorobjev, I. A., Goldfeld, A. E., & Barteneva, N. S. (2017). Imaging flow cytometry analysis of intracellular pathogens. *Methods*, *112*, 91–104. https://doi.org/10.1016/j.ymeth.2016.09.007

Horn, J., Stelzner, K., Rudel, T., & Fraunholz, M. (2018). Inside job: *Staphylococcus aureus* host-pathogen interactions. *International Journal of Medical Microbiology*, *308*, 607–624. https://doi.org/10.1016/j.ijmm.2017.11.009

Jain, S., Chowdhury, R., Datta, M., Chowdhury, G., & Mukhopadhyay, A. K. (2019). Characterization of the clonal profile of methicillin resistant *Staphylococcus aureus* isolated from patients with early post-operative orthopaedic implant-based infections. *Annals of Clinical Microbiology and Antimicrobials*, *18*, 8.

Jevon, M., Guo, C., Ma, B., Mordan, N., Nair, S. P., Harris, M., … Meghji, S. (1999). Mechanisms of internalization of *Staphylococcus aureus* by cultured human osteoblasts. *Infection and Immunity*, *67*, 2677–2681. https://doi.org/10.1128/IAI.67.5.2677-2681.1999

Josse, J., Guillaume, C., Bour, C., Lemaire, F., Mongaret, C., Draux, F., … Gangloff, S. C. (2016). Impact of the maturation of human primary bone-forming cells on their behaviour in acute or persistent *Staphylococcus aureus* infection models. *Frontiers in Cellular and Infection Microbiology*, *6*, 64.

Josse, J., Velard, F., & Gangloff, S. C. (2015). *Staphylococcus aureus vs* Osteoblast: Relationship and consequences in osteomyelitis. *Frontiers in Cellular and Infection Microbiology*, *5*, 85. https://doi.org/10.3389/fcimb.2015.00085

McPherson, J. C., Runner, R. R., Shapiro, B., Walsh, D. S., Stephens-DeValle, J., & Buxton, T. B. (2008). An acute osteomyelitis model in traumatized rat tibiae involving sand as a foreign body, thermal injury, and microbial contamination. *Comparative Medicine*, *58*, 369–374.

Moore, A. J., Whitehouse, M. R., Gooberman-Hill, R., Heddington, J., Beswick, A. D., Blom, A. W., & Peters, T. J. (2017). A UK national survey of care pathways and support offered to patients receiving revision surgery for prosthetic joint infection in the highest volume NHS orthopaedic centres. *Musculoskeletal Care*, *15*, 379–385. https://doi.org/10.1002/msc.1186

Peng, K. T., Huang, T. Y., Chiang, Y. C., Hsu, Y. Y., Chuang, F. Y., Lee, C. W., & Chang, P. J. (2019). Comparison of methicillin-resistant *Staphylococcus aureus* Isolates from cellulitis and from osteomyelitis in a Taiwan Hospital, 2016–2018. *Journal of Clinical Medicine*, *8*, 816.

Purrello, S. M., Garau, J., Giamarellos, E., Mazzei, T., Pea, F., Soriano, A., & Stefani, S. (2016). Methicillin-resistant *Staphylococcus aureus* infections: A review of the currently available treatment options. *Journal of Global Antimicrobial Resistance*, *7*, 178–186.

Sinha, B., & Fraunholz, M. (2010). *Staphylococcus aureus* host-cell invasion and post-invasion events. *International Journal of Medical Microbiology*, *300*, 170–175. https://doi.org/10.1016/j.ijmm.2009.08.019

Stefani, S., Chung, D. R., Lindsay, J. A., Friedrich, A. W., Kearns, A. M., Westh, H., & Mackenzie, F. M. (2012). Meticillin-resistant *Staphylococcus aureus* (MRSA): Global epidemiology and harmonisation of typing methods. *International Journal of Antimicrobial Agents*, *39*, 273–282. https://doi.org/10.1016/j.ijantimicag.2011.09.030

Strobel, M., Pförtner, H., Tuchscherr, L., Völker, U., Schmidt, F., Kramko, N., … Niemann, S. (2016). Post-invasion events after infection with *Staphylococcus aureus* are strongly dependent on both the host-cell type and the infecting *S. aureus*strain. *Clinical Microbiology & Infection*, *22*, 799–809.

Trouillet, S., Rasigade, J. P., Lhoste, Y., Ferry, T., Vandenesch, F., Etienne, J., & Laurent, F. (2011). A novel Flow Cytometry-based assay for the quantification of *Staphylococcus aureus* adhesion to and invasion

of eukaryotic cells. *Journal of Microbiological Methods*, *86*, 145–149. https://doi.org/10.1016/j.mimet.2011.04.012

Tuchscherr, L., & Löffler, B. (2016). *Staphylococcus aureus* dynamically adapts global regulators and virulence factor expression in the course from acute to chronic infection. *Current Genetics*, *62*, 15–17.

Tuchscherr, L., Medina, E., Hussain, M., Völker, W., Heitmann, V., Niemann, S., … Löffler, B. (2011). *Staphylococcus aureus* phenotype switching: An effective bacterial strategy to escape host immune response and establish a chronic infection. *EMBO Molecular Medicine*, *3*, 129–141.

Valour, F., Trouillet-Assant, S., Rasigade, J. P., Lustig, S., Chanard, E., Meugnier, H., … Lyon BJI Study Group (2013). *Staphylococcus epidermidis* in orthopedic device infections: The role of bacterial internalization in human osteoblasts and biofilm formation. *PLoS ONE*, *28*(8), e67240. https://doi.org/10.1371/journal.pone.0067240

Wright, K. M., & Friedland, J. S. (2004). Regulation of chemokine gene expression and secretion in *Staphylococcus aureus*-infected osteoblasts. *Microbes and Infection*, *6*, 844–852.

How to cite this article: Bongiorno D, Musso N, Lazzaro LM, Mongelli G, Stefani S, Campanile F. Detection of methicillin-resistant *Staphylococcus aureus* persistence in osteoblasts using imaging flow cytometry. *MicrobiologyOpen*. 2020;9:e1017. https://doi.org/10.1002/mbo3.1017

APPENDIX 1

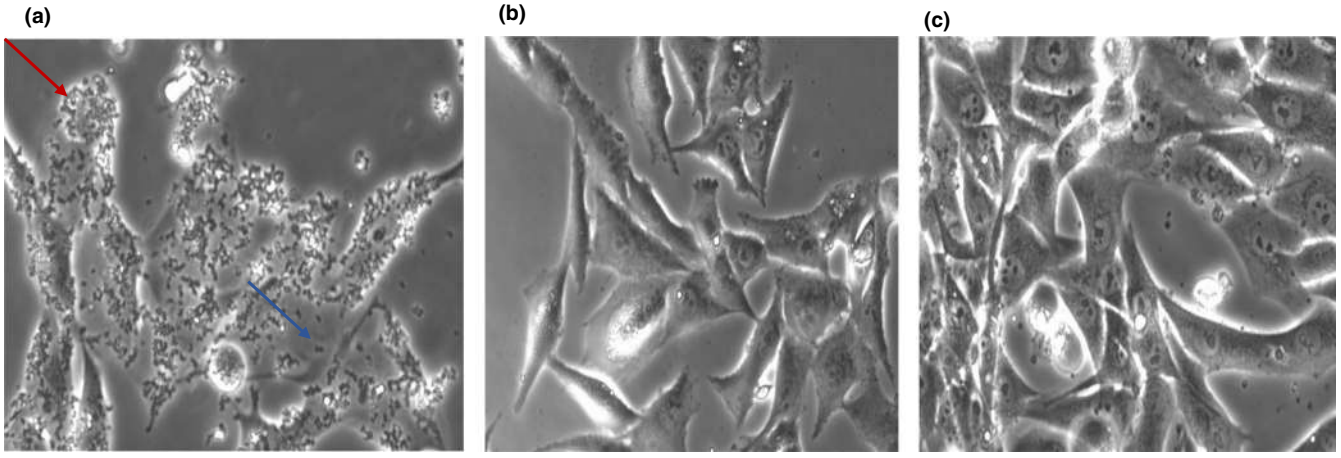

FIGURE A1 Image obtained with Leica DMI 4,000 20× (a, b and c). (a) MG-63 after 1h of infection with 7SA-ST8-SCC*mec*IV, bacterial cells were present all around the MG-63 cells (red arrow) and in the cell culture space between MG-63 cells (blue arrow); (b) after 2 hr of infection and 1 hr of lysostaphin treatment, there were no bacteria in cell culture spaces between MG-63 cells, and (c) the MG-63 cell culture after 24 hr of infection

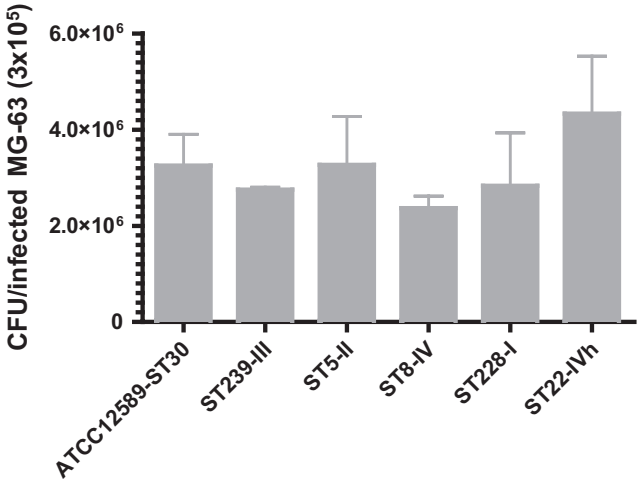

FIGURE A2 Invasion rate of MRSA strains from different genetic backgrounds. After 2 hr of infection at an MOI of 100:1, external and adherent bacteria were removed by lysostaphin treatment for 1 hr. The MG-63 cells infected with the different strains were osmotically lysed, and the number of intracellular bacteria was determined by plating serial dilutions of the lysates on blood agar plates and counting the colonies grown after overnight incubation at 37°C. The graph reports the mean ± *SD* for each clone for two different experiments

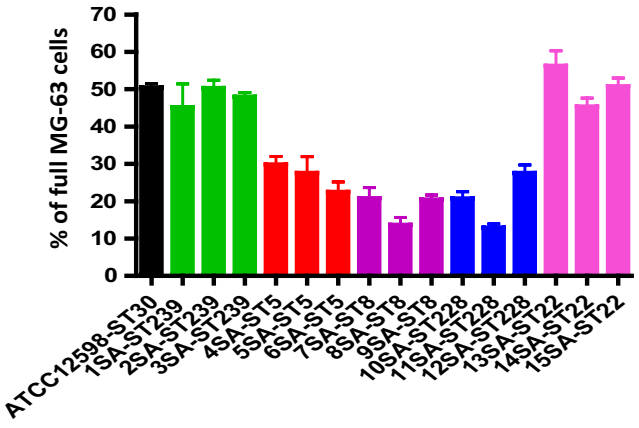

FIGURE A3 Evaluation of the internalization frequency by IFC. At 24 hr p.i. at an MOI of 100:1, external and adherent bacteria were removed by lysostaphin treatment. The MG-63 cells infected with the different strains were stained with the membrane-impermeable fluorochrome VBFL and analyzed on a flow cytometer (Amnis FlowSight Millipore), acquiring 10,000 events per sample. The graph reports the average amount of spots per cell ± *SD* for each strain for three different experiments

APPENDIX 2

TABLE A1 The table reports the phenotypical and molecular characteristics of the sample included in the study

LAB CODE	ST-SCC*mec*-Spa type	Source	FOX	CN	DA	E	CIP	TE	SXT	K	RD	BPR	DAL	CPT	LNZ	DPT	TGC	FU	VA	TC	GRD
1SA	239-III- t030	Wound	R	R	R	R	S	R	S	R	>32	2	0.125	2	2	1	0.25	>256	0.5	0.25	VSSA
2SA	241-III-t037	Wound	R	R	Ri	R	R	R	R	R	2	2	0.125	2	2	0.5	0.25	>256	1	2	VSSA
3SA	239-III-t037	Blood	R	R	Ri	R	R	R	R	R	2	1	0.25	2	2	1	0.25	>256	1	0.5	VSSA
4SA	5-II-t002	Blood	R	R	Ri	R	R	R	S	S	16	4	0.125	4	4	0.5	0.5	4	1	2	VSSA
5SA	5-II-t2154	Blood	R	R	S	R	R	R	S	R	>32	2	0.012	4	32	0.5	0.5	>256	1	0.5	hVISA
6SA	5-II-t002	CVC	R	S	R	R	R	S	S	R	0.008	4	0.125	2	1	1	0.125	0.064	1	0.5	hVISA
7SA	8-IV-t008	Hip fistula	R	R	R	R	R	R	S	R	>32	2	0.125	2	4	1	0.125	0.064	2	2	hVISA
8SA	8-IVc-t008	Bronchial	R	S	S	S	R	S	S	S	0.008	2	0.125	2	0.5	0.5	0.125	0.125	1	1	VSSA
9SA	8-IVc-t008	Bronchial	R	R	S	R	R	S	S	R	0.016	1	0.064	1	0.5	0.5	0.125	0.125	2	0.5	hVISA
10SA	228-I-t041	Blood	R	R	R	R	R	S	S	R	>32	2	0.125	1	8	1	0.125	0.125	1	1	VSSA
11SA	228-I-t041	Knee biopsy	R	R	R	R	R	I	S	R	2	2	0.064	4	2	0.5	0.125	0.064	2	1	hVISA
12SA	228-I-t001	CVC	R	R	Ri	R	R	S	S	R	0.016	2	0.064	2	0.5	0.5	0.125	0.125	1	2	VSSA
13SA	22-IVh-t032	Blood	R	R	S	S	R	R	S	R	>32	0.5	0.125	1	0.5	0.5	0.06	0.125	1	0.25	VSSA
14SA	22-IVh-t032	Blood	R	S	Ri	R	R	S	S	S	0.008	1	0.064	1	1	1	0.125	0.064	0.5	0.25	VSSA
15SA	22-IVh-t902	Blood	R	S	Ri	R	S	R	S	S	>32	1	0.125	0.5	2	2	0.064	0.125	1	0.25	VSSA

Abbreviations: FOX, cefoxitin; CN, gentamicin; DA, clindamycin; E, erythromycin; CIP, ciprofloxacin; TE, tetracycline; SXT, trimethoprim/sulfamethoxazole; K, kanamycin; RD, rifampin; BPR, ceftobiprole; DAL, dalbavancin; CPT, ceftaroline; LNZ, linezolid; DPT, daptomycin; TGC, tigecycline; FU, fusidic acid; VA, vancomycin; TC, teicoplanin; GRD, MIC test strip glycopeptide resistance detection; Ri, Inducible clindamycin resistance; clone characterization by means of: ST, Sequence Type; SCC*mec*, Staphylococcal Cassette Chromosome *mec*; *spa* type, staphylococcal protein A.

TABLE A2 The statistical analysis relative to strain invasiveness was performed by comparing the rate of infection of each strain with the rate of infection of ATCC12598 as control for cell culture method at 3 hr p.i., using *t* test, *p* value and 95% of confidence

t Test	ATCC12598-ST30	ST239-SCCmecIII	ST5-SCCmecII	ST8-SCCmecIV	ST228-SCCmecI	ST22-SCCmecIVh
Rate of Infection CFU/infected MG-63	$3.2 \times 10^6 \pm 3.7 \times 10^5$	$2.7 \times 10^6 \pm 2.8 \times 10^4$	$3.3 \times 10^6 \pm 5.8 \times 10^5$	$2.4 \times 10^6 \pm 1.4 \times 10^5$	$2.8 \times 10^6 \pm 6.3 \times 10^5$	$4.3 \times 10^6 \pm 6.8 \times 10^5$
p value	—	.2548	.9819	.0932	.6016	.2394
95% confidence interval	—	-1.545×10^6 to 5.455×10^5	-1.904×10^6 to 1.937×10^6	-2.001×10^6 to 2.34×10^5	-2.461×10^6 to 1.627×10^6	-1.095×10^6 to 3.26×10^6

TABLE A3 The statistical analysis relative to strain invasiveness was performed by comparing the rate of infection of each strain with the rate of infection of ATCC12598 as control for cell culture method at 3 hr p.i., using *t* test, *p* value and 95% of confidence

t Test	ACTT12598-ST30	ST239-SCCmecIII	ST5-SCCmecII	ST8-SCCmecIV	ST228-SCCmecI	ST22-SCCmecIVh
% of internalization ± *SD*	51.18 ± 1.19	47.82 ± 1.68	26.59 ± 2.05	12.52 ± 3.185	20.25 ± 4.24	50.55 ± 3.71
p-Value of internalized bacteria recovered from spot counting versus ATCC12598	–	.2876	**.038***	**.0054*****	**.0120****	.9077
95% confidence interval	–	4.921 to −11.63	15.01 to −34.16	17.82 to 4.551	12.93 to 48.93	15.28 to −16.54

Note: The table reports the detailed statistical data obtained using *t* test versus ATCC12598: % of internalization, *p*-value and 95% confidence. Statistically significant *p*-value ≤.05*; highly significant ≤.01**; extremely significant ≤.001***.

The bold values are statistically significant.

TABLE A4 The statistical analysis relative to strain invasiveness was performed by comparing the rate of infection of each strain with the rate of infection of ATCC12598 as control for cell culture method at 3 hr p.i., using *t* test, *p* value and 95% of confidence

t Test	ATCC12598-ST30	1SA-ST239	2SA-ST239	3SA-ST239	4SA-ST5	5SA-ST5	6SA-ST5
% of internalization ± *SD*	50.49 ± 0.69	45.20 ± 3.58	50.33 ± 1.19	47.98 ± 0.63	29.82 ± 1.2	27.59 ± 2.5	22.49 ± 1.58
p-Value N cells versus ATCC12598	—	.3380	.9261	.0791	**.0012****	**.006****	**.0008****
95% confidence interval	—	−20.09 to −9.513	−5.320 to 4.994	−5.568 to −0.5416	−26.12 to −15.22	−33.34 to −12.46	−34.49 to −21.50

Note: The table reports the detailed statistical data obtained using *t* test versus ATCC12598: % of internalization, *p*-value and 95% of confidence. Statistically significant *p*-value ≤.05*; highly significant ≤.01**, extremely significant ≤.001***.

The bold values are statistically significant.

TABLE A5 The statistical analysis relative to strain invasiveness was performed by comparing the rate of infection of each strain with the rate of infection of ATCC12598 as control for cell culture method at 3 hr p.i., using *t* test, *p* value and 95% of confidence

t Test	ATCC12598-ST30	ST239-SCC*mec*III	ST5-SCC*mec*II
Rate of Infection CFU/infected MG-63	$1.9 \times 10^6 \pm 4.6 \times 10^5$	$2.5 \times 10^6 \pm 1.8 \times 10^5$	$1.5 \times 10^6 \pm 3.8 \times 10^5$
p Value	—	.99	.169
95% confidence interval	—	-3.774×10^5 to 3.741×10^6	-6.592×10^5 to 2.666×10^6

TABLE A6 The statistical analysis relative to strain invasiveness was performed by comparing the rate of infection of each strain with the rate of infection of ATCC12598 as control for cell culture method at 3 hr p.i., using *t* test, *p* value and 95% of confidence.

t Test	ATCC12598-ST30	ST239-SCC*mec*III	ST5-SCC*mec*II	ST8-SCC*mec*IV	ST228-SCC*mec*I	ST22-SCC*mec*IVh
Average spots/infected MG−63	$3.9 \times 10^5 \pm 2.1 \times 10^4$	$2.6 \times 10^5 \pm 3.6 \times 10^4$	$1.3 \times 10^5 \pm 2.5 \times 10^4$	$1.1 \times 10^5 \pm 2.4 \times 10^4$	$1.08 \times 10^5 \pm 2.6 \times 10^4$	$3.5 \times 10^5 \pm 4.7 \times 10^4$
p Value	—	.084	**.002**	**.004**	**.0049**	.5762
95% confidence interval	—	-3.14×10^5 to 2.84×10^4	1.76×10^5 to 3.37×10^4	1.69×10^5 to 3.91×10^4	1.62×10^5 to 4.01×10^4	-1.61×10^5 to 2.40×10^4

Note: Statistical data versus ATCC12598, using *t* test, *p* value and 95% of confidence. Statistically significant *p*-value ≤.05*; highly significant ≤.01**, extremely significant ≤.001***.

The bold values are statistically significant.

7SA-ST8	8SA-ST8	9SA-ST8	10SA-ST228	11SA-ST228	12SA-ST228	13SA-ST22	14SA-ST22	15SA-ST22
20.78 ± 1.659	13.68 ± 1.34	20.43 ± 0.72	20.74 ± 1.04	12.89 ± 0.59	27.59 ± 1.12	56.24 ± 2.34	45.37 ± 1.31	50.70 ± 1.27
.0009**	**.0002****	**<.0001*****	**.0002**	**<.0001**	**.0009**	.1573	.0633	.8725
−36.72 to 22.70	−41.74 to −31.87	−33.44 to 29.69	−34.33 to −25.18	−40.54 to −32.56	−28.26 to −17.54	−4.005 to 15.51	−10.78 to 0.5308	−5.169 to 5.769

ST8-SCC*mec*IV	ST228-SCC*mec*I	ST22-SCC*mec*IVh
$2.5 \times 10^6 \pm 4.3 \times 10^5$	$2.1 \times 10^6 \pm 1.3 \times 10^5$	$3.6 \times 10^6 \pm 1.7 \times 10^6$
1.0	.4881	.5585
-1.763×10^6 to 1.763×10^6	-9.670×10^5 to 1.701×10^6	-6.129×10^6 to 3.84×10^6

Part II: study of the metabolic activity by cellular vitality assay and expression studies of diverse marker during osteoblast infections

The second part focuses on the analysis of potential alterations of MG63 cell metabolic activity and cellular growth, after infection at different time periods, and the evaluation of the expression levels of transcription of selected genes involved in the *S. aureus*/osteoblasts interaction, in two different invasive MRSA isolates, ST239-SCC*mec* III-t036 and ST228-SCC*mec* I-t041.

To evaluate the alterations in human osteoblast metabolic status induced during internalization and persistence (3h and 24h post-infection) in the same experimental conditions, the "3-(4,5-di methylthiazol-2-yl)-2,5-diphenyltetrazoliumbromide reduction assay (MTT) assay was performed, in order to analyze the viability of MG-63 cells. The obtained absorbance value is directly proportional to the number of living cells. **(Fig. 5)**

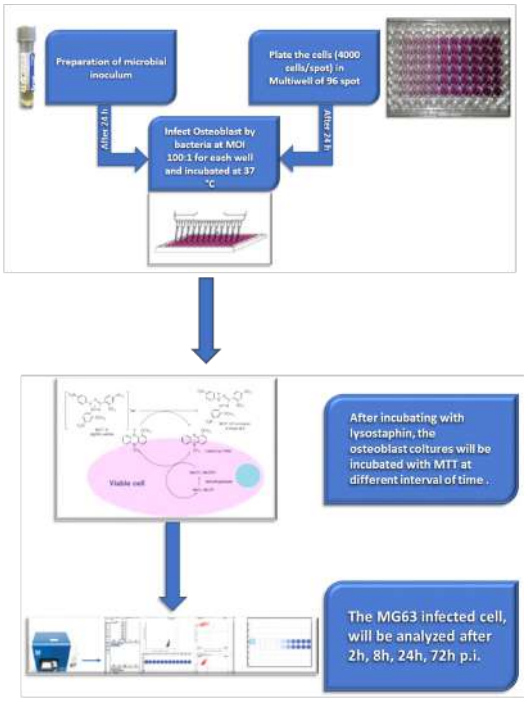

Figure 5 *Workflow of eukaryotic cell viability (MTT), conducted in cell line MG63 infected by S. aureus.*

At 3h p.i., MG-63 cells infected with ST228-I strain showed a statistically significant increase in the metabolic activity, compared to the control MG-63 uninfected cells: +12.27% ($p<0.001$) and +7.57% ($p<0.05$), respectively. Whereas, ST239-III strain induced only a slight decrease in metabolic activity (-2.47%). At 24h p.i. of intracellular persistence, ST239-III induced a statistically significant decrease in metabolic activity of MG-63 cells, compared to the control uninfected cells: -7.11% ($p<0.05$) and -18.32% ($p<0.001$), respectively. While, ST228-I strain induced only a slight increase in metabolic activity (+3.79%).

As previously observed, the ability of MRSA ST239-III to internalized and persist in MG-63 osteblasts was similar to that of ATCC12598-ST30 invasive control strain, while MRSA ST228-I showed a different behavior. These differences among clones were evaluated also by measuring the MG-63 metabolic *status* in term of cytotoxicity, demonstrating that ST239 was immediately able to decrease the cell metabolic activity at 3h p.i. maintaining it out 24h p.i., while ST228 only slightly affects the metabolic *status* of the MG63 cells.

The expression levels of transcription of selected genes involved in regulation (*sigB, sarA, sarS, agr,rot*), adhesion- MSCRAMMS (*bbp, fnbA/B, sdrE*), toxicity (*psmA, hla, hldI*), and bacterial metabolism (*uhp*T) were

further analyzed to look for a potential relationship between variation in gene expression and ability of *S. aureus* to internalize and persist in MG-63 cells, as well as their damaging potential.

The gene expression was evaluated at 3h p.i. and 24h p.i. stages, in comparison with non-internalized bacteria (baseline condition). All results of the expression studies were compared to ATCC 12598, used as reference sample.

After 3 h p.i., ST239-III was able to internalized in 50% of MG-63 cells, while after 24 h p.i. persisted in 45%, displaying a significant increase in the expression of *bbp*, necessary for adhesion and invasion in MG63 cells, and an increase in *agr*A expression, resulting in an up-regulation of *hla* and *psm*A, associated with a good ability to internalize in MG63 cells. At 24h p.i., this strain stably persisted intracellularly and exerted a highly significant cytotoxic activity against osteoblasts, due to the overexpression of *hla*, as well as an increased expression of the genes involved in adhesion. No differences were found in the expression of the genes involved in adaptation to environmental stress (*sar*A, *sig*B, *sar*S, *agr*) and those involved in adherence (*fnb*A and *fnb*B) respect to the baseline condition. In conclusion, this clone is able to stably infect MG-63 cells at 24 h p.i., exerting cytotoxic activity against osteoblasts, and demonstrating to be more prone to persistent infections.

After 3 h p.i., ST228-I strain internalized in 30% of MG-63 cells while after 24 h p.i.persisted in 20%. This clone showed to be less able to internalize and persist inside the cells, compared to ATCC12598 and ST239-III, displaying a baseline level of *agr*A expression and an increase in *sig*B and *sar*A expression, leading to up-regulation of the surface proteins and up-regulation of secreted toxins, such as PSMα, Hla, and Hld, associated with a significant non-cytotoxic activity inside osteoblasts, and lower ability to internalize into and infect MG63 cells. After 24h of intracellular persistence, all regulatory genes were down-expressed, in particular *rot* and consequently the genes involved in adhesion and virulence. The down-expression of PSMα suggests that ST228 bacteria exert their potential to damage osteoblasts by a cytotoxic effect. ST228 is not capable of activate a sufficient cellular reaction but seemed to “succumb” inside MG-63 cells. Consequently, this strain was demonstrated to be less able to internalize.

The modulation of the *agr*, *sigB*, *rot*, *hla*, and *fnbA* expression was previously associated with the switch from extracellular to intracellular behavior, due to changes in the expression of the fibronectin-binding- and adhesion-binding proteins, important for host/cell invasion but not required for intracellular persistence.

These results support the idea that variations in the expression leves of the gene tested were related to the degree of invasiveness and persistence in MG-63 cells. The bacteria can differently adapt strategies thanks to a costant interplay among regulatory and adhesion/toxin genes, rapid reaction to changing environmental conditions and dynamic adjustment of their virulence factor expression levels, at different times of infection.

Received: 8 September 2020 | Revised: 9 February 2021 | Accepted: 12 February 2021

DOI: 10.1002/mbo3.1178

ORIGINAL ARTICLE

MicrobiologyOpen Open Access WILEY

Staphylococcus aureus ST228 and ST239 as models for expression studies of diverse markers during osteoblast infection and persistence

Dafne Bongiorno[1] | Nicolò Musso[2] | Giuseppe Caruso[3] | Lorenzo Mattia Lazzaro[1] | Filippo Caraci[3,4] | Stefania Stefani[1] | Floriana Campanile[1]

[1]Department of Biomedical and Biotechnological Sciences (BIOMETEC), Medical Molecular Microbiology and Antibiotic Resistance laboratory (MMARLab, University of Catania, Catania, Italy

[2]Department of Biomedical and Biotechnological Sciences (BIOMETEC), University of Catania, Catania, Italy

[3]Department of Drug Sciences and Health Science, University of Catania, Catania, Italy

[4]Oasi Research Institute-IRCCS, Troina, Italy

Correspondence
Dafne Bongiorno, Department of Biomedical and Biotechnological Sciences (MMAR*Lab*), University of Catania, Via Santa Sofia, 97, 95123 Catania, Italy.
Email: d.bongiorno@unict.it

Funding information
Ministry of Research, Grant/Award Number: PRIN2017SFBFER; University of Catania

Abstract

The ability of *S. aureus* to infect bone and osteoblasts is correlated with its incredible virulence *armamentarium* that can mediate the invasion/internalization process, cytotoxicity, membrane damage, and intracellular persistence. We comparatively analyzed the interaction, persistence, and modulation of expression of selected genes and cell viability in an ex vivo model using human MG-63 osteoblasts of two previously studied and well-characterized *S. aureus* clinical strains belonging to the ST239-SCC*mec*III-t037 and ST228-SCC*mec*I-t041 clones at 3 h and 24 h post-infection (p.i). *S. aureus* ATCC12598 ST30-t076 was used as a control strain. Using imaging flow cytometry (IFC), we found that these strains invaded and persisted in MG-63 osteoblasts to different extents. The invasion was evaluated at 3 h p.i and persistence at 24 h p.i., in particular: ATCC12598 internalized in 70% and persisted in 50% of MG-63 cells; ST239-SCC*mec*III internalized in 50% and persisted in 45% of MG-63 cells; and ST228-SCC*mec*I internalized in 30% and persisted in 20% of MG-63 cells. During the infection period, ST239-III exerted significant cytotoxic activity resulting from overexpression of *hla* and *psm*A and increased expression of the genes involved in adhesion, probably due to the release and re-entry of bacteria inside MG-63 cells at 24 h p.i. The lower invasiveness of ST228-I was also associated with non-cytotoxic activity inside osteoblasts. This clone was unable to activate sufficient cellular reaction and succumbed inside MG-63 cells. Our findings support the idea of considering new strategies, based on a translational approach—eukaryotic host–pathogen interaction (EHPI)—and to be applied on a large scale, to predict *S. aureus* /osteoblast interaction and treat bone infections. Such strategies rely on the study of the genetic and biochemical basis of both pathogen and host.

KEYWORDS
crosstalk mechanism, MRSA, osteoblast, ST228, ST239, virulence toxin

Dafne Bongiorno, Nicolò Musso and Giuseppe Caruso are equally contributed to the paper.

1 | INTRODUCTION

The human pathogen *Staphylococcus aureus* can adapt to the host/environment, infect any organ, and damage tissues, causing severe infections, and can resist antibiotics, in particular beta-lactams and methicillin (Tong et al., 2015). It is one of the main pathogens responsible for recurrent osteomyelitis (OM), accounting for 50% to 70% of cases, and prosthetic joint infections (PJIs) (Mruk & Record, 2012; Wu et al., 2019). PJIs can have a dramatic impact on a patient's quality of life, often requiring surgical intervention and prosthesis removal, as well as prolonged antibiotics treatment (Moore et al., 2017; Purrello et al., 2016; Stefani et al., 2012). These infections are often due to healthcare-associated methicillin-resistant *S. aureus* (HA-MRSA) belonging to clonal complex 5 (Muñoz-Gallego et al., 2017; Peng et al., 2019; Pérez-Montarelo et al., 2018) and associated with the staphylococcal chromosomal cassette (SCC*mec*) I and III (Hussain et al., 2009). Among them, ST239-III is probably the oldest pandemic MRSA clone, first discovered in 1970, isolated in most countries worldwide, and the most widespread in Europe (Campanile et al., 2015; Monecke et al., 2018; Szymanek-Majchrzak et al., 2018). ST228-SCC*mec*I is one of the most widespread clones in Italy, associated with nosocomial infections (Bongiorno et al., 2018; Campanile et al., 2012).

Assessing the interaction between *S. aureus* isolates and osteoblasts during PJIs and OM includes three crucial events: adhesion, invasion, and post-invasion, where *S. aureus* controls the expression of adhesion and virulence determinants with its large armamentarium of regulatory genes.

Many studies have been carried out in this field. Different authors have shown the role of many regulators involved in the invasion and adaptation to host tissue. The role of *sig*B in persistence and stress response, together with its link to *sar*A and, consequently, to its action on the *agr* locus was studied in osteoblasts, in an in vivo model, using two different strains of *S. aureus*; in particular, the authors used the wild-type and the defective strain for *agr, sig*B, and *sarA* (Tuchscherr et al., 2015). The global regulatory system—*agr* locus—cell density-dependent, controls virulence factor expression. Through its effector molecule RNAIII, the *agr* locus controls the post-transcriptional regulation of proteins involved in cell–surface interaction and virulence cytotoxic factors (Painter et al., 2014).

Two other genes belonging to the SARA protein family are involved in the regulation of virulence genes: *sarS* (SarH1), whose expression is repressed by *sar*A and *agr*, is a repressor of *hla* and *etb* and is a positive regulator of *spa* and *rot*, the "repressor of toxin," which is a repressor of enterotoxin B (*seb*) and alpha-toxin (*hla*) and is repressed by the *agr* effector RNAIII and SarA (Jenul & Horswill, 2018).

In the process of adhesion, cell surface proteins (adhesins) of the Microbial Surface Component Recognizing Adhesive Matrix Molecules (MSCRAMM) play an important role in the pathogenesis of osteoarticular infections (OM and PJIs). Among these, an important role is played by: the fibronectin-binding proteins A and B (FnbA/B); the fibrinogen-binding protein clumping factors A and B (ClfA/B); the bone sialoprotein binding protein (Bbp); the collagen adhesin (CNA) (Otsuka et al., 2006; Pérez-Montarelo et al., 2018); and SdrE, a serine–aspartate (SD) protein that anchors the cell wall interacting with complement factor H and facilitates colonization through adherence to the cell surface or extracellular matrix (ECM) components (Herr & Thorman, 2017).

S. aureus can invade endothelial cells and osteoblasts using the cell surface integrin $\alpha5\beta1$, binding Fn on the surface of human cells. In particular, as already demonstrated, FnBPA and FnBPB are involved not only in adhesion but also in internalization (Shinji et al., 2011). Pore-forming proteins, such as Panton–Valentine leukocidin (PVL) and α- and δ-hemolysin (Hla and Hld), together with phenol-soluble modulins (PSMs), were able to induce local complications such as bone deformation, systemic complications as severe sepsis in rabbit osteomyelitis, or neutrophil and osteoblast cytotoxicity in an ex vivo model (Davido et al., 2016). The *hla* gene was frequently present in strains associated with osteoarticular bacteremia (Pérez-Montarelo et al., 2018). PSMs are small peptides with amphipathic properties that destabilize the lipid bilayer of the host cell; this activity is related to receptor-independent cytotoxicity to osteoblasts and specialized cells such as the neutrophils. PSMs are also implicated in biofilm formation, in bacterial interference, and in cell-cycle disruptions (Davido et al., 2016).

During the infection process, *S. aureus* can use alternative carbon sources and, in particular, glucose-6-phosphate (G6P); the uptake of these alternative carbon sources occurs through the hexose phosphate antiporter UhpT (Yang et al., 2016).

After observing that interaction, internalization, and persistence during an ex vivo osteoblast infection are a strain-dependent process, we selected two strains belonging to different genetic backgrounds showing a preliminary difference in their ability to internalize as a model of infection to study how differently they adapt their strategies to react to changing environmental conditions and how they adjust their virulence factor expression at different times of infection inside the MG-63 cell line.

2 | MATERIALS AND METHODS

2.1 | Strains included in the study

The study sample consisted of 2 invasive MRSA isolates, 2SA ST239-SCC*mec*III-t036 and 10SA ST228-SCC*mec*I-t041, already molecularly characterized using internationally recognized standard genotyping methods to determine MRSA clones. These strains were selected from a large collection of 15 MRSA strains phenotypically and molecularly (SCC*mec-spa* type) characterized as previously reported (Bongiorno et al., 2018; Campanile et al., 2015) and tested for their ability to internalize and persist in MG-63 human osteoblasts (Bongiorno et al., 2020).

The invasive ATCC12598 isolate (Cowan ST30-t076) (ATCC® Standards Development Organization, LGC Standards S.r.l.) was used, as previously described, as a control strain for invasion and persistence assays and the statistical analysis of the results obtained

at imaging flow cytometry (IFC), as previously reported (Bongiorno et al., 2020).

2.2 | agr, toxin, and MSCRAMM characterization

The genomic DNA used as a template for PCR amplification was extracted with QIAamp® DNA Mini Kit (cat. No. 51306, Qiagen) following the manufacturer's instructions with some modifications. Briefly, a bacterial suspension was centrifuged and the pellet was resuspended in 200 µl of physiological saline solution 0.9% and subjected to freezing and thawing twice. After centrifugation, the bacterial pellet was resuspended in 180 µl of enzyme solution: 20 mg/ml lysozyme (cat. No. 10837059001, Sigma-Aldrich, Merck KGaA) and 100 µg/ml lysostaphin (cat. No. L7386-15MG, Sigma-Aldrich, Merck KGaA) in Tris-EDTA (TE) buffer, pH 8.0 (cat. No. AM9849, Ambion, Invitrogen). Apart from these differences, the indications provided by the manufacturer were followed.

The toxin and MSCRAMM genes included in the study and listed in Table A1 were tested as previously described (Stefani et al., 2009). The *agr* locus was typed using a multiplex PCR assay (Gilot et al., 2002). The *cna* gene was PCR-tested using the following primers in 5′-3′: F-GGAAAACGACCAACTGAAATCAAAG, R-TCTGGCGTATATTTATTCGTCACAATC. PCR was performed at 57°C, the product size was 239 bp, and the MW2 strain was used as an internal control.

PCR amplification was carried out in a Veriti Thermal Cycler (Applied Biosystems, Thermo Fisher) in a total volume of 25 µl containing 2× Multiplex PCR Master Mix (cat. No. BR0200804, biotechrabbit GmbH) and 10 ng template DNA.

2.3 | δ-Hemolysin production

δ-Hemolysis production was evaluated by cross-streaking perpendicularly our sample to *S. aureus* RN4220, using 5% sheep blood agar Columbia base with 6 mg/L vancomycin, as previously described. The

TABLE 1 Regulators, MSCRAMMs, toxins, and other genes used to evaluate gene expression in real-time PCR

Gene expression evaluated in real-time PCR					
Category	**Gene**	**Product size bp**	**Function**	**Primer Sequence 5'-3'**	**GenBank Acc. number**
Regulators	*sig*B	103	RNA polymerase sigma factor, in response to changes in environmental conditions.	ATGTACGTTTATTGAAGGATTG AGAACGGCAATTAAGAAATTA	AY197753.1
	*sar*A	151	Transcription regulator, regulating the expression of virulence factors	ACATGGCAATTACAAAAATCAATGAT CATCAGCGAAAACAAAGAGAAAGA	U46541.1
	*sar*S	187	Transcription regulator, regulating the expression of virulence factors	TCAACAAGAAAACACACTTCCAT ACGTTCTGCAATTTTCTCTCGT	NC_7793
	*agr*A	145	Accessory gene regulator-mediated quorum sensing plays a major role in staphylococcal pathogenesis	Aactgcacatacacgcttaca aaatctcacagactcattgcc	BX571856.1
	rot	168	Repressor of toxins regulatory protein	CGGGATTGTTGGGATGTTTG TCGCTTTCAATCTCGCTGAA	CP_026073
MSCRAMMs	*bbp*	172	Adhesin binding to bone sialoprotein	GATGCTAATGAACCTGGTATCAAAGAT CAGGTTACACGCCAACGGTTA	BX571856.1
	*fnb*A	75	Adhesin binding to fibronectin and elastin	ACAAGTTGAAGTGGCACAGCC CCGCTACATCTGCTGATCTTGTC	KP096552.1
	*fnb*B	87	Adhesin binding to fibronectin and elastin	TTCCTGTAGTTTCCTTATCAGCAACTT GCTTGCACAGTTGTTGGTG	BA000033.2
	*sdr*E	211	surface protein serine-aspartate repeat protein E	GGCGACGGTACTGTTAAACC CTCCGTCTTTCAAACCACCG	NC_007793
Toxins	*psmα*	198	Phenol-soluble modulin α	TCATCGCTGGCATCATTAAAGTTA ATAGATATGAACATCTTATTTGAAGGGG	JQ066321.1
	hla	202	α-hemolysin	caactgataaaaaagtaggctggaaagtgat ctctattatcttcagggttttcaccaga	BA000033.2
	hld	187	Delta-hemolysin	TGGTTATTAAGTTGGGATGGCT GGAAGGAGTGATTTCAATGGCA	NC_007793
Others	*Uhp*T	195	hexose phosphate antiporter	GTCGTCGTGCAATTGTAGCT CGTTTGCTACACTGATGGCA	NC_007793
	*gyr*B	160	DNA gyrase subunit B	GTGAAGGTATGACAGCAATTATATCTATCAA ATATGAAAATCCACAAGTCGCACG	BX571856.1

TABLE 2 Molecular characteristics of the samples included in the study

Code	ST-SCC*mec*-spa type-agr type	Source	δ-hemolysis	Pathotype profile									
				MSCRAMMs (adhesins)						Toxins			
				*fnb*A	*ica*A	*sdr*E	*clf*A	*clf*B	*cna*	*luk-PV*	*eta*	*etb*	*hlb*
ATCC12598	ST30-MSSA-t976-III	–	+	+	+	+	+	+	+	+	–	–	–
2SA	ST239-HAMRSA-III-t037-I	Blood	+	+	+	+	+	+	+	–	–	–	+
10SA	ST228-HAMRSA-I-t041-II	Blood	–	+	+	+	+	+	+	+	–	–	–

Clone characterization through: ST—sequence type; SCC*mec*—Staphylococcal Cassette Chromosome *mec*; *spa* type—staphylococcal protein A; *agr* type—locus *agr*; delta—hemolysis production; *fnb*A—fibronectin-binding protein A; *ica*A—intracellular adhesion; *sdr*E—platelet aggregation; *clf*A/B—clumping factor A/B; *cna*—adhesin binding to collagen; *luk*-PV—Panton–Valentine leukocidin; *eta/b*—exfoliative toxin A/B; *hlb/d/g*—hemolysins beta/delta/gamma; *tst*—toxic shock syndrome toxin; *se*A-P—Staphylococcal enterotoxin from A to P; *spa*—protein A; *agr*—accessory gene regulated.

S. aureus reference strains Mu3 (hVISA) and MU50 (VISA) were used as controls for strong hemolysis activity, and NRS149 (VSSA) was used as a control for absent hemolysis activity (Cafiso, Bertuccio, Spina, Purrello, Blandino, et al., 2012).

2.4 | Eukaryotic cell culture preparation

Infection experiments were performed on the human osteosarcoma cell line MG-63 (ATCC® CRL-1427™, Standards Development Organization, LGC Standards S.r.l.), as previously described (Bongiorno et al., 2020).

A single 6-well plate was used for the imaging flow cytometry (IFC), a single 6-well plate was used for RNA extraction, and a 96-well plate was used for the evaluation of eukaryotic cell metabolism. All experiments were performed twice in triplicate.

2.5 | Evaluation of the frequency of internalization and intracellular persistence by IFC

The frequency of internalization was evaluated in a cell culture model of infection in MG-63 osteoblasts at a multiplicity of infection (MOI) of 100:1, as previously reported (Bongiorno et al., 2020). In this work, we evaluated, by IFC, bacterial internalization at 3 h p.i., and persistence at 24 h p.i, as previously reported (Bongiorno et al., 2020). Briefly, bacterial isolates were grown in Brain Heart Infusion Broth (BHI) (cat. No. CM1135, Oxoid Limited, Thermo Fisher Scientific Inc) at 37°C overnight. The bacterial concentration was evaluated by optical density (OD) at 600 nm. Bacterial suspensions were prepared using MEM supplemented with 10% fetal bovine serum (FBS) (cat. No. 16000044, GIBCOTM, Thermo Fisher Scientific). MG-63 cultures were infected for 2 h and 24 h in antibiotic-free conditions; extracellular bacterial lysis was carried out for 1 h at 37°C with 100 mg/ml lysostaphin (cat. No. L7386-15MG, Sigma-Aldrich, Merck KGaA). Infected cells were first washed with 1X phosphate-buffered saline (PBS) (cat. No. P5493, Sigma-Aldrich, Merck), followed by an incubation step of 3–5 min at 37°C with 0.05% trypsin-EDTA solution (cat. No. T4049, Sigma-Aldrich, Merck). The cellular suspension was reversibly permeabilized with saponin 0.1% (cat. No. 558255, Sigma-Aldrich, Merck) in PBS. Saponin interacts with membrane cholesterol, selectively removing it and leaving holes in the membrane. This transient permeabilization does not require cell fixing. After 15 min in saponin, bacterial cells were labeled with 0.08 μg/ml BODIPY™ FL-Vancomycin (VBFL) (cat. No. V34850, Invitrogen™), the membrane-impermeable green fluorochrome vancomycin analog that specifically binds the cell-wall peptidoglycan of Gram-positive bacteria and does not penetrate intact cells. The suspensions were then washed three times with PBS to remove the transient permeabilization and checked under the microscope to ensure that the cells had maintained their cell integrity and that their cell wall was intact. The labeled cellular suspension was analyzed using a FlowSight® Imaging Flow Cytometer (Amnis® FlowSight® Millipore, Merck).

We acquired 10,000 events per sample, and as quality control, we used the stained and unstained bacterial suspension to exclude autofluorescence; a negative control of infected, but not permeabilized, cells was also acquired to guarantee the exclusively intracellular localization of green spots. Acquisition analysis was performed using the powerful INSPIRE® and IDEAS® software (Amnis, EMD Millipore).

2.6 | Eukaryotic cellular metabolic assay

To evaluate the metabolic status of MG-63 cells following infection with *S. aureus* for 3 h p.i. and 24 h p.i., we used the MTT ([3-(4,5-dimethylthiazol-2-yl)-2,5-diphenyltetrazolium bromide]) assay (Fresta et al., 2018; Pedotti et al., 2017). The formazan crystals obtained at the end of the procedure were dissolved by dimethyl sulfoxide, and the multiplate reader Synergy™ H1 (BioTek) was used to determine the colorimetric differences, detected as absorbance at 569 nm, between samples. The values obtained for the infected cells were expressed as percent variation from the metabolic status detected in not infected (control) cells (as 100%).

hld	*hlg*	*tst*	*sea*	*seb*	*sec*	*sed*	*see*	*seg*	*seh*	*sei*	*sej*	*seK/q*	*sel*	*sem*	*sen*	*seo*	*sep*
+	+	−	−	−	−	−	−	+	−	+	−	−	−	+	−	−	−
+	+	−	−	−	−	−	−	−	−	−	−	−	−	−	−	−	−
+	+	−	+	−	−	−	−	+	−	+	−	−	−	+	−	+	−

2.7 | qRT-PCR expression study

We have investigated the expression level of transcription of some selected genes involved in the bacteria/osteoblast interaction. The primers used for real-time PCR, reported in Table 1, were designed by the Flexi® Vector Primer Design Tool. Real-time PCR experiments on the total RNA extracted from infected cell cultures were carried out at 3 h p.i. and 24 h p.i.

RNA extraction was performed using the RNeasy Mini Kit (cat. No. 74104, Qiagen, Milan) following the manufacturer's instructions, with some modifications. Briefly, bacteria internalized in MG-63 at 3 h p.i. and 24 h p.i. were collected in 500 µl of RNAprotect Bacteria buffer (cat. No. 76506, Qiagen). This first reaction series was carried out at a controlled temperature of about 4°C, vortexed, and incubated for 5 min at room temperature. After centrifugation, the pellet was resuspended in 100 µl of TE buffer containing: 20 µl QIAGEN Proteinase K (cat. No. 9131, Qiagen), 150 mg/ml lysozyme (cat. No. 10837059001, Sigma-Aldrich, Merck KGaA), and 20 mg/ml lysostaphin (cat. No. L7386-15MG, Sigma-Aldrich, Merck KGaA). Apart from these differences, the indications provided by the manufacturer were followed.

RNA quality was tested by Qubit® 3.0 Fluorometer (cat. No. Q33216, Life Technologies, Thermo Fisher Scientific Monza) using the Qubit RNA HS Assay Kit (250 pg/µl and 100 ng/µl). The RNA was normalized at 100 ng to obtain the cDNA using the QuantiTect Reverse Transcription Kit (cat. No. 205311, Qiagen), and the amplifications were performed using the QuantiTect SYBR Green PCR Kit (cat. No. 204145, Qiagen) at a final cDNA concentration of 25 ng/µl and 2uM primers per PCR. Each sample amplification consisted of a total reaction volume of 10 µl (5 µl PCR Master Mix +1 µl specific primers +4 µl of cDNA (25 ng/µl). Reactions were run in triplicate under the following conditions: PCR initial activation step for 15 min at 95°C; denaturation for 15 s at 94°C; annealing for 30 s at 60°C; and extension for 30 s at 72°C, the acquisition of fluorescence was done for 50 cycles. The negative control consisted of a reaction in the absence of cDNA (5 µl PCR Master Mix +1 µl specific primers +4 µl of TE buffer) indicated as NTC (no template control).

qPCRs were performed in a LightCycler® 480 Real-Time PCR System (Roche, Monza, Italy). PCR efficiencies, melting curve analysis, and expression rate were calculated using the LightCycler® 480 software (Roche, Monza, Italy). *gyr*B primers were used as the internal control.

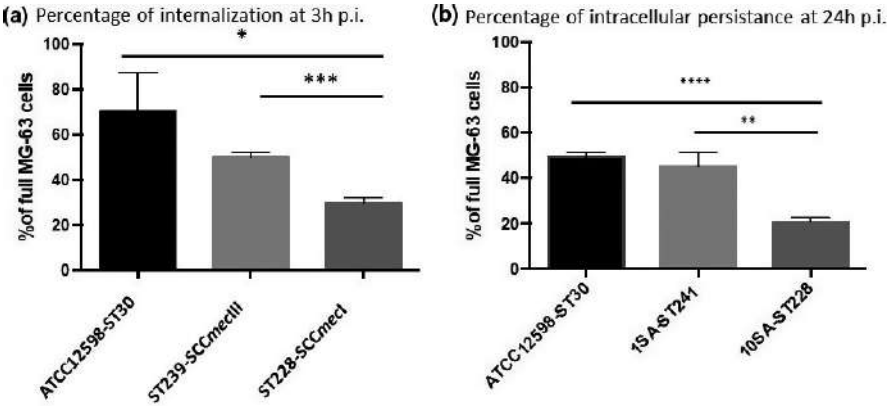

FIGURE 1 Evaluation of the internalization frequency by IFC evaluation and cellular metabolism viability, at 3 h p.i. and 24 h p.i. at an MOI of 100:1. (a) The graph reports the percentage of spots at 3 h p.i. for cell ±SD for each strain for three different experiments. (b) The graph reports the percentage of spots at 24 h p.i. for cell ±SD for each strain for three different experiments. Statistical data were obtained using Student's *t* test versus ATCC12598: *p*-value, 95% confidence interval, and *R*-squared. Statistically significant *p*-value: ≤0.05*; ≤0.01**; ≤0.001***; and ≤0.0001****

TABLE 3 Evaluation of the internalization frequency by IFC evaluation and cellular metabolism viability, at 3 h p.i. and 24 h p.i. at an MOI of 100:1

Student's *t*-test	ST239-SCC*mec*III versus ATCC12598-ST30	ST228-SCC*mec*I versus ATCC12598-ST30	ST228-SCC*mec*I versus ST239-SCC*mec*III
A. Statistical details of internalization at 3 h p.i.			
p-value	0.1138	0.0152	0.0004
p value summary	ns	*	***
Significantly different? ($p < 0.05$)	No	Yes	Yes
95% confidence interval	−47.57 to 7.527	−68.02 to −12.90	−25.62 to −15.26
R squared	0.5044	0.8059	0.9677
B. Statistical details of internalization at 24 h p.i.			
p-value	0.3226	<0.0001	0.0028
p-value summary	ns	****	**
Significantly different? ($p < 0.05$)	No	Yes	Yes
95% confidence interval	−14.66 to 6.192	−32.96 to −24.43	−34.83 to −14.11
R squared	0.2411	0.9887	0.915

(A) The table reports the detailed statistics of internalization at 3 h p.i. (B) The table reports the detailed statistics of internalization at 24 h p.i. Statistical data were obtained using the Student's *t*-test versus ATCC12598: *p*-value, 95% confidence interval, and *R*-squared. Statistically significant *p*-value: ≤0.05*; ≤0.01**; ≤0.001***, ≤0.0001****.

TABLE 4 Cellular metabolic status during infection and persistence. Cellular metabolic status was determined using the MTT assay

MG-63 cells infected with	% of cellular metabolic status	Significance	Standard deviation	Variation
(A) MG-63 Cellular metabolic *status* at 3 h p.i.				
ATCC12598	112.27	***	7.59	+12.27
ST239-SCC*mec*III	97.53	###	2.97	−2.47
ST228-SCC*mec*I	107.57	*; θθθ	8.82	+7.57
(B) MG-63 cellular metabolic status at 24 h p.i.				
ATCC12598	92.89	*	4.25	−7.11
ST239-SCC*mec*III	81.67	***; ###	5.94	−18.32
ST228-SCC*mec*I	103.79	###; θθθ	8.69	+3.79

Data are the mean of at least 8 independent experiments and are expressed as a percent variation with respect to the cellular metabolic status detected in control, uninfected cells (100%). (A) Cellular metabolic status 3 h p.i. (B) cellular metabolic status at 24 h p.i. Statistical significance was assessed using ANOVA and Sidak's multiple comparison tests (post hoc test), and the threshold was set *p*-value: Statistically significant *p*-value: ≤0.05*; ≤0.01**; and ≤0.001***. Symbols used: (*) versus empty MG63 cells (control); (#)versus ATCC12598; (θ) versus ST239-SCC*mec*III.

The relative RNA expression level for each sample was calculated using the $2^{-\Delta\Delta CT}$ method (threshold cycle (CT) value of the gene of interest vs. CT value of the housekeeping gene) (Fresta et al., 2020). For accurate gene expression measurements with qRT-PCR, the results were normalized to the housekeeping gene *gyr*B (Cafiso et al., 2014; Cafiso, Bertuccio, Spina, Purrello, Campanile, et al., 2012; Chen et al., 2012).

2.8 | Statistical model

The statistical analysis and related graphs were obtained using GraphPad Prism 6 (GraphPad Software Inc.).

The statistical significance of cytofluorimetric analyses was assessed using Student's *t* test, and the number of single-cell events analyzed was never below 9980 cells out of 10,000 events at the outset (Bongiorno et al., 2020). The statistical significance of the MTT assay was evaluated using ANOVA and Sidak's multiple comparison test (*post hoc* test). The statistical significance of the expression analysis was assessed using ordinary one-way ANOVA and Bonferroni's multiple comparison test. The significance threshold was set to *p*-value ≤0.05 (*), *p*-value ≤0.01 (**), *p*-value ≤0.001 (***), and *p*-value ≤0.0001(****).

3 | RESULTS

3.1 | Genotypic characteristics, agr typing, and toxin detection

The molecular features of the strains in the study are reported in Table 2.

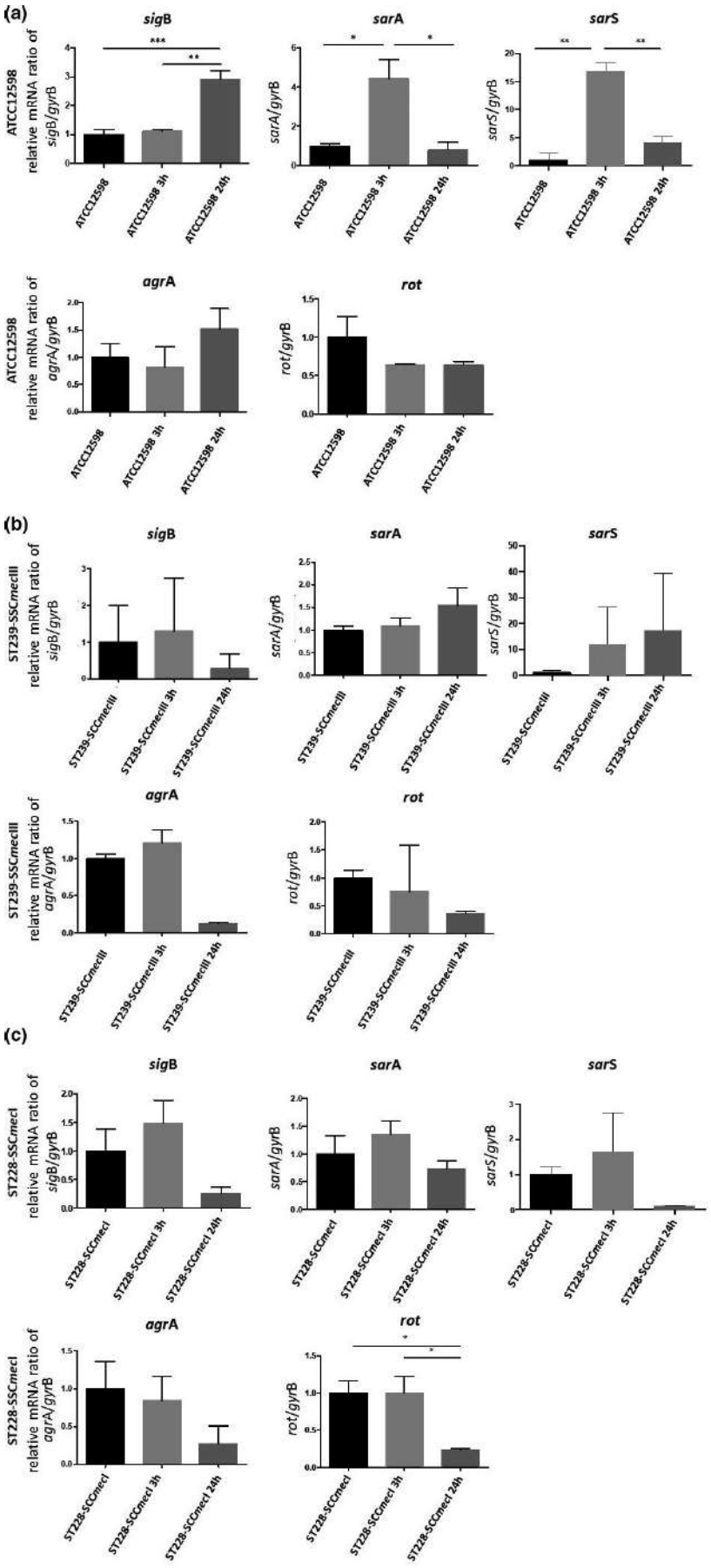

FIGURE 2 Evaluation of the relative mRNA expression of genes involved in regulation in ATCC12598, ST239, and ST228 strains at 3 h p.i. and 24 h p.i. versus baseline condition. Horizontal bars report the statistical analysis. Statistically significant *p*-value ≤0.05 (*); ≤0.01 (**); and ≤0.001 (***)

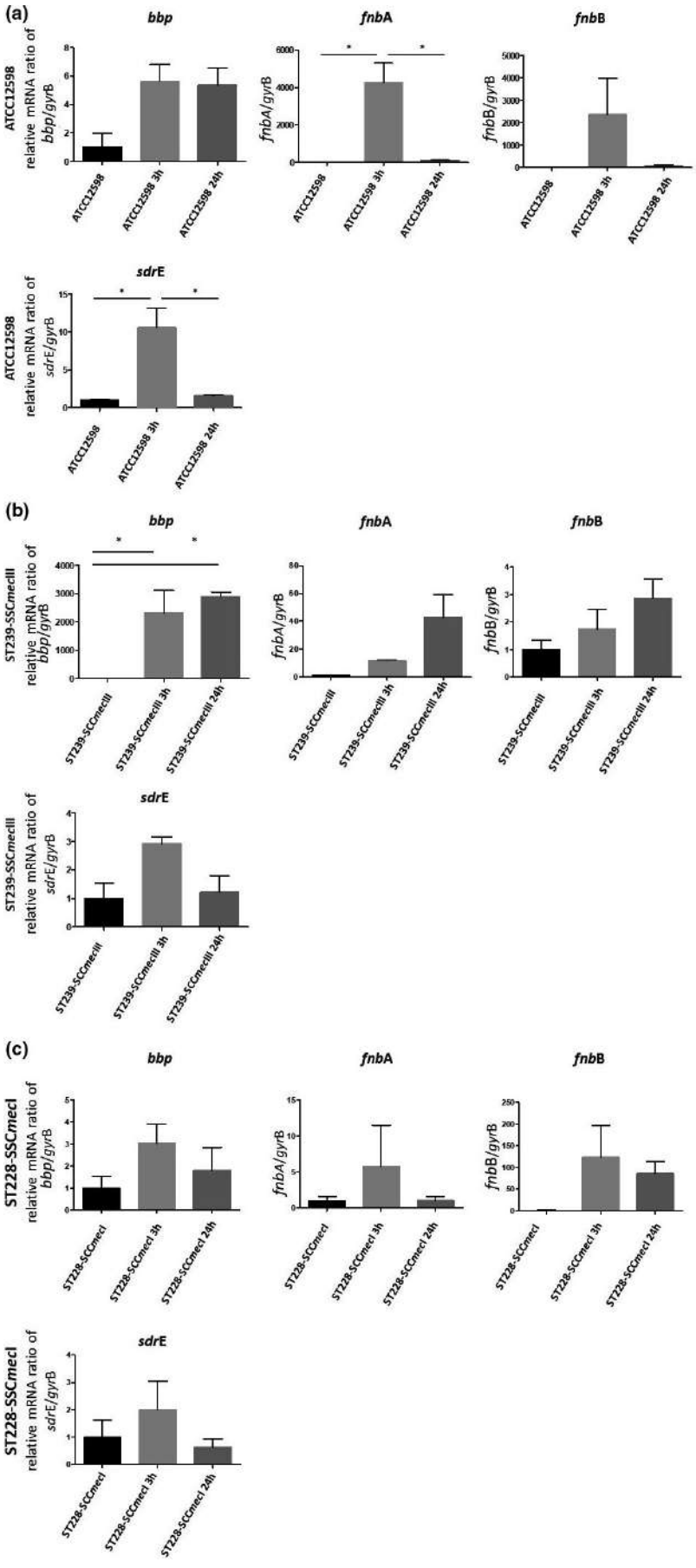

FIGURE 3 Evaluation of the relative mRNA expression of genes involved in regulation in ATCC12598, ST239, and ST228 strains at 3 h p.i. and 24 h p.i. versus baseline condition. Horizontal bars report the statistical analysis. Statistically significant *p*-value ≤0.05 (*); ≤0.01 (**); ≤0.001 (***)

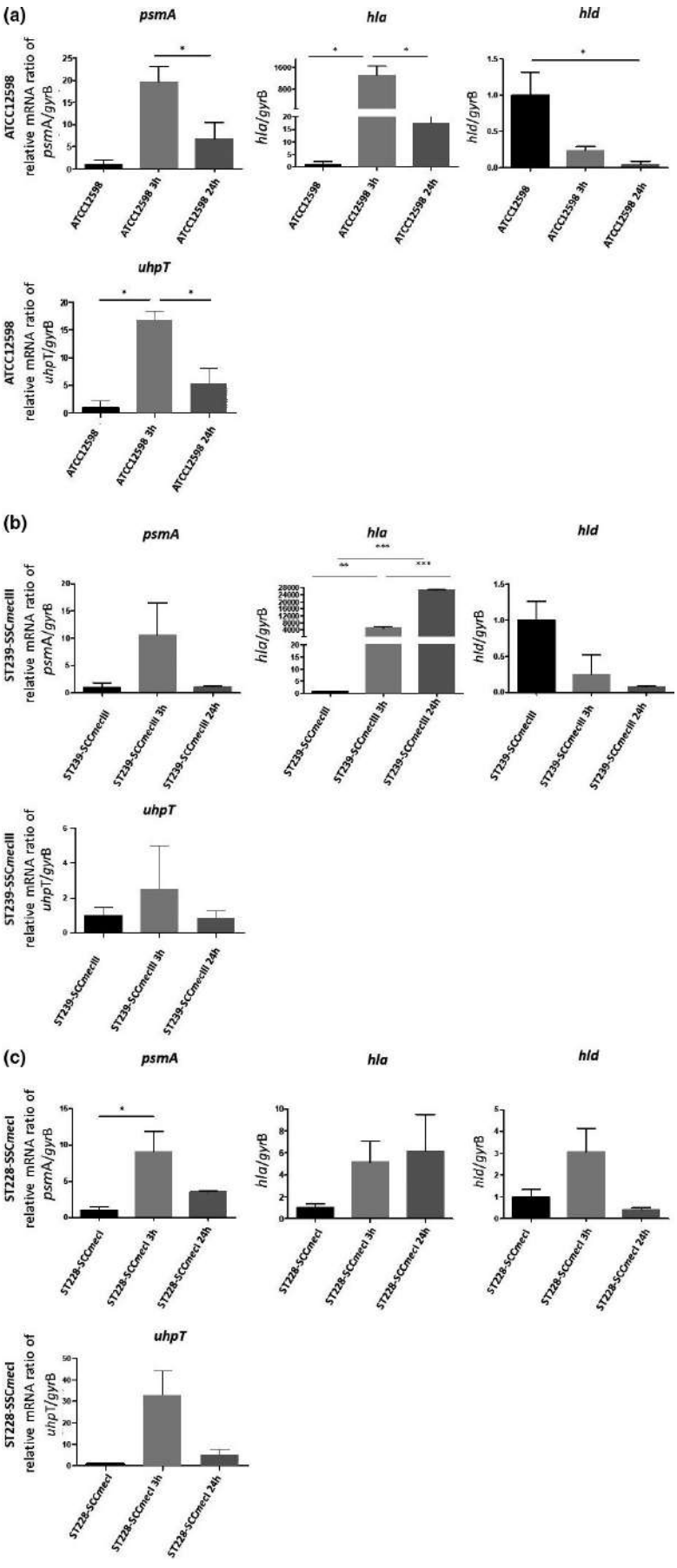

FIGURE 4 Evaluation of the relative mRNA expression of toxin and metabolic genes in ATCC12598, ST239, and ST228 strains at 3 h p.i. and 24 h p.i. versus baseline condition. Horizontal bars report statistical analysis. Statistically significant *p*-value ≤0.05 (*); ≤0.01 (**); and ≤0.001 (***)

TABLE 5 The up/down-regulation of the genes considered in the study, at 3 h p.i. and 24 h p.i

Regulator genes	*sigB*			*sarA*			*sarS*			*agr*			*rot*		
Exp time	3 h versus basal	24 h versus basal	3 h versus 24 h	3 h versus basal	24 h versus basal	3 h versus 24 h	3 h versus basal	24 h versus basal	3 h versus 24 h	3 h versus basal	24 h versus basal	3 h versus 24 h	3 h versus basal	24 h versus basal	3 h versus 24 h
ATCC12598	=	**↑	***↑	*↑	ns=	*↑	**↑	↑	**↑	=	↑	↓	↓	↓	=
ST239-SCCmecIII	↑	↓	↑	=	↑	↓	↑	↑	↓	↑	↑	↑	↓	↓	↑
ST228-SCCmecI	↑	↓	↑	↑	↑	↑	↓	↑	↓	↓	↓	↑	=	*↓	*↑

MSCRAMM genes	*bbp*			*fnbA*			*fnbB*			*sdrE*		
Exp time	3 h versus basal	24 h versus basal	3 h versus 24 h	3 h versus basal	24 h versus basal	3 h versus 24 h	3 h versus basal	24 h versus basal	3 h versus 24 h	3 h versus basal	24 h versus basal	3 h versus 24 h
ATCC12598	↑	↑	=	*↑	=	*↑	↑	=	↑	*↑	=	*↑
ST239-SCCmecIII	*↑	*↑	↓	↑	↑	↓	↑	↑	↓	↑	=	↑
ST228-SCCmecI	↑	↑	↑	↑	=	↑	↑	↑	↑	↑	↓	↑

Toxin genes	psmA			*hla*			*hld*		
Exp time	3 h versus basal	24 h versus basal	3 h versus 24 h	3 h versus basal	24 h versus basal	3 h versus 24 h	3 h versus basal	24 h versus basal	3 h versus 24 h
ATCC12598	↑	↑	*↑	*↑	↑	*↑	↓	*↓	↓
ST239-SCCmecIII	↑	=	↑	**↑	***↑	***↓	↓	↓	s↑
ST228-SCCmecI	*↑	↑	↑	↑	↑	↑	↑	↓	↑

Other genes	*uhpT*		
Exp time	3 h versus basal	24 h versus basal	3 h versus 24 h
ATCC12598	*↑	↑	*↑
ST239-SCCmecIII	↑	=	↑
ST228-SCCmecI	↑	↑	↑

Statistically significance: not significant (gray arrow), *p*-value: ≤0.05 (*); ≤0.01 (**); and ≤0.001 (***).

↑Up-regulated.

↓Down-regulated.

↑Up-Regulated But No Significant difference.

↓Down-regulated but no significant difference.

= same expression level as a basal condition.

S. aureus ATCC12598 was associated with *agr* type III, while ST239-III was associated with *agr* type I and ST228-I with *agr* type II. δ-Hemolysis production was observed in ATCC12598 and ST239-III but not in ST228-I.

Genes responsible for adhesion, such as *fnb*A, *ica*A, *clf*A/B, *cna*, and *sdr*E (the latter being responsible for platelet aggregation), were present in all strains. The strain belonging to ST239-III showed a toxin gene pattern extremely different from that of ATCC12598; in fact, neither the exfoliative toxin (*eta/b* genes) nor the toxic shock syndrome toxin (*tst)* and the staphylococcal enterotoxin (*es*A-P genes) were found. ST228-I showed a toxin gene pattern similar to ATCC12598 (*luk-PV*, *seg*, *sei*, *sem*) besides carrying enterotoxin A and O genes (*sea* and *seo*). All strains showed the presence of *hld*, and *hlg* and ST239-III also carried the *hlb* gene. All strains carried the genes responsible for adhesion/invasion, toxicity, and microbial metabolism used in the subsequent expression studies.

3.2 | Evaluation of bacterial intracellular internalization and persistence

We used imaging flow cytometry (IFC) to evaluate the number of bacteria that internalized and persisted in MG-63 cells. We previously demonstrated the power of IFC in precisely estimating the percentage of osteoblasts infected with *S. aureus* strains in a sample of 10,000 MG-63 cells. Here, we report the internalization rate, expressed as a percentage of internalization at 3 h p.i. and the persistence rate at 24 h p.i (Figure 1 and Table 3).

At 3 h p.i., ATCC12598 internalized in 70 ± 17.04% of MG-63 cells, a slightly lower ability to internalize was found for the ST239-III clone (50.24 ± 2.26%), while ST228-I showed the lowest internalization rate, at 29.8 ± 2.31% ($p = 0.015$). The lower ability to internalize the ST228-I strain was also evident when compared to ST239-III ($p = 0.0004$) (Figure 1a and Table 3A). Persistence inside cells was measured at 24 h p.i.: 49 ± 1.96% of the ATCC12598 bacterial cells persisted inside MG-63 cells; the same ability to persist was found in the ST239-III clone (45.2 ± 6.2%), while ST228-I showed a lower rate of persistence, 20.7 ± 1.80% ($p < 0.0001$). The lower ability to persist of ST228-I was also evident when compared to ST239-III ($p = 0.0028$) (Figure 1b and Table 3B).

This technique allowed us to estimate the percentage of MG-63 cells that were internalized (full vs. empty cells) and the number of bacteria that internalized in a sample of 10,000 MG-63 cells; moreover, we were able to establish bacterial persistence at 24 h p.i.

3.3 | Analysis of MG-63 cell metabolic status

Alterations in the metabolic status of human osteoblasts induced during internalization and persistence were evaluated in the same experimental condition by analyzing the MG-63 cell viability at 3 h p.i. and 24 h p.i. (Table 4).

At 3 h p.i., MG-63 cells infected with ATCC12598 and ST228-I strains showed a statistically significant increase of +12.27% ($p < 0.001$) and +7.57% ($p < 0.05$), respectively, in their metabolic activity compared with control uninfected MG-63 cells, whereas the ST239 strain induced only a slight decrease in their metabolic activity (−2.47%).

A statistically significant decrease ($p < 0.001$) was found when comparing the cellular metabolic status of MG-63 infected with ST239-III versus ATCC12598, while no statistical difference was observed when comparing the toxicity of MG-63 cells infected with ST228-I versus ATCC12598. A statistical difference in the human cell metabolic status was detected by comparing MG-63 infected with ST239-III and ST228-III with each other ($p < 0.001$) (Table 4A).

At 24 h p.i., ATCC12598 and ST239-III intracellular persistence induced a statistically significant decrease of −7.11% ($p < 0.05$) and −18.32% ($p < 0.001$), respectively, in the metabolic activity of MG-63 cells, compared with uninfected control cells, while the ST228-I strain showed only a slight increase in their metabolic activity (+3.79%).

A statistically significant decrease ($p < 0.001$) was found when comparing the cellular metabolic status of MG-63 cells infected with ST239-III and ST228-I versus ATCC12598. Statistically significant differences in MG-63 cell metabolic status were found by comparing the results obtained from cells infected with ST239-III and ST228-I ($p < 0.001$) (Table 4B).

Testing MG-63 cells viability led us to understand the changes in the cellular metabolic status that were induced at 3 h p.i. and at 24 h p.i by the different strains used in the study.

3.3.1 | Expression studies

We decided to study the expression of different staphylococcal genes involved in regulation (*sig*B, *sar*A, *sar*S, *agr*, and *rot*), adhesion—MSCRAMMS (*bbp*, *fnb*A/B, and *sdr*E), toxicity (*psm*A, *hla*, and *hld*), and bacterial metabolism (*uhp*T) to look for a potential relationship between variation in gene expression and the ability of *S. aureus* to internalize and persist in MG-63 cells, as well as their damaging potential.

During the experiments of MG-63 cell infection, the RNA was extracted and the expression of some regulatory, adhesion, and toxin genes was evaluated at 3 h p.i. and 24 h p.i. in comparison with non-internalized bacteria (baseline condition). All experiments were the average of three biological experiments and are reported in Figures 2–4 and Table 5, with genes subdivided based on their function.

The expression of the regulatory genes is reported in Figure 3a–c and Table 5.

In ATCC12598, *sig*B was significantly up-regulated at 24 h p.i, *sar*A and *sar*S were up-regulated at 3 h p.i. In particular, the *sig*B gene mRNA expression showed a strong, statistically significant increase at 24 h p.i. (+2.92 ± 0.27-fold change (fd); $p \leq 0.001$) versus the baseline condition and comparing 24 h versus 3 h p.i. ($p \leq 0.01$). The *sar*A gene mRNA expression showed an increase at 3 h versus baseline condition (+4.4 ± 0.98 fd, $p \leq 0.05$) and a statistically

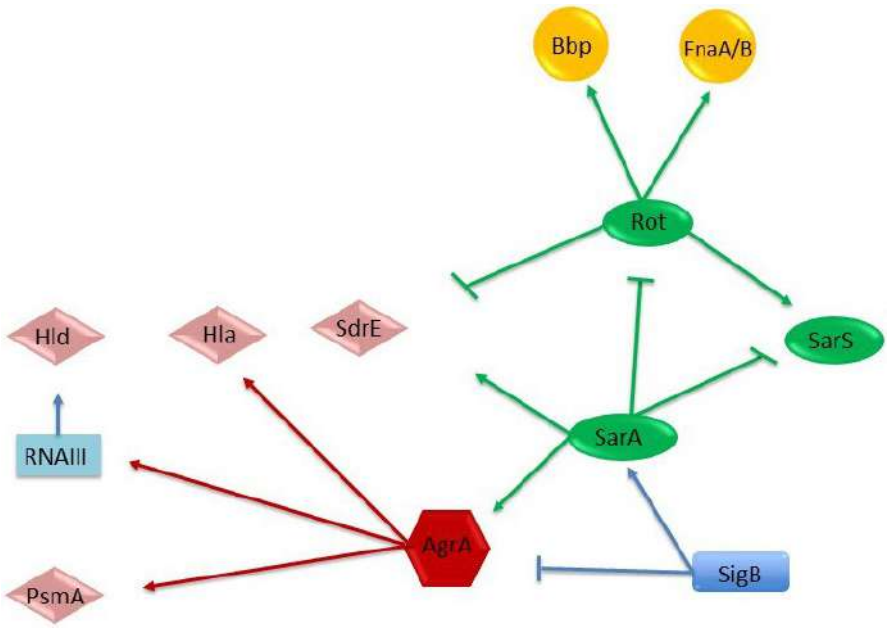

FIGURE 5 Regulation of adhesion and virulence determinants in *S. aureus* by global regulatory loci. Arrows stand for activation; bars for repression. The molecules that act as activators or repressors (members of SarA protein family, SarA, SarS, and *rot*), that is, regulating protease expression, are represented in green ovals; the alternate sigma factor (SigB) in blue rectangles; the *agr* quorum-sensing system (AgrA) in red hexagons; the toxins in pink rumbles (Hla, Hld, SdrE, and PsmA); and the adhesion factors in yellow circles (Bbp and FnaA/B) (Jenul & Horswill, 2018; Romilly et al., 2014).

significant decrease at 24 h versus baseline condition (+0.79 ± 0.36 fd, $p \leq 0.05$). The *sar*S gene mRNA expression showed an increase at 3 h versus baseline condition (+7.45 ± 0.65 fd, $p \leq 0.01$) and a statistically significant decrease at 24 h versus baseline condition (+1.83 ± 0.45 fd, $p \leq 0.01$).

Although in the ST239-III and ST228-I strains the *sig*B, *sar*A, and *sar*S gene expressions were not statistically significant, some variations were observed compared with the baseline condition. In ST239-III, the *sig*B gene expression showed a decrease at 24 h p.i; the *sar*A gene expression exhibited an increment at 24 h p.i., and the *sar*S gene expression showed a progressive increase at 3 h p.i. and 24 h p.i. In ST228-I, the *sig*B, *sar*A, and *sar*S gene expression showed a slight increase at 3 h p.i., followed by a decrease at 24 h p.i.

The *rot* gene was significantly down-regulated at 24 h p.i. in the ST228 strain only. The *rot* gene mRNA expression in the ST228 strain showed a statistically significant decrease at 24 h p.i. versus baseline condition (+0.23 ± 0.016 fd, $p \leq 0.05$) and versus 3 h p.i. ($p \leq 0.05$). Although no statistical differences were observed for ATCC12598 and ST239-III, there was a down-regulation versus baseline condition.

The expression of the MSCRAMM genes is reported in Figure 3a–c and Table 5. All MSCRAMM genes were differently modulated in our sample.

In the ATCC12598 strain, the *fnb*A gene mRNA expression showed a statistically significant increase at 3 h p.i. versus baseline condition (+4255.6 ± 1052.8 fd, $p \leq 0.05$) and a statistically significant decrease at 24 h p.i. versus 3 h (+86.9 ± 28.03 fd, $p \leq 0.05$). The *sdr*E gene mRNA expression exhibited a statistically significant increase at 3 h p.i. versus baseline condition (+10.63 ± 2.48 fd, $p \leq 0.05$) and a statistically significant decrease at 24 h p.i. versus 3 h (+1.55 ± 0.1 fd, $p \leq 0.05$).

The *bbp* gene mRNA expression showed a statistically significant increase (+2318.32 ± 801.5 fd, $p \leq 0.05$) in the ST239-III strain at 3 h p.i. versus baseline condition and at 24 h p.i. versus baseline condition (+2897.22 ± 156.12 fd, $p \leq 0.05$). For the *fnb*B gene and the other strains, no other statistical differences were observed in each condition considered. Expression of toxin genes and the sugar phosphate antiporter gene is reported in Figure 4a–c and Table 5.

The *psm*A gene mRNA expression in the ATCC12598 strain showed a statistically significant increase (+6.75 ± 3.75 fd, $p \leq 0.05$) at 3 h p.i. vs. 24 h p.i. In the ST228-I strain, this gene was statistically significantly up-regulated (+32.84 ± 11.5 fd, $p \leq 0.05$) at 3 h p.i versus baseline condition.

The *hla* gene mRNA expression showed a significant increase in the ATCC12598 strain (+1308.64 ± 323.75 fd, $p \leq 0.05$) at 3 h p.i. versus baseline condition and a statistically significant decrease when comparing 24 h p.i. versus 3 h p.i. (17.58 ± 6.4 fd; $p \leq 0.05$). In the ST239-III strain, this gene showed a statistically significant increase at 3 h p.i. and 24 h p.i. when comparing 3 h p.i. versus baseline condition (4922.01 ± 840.23 fd, $p \leq 0.01$ and 26698.18 ± 130.85 fd, $p \leq 0.001$) and when comparing 3 h p.i versus 24 h p.i. ($p \leq 0.001$). The *hld* gene mRNA expression showed a significant decrease in ATCC12598 at 24 h p.i. versus baseline condition (0.04 ± 0.04 fd; $p \leq 0.05$). For the other strains, in each condition considered, no statistically significant differences were observed. The mRNA expression of the *uhp*T gene showed a statistically significant difference in the ATCC12598 strain only, in particular, an up-regulation when comparing 3 h p.i. versus baseline condition (16.85 ± 1.5 fd; $p \leq 0.05$) and a down-regulation when comparing 24 h p.i. versus 3 h p.i. (5.32 ± 2.27 fd; $p \leq 0.05$).

These findings support the idea that variations in the regulator, MSCRAMM, toxins, and metabolic gene transcription were related to the degree of invasiveness and persistence in MG-63 cells.

4 | DISCUSSION

Internalization of *S. aureus* in non-phagocytic cells is an attractive field of study owing to the particular ability of this microorganism to generate chronic diseases.

The process of internalization includes different phases: In the early phase, microbial surface proteins (MSCRAMMs) are implicated in host cell adhesion and invasion, fighting against the immune system and entering the deep tissue structure (Painter et al., 2014); subsequently, the pathogenicity and virulence of *S. aureus* depend on the ability to produce several virulence factors including enterotoxins (SEs) and toxic shock syndrome toxin-1 (TSST), pore-forming toxins (hemolysins; Panton–Valentine leukocidin; phenol-soluble modulins), exfoliative toxins (ETs), protein A, and several enzymes able to damage host cells by their cytotoxic/cytolytic activity and through modulation of immune responses.

In a previous study, we analyzed the different proclivity of the main staphylococcal clones to invade, internalize, and persist within human cells, using a highly performing IFC assay. In particular, we demonstrated that ST5-II, ST8-IV, and ST228-I showed a statistically significant lower aptitude to intracellular subsistence, while ST239-III and ST22-IVh isolates had intracellular frequencies equal to, or greater than, those of the invasive ATCC12598 strain, suggesting their possible role as invasive and persistent clones responsible for chronic and recurrent infections (Bongiorno et al., 2020).

Based on the above observations, we used the same infection models to examine the differential expression of a set of genes responsible for the adhesion, invasion, and internalization of two *S. aureus* clones ST239-III and ST228-I compared with the control invasive ATCC12598 isolate.

The pathotype gene profile of the two strains included in the study showed only a few differences.

S. aureus ST228-I is one of the most predominant clones associated with orthopedic infection (Jain et al., 2019) showing a high rate of virulence, drug resistance, and longer duration of hospitalization. It exhibited two more enterotoxins (SEA and SEO), suggesting a potentially augmented role in eliciting and deregulating the immune system of the host (Hussain et al., 2009).

Conversely, ST239-III was the only strain carrying the *hlb* gene coding for a pore-forming toxin involved in chronic skin infections and phagosomal escape (Katayama et al., 2013) and producing δ-hemolysis, demonstrating that the *agr* locus is not defective. Moreover, this strain, belonging to the ST239 clone, did not carry the other toxin genes; therefore, its ability to damage host cells is related to *hla* and *psmα* or other unknown factors.

To further investigate these differences, we evaluated the expression of a selected set of genes grouped into three different general categories, that is, regulators, adhesion factors (MSCRAMMs), and toxins (Table 6, Figure 5). Moreover, to evaluate the metabolic activity of internalized bacteria, we evaluated a hexose phosphate antiporter for G6P. The expression of the regulatory global network SigB, SarA, SarS, *agr* locus, and Rot controls the expression of a set

TABLE 6 Comparison of % internalized MG-63, cellular metabolic status, adhesin, and toxin gene regulation

Strains	Time	MG-63 internalized	% of Cellular metabolic status variation versus uninfected MG-63	Regulator Expression					Adhesin and Toxin Expression						Metabolism expression
				sigB	*sarA*	*sarS*	*agr*	*rot*	*bbp*	*fnbA*	*fnbB*	*sdrE*	*psmA*	*hla*	*hld*	*uhpT*
ATCC12598	3h	70%	+12.27 ↑	=	↑**	↑**	=	↓	↓	↑*	↓	↑*	↑*	↑*	↓	↑*
	24h	~50%	−7.11 ↓	↑**	=	↓	↓	↓	↓	=	=	=	↓	↓	↓*	↓
ST239-SCC*mec*III	3h	50%	−2.47 ↓	↓	=	↓	↓	↓	↓*	↓	↓	↓	↓	↑*	↓	↓
	24h	45%	−18.32 ↓	↓	↓	↓	↓	↓	↓*	↓	↓	=	=	↑*	↓	=
ST228-SCC*mec*I	3h	~30%	+7.57 =	↓	↓	↓	↓	=	↓	↓	↓	↓	↑*	↓	↓	↓
	24h	20%	+3.29 =	↓	↓	↓	↓	↓*	↓	=	=	↓	↓	↓	↓	↓

Statistical significance: not significant (gray arrow), *p*-value: ≤0.05 (*); ≤0.01 (**); and ≤0.001 (***).

of virulence factors involved in adhesion and cytotoxic/cytolytic activities.

The genes responsible for invasiveness and persistence were analyzed by comparing the ability to infect and internalize into MG-63 osteoblasts, according to their cytotoxic potential (based on the cellular metabolic status of infected MG-63 osteoblasts) and the expression levels of surface and secreted toxins at 3 h and 24 h p.i.

As preliminarily observed and now confirmed (Bongiorno et al., 2020), the ability of ATCC12598-ST30 and MRSA ST239-III to internalize and persist in MG-63 is quite similar (ATCC12598 internalized into 70% of MG-63 cells and persisted in 49% of MG-63 cells; ST239-III internalized into 50% of MG-63 cells and persisted in 45% of MG-63 cells), while MRSA ST228-I behaves differently (internalized into 29% of MG-63 cells and persisted in the 20% of MG-63 cells).

These differences among clones were also evaluated by measuring the metabolic status of MG-63 cells in terms of cytotoxicity, demonstrating that ST239-III was immediately able to decrease the metabolic activity of cells at 3 h p.i. (cellular metabolic status detected −2.47 vs. uninfected MG-63 cells) and further damaged cells at 24 h p.i. (cellular metabolic status detected −18.32 vs. uninfected MG-63 cells). The ATCC12598 clone was able to interfere with the MG-63 cells at 24 h p.i. (cellular metabolic status detected −7.11 vs. uninfected control MG-63), while ST228 affected the metabolic status of the cells only slightly.

These results are in agreement with other studies (Botelho et al., 2019), demonstrating that the ST239-III clone can adapt to diverse pathological conditions (diverse syndromes) and undergo genomic adaptations, thus developing a distinct pattern of virulence-associated genes.

The ATCC12598 strain was included as an invasive model. It displayed, at 3 h p.i., a higher ability to infect and internalize into MG-63 human osteoblasts (70%), associated with a significant increase in the cellular metabolic status compared with the uninfected cell line. At 24 h p.i., although intracellular persistence decreased to 50%, ATCC12598 bacteria exerted a high intracellular cytotoxic activity against osteoblasts, as demonstrated by a decrease in the cellular metabolic status. The regulation of gene expression in ATCC12598 during the internalization and, especially, the persistence steps, followed an expected scheme: A significant increase in the expression of genes involved in adaptation to environmental stress (in particular *sar*A, *sig*B), resulting in up-regulated expression of genes involved both in adherence (in particular to *fnb*A and *sdr*E) in and virulence (*psm*A and *hla*) at 3 h p.i, although *rot*, the toxin repressor gene, did not undergo statistically significant changes, which is still in line with the expression of toxins.

In particular, *psm*A and *hla* overexpression may be related to the 20% decrease in persistence; moreover, the overexpression of α-hemolysin may enhance internalization and survival by modulating osteoblast expression of β1 integrin, as previously reported (Goldmann et al., 2016), and may also be involved in pore formation and cellular lysis, which might explain the decrease in cellular metabolism associated with enhanced cytotoxic activity. This is in line with previous studies in which *hla* expression was a requirement for the pathogenesis of the invasive disease (Oliveira et al., 2018). At 24 h p.i, an over decrease in the expression of regulatory genes was observed, except for *sig*B, probably due to cellular stimulation, which resulted in a decreased expression of genes involved in adhesion (*fnb*A and *sdr*E) and virulence (*psm*A and *hla*). We can conclude that, for the ATCC12598 strain, all events involving both adhesion/invasion and damage to host cells occurred within 3 h p.i. Furthermore, its metabolism, adapted to intracellular conditions, showed up-regulation of the alternative antiporter of carbon source (UhpT) at 3 h p.i., as confirmed by the 12% increase in the cellular metabolic status, while there was a significant decrease in metabolism at 24 h p.i. versus 3 h p.i., as confirmed by the loss of −7.11% of the cell metabolic status. As the *hld* gene expression was down-regulated in ATCC12598, we can conclude that this gene was not involved in cellular adaptation or invasion.

The strain belonging to ST239-III, which did not show any toxin gene (Botelho et al., 2019) except for *sdr*E and *hla*, *hlb* and *hld*, was able to infect (3 h p.i.) 50% of MG-63 human osteoblasts and induced a slowdown of the cell metabolic activity, which may be due to the production of hemolysins Hlb, Hla, and PsmA. The ST239-III strain displayed, at 3 h p.i., a significant increase in *bbp* that is necessary for adhesion and invasion in MG-63 cells, and an increase in *agr*A expression (although not statistically significant), resulting in an up-regulation of *hla* and an increase in *psm*A expression (although not statistically significant), associated with a good ability to internalize into and infect MG-63 cells. At 24 h p.i., ST239-III bacteria stably persisted intracellularly (45%) and exerted a highly significant cytotoxic activity against osteoblasts, due to the overexpression of *hla*, as demonstrated by a remarkable decrease in the cellular metabolic status, also confirmed by the expression of the *uhp*T gene (although not statistically significant). Some studies have demonstrated the importance of this toxin for *S. aureus* pathogenicity, phagosomal escape, and induction of biofilm formation (Katayama et al., 2013; Tajima et al., 2009). At 24 h p.i., increased expression of the genes involved in adhesion was detected. A possible explanation could be that bacterial cells exit and enter MG-63 cells through their membrane, using the integrins located in the cell wall.

The significantly higher rates of intracellular invasion by ST239-III bacteria could justify their cytotoxicity despite the loss of toxin production and contribute to their survival in a higher number. These findings suggest that ST239-III is associated with an intracellular adaptation that leads to decreased virulence and host immune escape, making this clone more prone to persistent infections.

During internalization and persistence, we did not find any difference in the expression of the genes involved in adaptation to environmental stress (*sar*A, *sig*B, sarS, *agr*) and of those involved in adherence (*fnb*A and *fnb*B) with respect to the baseline condition; this phenomenon could be probably because these genes were normally overexpressed at the baseline condition, while, under the same conditions, the genes involved in toxicity and phagosomal escape (*psm*A and *hla*) were down-regulated. This regulation was in line with *rot* expression.

On the contrary, the strain belonging to ST228-I was found to be less able to internalize (30%) at 3 h p.i.; correlation analysis between regulatory genes and virulence factors showed that at 3 h p.i., the ST228-I strain displayed a baseline level of *agr*A expression and an up-regulation of *sig*B and *sar*A, leading to up-regulation of the surface proteins and up-regulation of secreted toxins, such as PSMα, Hla, and Hld, associated with a significant non-cytotoxic activity inside osteoblasts, and a lower ability to internalize into and infect MG-63 cells. Even if these variations were not statistically significant, their expression levels showed an expected scheme. This strain is also characterized by the presence of the *pls* gene, carried by SCC*mec*I, known to be involved in the failure to adhere to the cell surface (Hussain et al., 2009).

After 24 h of intracellular persistence, all regulatory genes were down-expressed, in particular, *rot* and consequently the genes involved in adhesion and virulence (except for an increased expression of *hla* at 3 h p.i.): 20% of MG-63 cells were infected, and the cellular metabolic status did not show any variation compared with the uninfected cell line; the expression of *uhp*T supported these results.

The impact of PSMα suggests that regardless of the lower invasiveness, ST228 bacteria exert their potential to damage osteoblasts by a cytotoxic effect. ST228 is not capable of activating a sufficient cellular reaction; quite on the contrary, it seemed to "succumb" inside MG-63 cells. This variation in the expression of *agr*, *sig*B, *rot*, *hla*, and *fnb*A was previously associated with the switch from an extracellular to an intracellular behavior, due to changes in the expression of the fibronectin-binding protein and adhesion-binding protein, important for host/cell invasion but not required difficult for intracellular persistence (Tuchscherr & Löffler, 2016).

Although *rot* variations were not statistically significant, except for the ST228-I strain at 24 h p.i., they were still in line with the variations found in the toxin genes. Two further considerations are necessary: The regulation of toxin production was not dependent on *rot* regulation only, but also on other members of the SarA family, accessory sensor/regulators (RSP), and/or two-component systems (i.e., SaeRS) (Horn et al., 2018); and *rot* was regulated by other genes, which have not been considered in this context, such as *rbf* (Gimza et al., 2019).

Our results, arising from the qualitative and quantitative assays of virulence and toxin factors, are in line with recently published studies according to which the genetic and phenotypic different characteristics of staphylococcal strains favor the infection process, invasiveness, and persistence inside host cells (Davis & Isberg, 2019; Recker et al., 2017; Tuchscherr et al., 2019). In our study, we analyzed two different genetic backgrounds to elucidate how bacteria can differently adapt strategies thanks to the interplay among regulatory and adhesion/toxin genes and rapidly react to changing environmental conditions and dynamically adjust their virulence factor expression at different times of infection. This ability was identified in the ST239-III clone and not in others.

5 | CONCLUSION

We found that the ST239-III clone was able to infect, at 3 h p.i., 50% of MG-63 human osteoblasts, and this rate stably persisted at 24 h p.i.; during the infection period, it exerted a highly significant cytotoxic activity against osteoblasts, due to the overexpression of *hla*, as demonstrated by a remarkable decrease in the cellular metabolic status. The increase in *hla* and, to a lesser extent, of *psm*A has as a consequence the increased expression of genes involved in adhesion (*bbp*), probably due to the release and re-entry of bacteria inside MG-63 cells at 24 h p.i. Our results lead us to conclude that the ST239-III clone is more prone to persistent infections. Recent data from our group considering pro-inflammatory and pro-oxidant response in an ST239-III osteoblast infection demonstrated a significant increase in gene expression of both interleukin-6 and TNF-α (Musso et al., 2021).

On the contrary, ST228-I was found to be less able to internalize (30%), compared with the control strain and ST239-III at 3 h p.i., and to persist (20%) at 24 h p.i., and this lower invasiveness was also correlated with the non-cytotoxic activity inside osteoblasts. This is probably due to the presence of the *pls* gene in SCC*mec*I, which is involved in the failure to adhere to the cell surface. This clone is not able to activate a sufficient cellular reaction and succumbs inside MG-63 cells.

Our idea is to consider new strategies, including a clonal and translational approach. We believe that our translational approach—eukaryotic host–pathogen interaction (EHPI)—based on the study of the genetic and biochemical basis of both pathogen and host can be applied on a large scale to predict *S. aureus* /osteoblast interaction and treat bone infections.

ETHICS STATEMENT

None required.

ACKNOWLEDGEMENTS

Some of the results of this study were presented at the 29th ECCMID (O0927) and the 44th Italian Society of Microbiology (SIM) congress (P127). We would like to thank the BRIT laboratory at the University of Catania (Italy) for valuable technical assistance and use of their laboratories. We also wish to thank the PharmaTranslated (http://www.pharmatranslated.com/) and in particular to Silvia Montanari for language support. The manuscript was partially supported by: a research grant project number PRIN2017SFBFER from the Ministry of Research (MIUR) Italy; a research grant from a private company; a research grant entitled "Fragment-sized covalent inhibitors of MAOs to fight neurodegenerative diseases and repositioning against the 3CLPro main protease of the SARS-COV-2 and bacterial resistances [CovDock], 'Programma PIACERI – Linea di intervento 2'. University of Catania, Dept. of Biomedical and Biotechnological Sciences."

CONFLICT OF INTEREST

None declared.

AUTHOR CONTRIBUTIONS

Dafne Bongiorno: Conceptualization (equal); Investigation (equal); Methodology (equal); Project administration (lead); Validation

(equal); Visualization (equal); Writing-original draft (equal); Writing-review & editing (equal). **Nicolò Musso:** Conceptualization (equal); Formal analysis (equal); Investigation (equal); Methodology (equal); Project administration (supporting); Validation (equal); Visualization (equal); Writing-original draft (equal); Writing-review & editing (supporting). **Giuseppe Caruso:** Formal analysis (equal); Investigation (equal); Methodology (equal); Validation (equal); Visualization (equal). **Lorenzo Mattia Lazzaro:** Formal analysis (supporting); Investigation (supporting). **Filippo Caraci:** Resources (equal). **Stefania Stefani:** Funding acquisition (equal); Resources (equal); Supervision (equal); Writing-review & editing (equal). **Floriana Campanile:** Conceptualization (equal); Funding acquisition (equal); Methodology (supporting); Resources (equal); Supervision (equal); Writing-review & editing (equal).

DATA AVAILABILITY STATEMENT

All data generated or analyzed during this study are included in this published article.

ORCID

Dafne Bongiorno https://orcid.org/0000-0002-8672-0484
Nicolò Musso https://orcid.org/0000-0003-2451-1158
Giuseppe Caruso https://orcid.org/0000-0003-1571-5327
Filippo Caraci https://orcid.org/0000-0002-9867-6054
Stefania Stefani https://orcid.org/0000-0003-1594-7427
Floriana Campanile https://orcid.org/0000-0002-8405-5425

REFERENCES

Bongiorno, D., Mongelli, G., Stefani, S., & Campanile, F. (2018). Burden of rifampicin- and methicillin-resistant *Staphylococcus aureus* in Italy. *Microbial Drug Resistance*, *24*, 732–738.

Bongiorno, D., Musso, N., Lazzaro, L. M., Mongelli, G., Stefani, S., & Campanile, F. (2020). Detection of methicillin-resistant *Staphylococcus aureus* persistence in osteoblasts using imaging flow cytometry. *Microbiologyopen*. *2020*, e1017. https://doi.org/10.1002/mbo3.1017

Botelho, A. M., Cerqueira e Costa, M. O., Moustafa, A. M., Beltrame, C. O., Ferreira, F. A., Côrtes, M. F., Costa, B. S., Silva, D. N., Bandeira, P. T., Lima, N. C., & Souza, R. C. (2019). Local diversification of methicillin-resistant *Staphylococcus aureus* ST239 in South America after its rapid worldwide dissemination. *Frontiers in Microbiology*, *10*, 82. https://doi.org/10.3389/fmicb.2019.00082. eCollection.

Cafiso, V., Bertuccio, T., Purrello, S., Campanile, F., Mammina, C., Sartor, A., Raglio, A., & Stefani, S. (2014). dltA overexpression: A strain-independent keystone of daptomycin resistance in methicillin-resistant *Staphylococcus aureus*. *International Journal of Antimicrobial Agents*, *43*(1), 26–31. https://doi.org/10.1016/j.ijantimicag.2013.10.001

Cafiso, V., Bertuccio, T., Spina, D., Purrello, S., Blandino, G., & Stefani, S. (2012). A novel δ-hemolysis screening method for detecting heteroresistant vancomycin-intermediate *Staphylococcus aureus* and vancomycin-intermediate *S. aureus*. *Journal of Clinical Microbiology*, *50*(5), 1742–1744. https://doi.org/10.1128/JCM.06307-11

Cafiso, V., Bertuccio, T., Spina, D., Purrello, S., Campanile, F., Di Pietro, C., Purrello, M., & Stefani, S. (2012). Modulating activity of vancomycin and daptomycin on the expression of autolysis cell-wall turnover and membrane charge genes in hVISA and VISA strains. *PLoS One*, *7*(1), e29573. https://doi.org/10.1371/journal.pone.0029573

Campanile, F., Bongiorno, D., Falcone, M., Vailati, F., Pasticci, M. B., Perez, M., Raglio, A., Rumpianesi, F., Scuderi, C., Suter, F., Venditti, M., Venturelli, C., Ravasio, V., Codeluppi, M., & Stefani, S. (2012). Changing Italian nosocomial-community trends and heteroresistance in *Staphylococcus aureus* from bacteremia and endocarditis. *European Journal of Clinical Microbiology and Infectious Diseases*, *31*(5), 739–745. https://doi.org/10.1007/s10096-011-1367-y. Epub 2011 Aug 7.

Campanile, F., Bongiorno, D., Perez, M., Mongelli, G., Sessa, L., Benvenuto, S., Gona, F., Varaldo, P. E., & Stefani, S. (2015). Epidemiology of *Staphylococcus aureus* in Italy: First nationwide survey, 2012. *Journal of Global Antimicrobial Resistance*, *3*(4), 247–254. https://doi.org/10.1016/j.jgar.2015.06.006

Chen, L., Shopsin, B., Zhao, Y., Smyth, D., Wasserman, G. A., Fang, C., Liu, L., & Kreiswirth, B. N. (2012). Real-time nucleic acid sequence-based amplification assay for rapid detection and quantification of *agr* functionality in clinical *Staphylococcus aureus isolates*. *Journal of Clinical Microbiology*, *50*(3), 657–661. https://doi.org/10.1128/JCM.06253-11.

Davido, B., Saleh-Mghir, A., Laurent, F., Danel, C., Couzon, F., Gatin, L., Vandenesch, F., Rasigade, J. P., & Crémieux, A. C. (2016). Phenol-soluble modulins contribute to early sepsis dissemination not late local USA300-osteomyelitis severity in rabbits. *PLoS One*, *11*(6), e0157133. https://doi.org/10.1371/journal.pone.0157133

Davis, K. M., Isberg, R.. (2019). One for all, but not all for one: Social behavior during bacterial diseases. *Trends in Microbiology*, *27*(1), 64–74. https://doi.org/10.1016/j.tim.2018.09.001

Fresta, C. G., Chakraborty, A., Wijesinghe, M. B., Amorini, A. M., Lazzarino, G., Lazzarino, G., Tavazzi, B., Lunte, S. M., Caraci, F., Dhar, P., & Caruso, G. (2018). Non-toxic engineered carbon nanodiamond concentrations induce oxidative/nitrosative stress, imbalance of energy metabolism, and mitochondrial dysfunction in microglial and alveolar basal epithelial cells. *Cell Death & Disease*, *9*, 245. https://doi.org/10.1038/s41419-018-0280-z

Fresta, C. G., Fidilio, A., Lazzarino, G., Musso, N., Grasso, M., Merlo, S., Amorini, A. M., Bucolo, C., Tavazzi, B., Lazzarino, G., Lunte, S. M., Caraci, F., & Caruso, G. (2020). Modulation of Pro-oxidant and pro-inflammatory activities of M1 macrophages by the natural dipeptide carnosine. *International Journal of Molecular Sciences*, *21*(3), E776. https://doi.org/10.3390/ijms21030776

Gilot, P., Lina, G., Cochard, T., & Poutrel, B. (2002). Analysis of the genetic variability of genes encoding the RNA III-activating components Agr and TRAP in a population of *Staphylococcus aureus* strains isolated from cows with mastitis. *Journal of Clinical Microbiology*, *40*(11), 4060–4067. https://doi.org/10.1128/JCM.40.11.4060-4067.2002

Gimza, B. D., Larias, M. I., Budny, B. G., & Shaw, L. N. (2019). Mapping the global network of extracellular protease regulation in *Staphylococcus aureus*. *mSphere*, *4*(5):e00676–19. https://doi.org/10.1128/mSphere.00676-19.

Goldmann, O., Tuchscherr, L., Rohde, M., & Medina, E. (2016). α-Hemolysin enhances *Staphylococcus aureus* internalization and survival within mast cells by modulating the expression of β1 integrin. *Cellular Microbiology*, *18*(6), 807–819.

Herr, A. B., & Thorman, A. W. (2017). Hiding in plain sight: Immune evasion by the staphylococcal protein SdrE. *The Biochemical Journal*, *474*(11), 1803–1806. https://doi.org/10.1042/BCJ20170132

Horn, J., Stelzner, K., Rudel, T., & Fraunholz, M. (2018). Inside job: *Staphylococcus aureus* host-pathogen interactions. *International Journal of Medical Microbiology*, *308*(6), 607–624. https://doi.org/10.1016/j.ijmm.2017.11.009

Hussain, M., Schäfer, D., Juuti, K. M., Peters, G., Haslinger-Löffler, B., Kuusela, P. I., & Sinha, B. (2009). Expression of PLS (plasmin sensitive) in *Staphylococcus aureus* negative for PLS reduces adherence and cellular invasion and acts by steric hindrance. *Journal of Infectious Diseases*, *200*(1), 107–117. https://doi.org/10.1086/599359.

Jain, S., Chowdhury, R., Datta, M., Chowdhury, G., & Mukhopadhyay, A. K. (2019). Characterization of the clonal profile of methicillin resistant *Staphylococcus aureus* isolated from patients with early postoperative orthopedic implant-based infections. *Annals of Clinical Microbiology and Antimicrobials*, *18*(1), 8. https://doi.org/10.1186/s12941-019-0307-z

Jenul, C., & Horswill, A. R. (2018). Regulation of *Staphylococcus aureus* virulence. *Microbiology Spectrum*, *7*(2), https://doi.org/10.1128/microbiolspec.GPP3-0031-2018

Katayama, Y., Baba, T., Sekine, M., Fukuda, M., Hiramatsu, K.. (2013). Beta-hemolysin promotes skin colonization by *Staphylococcus aureus*. *Journal of Bacteriology*, *195*(6), 1194–1203. https://doi.org/10.1128/JB.01786-12

Monecke, S., Slickers, P., Gawlik, D., Müller, E., Reissig, A., Ruppelt-Lorz, A., Akpaka, P. E., Bandt, D., Bes, M., Boswihi, S. S., Coleman, D. C., Coombs, G. W., Dorneanu, O. S., Gostev, V. V., Ip, M., Jamil, B., Jatzwauk, L., Narvaez, M., Roberts, R., … Ehricht, R. (2018). Molecular typing of ST239-MRSA-III from diverse geographic locations and the evolution of the SCCmec III element during its intercontinental spread. *Frontiers in Microbiology*, *9*, 1436. https://doi.org/10.3389/fmicb.2018.01436

Moore, A. J., Whitehouse, M. R., Gooberman-Hill, R., Heddington, J., Beswick, A. D., Blom, A. W., & Peters, T. J. (2017). A UK national survey of care pathways and support offered to patients receiving revision surgery for prosthetic joint infection in the highest volume NHS orthopaedic centres. *Musculoskeletal Care*, *15*, 379–385. https://doi.org/10.1002/msc.1186

Mruk, A. L., & Record, K. E. (2012). Antimicrobial options in the treatment of adult staphylococcal bone and joint infections in an era of drug shortages. *Orthopedics*, *35*(5), 401–407. https://doi.org/10.3928/01477447-20120426-07

Muñoz-Gallego, I., Lora-Tamayo, J., Pérez-Montarelo, D., Brañas, P., Viedma, E., & Chaves, F. (2017). Influence of molecular characteristics in the prognosis of methicillin-resistant *Staphylococcus aureus* prosthetic joint infections: Beyond the species and the antibiogram. *Infection*, *45*(4), 533–537. https://doi.org/10.1007/s15010-017-1011-6. Epub 2017 Apr 7.

Musso, N., Caruso, G., Bongiorno, D., Grasso, M., Bivona, D. A., Campanile, F., Caraci, F., & Stefani, S. (2021). Different modulatory effects of four methicillin-resistant *Staphylococcus aureus* clones on MG-63 osteoblast-like cells. *Biomolecules*, *11*(1), 72. https://doi.org/10.3390/biom11010072

Oliveira, D., Borges, A., & Simões, M. (2018). *Staphylococcus aureus* toxins and their molecular activity in infectious diseases. *Toxins*, *10*(6), 252. https://doi.org/10.3390/toxins10060252.

Otsuka, T., Saito, K., Dohmae, S., Takano, T., Higuchi, W., Takizawa, Y., Okubo, T., Iwakura, N., & Yamamoto, T. (2006). Key adhesin gene in community-acquired methicillin-resistant *Staphylococcus aureus*. *Biochemical and Biophysical Research Communications*, *346*(4), 1234–1244. https://doi.org/10.1016/j.bbrc.2006.06.038

Painter, K. L., Krishna, A., Wigneshweraraj, S., & Edwards, A. M. (2014). What role does the quorum-sensing accessory gene regulator system play during *Staphylococcus aureus* bacteremia? *Trends in Microbiology*, *22*(12), 676–685. https://doi.org/10.1016/j.tim.2014.09.002. Epub 2014 Oct 6.

Pedotti, S., Ussia, M., Patti, A., Musso, N., Barresi, V., & Condorelli, D. F. (2017). Synthesis of the ferrocenyl analogue of clotrimazole drug. *Journal of Organometallic Chemistry*, *830*, 56–61. https://doi.org/10.1016/j.jorganchem.2016.12.009

Peng, K. T., Huang, T. Y., Chiang, Y. C., Hsu, Y. Y., Chuang, F. Y., Lee, C. W., & Chang, P. J. (2019). Comparison of methicillin-resistant *Staphylococcus aureus* isolates from cellulitis and from osteomyelitis in a Taiwan Hospital, 2016–2018. *Journal of Clinical Medicine*, *8*(6), 2016–2018. https://doi.org/10.3390/jcm8060816

Pérez-Montarelo, D., Viedma, E., Larrosa, N., Gómez-González, C., Ruiz de Gopegui, E., Muñoz-Gallego, I., San Juan, R., Fernández-Hidalgo, N., Almirante, B., & Chaves, F. (2018). Molecular epidemiology of *Staphylococcus aureus* bacteremia: Association of molecular factors with the source of infection. . *Frontiers in Microbiology*, *9*, 2210. https://doi.org/10.3389/fmicb.2018.02210. eCollection 2018.

Purrello, S. M., Garau, J., Giamarellos, E., Mazzei, T., Pea, F., Soriano, A., & Stefani, S. (2016). Methicillin-resistant *Staphylococcus aureus* infections: A review of the currently available treatment options. *Journal of Global Antimicrobial Resistance*, *7*, 178–186. https://doi.org/10.1016/j.jgar.2016.07.010

Recker, M., Laabei, M., Toleman, M. S., Reuter, S., Saunderson, R. B., Blane, B., Török, M. E., Ouadi, K., Stevens, E., Yokoyama, M., & Steventon, J. (2017). Clonal differences in *Staphylococcus aureus* bacteremia-associated mortality. *Nature Microbiology*, *2*(10), 1381–1388. https://doi.org/10.1038/s41564-017-0001-x. Epub 2017 Aug 7.

Romilly, C., Lays, C., Tomasini, A., Caldelari, I., Benito, Y., Hammann, P., Geissmann, T., Boisset, S., Romby, P., & Vandenesch, F. (2014). A non-coding RNA promotes bacterial persistence and decreases virulence by regulating a regulator in *Staphylococcus aureus*. *PLoS Path*, *10*(3), e1003979. https://doi.org/10.1371/journal.ppat.1003979

Shinji, H., Yosizawa, Y., Tajima, A., Iwase, T., Sugimoto, S., Seki, K., & Mizunoe, Y. (2011). Role of fibronectin-binding proteins A and B in *in vitro* cellular infections and *in vivo* septic infections by *Staphylococcus aureus*. *Infection and Immunity*, *79*(6), 2215–2223. https://doi.org/10.1128/IAI.00133-11. Epub 2011 Mar 21.l

Stefani, S., Bongiorno, D., Cafiso, V., Campanile, F., Crapis, M., Cristini, F., Sartor, A., Scarparo, C., Spina, D., & Viale, P. (2009). Pathotype and susceptibility profile of a community-acquired methicillin-resistant *Staphylococcus aureus* strain responsible for a case of severe pneumonia. *Diagnostic Microbiology and Infectious Disease*, *63*(1), 100–104. https://doi.org/10.1016/j.diagmicrobio.2008.09.012

Stefani, S., Chung, D. R., Lindsay, J. A., Friedrich, A. W., Kearns, A. M., Westh, H., & Mackenzie, F. M. (2012). Methicillin-resistant *Staphylococcus aureus* (MRSA): Global epidemiology and harmonization of typing methods. *International Journal of Antimicrobial Agents*, *39*, 273–282. https://doi.org/10.1016/j.ijantimicag.2011.09.030. Epub 2012 Jan 9.

Szymanek-Majchrzak, K., Mlynarczyk, A., & Mlynarczyk, G. (2018). Characteristics of glycopeptide-resistant *Staphylococcus aureus* strains isolated from inpatients of three teaching hospitals in Warsaw, Poland. *Antimicrobial Resistance & Infection Control 7*, 105. https://doi.org/10.1186/s13756-018-0397-y. eCollection

Tajima, A., Iwase, T., Shinji, H., Seki, K., & Mizunoe, Y. (2009). Inhibition of endothelial interleukin-8 production and neutrophil transmigration by *Staphylococcus aureus* beta-hemolysin. *Infection and Immunity*, *77*(1), 327–334. https://doi.org/10.1128/IAI.00748-08. Epub 2008 Oct 20.

Tong, S. Y., Davis, J. S., Eichenberger, E., Holland, T. L., & Fowler, V. G. (2015). *Staphylococcus aureus* infections: Epidemiology, pathophysiology, clinical manifestations, and management. *Clinical Microbiology Reviews*, *28*(3), 603–661. https://doi.org/10.1128/CMR.00134-14

Tuchscherr, L., Bischoff, M., Lattar, S. M., Noto Llana, M., Pförtner, H., Niemann, S., Geraci, J., Van de Vyver, H., Fraunholz, M. J., Cheung, A. L., Herrmann, M., Völker, U., Sordelli, D. O., Peters, G., & Löffler, B. (2015). (2015) Sigma factor SigB Is crucial to mediate *Staphylococcus aureus* adaptation during chronic infections. *PLoS Path*, *11*(4), e1004870. https://doi.org/10.1371/journal.ppat.1004870. eCollection.

Tuchscherr, L., & Löffler, B. (2016). *Staphylococcus aureus* dynamically adapts global regulators and virulence factor expression in the course from acute to chronic infection. *Current Genetics*, *62*(1), 15–17. https://doi.org/10.1007/s00294-015-0503-0

Tuchscherr, L., Pöllath, C., Siegmund, A., Deinhardt-Emmer, S., Hoerr, V., Svensson, C. M., Thilo Figge, M., Monecke, S., & Löffler, B. (2019). Clinical *S. aureus* isolates vary in their virulence to promote adaptation to the host. *Toxins*, *11*(3), 135. https://doi.org/10.3390/toxins11030135

Wu, S., Huang, F., Zhang, H., & Lei, L. (2019). *Staphylococcus aureus* biofilm organization modulated by YycFG two-component regulatory pathway. *Journal of Orthopaedic Surgery and Research*, *14*(1), 10, https://doi.org/10.1186/s13018-018-1055-z

Yang, Y., Sun, H., Liu, X., Wang, M., Xue, T., & Sun, B. (2016). Regulatory mechanism of the three-component system HptRSA in glucose-6-phosphate uptake in *Staphylococcus aureus*. *Medical Microbiology and Immunology*, *205*(3), 241–253. https://doi.org/10.1007/s00430-015-0446-6.

SUPPORTING INFORMATION

Additional supporting information may be found online in the Supporting Information section.

How to cite this article: Bongiorno D, Musso N, Caruso G, et al. *Staphylococcus aureus* ST228 and ST239 as models for expression studies of diverse markers during osteoblast infection and persistence. *MicrobiologyOpen*. 2021;10:e1178. https://doi.org/10.1002/mbo3.1178

PUBLISHED WORK

Bongiorno D, Musso N, Lazzaro LM, Mongelli G, Stefani S, Campanile F. Detection of methicillin-resistant Staphylococcus aureus persistence in osteoblasts using imaging flow cytometry. Microbiologyopen. 2020 May;9(5):e1017.

Bongiorno D, Musso N, Caruso G, Lazzaro LM, Caraci F, Stefani S, Campanile F. Staphylococcus aureus ST228 and ST239 as models for expression studies of diverse markers during osteoblast infection and persistence. Microbiologyopen. 2021 Mar;10(2): e1178.

Stracquadanio S, Musso N, Costantino A, Lazzaro LM, Stefani S, Bongiorno D. Staphylococcus aureus Internalization in Osteoblast Cells: Mechanisms, Interactions and Biochemical Processes. What Did We Learn from Experimental Models? Pathogens. 2021 Feb 19;10(2):239.

3. REFERENCES

Campanile, F., Bongiorno, D., Perez, M., Mongelli, G., Sessa, L., Benvenuto, S., Stefani, S. (2015). Epidemiology of Staphylococcus aureus in Italy: First nationwide survey. Journal of Global Antimicrobial Resistance, 3, 247–254.

Cheung A. L., Eberhardt K., and Heinrichs J. H. 1997. Regulation of protein A synthesis by the *sar* and *agr* loci of Staphylococcus aureus. Infect. Immun. 65:2243–2249.

Diseases, 200(1), 107–117.

Hussain, M., Schäfer, D., Juuti, K. M., Peters, G., Haslinger-Löffler, B.,Kuusela, P. I., & Sinha, B. (2009). Expression of PLS (plasmin sensitive) in *Staphylococcus aureus* negative for PLS reduces adherence and cellular invasion and acts by steric hindrance. Journal of Infectious Diseases, 200(1), 107–117.

Lowy FD. Staphylococcus aureus infections. N Engl J Med. 1998 Aug 20;339(8):520-32.

Manna A. C., Ingavale S. S., Maloney M., van Wamel W. & Cheung A. L. (2004) J. Bacteriol. 186, 5267–5280.

Peng, K. T., Huang, T. Y., Chiang, Y. C., Hsu, Y. Y., Chuang, F. Y., Lee, C. W., & Chang, P. J. (2019). Comparison of methicillin-resistant *Staphylococcus aureus* Isolates from cellulitis and from osteomyelitis in a Taiwan Hospital, 2016–2018. Journal of Clinical Medicine, 8, 816.

Post V., P. Wahl, I. Uçkay, P. Ochsner, W. Zimmerli, S. Corvec, C. Loiez, R. G. Richards and T. F. Moriarty, "Phenotypic and genotypic characterisation of *Staphylococcus aureus* causing musculoskeletal infections," Med Microbiol, pp. 565-576, 2014.

Tuchscherr L, Heitmann V, Hussain M, Viemann D, Roth J, von Eiff C, Peters G, Becker K, Löffler B (2010) Staphylococcus aureus small-colony variants are adapted phenotypes for intracellular persistence. J Infect Dis 202:1031–1040

CHAPTER II

Ceftobiprole activity against Enterococcus faecalis: resistance development, interaction with multiple low-reactive Penicillin-Binding-Proteins (PBPs) and PBP4 alterations

1. INTRODUCTION

1.1. The Genus *Enterococcus*

Enterococci are leading causes of health care-associated infections (HAI's) globally, in particular urinary tract, soft tissue and device-associated infections, mainly responsible of bacteraemia, burn and surgical site wound infections, abdomen and biliary tract infections, infection of catheters and other implanted medical devices, considered the third most common cause of native valve endocarditis, after *Staphylococcus aureus* and Streptococci, and the third most commonly isolated nosocomial pathogens, accounting for 12% of all hospital infections **(Hollenbeck and Rice,2012)**.

The term "enterocoque" was first coined in 1899 by Thiercelin, when he described gut commensal bacteria with the ability to become pathogenic (**Thiercelin ME, 1899),** considered part of the genus *Streptococcus* and classified as group D streptococci until the mid- 1980, due to morphological and some biochemical similarities. It was only in 1984 that the formal proposal of the genus *Enterococcus* became more accepted, and it appeared as a properly recognized genus separated from the streptococci. The genus "*Enterococcus*" comprises a ubiquitous group of Gram-positive bacteria that are of great relevance to the human health for their role as major causative agents of healthcare associated infections. The members of this species are resilient and versatile, able to survive under harsh conditions, making them well adapted to the health care environment, isolated from soil, surface waters and seawater, in association with plants; in fermented food products; as part of the gut microbiota of both vertebrate and invertebrate and as causative agents of human disease **(García-Solache M and Rice LB, 2019).** Morphologically, they are non-spore forming ovoid bacteria that exist individually or as pairs, chains, or groups, chemo-organotrophic, facultative anaerobes with homofermentative metabolism, with lactic acid as the predominant final product of carbohydrate fermentation. Most enterococci are oxidase and catalase negative, salt-tolerant (as high 6.5%), resistant to 40% bile, esculin hydrolytic and able to grow in the presence of sodium azyde (up to 0.4%). Almost all species descripted and tested produce β-glucosidase; leucine arylamidase; acid from the sugars D-fructose, galactose, β-gentiobiose, glucose, lactose, maltose, D-mannose, ribose, trehalose, cellobiose and N-acetylglucosamine; and the glycosides salicin, methyl β-D-glucoside, amygdalin, and arbutin. Furthermore, enterococci are urease negative and don't produce acid from D-arabinose erythritol, D- and L-fucose, methyl -D-xyloside, and L-xylose. The growth occurs at between 10°C and 45°C, with optimal growth for most species at 35°C to 37°C, and the cells are non-motile and remarkably resistant to desiccation. They possess a low-GC genome content of about 34-45%, a genome size ranging from 2.3 to 5.4 Mb with 2.154 to 5.107 predicted genes **(Zhong Z. et al., 2017).** The separation of *Enterococcus faecalis* and *Enterococcus faecium* into two different species based on the ability of the former to tolerate potassium tellurite and produce black colonies. Additional biochemical tests, such as testing of the ability to reduce tetrazolium salts to the chromogenic formazan in the presence of glucose, were introduced along the way to improve species identification **(García-Solache M., Rice L.B., 2019).** If grown on horse-blood agar, the Enterococci can be α, β, γ-hemolytic and form 1- to 2-mm colonies with a wet appearance**.** Based on their metabolic capabilities, different selective culture media have been developed for the isolation of enterococci; these selective media frequent contains bile salts, sodium azide, antibiotics and aesculin or tetrazolium salts. The identification of enterococci at the species level has clinical relevance due to the antibiotic resistance profiles of the different pathogenic enterococci. Molecular-based-methods have the potential advantages of increased diagnostic accuracy, providing information about antimicrobial resistance, and reduced time and cost compared to phenotypic testing. Among the newer system are matrix-assisted laser desorption ionization-time of flight mass spectrometry (MALDI-TOF), nucleic acid amplification tests (NAATs), sequencing and different method

based on PCR and on real-time-quantitative polymerase-chain-reaction. (RTq-PCR), and the "multi-locus-sequence-typing" (MLST). Different genes have been used for diagnostic and phylogenetic purposes, including *16S* rRNA gene sequencing to allows discrimination of enterococci, the "D.alanine:D-alanine" (*ddl*), ATP-synthase (*atpA*), *groES*, *groEL*, "superoxide dismutase"(*sod*) and "elongation factor" (*tuf*) **(Ke D. et al, 1999)** .

The incidence of enterococcal infections has been increasing steadily since the 1970 **(Guzman Prieto AM et al., 2016)**. In humans, two species cause the majority of enterococcal infections: *Enterococcus faecalis* and *Enterococcus faecium*. Together, *E. faecalis* and *E. faecium* cause about 75% of all typed of enterococcal infections. , while non-typed enterococci comprise about 24.6% of all enterococcal infections (*E. gallinarum; E. durans; E. hirae; E. raffinosus*). This success is due to their intrinsic resistance to many antimicrobials , such as all cephalosporin, aminoglycosides, clindamycin, and trimethoprim-sulfamethoxazole, which results in the occurrence of many cases of multidrug resistance ,prolonging hospitalization-time, increases treatment cost and the risk of treatment failure and death, in addition to acquire new resistant traits, due to remarkably plastic genome that allows these two species to readily acquire resistance to further antibiotics, such as high-level aminoglycoside resistance, high-level ampicillin resistance, and vancomycin resistance, either through mutation or by horizontal transfer of genetic elements conferring resistance determinants.

The timeline of the most important event characterizing the genus enterococci begins in 1899, with the first formal description of putative enterococci, as round enteric bacteria. In the 1964, the first description of the transfer of the chloramphenicol resistance, 15 years after its clinical introduction. Similar events for aminoglycosides and glycopeptides. Since the late 1980s, the prevalence of "vancomycin-resistant" profile (VRE). In the recent years there has been to increase of linezolid and daptomycin-resistant strain, newest antibiotics, although the majority of Enterococci remain susceptible. Finally, today, the insurgence and spread of the "multi-drug-resistant" strains (MDR**) (Fig.1)**.

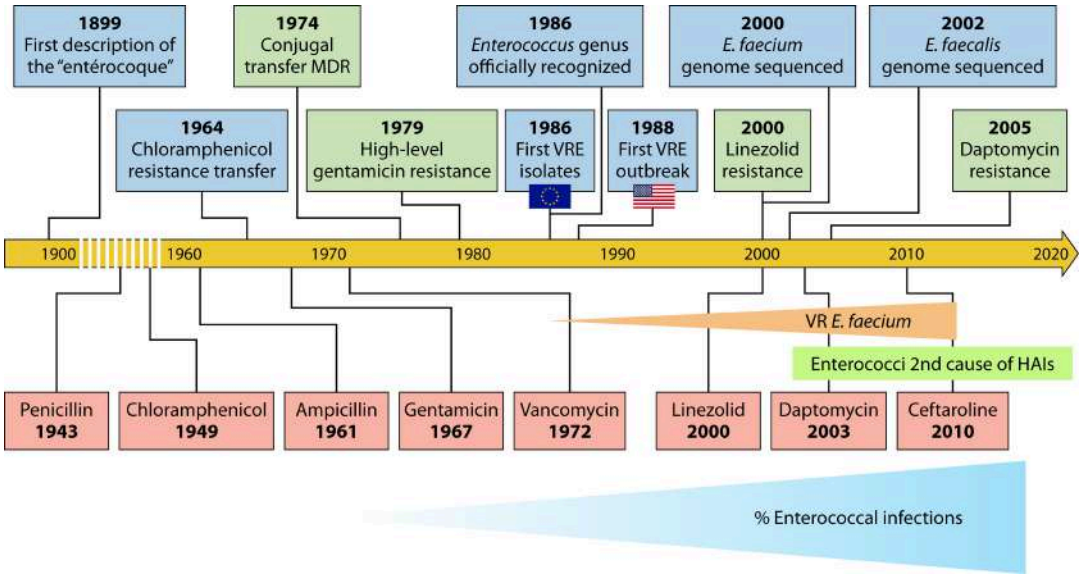

***Figure 1**. Timeline of relevant events in the history of enterococci as human pathogens (blue rectangles), appearance of antibiotic resistance (green rectangles), and antibiotic clinical debut (red rectangles). The timeline begins in 1899 with the first formal description of putative enterococci, as round enteric bacteria. The timeline then jumps to 1964 to the first description of the transfer of chloramphenicol resistance, only 15 years after its clinical introduction. Similar stories occurred for aminoglycosides and glycopeptides. Since the late 1980s, the prevalence of vancomycin-resistant (VR) E. faecium has been increasing, as has the overall percentage of enterococcal HAIs. Resistance to the newest introduced antibiotics, linezolid and daptomycin, emerged very rapidly after their clinical introduction, but the majority of enterococci remain susceptible. MDR, multidrug resistance (García-Solache M. et al., 2019).*

1.2. Virulence

The success of the genus enterococcus as pathogens in the hospital is related to their survival capabilities in a hostile antimicrobial-rich environment, due to their pathogenic potential and ability to cause disease, including the ability to evade the immune system; the capacity to attach to host cells, the extracellular matrix (EM), inert materials and a variety of medical devices, as well as the ability to form biofilms that make them more resistant to antibiotic killing and phagocytic attack.

Many proteins have been described in *E. faecalis* as part of its virulence repertoire.

- The microbial surface components recognizing adhesive matrix molecule (MSCRAMMs), surface elements that help to adhere to host tissue, starting the infection process. One of the best characterized MSCRAMM is Ace, a collagen-binding protein that enhances early heart valve colonization, suggesting an important role in the insurgence of endocarditis;
- Pilin gene cluster (PGCs), that encode LPxTG-like motif surface proteins that are responsible for the assembly of long filamentous structures extending from the surface, called pili, that can function as adhesin, and then associated to initial adherence and biofilm formation and implicated in the pathogenesis of endocarditis and UTI;
- Citolysin (Cyl), called also hemolysin, encoded by cyL_L and cyL_S genes, that promotes different infections. The encoded operon is located on mobile elements such as conjugative plasmids or within the pathogenicity island, (PAI), large elements that can be acquired by horizontal transfer and confer virulence to bacterial pathogens;
- Aggregation substance, a pheromone-induced surface protein that plays dual roles in mating pair formation during conjugation and virulence, involved in infective endocarditis and virulence, extracellular matrix adherence and phagocytosis protection. **(Coburn PS et al. 2003);**
- Gelatinase (*gel E*), a matrix metalloproteinase that hydrolyzes gelatin collagen, and other proteins, playing a key role in the development of endocarditis and inhibiting complemented-mediated responses **(Thurlow LR et al., 2010)**; *gelE* is cotranscribed with *sprE,* which encode a serine protease. The expression of both genes are under control of the *fsr* locus, a master regulator involved in the biofilm production, in the expression of surface proteins and metabolism;
- The cell wall-associated "enterococcal surface protein" **(Esp)** that contributes to cell adhesion in *E. faecalis* , involved in urethral colonization and endocarditis, promoting the biofilm formation;
- The phosphotransferase system (PTS) genes encoded transmembrane proteins that participate in sugar intake. The diversification of several PTS allows to Enterococci to use a broad variety of sugars as carbohydrate sources and better adapt to changing environments. PTS can act as a part if the general stress response, as virulence factors, helping the enterococci to colonize and survive within the host, and in biofilm and endocarditis development **(Sauvageot N. et al., 2017) (Fig.2).**

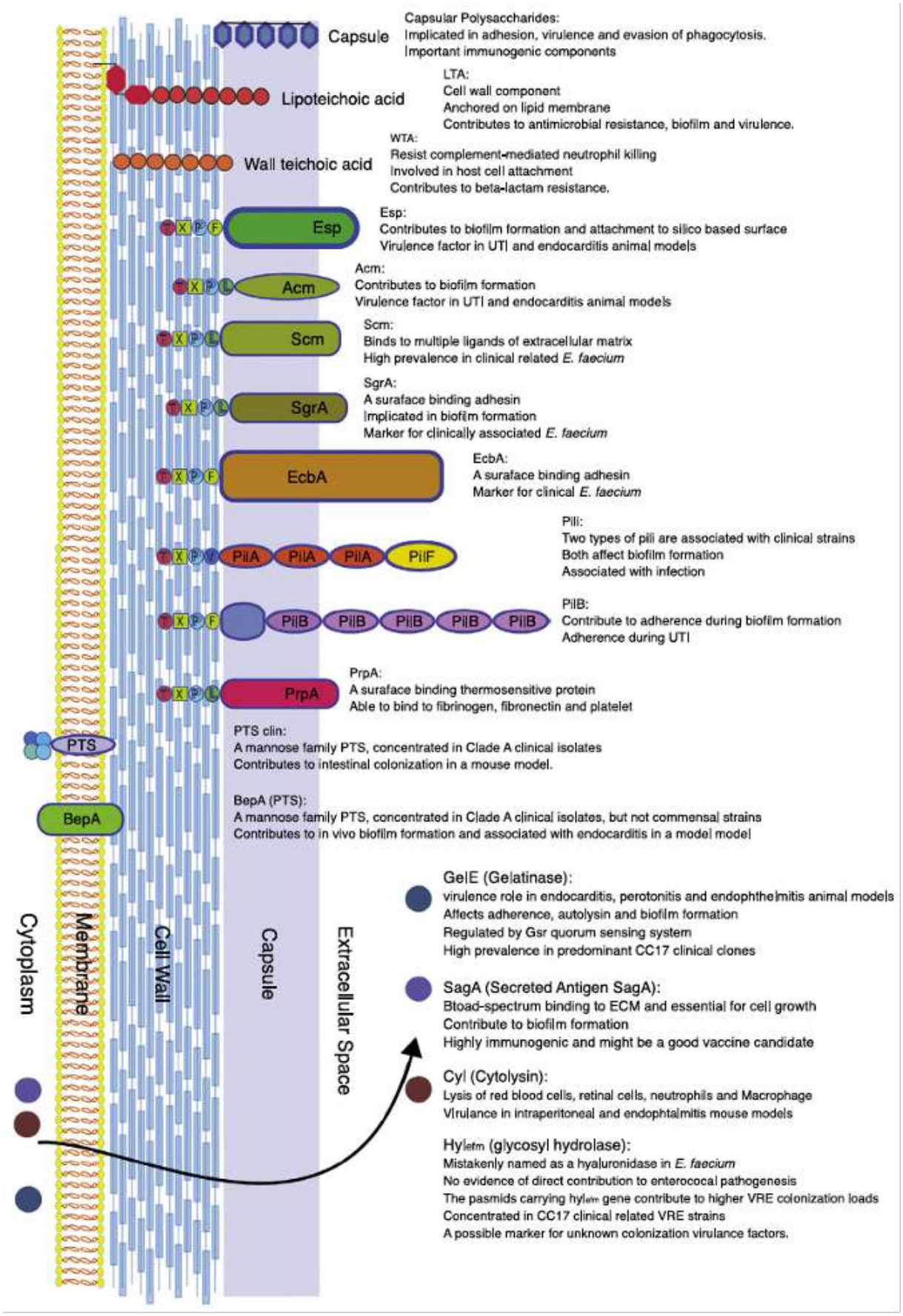

Figure 2. *Overview of Enterococcal virulence factor (Gao W. et al.,2018).*

1.3. Antibiotic resistance

The clinical importance of the genus *Enterococcus* is closely related to antibiotic resistance. *E. faecalis* and *E. faecium* are characterized by their reduced susceptibility to many agents that are quite active against streptococci and staphylococci, showing high-level resistance to almost all cephalosporin and all semi-synthetic penicillins. Although the resistance of these two species differs in important ways, it can generally be categorized as tolerance, intrinsic resistance and acquired resistance **(Fig.3).**

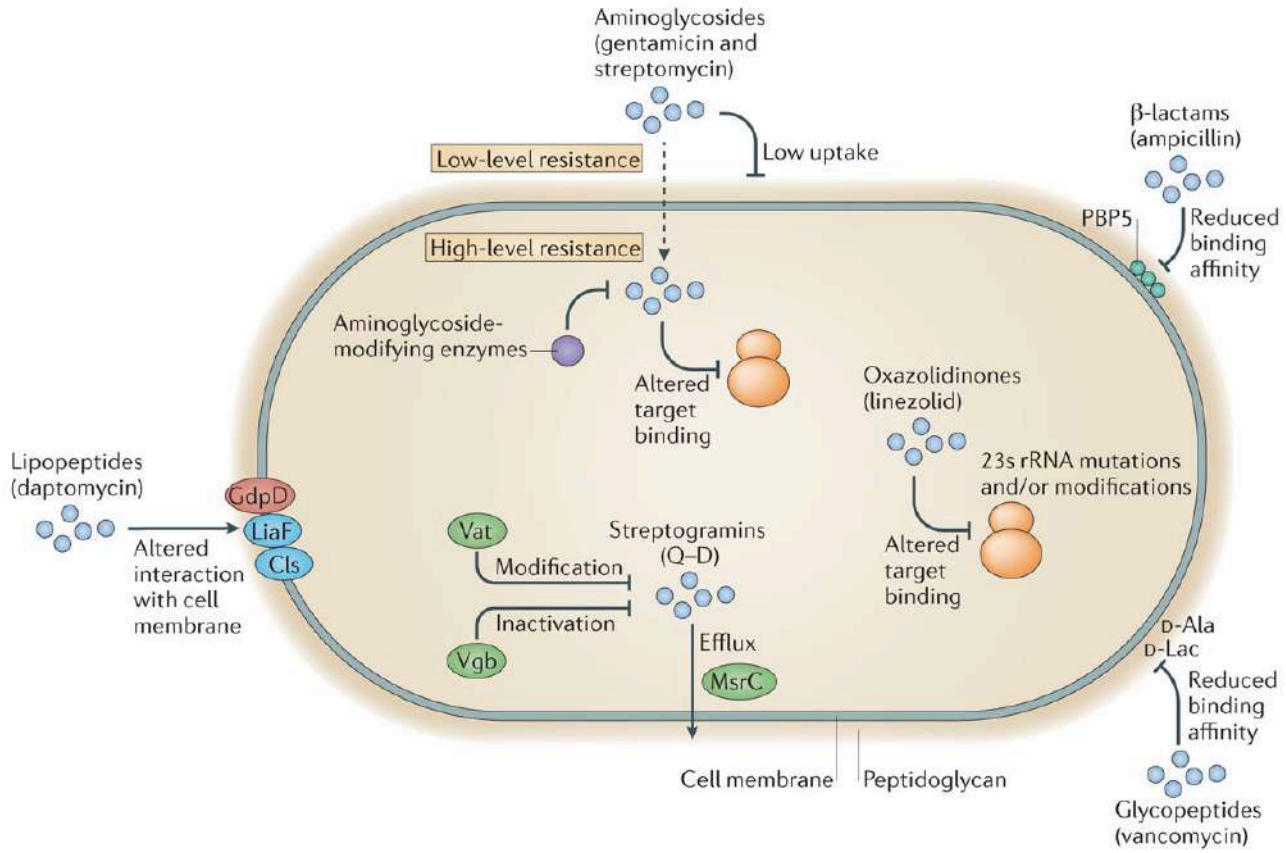

***Figure 3**. Main mechanisms of enterococcal antibiotic resistance Enterococci are intrinsically resistant to several antibiotics and can acquire mutations and exogenous genes that confer resistance to additional drugs. The main mechanisms of antibiotic resistance are shown. In Enterococcus faecium, resistance to ampicillin occurs through the production of penicillin-binding protein 5 (PBP5), which has low affinity for β- lactams. Enterococci exhibit intrinsic low-level resistance to aminoglycosides such as streptomycin or gentamicin owing to low uptake of these highly polar molecules. High-level resistance results from the acquisition of aminoglycoside-modifying enzymes or, for streptomycin, can result from ribosomal mutations that result in altered target binding. Resistance to the glycopeptide vancomycin occurs through a well-characterized mechanism of reduced vancomycin-binding affinity, involving alterations in the peptidoglycan synthesis pathway. Resistance of Enterococcus spp. to the streptogramin quinupristin–dalfopristin (Q– D) involves several pathways, including drug modification (by virginiamycin acetyltransferase (Vat)), drug inactivation (through virginiamycin B lysase (Vgb)) and drug efflux (via the ATP-binding cassette protein macrolide streptogramin resistance protein (MsrC)). Resistance to the oxazolidinone linezolid is rare, but the most common pathway involves mutation in the 23S ribosomal RNA ribosome-binding site. Resistance of E. faecalis to the lipopetide daptomycin has been shown to involve altered interactions with the cell membrane and requires the membrane protein LiaF and enzymes involved in phospholipid metabolism, such as a member of the glycerophosphoryl diester phosphodiesterase family (GdpD) and cardiolipin synthase (Cls) (Arias C.A., Murray B.E., 2012).*

1.3.1. Tolerance

Virtually, all clinical *E. faecalis* isolates are tolerant to the normally bactericidal cell-wall active agents, such β-lactams and glycopeptides. Tolerance implies that the bacteria can be inhibited by clinically achievable concentrations of the antibiotic but killed by concentrations far in excess of the inhibitory concentration. Tolerant bacteria escape the killing effect of bactericidal antibiotics, even at concentrations exceeding the MIC of the drug by several orders of magnitude, leading bactericidal drugs to become mere bacteriostatic agents **(Handwerger S. et al., 1985).** Tolerance has been linked to treatment failures in infections such as endocarditis, meningitis, osteomyelitis, and bacteraemia. Enterococcal tolerance can be overcome by combining cell-wall active agents with an aminoglycoside.

The mechanism by which β–lactam-aminoglycoside combinations yield synergistic bactericidal activity remains a mystery, but *in vitro* data indicate that a higher concentration of aminoglycoside enters cells that are also treated with agents that inhibit cell wall synthesis, which suggests that the cell wall active agents promote uptake of the aminoglycoside **(Mohr et al. 2009).**

1.3.2. Intrinsic resistance

Intrinsic resistance is encoded within the core genome of all members of the species. Among the species of greatest clinical interest, *E. faecalis* is intrinsically resistant to most β-lactams and only susceptible to a limited group of penicillins, such as ampicillin, penicillin and piperacillin **(Arias and Murray, 2012; Kristich et al., 2014a**). Enterococci show intrinsically susceptible to vancomycin but appear to be intrinsically resistant to a big plethora of antibiotics.

They are intrinsically resistant to macrolides, lincosamide and streptogramin, that act inhibiting protein synthesis by binding to the 50S subunit of the ribosome. The most common form of acquired resistance to macrolides is production of an enzyme that methylates a specific adenine in the 23S rRNA of the 50S ribosomal subunit, which reduces the binding affinity of the macrolide for the ribosome. This modification also reduces the binding of lincosamide and streptogramin B antibiotics to the ribosome. The responsible enzyme is typically encoded by the *ermB* gene, and the phenotype is often referred to as MLS_B. An efflux pump, encoded by the transferrable *mefA* gene, is also known to pump macrolides out of the cell, but confers a lower level of resistance than *ermB* (Clancy, et al., 1996).

E. faecalis strains exhibit different intrinsic susceptibilities to clindamicin (and lincosamide), quinopristin (streptogramin B class) dalfopristin (streptogramin class A), members of the streptogramin family that act synergistically, through activity conferred by expression of the *lsa* gene, related structurally to ATP-binding cassette (ABC)-efflux pumps, suggesting drug efflux as a possible mechanism, but lacks identifiable transmembrane sequences that would be expected of an authentic efflux pomp. The molecular mechanism of Lsa protein is based on ribosome protection **(Hollenbeck et al., 2012; Kristich et al., 2014; Wilson D.N. et al; 2020)**.

They show intrinsic resistance to trimetoprim-sulfamethoxazole. Most bacteria lack the ability to absorb folate from the environment and as such require de novo folate synthesis to produce nucleic acids. The antibiotic combination trimethoprim-sulfamethoxazole inhibits two sequential steps in the tetrahydrofolate synthesis pathway, thereby inhibiting folate synthesis and synergistically killing a broad spectrum of bacterial species. Enterococci are unusual in that they can absorb folic acid from the environment, bypassing the effects of trimethoprim-sulfamethoxazole **(Bushby et al., 1968).**

Enterococci are intrinsically resistant to clinically achievable concentration of amynoglicosides. This antibiotic class act by binding to the 16S rRNA of the 30S ribosomal subunit and interfering with protein synthesis. Enterococci generally exhibit a moderate level of intrinsic aminoglycoside resistance that has been attributed to poor uptake of antibiotics. Intrinsic resistance in *E. faecalis* is attributed to an inability of the aminoglycoside to the poor penetration of these agents through the enterococcal cell envelope (where they

act by inhibiting ribosomal protein synthesis). The reason for this poor penetration is not clear, but it has been postulated that enterococcal metabolism is essentially anaerobic, precluding aminoglycoside transport across the cytoplasmic membrane, which is an oxygen-dependent process. The impaired uptake of gentamicin can contribute directly to enhanced resistance. Also, these molecules have been inactived by covalent modifications on the hydroxylic and aminic group, due to enzymes naturally present in *E. faecalis.* Moderate species-specific intrinsic resistance to aminoglycosides in *E. faecium* is enhanced by a chromosomally encoded rRNA methyltransferase, EfmM that uses S-adenosyl methionine as a methyl donor to methylate a specific residue on 16S rRNA, in the context of the 30S ribosomal subunit. In addition, a chromosomally encoded 6'-N-aminoglycoside acetyltransferases (aac(6')-Ii) confers low-level intrinsic resistance **(Galimand et al., 2011; Hollenback et al., 2012).** They are intrinsically susceptible to tetracyclines and erythromycin, although acquired resistance to these agents is widespread (except for tygecycline). Newer agents as linezolid, tedizolid, daptomycin, televancin and oritavancin are active against enterococci. Fluoroquinolones have activity against enterococci. All enterococci exhibit decreased susceptibility to penicillin and ampicillin. For many strains, their level of resistance to ampicillin does not preclude the clinical use of this agent. In fact, in the clinical setting, ampicillin remains the treatment of choice for susceptible strains in patients who can tolerate this agent.

1.3.3. Acquired resistance

Acquired resistance in enterococci can occur through sporadic mutation or acquisition of foreign genetic material. Horizontal gene exchange among enterococci is due to the transfer of pheromone-sensitive, broad host range plasmids or through the movement of transposons. These elements may interact with each other and with the bacterial chromosome to form composite mobile elements.

Pheromone-responsive plasmids are found predominantly in *E. faecalis*. Chromosomally encoded lipoprotein fragments ("pheromones") released by recipient cells are sensed by nearby donor cells and stimulate production of aggregation substance (Asa1, PrgB and others), encoded by the plasmid. Aggregation substance interacts with enterococcal binding substance (EBS) on the surface of the recipient cell and stimulates recipient-donor contact that promotes conjugation **(Palmer K.L. et al.,2010)** These plasmids transmit genetic information in a highly efficient manner between *E. faecalis* strains but are largely restricted to this species.

pRUM plasmids in *E. faecium* are similar to pheromone-responsive plasmids in *E. faecalis* in that they transfer at a high frequency but exhibit a narrow host range **(Hegstad K. et al.,2010).**

In contrast, broad host range plasmids can transfer genetic information to other gram-positive and even gram-negative species, but at a lower frequency pheromone-responsive plasmids. Transfer of these plasmids requires close contact between cells. Inc.18-type plasmids are well-known broad host range plasmids that have been implicated in the transfer of vancomycin resistance determinants to *S. aureus* in recent years **(Périchon B. et al., 2009).**

Three types of transposons are responsible for most gene mobility in enterococci, Tn3 family transposons, composite transposons, and conjugative transposons **(Hegstad K. et al., 2010).** The prototypical Tn3 family transposons are Tn917 that confer macrolide, lincosamide and streptogramin B resistance (MLS_B) and Tn1546 that confer glycopeptide resistance, whereas the prototypical conjugative transposon is Tn916, which confers resistance to minocycline and tetracycline **(Rice LB. et al., 1998).** Composite transposons can readily be formed by the interaction of related IS elements that are liberally sprinkled throughout the genome of most clinical enterococcal strains. The movement of these IS elements not only confers mobility to resistance genes, but it promotes cointegration of plasmids with other plasmids and with the bacterial chromosome.

Glycopeptides resistance

Glycopeptides (vancomycin and teicoplanin) are used to treat serious infections due to resistant Gram-positive bacteria, inhibiting bacterial growth by interfering with peptidoglycan biosynthesis. These antibiotics form complex with the D-Ala-D-Ala peptide termini of peptidoglycan precursors on the outer surface of the cell, which prevents the cell wall biosynthetic enzymes (*i.e.*, the PBPs) from using them as substrates for transglycosylation and transpeptidation and, hence, impairment of cell wall integrity **(Kristich C.J. et al., 2014).** The acquisition of glycopeptide resistance by enterococci has been an epidemiological and antimicrobial dilemma for the past 25 years. In the early 1980's, first in Europe and then in the United States, have since emerged glycopeptide-resistant enterococci (GRE) as a major cause of nosocomial infections **(Hollenbeck B.L. et al., 2012).** Currently, in the United States, an estimate 30% of clinical enterococcus isolates are resistant to glycopeptides **(Farrell DJ et al. 2011).**

The biochemical basis for this resistance derives from modification of the antibiotic target. Glycopeptide-resistant enterococci produce altered peptidoglycan precursors in which the D-Ala-D-Ala termini have been modified in either D-Ala-D-lactate or D-Ala-D-Ser. These substitutions reduce the binding affinity of the antibiotics for the peptidoglycan precursors (~1000-fold reduction for D-Ala-D-lac; ~7 fold for D-Ala-D-Ser). The altered precursors can still serve as substrates for the cell wall biosynthetic enzymes to enable the construction of functional peptidoglycan, but the reduced affinity of glycopeptides renders the drugs unable to inhibit cell wall biosynthesis. The capacity to produce the alternative glycopeptide-resistant peptidoglycan precursors is encoded by resistance operons usually encoded on mobile genetic elements (and thus transferable to otherwise susceptible hosts). Specific types of glycopeptide resistance are encoded in the chromosome as part of the core genome of certain enterococcal species.

Nine distinct gene cluster (operon) conferring glycopeptide resistance in enterococci have been described to date. These determinants differ from each other both genetically and phenotypically, based on their physical location, encoded on a mobile genetic element or in the core genome; the specific glycopeptides to which they confer resistance, often distinguished operationally as providing resistance to both vancomycin and teicoplanin, or providing resistance to vancomycin but not teicoplanin; the level of resistance they confer; whether resistance is inducible or constitutively expressed; and the type of peptidoglycan precursor that is produced by their gene products.

These operons fall into two general categories: those that replace the terminal D-Ala with a D-lactate (*vanA, vanB, vanD, vanM, vanP*) **(Ever S. et al, 1993; Perichon B et al., 1997; Xu X et al.,2010; Xavier BB er al., 2021)** and those that replace the terminal D-Ala with a D-Serine (*vanC, vanE, vanG, vanL, vanN*) **(Fines M. et al., 1999; Lebreton F. et al., 2011; Sassi M. et al, 2011).**

The operons that encode D-Lac ligases result in high-level resistance with MICs 256 mg/ml (VanA, VanB, VanD and VanM), both to vancomycin and to teicoplanin, while operons that encode D-Ser ligases result in low-level resistance with MICs 8–16 mg/ml (VanC, VanE, VanG, VanL and VanN), and only to vancomycin, but remain susceptible to teicoplanin **(Hegstad K. et al., 2010; Fines M. et al.,2019; Lebreton F. et al.,2019; McKessar SJ et. Al., 2000).**

The Van gene cluster encode several functions: a regulatory module, namely a two-component signal trasduction system that is responsible for sensing the presence of glycopeptides and activating expression of the resistance genes in inducible Van types: enzymes that produce the modified peptidoglycan precursors, including enzymatic machinery that Is required to produce the appropriate substitute (D-Lac or D-Ser) , and a ligase that fuses D-Ala to either D-Lac or D-Ser to make the corresponding dipeptide that can be incorporated into peptidoglycan precursors via the normal biosynthetic machinery of the cell; and D,D-carboxypeptidases that eliminate any of the normal peptidoglycan precursor synthesized by the natural biosynthetic machinery of the cell, thereby ensuring that nearly all precursors reaching the cell surface are

of the modified variety **(Miller et al., 2014).** The Van gene clusters are typically referred to by the names given to the ligases they encoded (VanA, Van B, Van C, and so on) **(Fig. 4).**

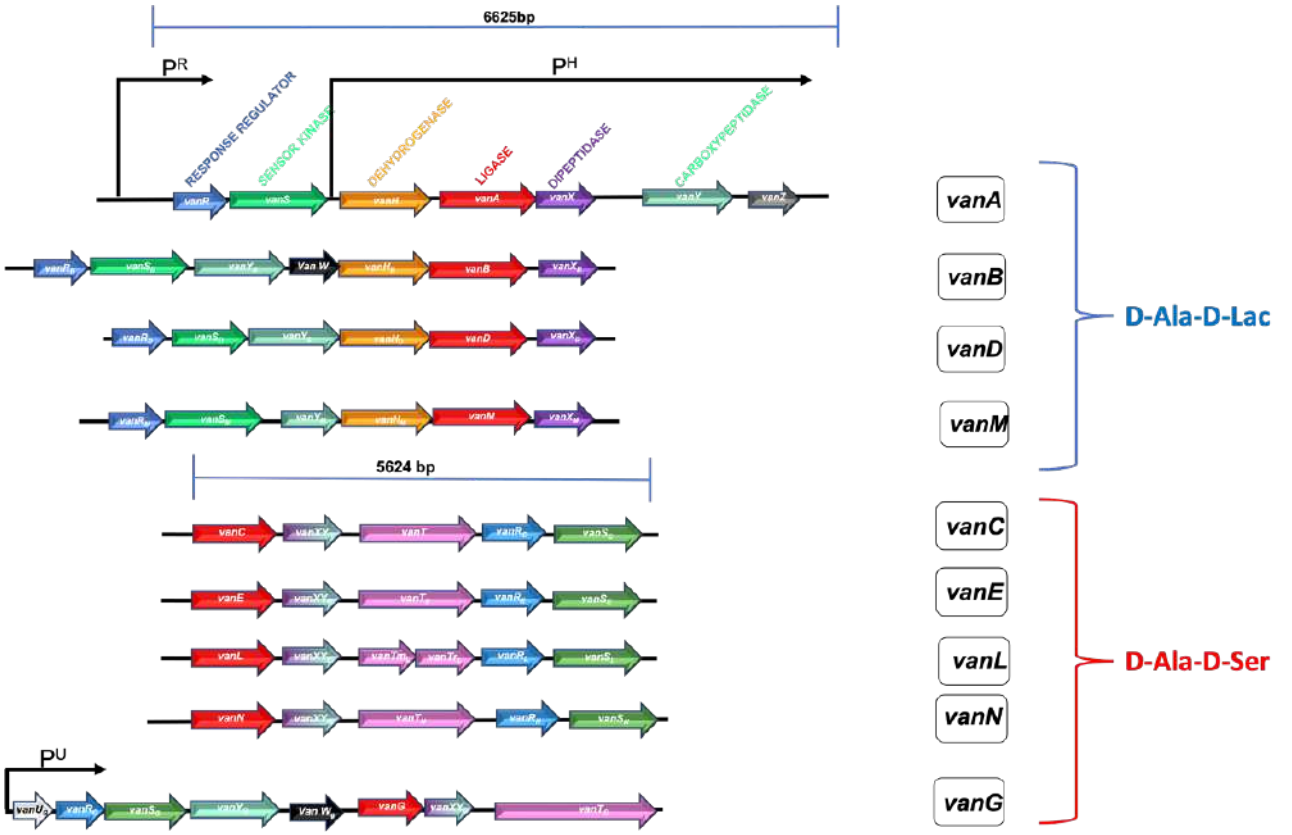

Figure 4*. Depictions of known glycopeptide resistance operons. (A) The four glycopeptide resistance operons that yield peptidoglycan precursors terminating in D-Ala-D-Lac. Arrows reflect the directions of transcription and relative sizes of the open reading frames. (B) The five glycopeptide resistance operons that yield peptidoglycan precursors terminating in D-Ala-D-Ser. See the text for descriptions of the open reading frame roles* (Adapted from Garcia-Solache et al., 2019).

The VanA and VanB types are the most common among clinical isolates.

The VanA determinant confers a high level of resistance to vancomycin and teicoplanin. Van A is typically encoded on Tn*1546* commonly carried on a plasmid or related transposon and includes seven open reading frames transcribed from two separate promoters. The regulatory apparatus is encoded by the VanR (response regulator) and VanS (sensor kinase) two component-system, which are transcribed from a common promoter, while the remaining genes are transcribed from a second promoter. The transmembrane sensor kinase is involved in detecting glycopeptides in the environment and phosphorylating VanR, which is converted from a repressor of operon transcription to an activator **(Artur M. et al., 1997).** VanR regulates 3 downstream genes, that encoded products that specify the production of modified peptidoglycan precursors: VanH, a dehydrogenase that reduces pyruvate to D-lactate, VanA that is a ligase that forms D-Ala-D-Lac dipeptide **(Artur M. et al., 1997),** which is then ligated to the UDP-MurNAc tripeptide peptidoglycan precursor by the cellular adding enzyme and VanX, a dipeptidase that cleaves D-Ala-D-Ala and VanY, a D,D-carboxypeptidase, necessary to eliminate the natural peptidoglycan precursors from the cell **(Reynolds PE et al., 1994)**. The last gene, VanZ, a protein with unknown function that contributes to resistance to the glycopeptide teicoplanin. **(Arthur M. et al., 1995).**

The VanB locus, confers moderate to high-level resistance to vancomycin, but did not induced by teicoplanin, usually acquired on Tn*5382/*Tn*1549* type transposons, which occur on plasmid or in the host chromosome. The genetic organization is similar to that of VanA , in that it contains two distinct promoter transcribing seven open reading frames, with any significant differences. Although VanB encodes a two-component

system (named VanRB and VanSB), this signaling system is considerably different from that encoded in VanA. VanB encodes homologs of VanH and the D-Ala-D-Ala ligase (encoded by VanB), as well as the peptidases (VanX and VanY). However, VanB lacks a homolog of VanZ, and instead encodes a protein named VanW, whose role in resistance is not fully understood **(Fig. 5).**

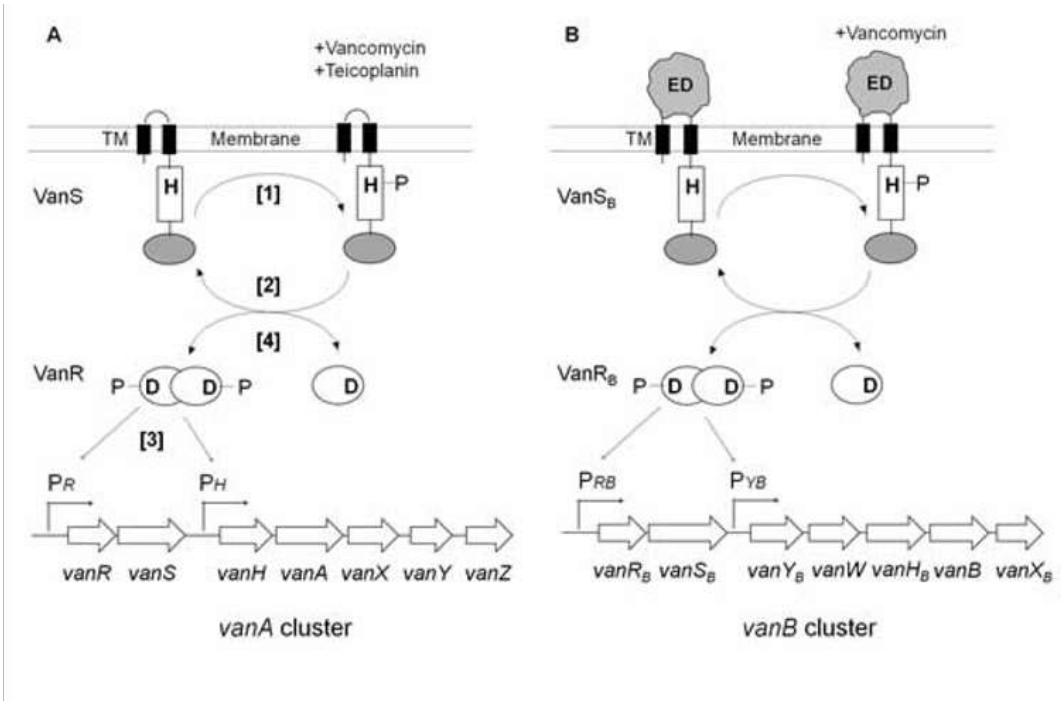

Figure 5 *Regulation of vancomycin resistance gene clusters. Comparison of VanA regulation (panel A) and VanB regulation (panel B). TheVanS (or VanSB) sensor kinases are anchored in the cytoplasmic membrane by two transmembrane segments (TM) that flankthe predicted sensory input domain. VanS (which is inducible by both vancomycin and teicoplanin) contains only a short extracellular loop, and may receive activating signals in, or immediately adjacent to, the membrane. VanSB (which is inducible by vancomycin, but not teicoplanin) contains a large extracellular domain (ED) that likely serves as the ligand-recognition domain. In both cases, the presence of the appropriate antibiotic stimulus leads to the activation of kinase activity and ATP-dependent autophosphorylation on a highly conserved His residue. This phosphoryl group is transferred to the VanR (or VanRB) response regulator, which leads to dimerization, enhanced binding to DNA, and activation of transcription from the two promoters found in the Van gene cluster. In the absence of inducing stimuli, VanS (VanSB) serves as a phosphatase to ensure that VanR (VanRB) remains in the inactive state and Van expression is off (Arthur & Quintiliani, Jr., 2001).*

In recent years it has been reported the emergence of enterococcal strains harboring a “silent” copy of vancomycin resistance genes, *vanHAX* operon, that confer to Vancomycin-susceptible enterococci (VSE) strains the capability to revert to the VRE phenotype during antibiotic treatment (exposure to vancomycin), and thus escape detection using drug sensitivity screening tests, severely compromising the success of therapy. For this reason, these strains were consequently termed vancomycin-variable enterococci (VVE) **(Thaker M.N. et al., 2015).**

VVE are Enterococci harbouring the *vanA* gene complex but being phenotypically vancomycin susceptible. Different VVE clones have caused nosocomial outbreaks, being detected only by molecular methods and cannot be cultured on selective vancomycin containing media. The detection of these strains is challenging since the clone is likely to be unrecognized, which facilitates further spread.

There are multiple factors that favor the restoration of resistance in these strains.

VVE typically lack the *vanS* (sensor) and *vanR* (regulator) genes despite harbouring the *vanHAX* gene cassette. It has been postulated that insertion of an ISL3-like element between the VanR binding site and the *vanHAX* promoter region is responsible for silencing of the *van-A* gene in VVE strains, resulting in a functional fitness gain

It has been shown that VVE strains, both *in vitro* and *in vivo* can revert into VRE phenotype under vancomycin exposure through the constitutive expression of the vancomycin resistance cassette *vanHAXYZ,* accomplished through a variety of changes in the DNA region upstream of the resistance genes that includes both a deletion of a likely transcription inhibitory secondary structure and the introduction of a new unregulated promoter, conferring resistance even in the absence of *vanRS* **(Kohler P. et al; 2018)**. The use of vancomycin to treat VVE infections could provide selective pressure that may lead to development of therapy induced resistance and treatment failure **(Coburn B. et al., 2014).**

Aminoglycoside resistance

The intrinsic mechanisms result in low level aminoglycoside resistance, while acquisition of mobile genetic elements typically underlies high-level aminoglycoside resistance in both *E. faecium* and *E. faecalis*, abolishing the synergistic bactericidal activity of aminoglycosides in combination with cell-wall-active agents that are important in the treatment of severe enterococcal infections, such as endocarditis **(Hollenbeck B.L. and Rice L.B., 2012).** Since the clinical utility of these combination has been recognized, strains that have expressed high levels of resistance to aminoglycosides have emerged (MICs of >500 g/ml for gentamicin and >2,000 g/ml for streptomycin) **(Shaw KJ et al., 1993)**.

High-level gentamicin resistance (HLGR) is usually acquired on a mobile element that encodes an aminoglycoside-modifying enzyme. Such enzymes can be phosphotransferases (APHs) that use ATP to phosphorylate a hydroxyl group on the antibiotic, acetyltransferases (AACs) that use acetyl-CoA to acetylate an amino group on the antibiotic, or nucleotidyltransferases (ANTs) that use ATP to adenylylate a hydroxyl group on the antibiotic. Alternatively, most frequently occurs through acquisition of a bifunctional gene encoding APH(2'')-Ia-AAC (6')-Ie **(Mederski-Samoraj BD. Et al., 1983),** that inactivate gentamicin (and structurally related aminoglycosides) by phosporylation at the 2'hydroxy position of gentamicin and simultaneous acetylation of the 6'hydroxy position of the other aminoglycosides. **(Ferretti JJ et al., 1986; Courvalin P.et al., 1980).** The modified antibiotic is no longer capable of binding to its target on the 30S ribosomal subunit and thereby loses antibacterial activity. Strains that contain *aph(2'')- Ia-aac(6')-Ie* are clinically resistant to all aminoglycosides except for streptomycin **(Chow JW et al., 2000).** This gene is most commonly flanked by IS*256* in a composite transposon designated Tn*4001* in *S. aureus* and Tn*5281* in *E. faecalis.* Expression of a second phosphotransferase [APH(2)-Ic] has been associated with lower gentamicin MIC (256 μg/ml) but still negates ampicillin-amynoglicoside synergism.

High-level resistance to streptomycin (HLSR) occurs most commonly through enzymatic modification of the antibiotic or by single point mutations to the ribosome. **(Shaw KJ et al., 1993).** Two well-described adenylyltransferases, Ant(6')-Ia and Ant(3'')-Ia, are capable of inactivating streptomycin (and structurally related aminoglycosides). **(Chow JW et al., 2000; Hollingshead S. et al. 1985).**

Other acquired AMEs have been identified in enterococci, including Aph(3')-IIIa, an aminoglycoside phosphotransferase that confers resistance to kanamycin **(Trieu-Cuot P. et al., 1983)** and Ant(4'')-Ia, a nucleotidyltransferase that confers resistance to tobramycin, amikacin, neomycin and kanamycin **(Carlier C. et al., 1983).** These enzymes are of less clinical significance, do not conferring gentamicin or streptomycin resistance.

Daptomycin resistance

Daptomycin is a cyclic lipopeptide with potent *in vitro* bactericidal activity against Gram-positive that acts by interacting with the cytoplasmic membrane in the presence of physiological concentrations of calcium, resulting in a variety of alterations in cell membrane characteristics. It is a cationic peptide whose first attraction to the cell membrane is through its interaction with phosphatidylglycerol, incorporating itself into the cell membrane of Gram-positive organisms in the presence of physiologic calcium concentrations and promotes leakage of intracellular potassium into the extracellular space, resulting in cell death by destruction of the transcellular potassium gradient **(Lakey JH et al., 1988; Alborn WE et al., 1991; Silverman JA et al., 2003)**. Because its mechanism of action is distinct from those of other antibiotics, daptomycin is useful for treatment of infections that are caused by multidrug-resistant Gram-positive strains. Daptomycin resistance has been observed in clinical isolates following daptomycin therapy, typically as a consequence of mutations in chromosomal gene.

In *E. faecalis*, resistance to daptomycin has a unique mechanism associated with a movement of the membrane phospholipids away from the septum, which may divert daptomycin from the septum.

Genome sequencing of the resistant *E. faecalis* strains revealed three mutated genes: *cls, gdpD* and *liaF.* Such mutations play a key role in the development of daptomycin resistance *in vivo.*

The *liaF* gene encoded LiaF (lipid II cycleinterfering antibiotic protein), part of the three-component LiaFSR regulatory system, which is known to coordinate the response of the cells envelope to antibiotics and antimicrobial peptides in some Gram-positive bacteria, which suggest that perturbation in the activity of this signal system may alter envelope properties in a such a way that daptomycin can no longer interact with, or insert into, the membrane efficiently. In *E. faecalis*, a deletion of isoleucine in position 177 of LiaF, is directly responsible for a Daptomycin -tolerant phenotype and is likely to negatively affect response to Daptomycin therapy, increasing Daptomycin MIC value from 1 to 4 ug/ml (breakpoint 4ug/ml) **(Munita et.al, 2013).** *gdpD* encoded to glycerophosphoryliester phosphodiesterase and *cls* a cardiolipinsynthase. Point mutation associated to *gdpD* did not increase the MIC, but the combination of mutation (*liaF* and *gdp*), increased the MIC to 12 ug/ml.

In *E. faecalis* the resistance phenotype was associated with redistribution of cardiolipin microdomains in the cellular membrane which were relocated from the septum (the principal target of DAP) to non-septal areas. These CL microdomain remodelling was associated with changes in the LiaFSR system. A novel mechanism of resistance involved a stepwise process in which mutations in LiaFSR resulted in mobilization of cardiolipin microdomains from the septum. As a result, DAP is diverted from the septum to other non-septal areas. The mechanism of resistance is completed by changing the content of cellular membrane phospholipids; the content of phosphatidylglycerol is decreased preventing Daptomycin oligomerization and cardiolipin microdomains may 'trap' the diverted antibiotic away from the septum and prevent it from reaching the inner leaflet of the cellular membrane **(Miller et al., 2014).**

Rifampicin resistance

Rifampicin Inhibits bacterial growth by binding the beta subunits of enterococcal DNA-dependent RNA polymerase (RpoB) and preventing initiation of transcription **(Miller et al.,2014).**

Most resistance to rifampicin results from mutations of specific sites in the gene encoding the beta subunit of the RNA polymerase, which reduces the affinity of rifampicin for the polymerase. Mutations in RpoB responsible for rifampicin resistance have been identified in numerous species of bacteria. Additional, enzymatic inactivation of rifampicin has been observed in a handful of cases. Although rifampicin has not been used extensively to treat enterococcal infections, acquired resistance to rifampicin is nonetheless common in enterococci. Presumably this is at least partially a consequence of commensal enterococci being exposed to rifampicin during treatment for non-enterococcal infections, but other as-yet-unknown factors may contribute to the occurrence of resistant enterococcal isolates as well **(Kristich et al., 2014).** Interestingly, a specific mutation in *rpoB* (H486Y) in both *E. faecalis* and *E. faecium* was shown to increase resistance to broad-spectrum cephalosporins but did not affect other classes of cell-wall acting antibiotics (including ampicillin and vancomycin). This could be due to differential transcription of genes related to cephalosporin resistance by the mutated polymerase **(Kristich C. et al.,2011).**

Quinolones resistance

Quinolones generally exhibit only moderate activity against enterococci, inhibiting the growth of bacteria by interfering with DNA replication, specifically by binding to the type II topoisomerases that control DNA supercoiling (DNA gyrase and DNA topoisomerase IV) and inhibiting their function, leading to lethal double-strand breaks in the DNA. Quinolone resistance in many species of bacteria occurs via mutations in the "quinolone resistance determining regions" of the gene that encode gyrase and topoisomerase IV. These

mutations prevent efficient binding of the antibiotic to the enzyme, which enables DNA replication to continue despite the presence of the antibiotic.

A second mechanism known to contribute to quinolone resistance in other species of bacteria is efflux of the antibiotic out of the cell. Such efflux is often a function of pumps with relatively broad or nonspecific substrate specificities, which are sometimes referred to as multidrug-resistance efflux pumps (MDRs). Gene encoding MDRs are usually found on the bacterial chromosome. These proteins are known to actively transport toxic compounds out of the cell.

A third new mechanism of quinolone resistance, found in *E. faecalis* is mediated by *qnr*, encoding for a Qnr protein family characterized by tandem pentapeptide repeats similar to the plasmid-borne quinolone resistance genes described in *Enterobacteriaceae*. These proteins protect the DNA gyrase and topoisomerase IV from inhibition by quinolones and the subsequent formation of the quinolone-gyrase complex **(Tran et al., 2005).** The inactivation of Qnr identified in the genome of *E. faecalis*, comprised of 42 predicted pentapeptide repeats, resulted in a modest decrease in resistance to fluoroquinolones. Overexpression of the corresponding gene yielded an increase resistance **(Kristich et al., 2014).**

Linezolid resistance

Linezolid is a member of the oxazolidinone family of antibiotics, with bacteriostatic activity, developed for use against multidrug-resistant Gram-positive bacteria. Linezolid interferes with bacterial growth by inhibiting protein synthesis through interaction with the translational initiation complex. It binds in the peptidyl-transferase center (PTC) and disrupts the docking of the aminoacyl-tRNA in the site A of the ribosome, thus inhibiting the delivery of peptides and the subsequent elongation of the polypeptide chain **(Shinabarger D. et al, 1997; Leach K. et al., 2007).** Most bacteria, including the enterococci, have multiple copies of the gene encoding 23S rRNA. *E. faecium* have six copies, while *E. faecalis* have four copies of the gene **(Lee ZM et al.,2009).** The level of resistance expressed depends upon the number of these genes that contain the relevant mutations **(Marshall SH et al., 2002).** In theory, the presence of multiple gene copies makes resistance from sporadic mutation less likely because the unaffected gene copies would mask the effect of the mutated gene. However, recombination between susceptible and resistant copies (referred to as “gene conversion”) will yield strains with multiple mutated copies under persistent linezolid selective pressure.

A variety of point mutations are involved in linezolid resistance, but G2576U represents the most common and spread worldwide. This mutation within the central loop of domain V of 23S rRNA prevents or reduces binding of the antibiotic to the ribosomal subunit. There is a direct correlation between the percentage of rRNA genes that carry a G2576U and the phenotypic level of linezolid resistance, which suggests that the percentage of ribosomes that carry rRNA with the G2576U substitution is the primary determinant for the level of linezolid resistance **(Martinez-Martinez L. et al., 1998; Pascual e Jacoby, 1998).** The recombination between rRNA genes after the emergence of the G2576U mutation may enable the amplification of the level of linezolid resistance in enterococci under the selective pressure imposed by antibiotic treatment.

Additionally, mutations in the ribosomal proteins L3 and L4, which border the peptidyl-transferase center where linezolid binds, are associated with an increase in the linezolid MICs. These mutations were originally described in linezolid-resistant staphylococci and have subsequently been identified in resistant enterococci as well (**Locke JB et al., 2009; Chen H. et al., 2013).** Nevertheless, resistance due to changes in ribosomal proteins L3, L4 and L22 appears to be extremely rare.

While in *E. faecium* linezolid resistance is typically associated with mutations in the 23S rRNA genes, in other enterococcal species and mainly in *E. faecalis,* the acquisition of *cfr* and *cfr*-like, *optrA* and *poxtA* resistance genes, often associated with mobile genetic elements, plays a critical role in oxazolidinone resistance mechanisms **(Brenciani A. et al., 2022).**

The acquisition of the plasmid-borne (pSCFS1) *cfr* or *cfr*(B) gene **(Kehrenberg C. et al. 2005),** which encodes a metyltransferase that post-transcriptionally modifies an adenosine (A2503) in the linezolid binding region of the bacterial 23S rRNA, preventing the antibiotic binding **(Fioriti S. et al., 2021).** The *cfr* gene has been associated with the mobile transposable element IS256, whose sequence is common in multi-drug-resistant staphylococci and enterococci, and this sequence has been found to mediate the transfer of antibiotic resistance genes, as well as altering the promoter sequence of regulatory proteins or activate the expression of existing resistance determinants **(Hennig S et al.,2010,).** This phenomenon could explain the ability of *cfr* to spread across species and propends the possibility of widespread dissemination in the clinical setting.

This metyltransferase confers resistance to a variety of antimicrobial classes, including phenicols, lincosamides, oxazolidinones, pleuromutilins and streptogramin A (PHLOPSA phenotype), as well as decreased susceptibility to the 16-membered macrolides spiramycin and josamycin. *Cfr* is commonly plasmid encoded and transferable and has been associated with outbreaks of linezolid resistance in a variety of Gram-positive species **(Campanile F., et al., 2013; Vester B., 2018).**

The plasmid-mediated resistance has also been attributed to the acquisition of *optrA,* which encodes a putative ABC-F protein **(Wang Y et al., 2015).** This is often located on chromosome or plasmid and can be transmitted by mobile genetic element such as transposons and insertion sequences. Originally thought to be responsible for the outflow of antibiotic molecules from the bacterial cell, today has been demonstrated its function as a ribosomal protection protein **(Sharkey *et al*., 2016,).**

Another gene has recently been identified that confers resistance to the linezolid, *poxtA* a Phenicol-Oxazolidinone-tetracycline resistance gene, recently described in *S. aureus* and *E. faecalis*, that encodes a ribosomal protection protein, yielding decreased susceptibility to phenicols, oxazolidinones and tetracyclines **(Sadowy, 2018)**. This gene is often associated with mobile genetic elements located upstream of a composite transposon Tn*6246,* and harbouring *fexB* (**Na SH et al., 2020).** PoxtA, similarly to OptrA, represents an ATP binding cassette protein of the F-subtype (ABC-F). The ABC proteins associated with antibiotic resistance (ARE), belong to the F lineage of the BC superfamily (ARE ABC-F) and include single polypeptides containing two conserved nucleotide binding domains separated by a linker of ~80 amino acids of variable composition, with no transmembrane domains. Recently, the resistance mechanism of ARE ABC-F proteins has been clarified and shown to be mediated by ribosomal protection. These proteins are not transporters but rather act via a direct target protection mechanism, conferring reduced susceptibility to phenicols and oxazolidinones, by a ribosomal protection mechanism by binding to the large ribosomal subunit and dislodging the bound antibiotic **(Antonelli A. et al., 2018).** PoxtA binds in the E-site of the ribosome, perturbing the CCA-end of the P-site tRNA, causing the shift by ~4 Å out of the ribosome and the retraction of its CCA-end from the peptydil-transferase-centre, corresponding to a register shift of approximately one aminoacid for an attached nascent polypeptide chain. The perturbation of the P-site tRNA by PoxtA thereby alters the conformation of the attached nascent chain to disrupt the drug binding site (**Crowe-McAuliffe C. et al., 2022)**.

Tetracyclines resistance

Tetracyclines exert their antibacterial effect by binding to the ribosome and interfering with the docking of aminoacyl-tRNA. This occurs via association with several loops of the 16S rRNA and the ribosomal protein S7. However, this is a reversible process, and these agents are bacteriostatic **(Schnappinger D. et al., 1996).**
Resistance is mediated by multiple genes, but follows two general strategies, efflux of the antibiotic and ribosomal protection. Efflux pumps encoded by *tetK* and *tetL* are plasmid-borne determinants that encode proteins with 14 α-helices that make up the transmembrane domains and confer resistance to tetracycline but not minocycline **(Chopra I. et al., 2001)**. Expression of resistance is regulated by translational attenuation in the absence of the antibiotic due to the formation of a stem loop structure in the mRNA, which masks the second of two ribosomal binding sites **(Schwarz S. et al., 1992).** In the presence of tetracycline, the ribosome complex is unable to synthesize the normal leader peptide, an alternate loop structure forms in the mRNA and the second binding site becomes accessible, allowing for synthesis of the efflux pump. The genes *tetM*,

tetO and *tetS* are chromosomal resistance determinants, which confer resistance to doxycycline and minocycline as well as tetracycline and can be transferred via the Tn*916* transposon **(Pepper K et al. 1987; Bentorcha F. et al., 1991)**. These genes encoded a protein with a significant homology to bacterial elongation factors (EFs), and like EFs they are able to hydrolyze GTP in the presence of the antibiotic, which alters ribosomal conformation and displaces bound tetracycline.

1.4. β-lactams resistance

Growth of most bacteria depends upon enzymatic linkage of pentapeptide precursor molecules into a peptidoglycan cell wall. The lack of similar structures in eukaryotic cells decrease the toxicity profiles of many of these agents, making them an ideal target against bacteria. Antibiotic in the β-lactam family inhibit bacterial growth by serving as suicide substrates for the D, D-transpeptidase (also known as penicillin-binding proteins, or PBP), the workhorses of the cell wall synthesis machinery, that catalyze cross-linking of peptidoglycan peptide side chain during the synthesis of mature peptidoglycan. Once modified by a beta-lactam antibiotic, PBPs are inactivated, thereby preventing continued cell wall synthesis. As such, the peptidoglycan synthesis and maintenance machinery as long been a target for antimicrobial therapy. Attachment of β-lactam agents to PBPs results in impaired cell wall synthesis and, in most cases, programmed cell death via creation of reactive oxygens species (ROS) **(Kohanski MA et al., 2007).**

Many enterococcal strains also exhibit tolerance to the bactericidal activity of the active β-lactams, with minimal bactericidal concentration greatly exceeding MICs **(Hodges TL et al., 1992).** The enterococci were not killed by penicillin when exposed to drug concentrations in the range of the MIC. This tolerance has clinical significance in the treatment of endocarditis, with cure rates with β-lactams antibiotics alone being approximately 40%. Tolerance in *E. faecalis* has been attributed to removal of reactive oxygen species by the enzyme superoxide dismutase **(Bizzini A. et al., 2009).** Tolerance may be induced when penicillin is administered by pulsed dosing. As such, penicillin-naïve enterococcal strains may appear susceptible *in vitro* but develop tolerance after exposure to the drug **(Krogstad DJ et al.,1980; Hodges TL et al., 1992).**

The intrinsic enterococcal resistance to β-lactams is attributable to a low affinity PBPs. As a result, in *E. faecalis,* the minimal inhibitory concentration for penicillin is typically 2-8 μg/ml, and 8-16 μg/ml for *E. faecium*, much higher than MICs for streptococci and related Gram-positive organisms that do not contain chromosomally-encoded low-affinity PBP genes **(Murray BE. et al., 1992).** Strains with deleted *pbp* genes exhibit reduced MICs for active β-lactams and reductions into the susceptible range for active β-lactams that have poor activity against wild-type strains **(Arbeloa A. et al., 2004; Rice LB et al., 2004).** The extension of nonsusceptibility to beta-lactam antibiotic varies among the different classes of beta-lactams and between enterococcal species. Penicillins show the most activity against enterococci, carbapenems slightly less, and cephalosporins exhibit the least activity. Insofar, ampicillin remains an effective therapy for susceptible enterococcal infections, while cephalosporins are completely ineffective against enterococci. In fact, prior use of cephalosporins is a major risk factor for the acquisition of an enterococcal infection.

1.4.1. Penicillin resistance

As noted above, enterococci are intrinsically resistant to most β-lactams, being susceptible to only a limited number of penicillins like ampicillin, meziocillin, penicillin and piperacillin. Resistance to these penicillins is achievable through two mechanisms: the production of β-lactamases and the expression of low affinity PBP **(Rice LB. et al.,1995).**

<u>β-lactamases</u>

The β-lactamases are the enzymes that inactivates the antibiotic through cleavage of the β-lactam ring, described in both *E. faecalis* and *E. faecium* **(Fig 6).** Plasmid-mediated *bla* genes, encoding β-lactamases were first described in *E. faecalis* in 1983 **(Murray BE et al., 1983).** Since that time, enterococcal β-lactamase production has been rare and described predominantly in *E. faecalis*. *In vitro* hydrolysis studies have shown that the enterococcal β-lactamase, like the ones in staphylococci, has greatest activity against penicillin, ampicillin, and ureidopenicillins; little or no activity against most cephalosporins, penicillinase-resistant semisynthetic penicillins, imipenem, and intermediate activity against ticarcillin **(Murray BE., 1992).** Molecular analysis shows that in all cases, this β-lactamase is identical to that of that produced by *S. aureus*, in some cases within genetic region identical to that of the *S. aureus* β-lactamase transposon Tn552 **(Rice LB et al., 1992).**

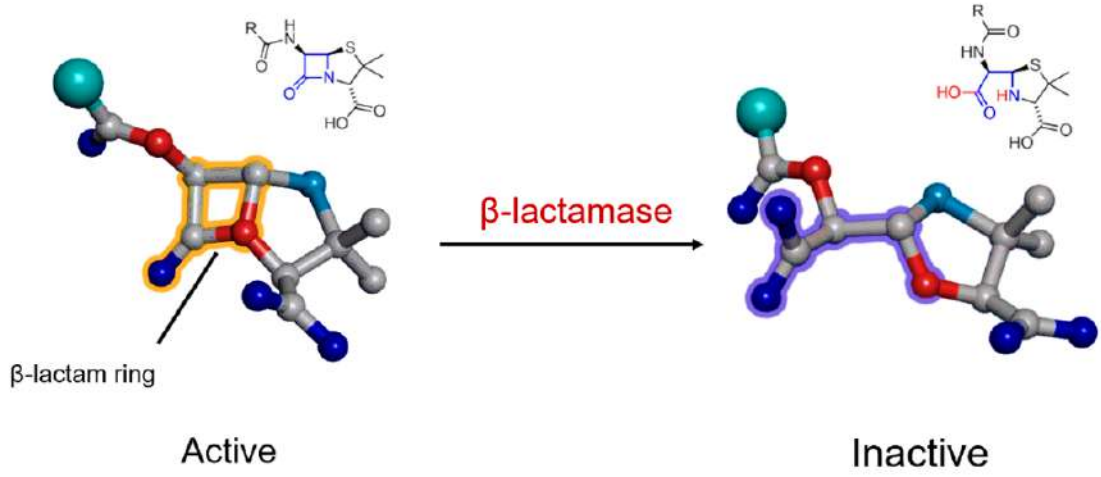

***Figure 6**. Hydrolysis of penicillin by β-lactamase*

Originally described in staphylococci, the gene *blaZ* encodes a β-lactamases as part of an operon with *blaR1,* a transmembrane sensor and signal transducer, and *blaI,* a repressor gene **(Fig. 7).** Expression of the β-lactamases is governed by a membrane-bound β-lactam sensor/signal transducer protein, BLAR1, which senses the presence of the antibiotic in the milieu and regulates transcription of the antibiotic resistance genes. This regulation is via derepression of the requisite genes by the proteolytic activity of the cytoplasmic domain of BlaR1. It degrades the gene repressor BlaI, *blaI* gene product, which leads to transcription of the genes *blaI, blaR1 and blaZ* **(Leticia I. et al., 2010).**

The staphylococcal plasmids encode for a type A penicillinase, and the genes have previously been designated *blaZ.* Immediately upstream of the staphylococcal β-lactamase structural gene and reading in the opposite direction is an open reading frame for the putative repressor; together they are assumed to regulate β-lactamase production. Marked differences in the restriction sites in the corresponding regions of two enterococcal Bla+ plasmids suggest that these genes are not present in enterococci or are markedly altered. **(Smith, M. C. et al., 1992).** Only part of the antirepressor sequence is present, and there isn't region that is homologous to the repressor gene **(Zscheck, K. et al., 1992).** The lack of a repressor presumably explains why production of this β-lactamase in enterococci is constitutive while it is inducible in staphylococci. It does not, however, explain why the amount of enzyme produced is smaller in enterococci.

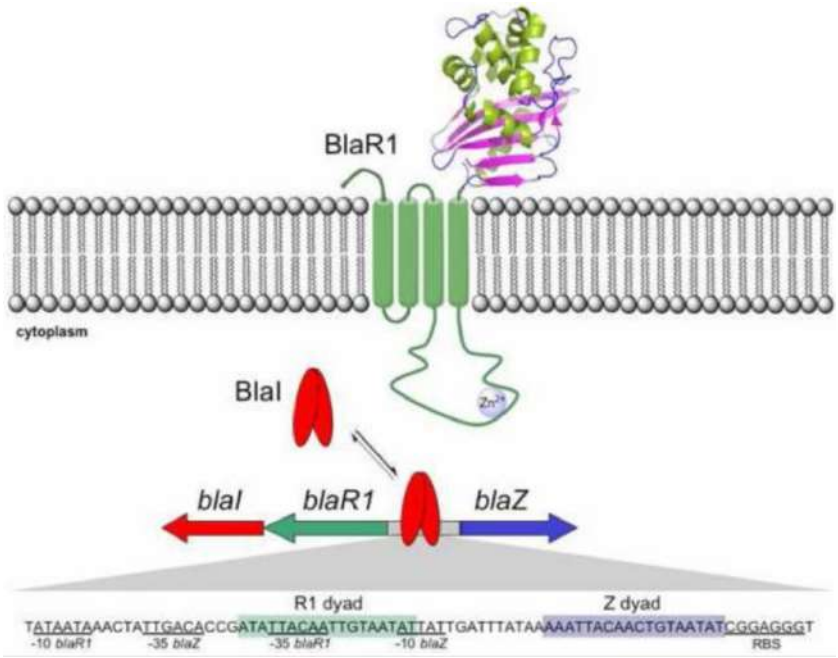

Figure 7 *The sensor and repressor of the bla operon are involved in the onset of beta-lactam resistance (Llarrull LI. Et al., 2010).*

The *bla* operator consists of two distinct binding sites for the repressor, referred to as the R1 dyad (which is upstream of the *blaR1 gene)* and the Z dyad (located upstream of the *blaZ* gene). The R1 dyad contains an 18-bp palindrome, while the Z dyad contains an 18-bp imperfect palindrome. A 13-bp-linker separates the two dyads. Sequence analysis of enterococci possessing the entire operon showed amino acid sequence identity of 97, 95 and 96% to the *blaZ, blaI* and *blar1* genes, respectively of *S. aureus,* reinforcing evidence that these genes likely originated in staphylococci **(Sarti M. et al., 2012).**

The *S. aureus* β-lactamase is a narrow-spectrum enzyme that is active only against the penicillins that happen to have activity against *E. faecalis*, nevertheless, this phenomenon is rarely described among *E. faecalis* strain. Expression of the β-lactamase in *E. faecalis* differs from that in *S. aureus* in that β-lactamase transcription is not inducible by exposure to β-lactam, and it appears that the enzyme remains membrane bound. In contrast to staphylococci, *blaZ* in enterococci is expressed constitutively and at a much lower level, resulting in a clinically inoculum effect. Thus, when inoculating bacteria at concentrations for routine susceptibility testing (generally 1×10^5 organisms per ml), the enterococci produce so little enzyme that they test susceptible, while at high inoculum, such as during infection, the presence of more enzyme leads to resistance.

Even though enzyme production is constitutive, several enterococci produce much less enzyme than a typical induced staphylococcus (**Zscheck, K. et al., 1991),** which likely explains the lack of phenotypic resistance of Bla+ enterococci unless a high inoculum is used. An inoculum effect is characteristic of Bla+ organisms, particularly Gram-positive bacteria which, lacking an outer membrane, have nothing which impedes the access of the drug to the enzyme and thus must depend on the total amount of enzyme produced by the population of bacterial cells to inactivate the drug. If the total amount of enzyme is insufficient, then the drug can overwhelm the enzyme, inactivate the susceptible target sites, and inhibit growth of the bacteria. A single cell and even a small number of cells may not produce enough enzyme to inactivate the antibiotic and will often appear susceptible; a large number of bacteria collectively produce more enzyme, can inactivate the antibiotic, and thus test resistant. Even Bla+ staphylococci show an inoculum effect and may test susceptible with an inoculum of 10^3 CFU/ml; however, they usually test resistant at the standard clinical laboratory inoculum of 10^5 CFU/ml, unlike Bla+ enterococci, presumably because most staphylococci produce more enzyme. Although all studies of Bla+ enterococci have shown an inoculum effect, the increase in the MIC with a large inoculum has been variable. Another difference between Bla+ enterococci and staphylococci is that the most strains of staphylococci release their enzyme into the extracellular medium and it can be

recovered from cell-free supernatants; with enterococci, we have not found the enzyme cell-free supernatants **(Murray BE et al, 1983).** The consequence of these differences is that expression stays at a low level and does not confer significant resistance with a standard inoculum **(Zscheck KK. Et al., 1993).** With a high inoculum, however, animal studies suggest that enterococcal β-lactamases production compromises β-lactam therapy but can be counteracted by the addition of a β-lactamase inhibitor **(Ingerman M. et al., 1987).** Once identified, however, the presence of a β-lactamase is of trivial clinical concern as the addition of the β-lactamase inhibitor sulbactam (i.e., ampicillin-sulbactam) is sufficient to restore the antibiotic efficacy. Reports of β-lactamase production in strains of *E. faecium* are quite rare, and the strains expressing it have not been extensively analyzed.

Low affinity Penicillin binding proteins expression

High level penicillin resistance in enterococci (Penicillin MIC>128 μg/ml), is commonly associated with the increased expression of low affinity PBP and accumulation of point mutation in the penicillin binding region **(Zapun et al., 2008),** yet implicate amino acid changes within the enzyme itself. These point mutation originate *de novo* in individual bacteria under selective pressure from antibiotic or chromosome to chromosome transfer of low affinity pbp genes has been documented *in vitro* and likely contributes to the dissemination of high-level penicillin resistance in *E. faecium* **(Rice LB et al.,2005).**

At present, according to internationally accepted criteria such as those of the Clinical and Laboratory Standards Institute (CLSI 2006, 2014) and the European Committee on Antimicrobial Susceptibility Testing (EUCAST 2014), *E. faecalis* susceptible to ampicillin can be considered susceptible to amoxicillin, piperacillin, and imipenem. However, susceptibility to ampicillin should not be used to predict susceptibility to penicillin, revealing the emergence of penicillin-resistant, ampicillin-susceptible *E. faecalis* (PRASEF) **(Infante et al., 2006).**

1.4.2. Ampicillin resistance

Ampicillin and penicillin are the most active β-lactams against enterococci inhibiting the synthesis of peptidoglycan. Intrinsic tolerance to the ampicillins due, as mentioned before, to the presence of a species-specific chromosomal gene, *pbp5/pbp4* with low binding affinity for ampicillin.

In *E. faecium*, *pbp5* exists in an operon with two other genes implicated in cell wall synthesis: *psr,* for PBP synthesis repressor and *ftsW,* involved during septum formation **(Rice LB. et al., 2001).**

High-level resistance to ampicillin (MIC 128 μg/ml or more) was first associated with increased production of the enzyme, requiring a higher concentration of antibiotic to saturate the active site and the mutation that occurs in the PBP4/PBP5 **(Fontana R. et al., 1994).**

In *E. faecalis*, pbp4 appears to exist independent from the operon structure described in *E. faecium*, and although it also encodes a class B PBP, it has a lower intrinsic tolerance to ampicillin (typical MICs of E. *faecalis* isolates are 1–4 μg/ml). Both overexpression of the enzyme and mutations in amino acid sequence have been implicated in higher levels of resistance, though neither method produced changes in MIC as dramatic as seen in *E. faecium* **(Duez C. et al., 2001; Ono S. et al., 2005).**

It has also been described *in vitro* an ampicillin resistance mechanism via L,D-transpeptidase known as $Ldt_{fm.}$**(Mainardi JL. Et al., 2000).** Constitutively expressed in *E. faecium*, Ldt_{fm} utilizes a tetrapeptide substrate (unlike the D,D-transpeptidases which act on pentapeptides) and is thought to be involved in the maintenance of peptidoglycan in the stationary phase. Mutations in a cryptic locus (*ddc*), coding for a putative two-component signal transduction system (TCS) induced expression of a D, D-carboxypeptidase (DdcY), which shares similarities with the *van* resistance cluster (discussed below) and produced the necessary tetrapeptide substrate **(Sacco E. et al., 2010).** Of note, this pathway would allow the synthesis of a functional cell wall in the presence of glycopeptides **(Cremniter J. et al., 2006).**

Ampicillin resistance has been rarely reported in *E. faecalis*, as this did not represent a clinical and therapeutic challenge. Until recently, it was assumed that ampicillin-susceptible *E. faecalis* was also susceptible to penicillin, but the clinical isolates have been exhibiting increasing levels of resistance to penicillin, due to the

emergence of Penicillin-Resistant Ampicillin-Susceptible (PRAS) isolates, eliminating β-lactams as a treatment options **(Guardabassi er al., 2010; Cabrera et al., 2020; Gawryszewska I. et al., 2021).**

1.4.3. Cephalosporin resistance

E. faecalis and *E. faecium* are intrinsically resistant to cephalosporin. Ceftaroline and ceftobiprole, fifth generation cephalosporins, have activity against *Enterococcus spp.*, but may be prone to emergence of resistant with increased clinical use. Ceftobiprole shows good *in vitro* activity against *E. faecalis* with no reports of resistance to date **(Arias CA et al., 2007)** but is ineffective against penicillin-resistant clinical strains of *E. faecium* **(Henry X et al., 2010).** The intrinsic resistant is associated with a decrease in binding affinity of cephalosporin for the enterococcal PBPs.

Additionally, several regulatory pathways controlled by bacterial two-component regulatory systems (TCS) have also been associated with the intrinsic resistance to cephalosporin. Among them, CroRS was shown to be important for cephalosporin resistance. CroS, a sensor with histidine kinase activity, phosphorylates the cognate response regulator CroR, which is postulated to alter transcription via a DNA binding domain. **(Comenge Y. et al., 2003).** The inactivation of CroRS rendered *E. faecalis* susceptible to extend spectrum cephalosporin, but not to a panel of antibiotics that perturb other cellular process **(Hartmann C. et al., 2010).** Analysis of the deletion mutant revealed that the loss of CroRS function did not alter the expression of PBP5, peptidoglycan precursor, production, or peptidoglycan crosslinking. CroRS TCS appeared to function in according to conventional models for TCSs, in that the CroS kinase could autophosphorylate itself in an ATP-dependent manner, followed by the transfer of the phosphoryl group to the CroR response regulator. CroR response regulator contains a functional DNA binding domain, which suggested that transcriptional remodelling is necessary for adaption to the stress imposed by cephalosporin.

A second signal transduction protein, IreK, is required for cephalosporin resistance in *E. faecalis*. Ire K exhibits a characteristics bipartite domain architecture that includes a "eukaryotic-type" Ser/Thr kinase coupled, through a putative transmembrane segment, to a series of five repeats of the PASTA domain, which bind to peptidoglycan or fragments thereof **(Squeglia, et al., 2011; Yeats, Finn, & Bateman, 2002).** Probably, that IreK could serve as a transmembrane receptor kinase that senses damage or perturbation of the peptidoglycan and initiates a signalling circuit to restore cell wall integrity. Analysis of an *E. faecalis* deletion mutant revealed that IreK is required for intrinsic cephalosporin resistance and for resistance to certain other cell-envelope stresses, such as detergents that are present in bile salts **(Kuch A. et al., 2012)**. Ire K exhibits protein kinase activity *in vitro,* and its kinase activity is required to promote cephalosporin resistance in *E. faecalis*. As with other members of this kinase family, IreK can catalyze autophosphorylation of threonine residues contained with a specific segment of the kinase domain known as the "activation loop". Phosphorylation at these sites is usually thought to lead to a conformational change, which results in enhanced activity of the kinase. IreP is a phosphatase that can dephosphorylate both IreK and substrates of IreK, *in vitro.* IreP mutants exhibit substantial hyperresistance to cephalosporins, a finding which is consistent with hyperactivation of the IreK kinase. Mutants that lack IreP exhibit a large reduction in fitness in the absence of cephalosporins, as compared to wild-type *E. faecalis,* which indicates that uncontrolled activation of cephalosporin resistance mechanisms imparts a significant fitness cost to the cell. A third protein, IreB, was demonstrated to be the target of both IreK and IreP and to negatively regulate the expression of cephalosporin resistance. This system seems to be specific to cephalosporin resistance, as MICs to ampicillin and other cell wall active agents were unchanged.

One protein that may be involved in the downstream effects of the IreK signaling pathway is MurA-A, one of a pair of homologs that catalyze the first committed step in peptidoglycan synthesis **(Vesić D et al., 2012).** Deletion of the gene coding for this enzyme resulted in a loss of resistance to cephalosporins despite the ability of the homolog MurAB to carry put enzymatic activity as a uridine diphos-phate N-acetylglucosamine, a-carboxyvinyl transferase.

Deletion of *murAA*, but not *murAB*, led to an increased susceptibility of *E. faecalis* to cephalosporins. This enhanced cephalosporin susceptibility does not reflect a general growth or cell-wall synthesis defect of the mutant, because the deletion mutant is not sensitized to antibiotics in general—or even to all antibiotics that

inhibit cell wall biosynthesis—but exhibits a loss of resistance specifically for extended spectrum cephalosporins and for fosfomycin (an antibiotic known to target MurA homologs). In addition, expression of *murAA*-enhanced cephalosporin resistance in an *E. faecalis* mutant that lacked IreK, which suggests that MurAA may function downstream of IreK in a pathway that leads to cephalosporin resistance. Further genetic analysis revealed that MurAA catalytic activity is necessary, but not sufficient, for this role **(Miller et al., 2014).**

1.5. Ceftobiprole

Cephalosporins are beta-lactam antimicrobials used to manage a wide range of infections, grouped into five generations based on their spectrum of coverage and their temporal discovery. Whenever the structure of cephalosporins modified, a new generation of cephalosporins are made **(Aiswarya P. Nath et al., 2020).**

Fifth generation cephalosorins include ceftobiprole, an advanced broad-spectrum antimicrobial with demonstrated superior *in vitro* antibacterial and bactericidal activity against Gram-positive, as well as methicillin-resistant *S. aureus* (MRSA) and *S.epidermidis* (MRSE), and penicillin-resistant *S. pneumoniae*. Ceftobiprole exhibited also bactericidal activity at concentration of 4, 8 and 16 mg/L against ampicillin susceptible, vancomycin-susceptible and vancomycin-resistant *E. faecalis* isolate, and β-lactamase producing strains **(Deshpande et al., 2003)**. The minimum inhibitory concentration at which 50%-90% of bacteria are inhibited (MIC_{50}-MIC_{90}) is lower than those for cefotaxime, ceftriaxone, ceftazidime and cefepime, demonstrates *in vitro* activity against *E. faecalis* isolated tested (MIC_{50} of 0.5 mg/L; MIC_{90} of 4 mg/L) and against ampicillin susceptible *E. faecium*, but not against ampicillin-resistant. (>32 mg/L).

In Gram positive strains, ceftobiprole Bactericidal activity is due to high affinity to multiple PBPs, including MRSA PBP2a **(Campanile et al., 2019)** and *E. faecalis* PBP4 **(Lazzaro et al., 2022)**,

The activity of this antibiotic is also effective against Gram negative bacilli among which AmpC-producing *E. Coli* and *Pseudomonas aeruginosa*, excluding extended spectrum β-lactamase producing strains like *H. influenzae*, *K. pneumoniae* **(Zhanel GG.et al., 2008).** Furthermore, Ceftobiprole show potent *in vitro* activity against *M. catarrhalis*, *P. mirabilis* and *Salmonella spp*; demonstrate limited activity against anaerobes such as *Bacteroides fragilis*, *Clostridium perfringens* and *C. difficile*, and generally against β-lactamase producing isolates. Based upon MIC_{90} data, ceftobiprole has comparable *in vitro* activity to cefepime against several Gram-negative pathogens but show poorly active against extended spectrum β-lactamase producing *E. coli, K. pneumoniae* and *P. mirabilis.* with MIC_{90} values of>16 and >32 mg/L.

Structurally, Ceftobiprole possess a bicyclic ring structure containing a four membered β-lactam ring fused to a six-membered dihydrothiazine ring and an oxymino aminothiadiazolyl substituent linked to the 7-aminogroup of the bicyclic cephalosporin ring, that confer stability against many common penicillinases and broad-spectrum β-lactamases. The vinylpyrrolidinone moiety at position 3 promote binding to penicillin-binding protein.

Ceftobiprole medocaril, the prodrug of Ceftobiprole, is converted by plasma esterases to ceftobiprole in < 30 minutes **(Fig. 8)** and shows several pharmacokinetic and pharmacodynamic properties that make it a very interesting molecule: high bactericidal activity, proven *in vitro* experimental model and animal studies *in vivo,* **(Arias CA et. Al., 2007);** low protein binding (16%), a high volume of distribution, and predominantly renal excretion (70-90%).

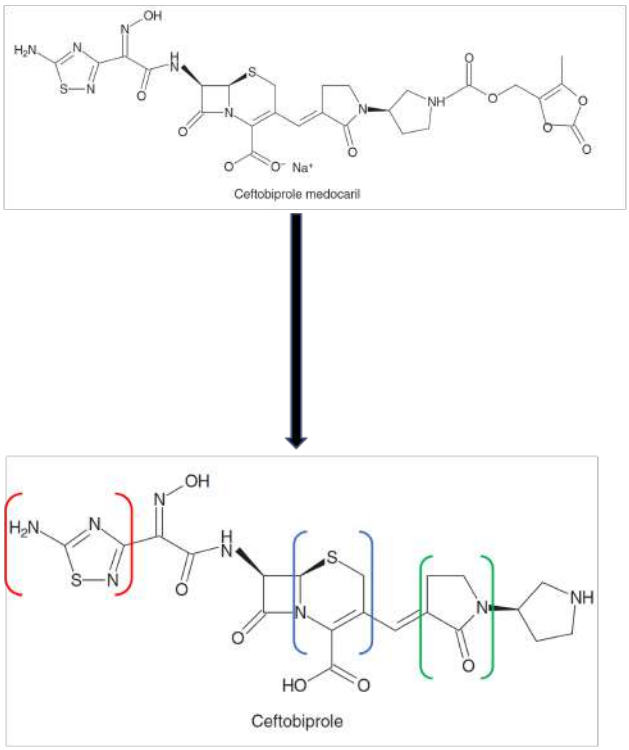

Figure 8. *Structural of prodrug ceftobiprole medocaril and ceftobiprole. Red: Oxyimino aminothiadiazolyl substituent; Blue: Dihydrothiazine ring; Green: Vinylpyrrolidinone moiety.*

Like other cephalosporins, the ceftobiprole mechanism of action is attributed to its ability to bind high affinity PBPs and irreversibly inhibit peptidoglycan biosynthesis by acylating the active-site serine of PBP, rapidly forming a stable, inhibitory complex. Moreover, it has been shown that ceftobiprole acylates *S. aureus* PBP2a more rapidly than other β-lactams antibiotics, forming a more stable acyl-enzyme complex through a unique mode of interaction with the protein **(Hebeisen et al., 2001).**

Another Ceftobiprole feature is that it appear stable to hydrolysis by staphylococcal and enterococcal penicillinases and it is relatively stable to class C β-lactamases, showing a low tendency to induce these enzymes, representing a poor substrate for these enzymes, which explains its excellent activity against β-lactamases-producing *E. faecalis* **(Queenan A et al., 2005; Heep M. et al., 2005),** but susceptible to hydrolysis by rare class A cephalosporinases and class B metallo-β-lactamases **(Page MG et. Al., 2006; Queenan A. et al., 2007).**

Ceftobiprole exhibits some promising features that may help to place it in a wide range of complex infections in the near future, like a very good activity against biofilm, once again showing synergy with rifampin and vancomycin **(Abbanat D et al., 2014),** and *in vitro* synergy with different antibiotic.

In vitro time kill studies shown that combinations of ceftobiprole with either amikacin or levofloxacin were synergistic against *P.aeruginosa* **(Kresken M. et al., 2007),** while the combinations of ceftobiprole with amynoglycosides were found to be synergistic against *E. faecalis*, including vancomycin-resistant isolate (VRE). Among enterococci, *E. faecium* showed indifference to almost all combinations while largely synergistic effects were seen in *E. faecalis* with ceftobiprole in combination with Linezolid, rifampicin and piperacillin-tazobactam. Ceftobiprole plus daptomycin combination represented the most potent combination in the time kill-model, with synergy against all isolates at the 1X MIC of ceftobiprole and 1 log10 CFU/ml reduction at the 2X and 4X MICs **(Campanile et al., 2019).**

The broad-spectrum activity of Ceftobiprole may make it an ideal alternative to complex multiple antibacterial regimens for the treatment of nosocomial infections, such as hospital and ventilator-associated

pneumoniae and polymicrobial infections and may be used in combination with vancomycin or linezolid for treatment of community acquired pneumoniae by CA-MRSA. Its activity is efficacious in the treatment of complicated skin infections.

To date, ceftobiprole has shown a reduced ability to develop antimicrobial resistance **(Morosini et al., 2019);** however, excessive clinical use can cause its onset **(Hollenbeck et al., 2012).** Strains subjected to increasing concentrations of this molecule have developed resistance *in vitro***.**

The prior exposure to cephalosporin is one of the most well-known risk factors for acquisition of an enterococcal infection (Shepard BD et al., 2002) because enterococci proliferate to abnormally high densities in the intestinal tract of patients receiving cephalosporin and subsequently escape to cause infection elsewhere.

Among the most frequent changes involved in ceftobiprole resistance in *E. faecalis* are mutations in PBP4 in the protein coding region and/or promoter.

For many years, low affinity PBP4 has been thought to be the primary PBP required for cephalosporin resistance, exhibiting intrinsically low reactivity, and enabling growth in its presence. The construction of Δ*pbp*4 mutant exhibited a substantial loss of resistance to cephalosporin in enterococci.

Djorić D, et al.,2020, confirm that exist other PBPs involved in cephalosporin-resistance and that exhibit a low intrinsic reactivity with cephalosporin *in vivo* and *in vitro*, required for growth in the presence of cephalosporins, among which thePBP2b. To evaluate their importance about enterococcal cephalosporin resistance, were construct deletion mutants, lacking the corresponding genes. Δ*pbp*2b mutants revealed a substantial loss of resistance to cephalosporin, similar to Δ*pbp*4 mutant. Complementation of this gene restores the original phenotype. Its intrinsically low reactivity enables PBP2b to avoid acylation (i.e., inactivation) by cephalosporin.

About the third classB PBP, encoded by *E. faecalis*, known as PBP2, It is impossible construct a mutant lacking PBP2, suggesting that it may be essential for viability, probably because this PBP is involved in cell division, but other studies suggest that this PBP is highly reactive with cephalosporin, *in vivo* and *in vitro*.

These data support the hypothesis that PBP4 and PBP2b acts collectively to determine cephalosporin resistance, performing distinct functions in enterococcal cells. PBP4 is important primarily to enable growth in the presence of cephalosporins, but the activity of PBP2b plays a more central role in overall peptidoglycan synthesis.

Finally, either of 2 classA PBP (PBP1a/ponA and PBP1b/PBPF) were required for cephalosporin resistance, which glycosyltransferase activity is required for peptidoglycan synthesis in cooperation with PBP4.

1.6. Penicillin binding protein

Bacterial peptidoglycan enable to bacteria to resist the intracellular pressure of several atmospheres that exists in the cell but also provides the bacterium with a well-defined cell-shape that is reproduced from generation to generation. This is made of glycan chains of alternating N-acetylglucosamine and N-acetylmuramic acid. **(Ghuysen JM, 1968; Schleifer e Kandler, 1972; Vollmer et al., 2008a).** Penicillin-binding proteins (PBPs) catalyze the polymerization of the glycan strand (transglycosilation) and the cross-linking between glycan chains (transpeptidation). Some PBPs can hydrolyze the last D-alanine of stem pentapetides (DD-carboxypeptidation) or hydrolyze the peptide bond connecting two glycan strands (endopeptidation). Endopeptidation and transpeptidation are reverse activities. Their role is synthesize new and remodel existing peptidoglycan.

The transpeptidation catalyzed by PBPs follow a three-step mechanism: the rapid, reversible formation of a complex between the enzyme and a peptidoglycan stem pentapeptide [L-Ala-g-D-Glu-A2pm (or L-Lys)-D-Ala-D-Ala], called the donor strand, is followed by the attack of the active serine in the carbonyl carbon atom of the C-terminal D-Ala-D-Ala peptide bond, leading to the formation of an acyl-enzyme intermediate and the concomitant release of the C-terminal D-Ala (acylation). The final step of deacylation consist of either hydrolysis with release of the shortened peptide (carboxypeptidation), or cross-link formation with a second peptidoglycan stem peptide called the acceptor strand (transpeptidation). This DD-peptidase activity is catalized by a common PB domain, which bind β-lactams antibiotics.

PB domain is made of two subdomains, a five stranded β-sheet covered by three α-helices and an all-helical domain. The active site lies at the interface of these two subdomains. **(Fig 9).**

There may be some flexibility between these two domains, and this can influence the binding capability of some PBPs towards various ligand **(Lim & Strynadka, 2002).** The active site encompasses nine residues broadly conserved on PBPs. The active serine is positioned at the beginning of helix a2 and is followed by a lysine to form a SxxK motif. A second motif, SxN, is situated in a loop between helices α4 and α5. Four conserved residues form the third motif KTG(T/S), a ninth residue, a glycine situated in the rear of the active site, are also strictly conserved**.** The carbonyl oxygen of the penultimate D-alanine lies in the oxyanion hole and its methyl group is inserted into a hydrophobic pocket. The carboxylate of the leaving D-alanine is oriented towards the two hydroxyl groups of the third motif. The asparagine of the second motif and the hydroxyls group of the third motif are important for the correct positioning of the substrate. **(Adediran et al., 2005).**

The acylation of PBPs requires the abstraction of a proton from the active serine. The lysine of the first motif, assumed deprotonated, can perform the withdrawal of the proton **(Nicola et al., 2005; Macheboeuf et al., 2006; Sauvage et al., 2007).** The proton can be back-donated to the leaving D-alanine amine group via the serine of the second motif. In the deacylation step, a proton of the acceptor must be abstracted to allow the activated group to attack the carbonyl carbon atom of the ester bond of the acyl-enzyme. The proton can be back donated to the active serine. Withdrawal of a proton from the acceptor group can be performed by the lysine of the third motif, which needs to be in a deprotonated form. The active site of PBPs can be seen a double lysine-serine system, one for acylation and one for deacylation, although both systems are not independent.

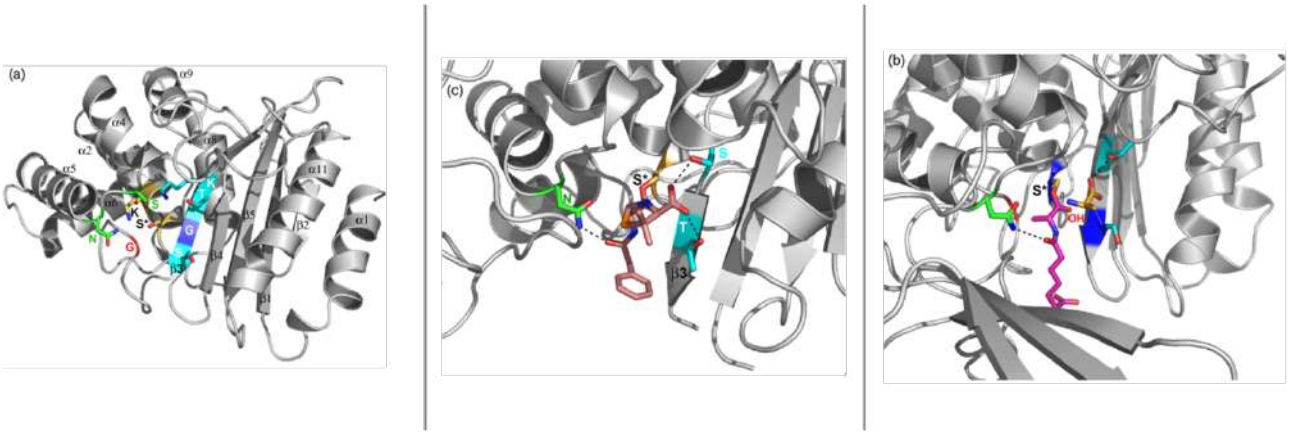

Figure 9 *a) Penicillin binding domain active site; Yellow:The first motif SxxK; Green: the second motif SxN ; Cyan: the third motif. Red. The glycine in the rear of the active site;b) PB domain active site acylated by a peptidoglycan mimetic peptide. The dipeptide D-a-aminopimelyl-e-D-alanine (magenta) is covalently linked to the active serine.OH indicates the oxyanion hole defined by the two backbone amine groups shown in dark blue The released D-alanine is shown in orange.H-bonds are shown as dashed lines.c) PB domain active site(Staphylococcus aureus PBP2a) acylated by benzylpenicillin.Benzylpenicillin and the active serine are shown in pink. The amidebond of benzylpenicillin side chain is wedged between strand b3 andthe asparagine of the second motif (green). The carboxylate is hydrogenbonded to both hydroxyl group of the third motif KSGT (cyan).*

The β-lactams antibiotics inhibit the enzymatic activity of PB domain, by playing on the structural similarity between penicillin and D-Ala-D-Ala dipeptide that ends the natural substrate of PBPs, the pentapeptide precursor of the peptidoglycan, forming a long-lived acyl-enzyme that impairs their peptidoglycan cross-linking capability. **(Tipper & Strominger, 1965; Ghuysen, 1991).**

X-ray structures show that many antibiotics covalently linked to the active site serine adopt a common standard positioning that shares some characteristics with the acyl-enzyme PBP4a-a-aminopimelyl-e- D-alanyl: the amide group of the side chain is inserted between the asparagine of the second motif ant the backbone of β3 strand; the carboxylate associated to the thiazolidine or to the dihydrothiazine ring of the antibiotic is hydrogen bonded to one or both hydroxyl groups of the KTGT motif, and the carbonyl oxygen lies in the oxyanion hole.

1.6.1. Main PBPs classification

Bacterial genome sequencing allowed to determine the exact number of PBPs of several bacteria species. Each bacteria show a variable number of PBPs, habitually classified as high molecular weight (HMW;> 45 kDa) PBPs and the low molecular weight (LMW; <45 kDa) PBPs.

HMM PBPs are multimodular PBPs, responsible for peptidoglycan polymerization and insertion into pre-existing cell wall (**Goffin & Ghuysen, 1998; Born et al., 2006).** Their topology consists of a cytoplasmatic tail, a transmembrane anchor, and two domains joined by β-rich linker located on the outer surface of the cytoplasmic membrane where peptidoglycan synthesis take place **(Macheboeuf et al., 2006; Lovering et al., 2007).** Based on number of reactions that can catalyze, the HMW-PBPs are classified in class A PBPs, bifunctional PBP with both glycosyltransferase and transpeptidase activity; class B PBPs, monofunctional, with only transpeptidase activity and class C PBP with carboxypeptidases and endopeptidases activity. **(Moon M.T. et al. 2018).**

The C-terminal penicillin binding (PB) domain of both classes has a transpeptidase activity, cataliyzing peptide cross-linking between two adjacent glycan chains. In class A, the N-terminal domain is responsible for their glycosyltransferase activity, catalyzing the elongation of uncross-linked glycan chains. In class B, the N-terminal domain play a role in cell morphogenesis by interacting with other proteins involved in the cell cycle **(H¨oltje, 1998; den Blaauwen et al., 2008; Zapun et al., 2008a).** LMM PBPs are monofunctional peptidyl-transferases with D, D-carboxypeptidase activity and with D,D-endopeptidase activity, sometimes are classified as class A, B and C, but frequently described with the general term of class C PBPs, with four

subcategories that will refer to their main PBP representative in *Escherichia coli*. (Type-4 for PBP similar to *Escherichia coli* PBP4; type-5 for enzyme similar to *E. coli* PBP5; type 7 for PBPs similar to *E. coli* PBP7 and type-AmpH for PBPs similar to *E. coli* AmpH).

The classification of class A-B-C PBPs is based on sodium dodecyl sulfate-polyacrylamide gel electrophoresis (SDS page) migration **(Table 1).**

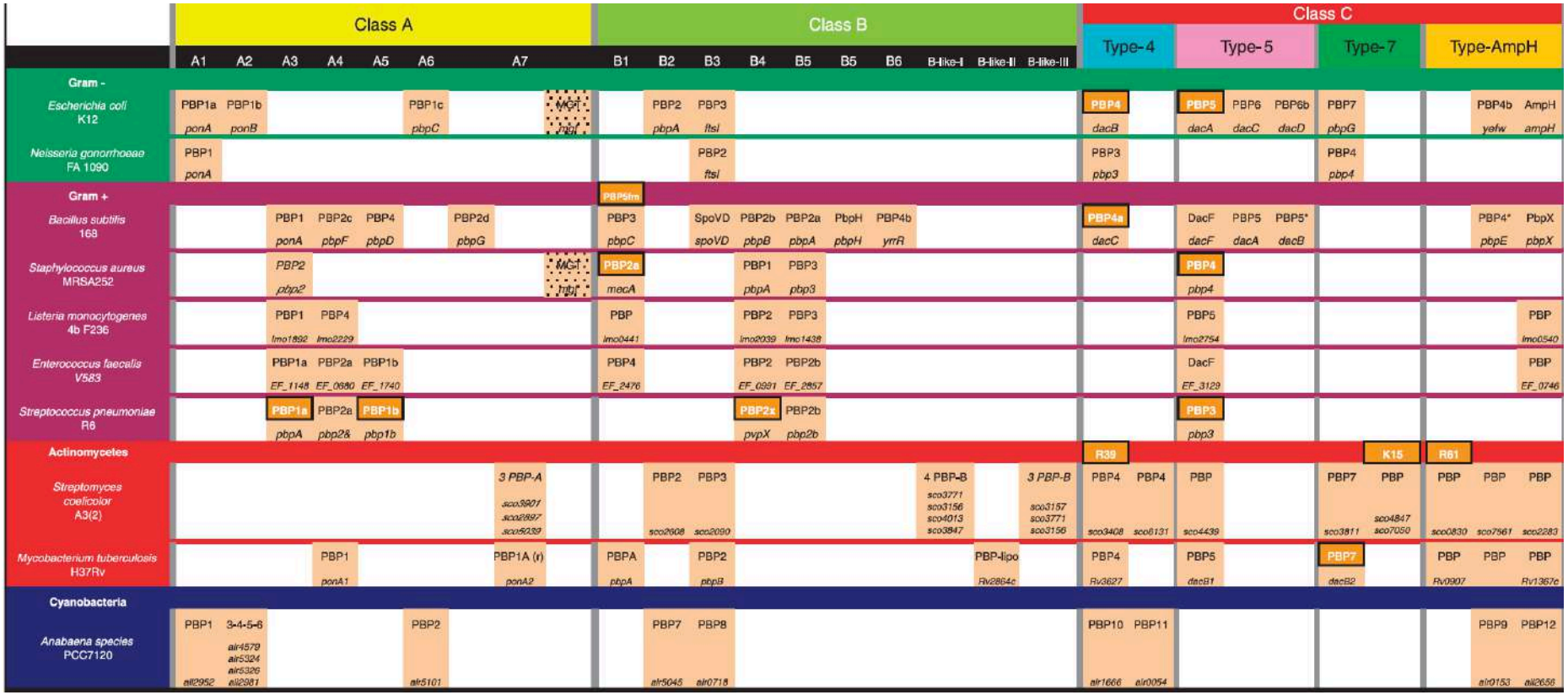

Table 1. *PBPs classification from 10 bacteria, following the Goffin e Ghuysen (1998) subdivision. The name of the PBP is given with its encoding gene (for most PBPs).*

1.6.2. PBPs in different species

The **Table 1** show the number of PBP in different species.

E. coli possess 12 PBP; 3 class A PBPs (PBP1a and PBP1b, monofunctional, with transpeptidases/transglycosylases activity, and PBP1c, which role is not understood);2 class B PBPs, monofunctional transpeptidases (PBP2, involved in the "elongase"process, and PBP3, a major protein of the divisome). **(den Blaauwen et al. 2008);** 7 LMW PBPs: PBP4 and PBP7, two endopeptidases that cleave cross-bridges between two glycan strands; PBP5, a major carboxypeptidase that cleaves the terminal D-Ala D-Ala bond, making the stem peptide unavailable for transpeptidation. **(Spratt & Strominger, 1976);** PBP6 and PBP6b with a carboxypeptidase activity; PBP4, with a undetermined role and AmpH, associated with peptydoglycan recycling.

Neisseria gonorrhoeae show 4 PBPs. PBP1, analogous to *E. coli* PBP1a and PBP2, homologous to *E. coli* PBP3. **(Ropp et al. 2002; Dowson et al. 1989)**. PBP3 and PBP4 have sequences similar to *E. coli* PBP4 and PB7. **(Stefanova et al. 2004).** The absence of an elongase complex is coherent whit its coccoid shape.

Bacillus subtillis possess 16 PBP. 4 class A PBPs: PB1, involved in the cell division machinery and is required for the efficient formation of the asymemetric sporulation septum **(Scheffers & Errington, 2004). ;** 6 class B PBPs: PBP2b a transpeptidase involved in the division cell process. **(Daniel et al., 2000)**; PBP4, the equivalent of *E. coli* PBP4, and PBP5, that are the major carboxypeptidase; 4 class C PBPs, among which PBP5* and dacF PBP5*., required for proper spore cortex synthesis **(Popham et al., 1995)**, and dacF that regulate the degree of cross-linking of spore peptidoglycan (**Popham et al., 1999)**, PBP4* and PBPX, involved in sporulation. **(Scheffers, 2005).**

Streptococcus pneumoniae has 3 class A PBPs, 2 class B PBPs and one type-5 class C PBPs. **(Hoskins et al., 1999; Morlot et al., 2005).**

Streptomyces genus probably because of their complex life cycle and their ability to produce β-lactam molecule possess a great number of PBPs that can be expressed at different stages of the bacterial development or when the bacterium produces β-lactams metabolites that can interfere with peptidoglycan biosynthesis.

Mycobacterium tuberculosis produces 2 class A PBPs, 2 class B PBPs and a lipoprotein sharing some motifs with the class B PBPs (**Goffin & Ghuysen, 2002).** 6 class C PBPs, one type-4, one type-5, one type-7 and three putative type- AmpH, complete the set of PBPs of M. tuberculosis.

Listeria monocytogenes has 6 PBPs **(Guinane et al., 2006),** including 2 class A PBPs (PBP1 and PBP4), 3 class B PBPs (PBP2, PBP3 and lmo0441), and 1 class C PBP of type-5 (PBP5) (**Zawadzka-Skomial et al., 2006).**

Staphylococcus aureus incorporates peptidoglycan at the division site and has no elongase complex. **(Zapun et al., 2008a)**. Its unique class A PBP localizes to the septum. The β-lactams susceptible strains have two class B PBPs (**Pinho et al., 2000; Pereira et al., 2007),** but resistant strains have acquired an additional PBP, PBP2a with a low sensitivity to β-lactams **(Zapun et al.,**

2008b). *S. aureus* possess only one LMM PB, of type 5, with a transpeptydase activity, necessary to achieve the high degree of cross-linking observed in the peptidoglycan of staphylococci. **(Wyke et al., 1981).**

All Enterococci produce at least five PBPs. The genome analysis of both *E. faecalis* and *E. faecium* revealed six putative PBP genes, 3 which are classes A protein (*pon*A, *pbp*F, *pbp*Z). and 3 class B PBPs (*pbp5, pbpA, pbpB*). **(Arbeloa et al., 2004).** PBP2 is encoded in a gene cluster involved in cell division, such as *ftsq,ftsA,ftsZ* and *divIVA,* suggesting that this PBP participates in septal PG synthesis during cell division and might therefore be essential for viability **(Dusanka D.et al., 2020).** The intrinsic resistance to β-lactams is due to the class B PBP, known as PBP4 (*E. faecalis*), and PBP5 (*E. faecium*) **(Duez et al., 2001a; Zapun et al., 2008b);** they possess only 2 class C PBP: DacF, a type-5 PBP,and a type-AmpH PBP**. (el Kharroubi et al., 1989).**

1.6.3. Focus on Class A PBPs

Class A PBPs can be grouped in at least seven subclasses. Subclasses A1 and A2 contain PBP belonged to Gram negative, while subclasses A3, A4 and A5 form three clusters of Gram-positive PBPs. Subclass A6 and A7 contains unusual PBP **(Goffin & Ghuysen, 1998).** The presence of a class A PBP is necessary for cell growth in most but not all bacteria. For example, in *E. coli*, the loss of PBP1a and PBP1b is tolerated but loss of both proteins is lethal even in the presence of PbP1c **(Denome et al., 1999).** In Gram positive bacteria, the PBPs of subclass A3 are the major class A PBPs and are recruited to the septum site. **(Scheffers & Errington, 2004; Leski & Tomasz, 2005).**

Likewise, the absence of all its class A PBPs is not lethal to B.subtilis. The strain lacking all four class A PBP is still viable and produces a peptidoglycan with only small structural differences from that of the wild type.

In the same way, in *E. faecalis* the deletion of the three class A PBPs is not lethal although this led to an increase in generation time and a decrease in peptydoglycan cross linking.

Arbeloa et al. have performed a combination of deletions that were introduced in all three class A PBP genes of *E. faecalis pon A*;(*pbpF* and *pbpZ*), to evaluate the role of the three class A PBP in intrinsic β-lactam resistance and their impact on bacterial growth. peptidoglycan cross-linking and susceptibility to cell wall synthesis inhibitors. The single deletion of any of the three class A PBP genes of *E. faecalis* had no impact on the MIC of beta-lactam antibiotic. Only the contemporary deletion of *ponA* and *pbpF* resulted in a large decrease (1000-fold) in ceftriaxone resistance, suggesting that these were required for intrinsic ceftriaxone resistance mediated by PBP5, and that are essential partners of PBP4. The contemporary deletion of *ponA*,*pbpF* and *pbpZ* led to a viable mutant, indicating that the class A are unessential to the cell survival.

As there is no monofunctional glycosyltransferase in *Enterococcus faecalis*, the glycan chain polymerization in the triple mutant must be performed by a novel type of glycosyltransferase **(Arbeloa et al., 2004).**

The PBP A structure it was determined by X ray **(Lovering et al., 2007).** The general fold is made of an N-terminal domain coupled to the C-terminal PB domain. The interdomain linker is composed of a small β-sheet and one α-helix. A small number of class A PBPs contain an additional C-terminal domain made of one or two repeating units know as Penicillin-binding protein and Serine/Threonine kinase Associated domain (PASTA) because this domain is also found in the C-terminal of serine/threonine kinase **(Yeats et al., 2002).** The PASTA domain is a small globular domain consisting of three β-strands and one α-helix.

A fibronectin type III domain (Fn3) can also be found at the C-terminus, often involved in cell surface binding, while a forkhead associated domain (FHA), consisting of a typical 11 stranded β-sandwiches fold, may be found at the N-terminus, involved in protein-protein interaction domains. **(Fig.10).**

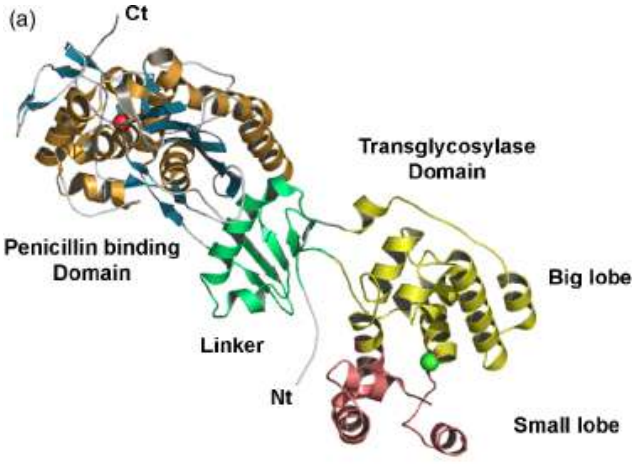

Figure 10 *Structure of class A PBPs. Green: linker region; Yellow and salmon: big and small lobes of the transglycosylase domain,respectivally. Redsphere: catalytic serine; Greensphere: catalytic glutamic acid (Sauvage et al., 2008).*

In presence or absence of substrate it was observed that the transpeptidase domain show an apoenzyme structure in "open" and "closed" forms, that may play a regulatory role in PBPA catalytic activity. Residues following the KTGT motif on strand β3 move away from strand β4 and an asparagine situated in the loop connecting these two strands makes hydrogen bond contacts with the backbone of a loop situated on other side of the active site, thus blocking the entry of the active site. In presence of substrate the active site retains a "canonical" configuration and the antibiotic forms with the class A PBP a classic acyl-enzyme.

The glycosyltransferase domain contains almost only α-helices and of a large and a small lobe separated by an extended cleft that contain the active site. All glycosyltransferase domains shared five conserved motifs: Motif 1 and motif 3, contain the two conserved catalytic glutamic acids and motif 2, which divides the cleft in two pockets is more likely to be involved in substrate recognition. These 3 motifs are found in the catalytic cleft. Motif 4 forms the black wall of the cleft and motif 5 is located in the large lobe farther from the active site, probably playing a structural role **(Lovering et al., 2007).** The bond with the substrate induces conformational change in the small subdomain and that some flexibility occurs around the linker region connecting the glycosyltransferase and the transpeptidase domain.

In class A PBPs, the N-terminal domain is responsible for their glycosyltransferase activity, catalyzing the elongation of uncross-linked glycan chains of the peptidoglycan.

The mechanism of glycan chain elongation by the glycosyltransferase proceeds by successive attacks of the growing chain (donor) at the reducing end by lipid II (acceptor) catalyzed by deprotonation of the 4-OH nucleophile of GlcNac by the active site base, concomitant with stabilization of the leaving diphosphoundecaprenyl group by the second glutamate, probably via a divalent metal **(Schwartz et al., 2002).** For the bifunctional PBPs, the transglycosilation can proceed while the transpeptidase domain is either inhibited by penicillin, mutation or is completely deleted. (**Terrak et al., 1999; Born et al., 2006).** In contrast, inactivation of the glycosyltransferase domain by mutation completely blocks the peptidoglycan polymerization.

1.6.4. Focus on class C PBPs

Type 4

Generally, there is one or zero type-4 class C PBP in bacteria.

Structurally, the transpeptidase domain is associated with two other domains, which are not in N-terminal or C-terminal position but are inserted in the transpeptidase domain in the way of matryoschka dolls. **(Sauvage et al., 2005),** i.e., the third domain is inserted in the second domain, which itself is inserted in the PB domain between the conserved motif 1 and 2 (of the PB domain), which role is unknown. Domain II has the topology of half a Rossmann fold, which is also the case of the N-terminal domain of MinC and the 1A region of FtsA, two proteins interacting with FtsZ and involved in the regulation of the septum formation in cell division, but the resemblance of these proteins to the domain II of type-4 PBPs remains limited. Domain III consists of two three-stranded β-sheets facing each other. The surroundings of the active site are specific to type-4 PBPs. The residue following motif 3 is invariably a leucine or a methionine, a hydrophobic residue turned inside the cavities that pushes the C-terminus of β3 strand slightly to the forefront of the active site. The residue following motif 3 is invariably a leucine or a methionine, a hydrophobic residue turned inside the cavities that pushes the C-terminus of β3 strand slightly to the forefront of the active site. Together with the residues pertaining to domain II, the residues of the C-terminus of β3 strand form a pocket that can accommodate the terminal H3N1–CH–COO group of the diaminopimelic acid, the antepenultimate amino-acid of the peptidoglycan stem peptide **(Sauvage et al., 2007).**Type-4 PBPs are very loosely associated with the cytoplasmic membrane and could be inserted into the peptidoglycan or exposed on the outer face of peptidoglycan where it would exert its endopeptidase activity and could thereby be indirectly involved in cell morphology **(Meberg et al., 2004),** in daughter cells separation **(Priyadarshini et al., 2006),** and implicated in biofilm formation **(Gallant et al., 2005). (Fig.11)**

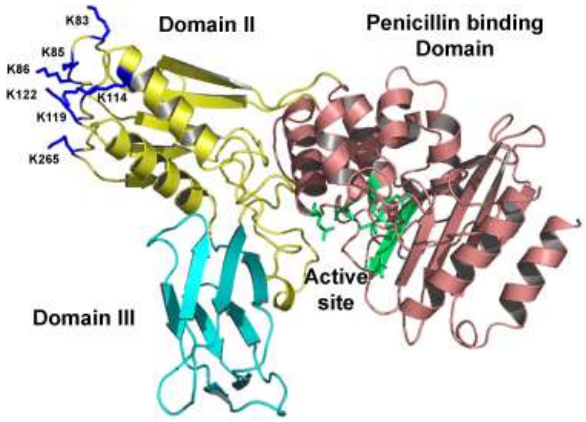

Figure 11 *Structure of type-4 PBPs. Salmon: PB domain; Yellow: domain II; Cyan: domain III. Green: acrive site, with conserved motifs residues shown as sticks. Blue sticks represente seven lysine residue (Sauvage et al., 2008).*

Of note is the absence of this protein in Gram positive cocci like staphilococci and enterococci.

Type 5

Type-5 PBPs are the most abundant LMW PBP produced by bacteria.

The fold of type-5 PBPs is biglobular. The PB domain is associated with a β-strand rich C-terminal domain that is essential for the correct functioning of the PBP5 and ends with an amphipathic helix that associates PBP5 to the cytoplasmatic membrane. The PB domain lacks the N-terminal helix, and a small loop extends on the top of the active sites. Except of *S. aureus* PBP4 , which shown to have a secondary transpeptidase activity **(Wyke et al., 1981),** generally type-5 PBPs are strict DD-carboxypeptidases unable to catalyze a transpeptidation reaction. (**Matsuhashi et al., 1979),** playing a major role in the control of cell diameter and correct septum formation.

Type 7

The structure of PBP7 differs from that of PBP5 by the absence of the C-terminal domain and the amphipathic helix that anchors PBP5 to the cytoplasmic membrane, lack the N-terminal helix and exhibit on the top of the active site a β-hairpin protuberance to anchor the protein to the plasma membrane. **(Fonzè et al., 1999).** They show an endopeptidase activity but had no carboxypeptidase activity, implicated in cell morphology **(Meberg et al., 2004)** and in daughter cells' separation. **(Fig. 12)**

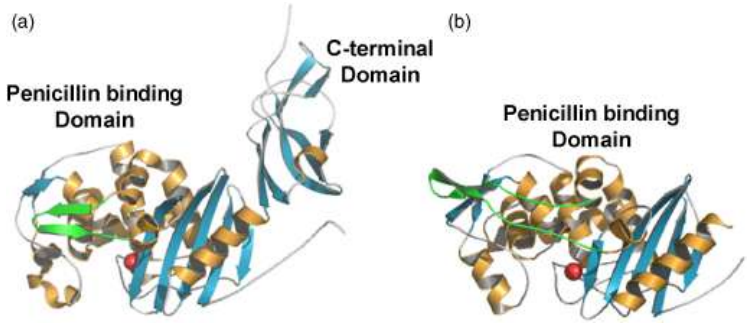

Figure 12 *Structures of type-5 and type 7 PBPs. The catalytic serine of the PB/DD-peptidase domain is shown as a red sphere. On the top of both active sites the b-hairpin protuberance is coloured in green (Sauvage et al., 2008).*

Type- Amph

The folding is similar to the PB domain of other classes PBP. The differences occur in loops or even secondary structures. The active site lies at the interface of the two subdomains and the first motif SxxK is similar to other PBPs. The conserved serine of the second motif (SxN) is, in type- AmpH PBPs, replaced by a tyrosine and this is the main feature that distinguishes the enzymes of this family. Although closely related to class C β-lactamases, this PBP show no β-lactamases activity. **(Henderson et al., 1997; Vega & Ayala, 2006).** The exact function of this protein is unknown, but probably, they play roles in the normal course of peptidoglycan synthesis, remodelling or recycling, like a weak DDcarboxypeptidase activity *in vitro* **(Vega & Ayala, 2006). (Fig.13)**

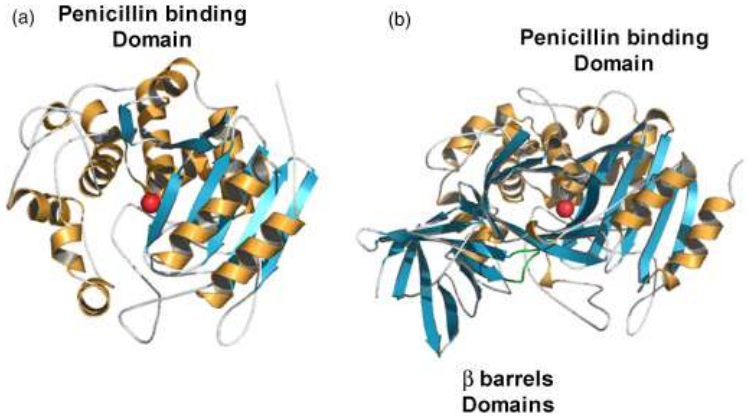

Figure 13*. Structures of type-AmpH PBPs. The catalytic serine of the PB/ peptidase domain is shown as a red sphere. The two additional b-barrels domains of the D-aminopeptidase are oriented in the front of the PB domain, and the loop impairing the active site entrance is highlighted in green. (Sauvage et al., 2008).*

1.6.5. Focus on class B PBP

The first HMW PBP whose crystal structure was resolved was *Streptococcus pneumoniae* PBP2X **(Pares et al., 1996)**, following by the structures of *Staphylococcus aureus* PBP2a **(Lim & Strynadka, 2002**) and *Enterococcus faecium* PBP5 **(Sauvage et al., 2002).** All this PBPs in this subclass are supposed to show a low affinity for penicillin. **(Zapun et al., 2008b**), and therefore confer beta-lactam resistance to their bacterial host by enabling peptidoglycan cross-linking to continue in the presence of beta-lactams when other PBPs have been acylated **(Dusanka et al.,2020).** Sequence alignment allowed to define five PBP B subclasses. **(Goffin & Ghuysen 1998).**

The subclass B2 contains an elongase complex specific to PBP2 type of Gram negative bacteria (e.g *E. coli* PBP2) whereas the subclass B3 contains divisome specific to PBP3 type of Gram-negative bacteria (e.g. *E. coli* PBP3) (**den Blaauwen et al., 2008).**

The PBPs belonged to subclass B4 are involved in division of Gram-positive bacteria, while subclass B5 contains enzyme from Gram-positive not directly involved in septation. Subclasses B-like I,II and III contains PBPs from mycobacteria, streptomycetes and related bacteria.

The fold of class B PBPs is made of a complex N-terminal domain coupled to the C-terminal transpeptidase domain. In the transpeptidase domain, the residue following motif 3 [KTG(T/S)] is, with very few exception, an alanine in class B PBPs [KTG(T/S)A], while it is a threonine or a serine in class A PBPs [KTG(T/S)(T/S)], and this might be related to their specific role as class A or class B PBPs. Gram negative PBP2 types are also distinguished in their active site by the presence of an aspartic acid at the third position of motif 2. The other subclasses have an asparagine as in the canonical active site of PBPs. The N-terminal domain was hypothesized to interact with other proteins. Or to serve as a pedestal for PBPs to reach their target **(H¨oltje, 1998; Macheboeuf et al., 2006)**. Small loops or domain may interact with other proteins. **(Leimanis et al., 2006).** The interdomain linker is made of four to six β-strands. Five conserved motifs (I-V) in or close to the linker constitute the signature of class B PBPs. The N-terminal domain should be seen as small subdomains

or loops that are connected to the interdomain linker. The number of residues in each loop or subdomain between the conserved motifs is characteristic of each subclass. **(Fig.14)**

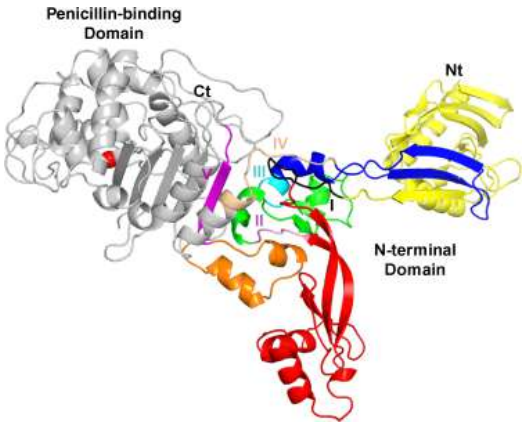

Figure 14 *Structure of class B PBPs The catalytic serine of the PB/transpeptidase domain is shown as a red sphere. The subdomain in yellow is delimited by the N-terminal helix and motif I (black). The red, green and blue subdomains are, respectively. delimited by motifs I and II (pink), motifs II and III (cyan), and motifs III and IV (wheat). The subdomain in orange is inserted in the PB domain between motif V (magenta) and the active serine of the PB domain (red sphere) (Sauvage et al., 2008).*

Class B PBP play a key role in peptidoglycan biosynthesis in different bacterial species. *E. coli* PBP2, localizes at the division site is essential for cell elongation and shape maintenance while PBP3 is essential for cell division since that cells with inactivated PBP3 grow as filaments. **(Spratt, 1977; Georgopapadakou et al., 1982).**

Bacillus subtilis PBP2A is required for normal outgrowth of spores. PBP2a and PBPH play redundant roles in determining the rod cells shape and the activity of one of these proteins is required for viability. **(Wei et al., 2003).** PBPH is expressed most strongly in late log phase and during the transition to stationary phase and may a play a unique role during that part of the life cycle.

Gram positive division specific PBs belong to subclass B4. They all possess a supplementary domain made of two repeating units known as PASTA domains, like class A PBPs.

Class B PBP play an important role in the β-lactams resistance. One resistance mechanism found in some Gram-positive bacteria is the presence of an endogenous or acquired penicillin resistant PBP that can take over the transpeptidase function of all other PBPs, like *S. aureus* PBP2a, *E. faecium* PBP5 and *E. faecalis* PBP4. Mutation or mosaics gene transfer are also frequently observed with naturally competent bacteria, mainly involving the division specific class B PBP (B3 PBP).

1.6.6. Role of low affinity PBP in Enterococci.

Reduced susceptibility to β-lactam antibiotics in enterococci results from expression of a single low-affinity class B PBP designated PBP4 in *E. faecalis* and PBP 5 in *E. faecium*.

The X-ray crystallography study has made it possible to determine the PBP4/PBP5 structure **(Moon T. et al., 2018)**., showing that these proteins lack the N-terminal membrane anchor, and identifying two different crystal forms of PBP5, which results in two distinct conformation: open and closed. **(Fig.15)**

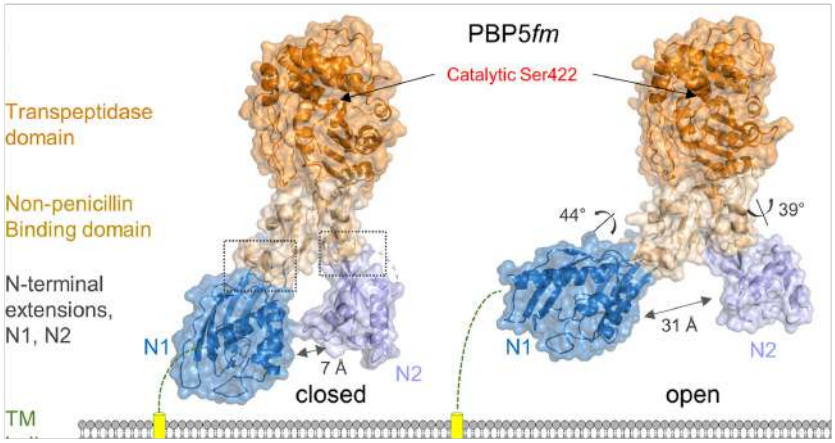

Figure 15 *Structural of four distinct domain of PBP4/PBP5. Left: closed conformation; Right: open conformation. Dark blue: N1 domain; Light blue: N2 domain; Beige: non-penicillin-binding-domain; Orange: TPase; Arrow: Catalytic seryne 422. The rotations of the N1 and N2 domains relative to the nBP/TPase domains, which result in a 24-Å opening of the cleft, are indicated, with the locations of the hinges shown as a dashed box.Yellow cylinder: N-terminal transmembrane helix (Moon T. et al. 2018).*

The structure of PBP4 was determined to 1.8 Å resolution and show that the PBP4 is composed of four distinct structural domains: two N-terminal domains (N1-N2), an N-terminal membrane-anchoring motif and N-terminal extension of unknown function that is hypothesized to mediate protein interactions and C-terminal transpetidase (TPase) domain; a non-penicillin-binding-domain (nPB) and a C-terminal catalytic Tpase domain, containing nucleophilic serine. **(Fig 16).**

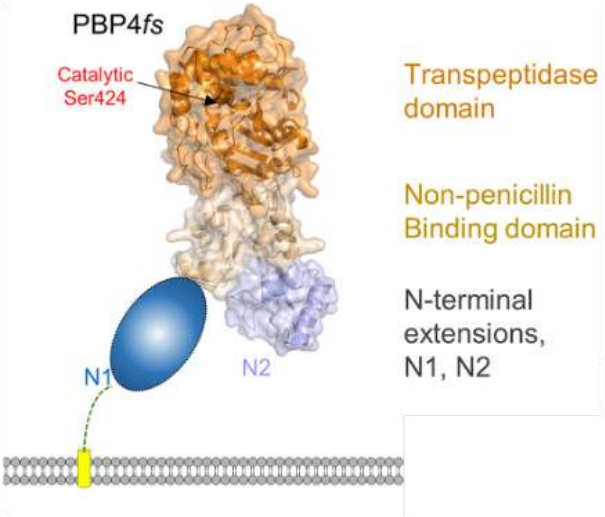

Figure 16*. E. faecalis PBP4 structure Moon T. et al. 2018).*

Except the N-terminal domain, all domains are composed of residues that are not linear in sequence, giving rise to an extensively interconnected topology **(Fig.17)**

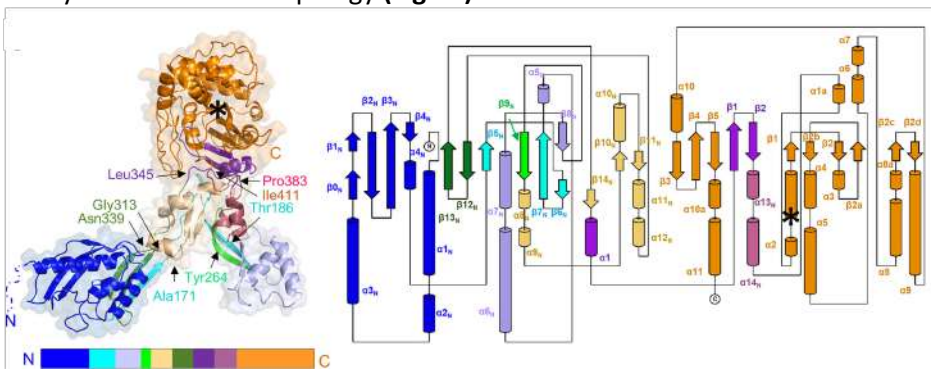

Figure 17*. Secondary structure (left) and topology map (right) of PBP5. Colors from the N-to-C terminus are indicated below the structure; a topology map of PBP5 is colored as in C. The location of the catalytic serine is indicated by an asterisk (Moon T. et al., 2018)*

The crystallography study reveals that the N1 and N2 domains are mobile, adopting a wide range of conformations relative to the TPase domain. In *E. faecium* PBP5, the transition from closed state to open state requires rotation of 44° and 39° by the N1 and N2 domains, respectively, causing a widening of the N1-N2 cleft from 7 Å (closed) to 31 Å (open). This mobile nature of the N1 domain it was been confirm by the structure of PBP4. No interpretable electron density was observed for the PBP4 N1 domain and this fact suggest that it adopts multiple conformation in the crystal. Similar observations were made for the N2 domain, in which adopting distinct positions and are related to one another by rotation of 39-52°. Despite the N-terminal domains are differentially conserved within the larger PBP family, it is unknown fact how these domain rotations affect and/or direct transpeptidase activity. It is assumed that they function as protein-protein interaction domains **(Höltje, J. V., 1998)**, or as molecular "spacer" **(Macheboeuf P. et al., 2006)**., constraining for example the catalytic site to remain a certain distance from the cell membrane.

The PBP active site is located in the TPase domain and is defined by three conserved motifs: *motif I,* which includes the catalytic serine (SXXK; ^{424}STFK^{427}/); *motif II*, which is involved in the protonation of the β-lactam leaving group (^{482}SDN^{484}) and *motif III* which facilitates substrate binding and defines the oxyanion hole (K(T/S)GT; ^{619}KTGT^{622}) **(Ghuysen, J. M., 1991)**. The nucleophilic serine (Ser-424) is located at the N-terminus of helix α2, whereas the oxyanion hole is defined by the backbone nitrogen atoms of the nucleophilic serine and the motif III threonine (Thr-622/Thr-620) These motifs are bordered above by the "lid" (aminoacids 445-473) and below by the C-terminal helix (amino acids 657-680), which together enclose the active site in a deep cleft. **(Fig. 18)**

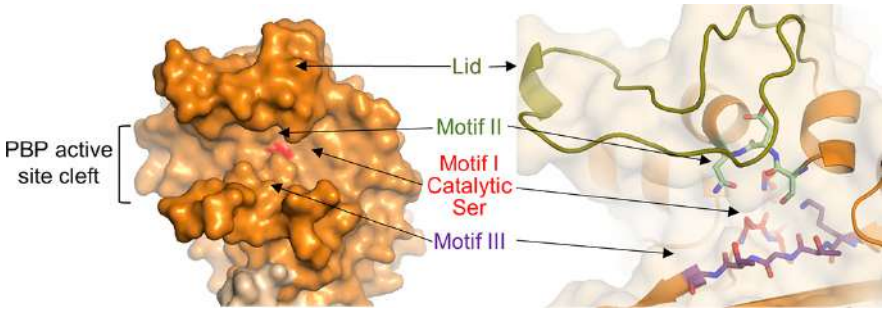

Figure 18 *Key elements of PBP TPase domains. Left, surface representation of the PBP5 active-site cleft, with the location of the catalytic serine highlighted in red. Right, the key conserved motifs of the PBP TPase domains, including motif I, which includes the catalytic serine (SXXK, red), motif II (SXN, mint), motif III (KTG(T/S), purple), and the lid (yellow-green), which covers that active site to form the deep cleft seen at the left (Moon T. et al. 2018).*

These PBP have unusually low affinities for β-lactams and their acylation rates are negligible compared with bacterial generation times, allowing the pathogens to survive antibiotic treatment. The prolonged β-lactam therapy can lead to the emergence of highly resistant strains. Unlike *E. faecium* strains, elevated resistance in *E. faecalis* strain is more rare, and emerged after prolonged β-lactam treatment, often due to PBP4 mutation. **(Rice L.B. et al., 2018).**

The β-lactam resistance of PBP4 and PBP5 has also been shown to due to the different formation of the acyl-PBP intermediate. The structures reveal that like PBP2a from *S. aureus,* the catalytic serine changes conformation upon acylation for a subset of β-lactams and that N-terminal domains of these enzyme undergo unprecedented conformational changes without impacting the structure of the catalytic pocket.

The binding between the β-lactam and PBP4/PBP5 does not lead to extensive conformational changes. These changes are exclusively localized to and around the catalytic pocket. Generally, as observed for PBP2a in *S. aureus*, the catalytic serines of PBP4-5 are not ideally positioned for nucleophilic attack. The strand β3 is twisted toward the catalytic pocket with the PBP4 Thr-622 carbonyl pointing toward the oxyanion hole. The catalytic serines of PBP4-5 rotate upward upon acylation, whereas strand β3 rotates upward and displaces the PBP4 Thr-622 carbonyl out of the oxyanion hole. The rotation of strand β3 depends on the nature of the β.lactams.

The second major conformational change associated with β-lactams acylation is the widening of the catalytic cleft that accommodates β-lactams and substrates. PBP4 are characterized by an unusually deep catalytic

pocket that is bounded by multiple structural elements, which includes a lid that braces the top of the catalytic pocket. This lid must open for β-lactams and substrate to access the catalytic serine. Once acylated, these elements maintain a more open conformation. It was shown that the N1 and N2 domains rotate independently of the TPase domain and do not alter the conformation of the catalytic site suggest that PBP4-5 may not be regulated by allostery, and that N1 and N2 domains are higly mobile despite their higly interconnected nature. The function of PBP domain mobility is unknown, but it is possible that these motions facilitate the building of the cell wall.

E. faecalis PBP4 show several behavior in correlation with the β-lactams classes of antibiotic. Moon et al. show that the active sites revealed strong density for all covalent acyl-enzyme adducts and that the acyl-adduct formation does not result in global conformational changes in PBP4/PBP5. The changes are localized to domain movements about the active site and changes in the structures of the active-sites motif. These changes are not identical between the free and β-lactam-bound structures but depend upon the particular acyl-adduct formed.

For example, the benzylpenicillin forms a covalent adduct with PBP4 via its catalytic serine, Ser-424. The benzylpenicillin carbonyl oxygen pointing toward the oxyanion hole defined by the backbone nitrogens atoms of Ser-424 and Thr-622. The benzylpenicillin is further stabilized by polar contacts with both PBP4 backbone atoms and the side chains of Ser-482 , Asn-484, Lys-619, Thr-620, and Thr-622 and the formation of intraprotein contacts between Lys-427 and Asn-484 and Ser-482. In apo-PBP the nucleophilic Ser-424 hydroxyl points down toward the oxyanion catalytic pocket. However, upon acylation with the Benzyl penicillin the Cβ –Oγ bond rotates by 150°. Oγ moves by 1.3 A and in acylated complex is now oriented away from the oxyanion hole, suggesting that the serine side chains is not ideally positioned for nucleophilic attack in the apo conformation. Because the β-lactam carbonyl now points toward the oxyanion hole, it displaces the carbonyl of Thr-622, which rotates out of the hole and upward toward the bound β-lactam moiety. This rotation of strand β3 results in the formation of two additional hydrogen bonds, the first between the β-lactam carbonyl and the amide hydrogen of Thr-622 and the second between the phenylacetamide nitrogen from benzylpenicillin and the Thr-620 side-chain hydroxyl. The Thr-618 side chain adopts a rotomer conformation that expands the active site to accommodate the β-lactam phenyl ring. Because the catalytic site of PBP4 is located in a deep, narrow cleft, the structural elements that enclose the catalytic site open in order to accommodate benzylpenicillin acylation. This results in a displacement of the "lid" moiety by 1.9 A for benzylpenicillin-acyl-PBP4 compared with its apo conformation. **(Fig. 19)**

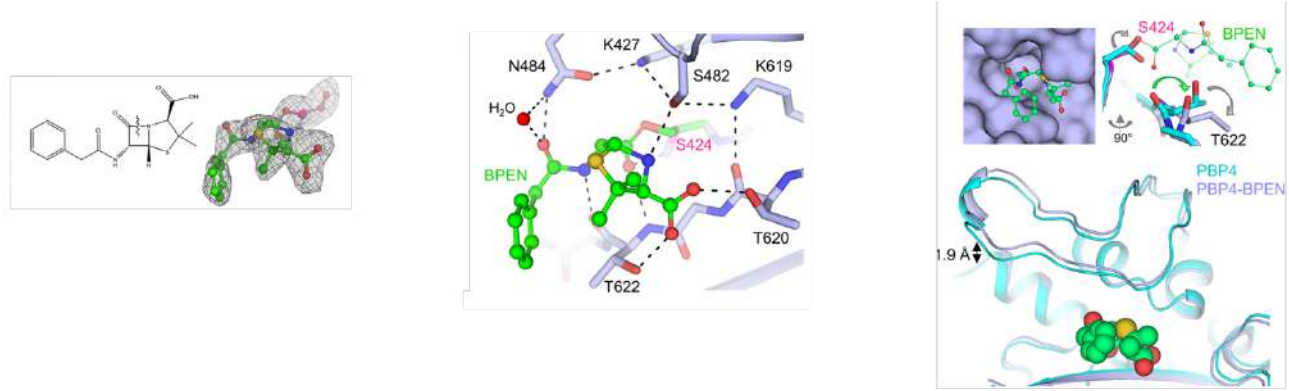

Figure 19 *PBP4 TPase catalytic cleft conformational changes after interaction with benzylpenicillin. Left: electron density for the benzylpenicillin-acylated Ser-424; Middle: active site in the benzylpenicillin-acyl-PBP4 structure. Green:penicillin; light blue: PBP4; Pink: Ser424. Right: Surface representation of PBP4 with bound benzylpenicillin. Overlay of nonacylated PBP4 (cyan) with benzylpenicillin-acyl-PBP4 (light blue; acylated Ser-424 in pink; view rotated by 90°). Conformational changes in backbone and side-chain atoms are highlighted with arrows. Overlay orientation opening of the lid to accommodate benzylpenicillin binding (Moon T. et al. 2018).*

Also, imipenem forms a covalent adduct with Ser-424 in similar way, but with any differences. The Ser-424 rotates out of the oxyanion hole to form the acyl-enzyme adduct. However, unlike in benzylpenicillin, where the β-lactam carbonyl points downward into the oxyanion hole, the imipenem carbonyl point upward, away from the oxyanion hole, where its hydrogen-bonds with Lys-4227 and Asn-484. The carbonyl of motif III Thr-

622 does not rotate put of the oxyanion hole, but instead retains the twisted conformation of β3 observed in the apo state. Polar contacts are observed between imipenem and the backbone and/or side chain atoms of Ser-482, Thr-620, and Thr-622. As observed for benzylpenicillin, both the lid and central β-sheet of PBP4 open to accommodate imipenem acylation, to a much lesser extent, with the lid moving by only 0.7 A. **(Fig.20)**

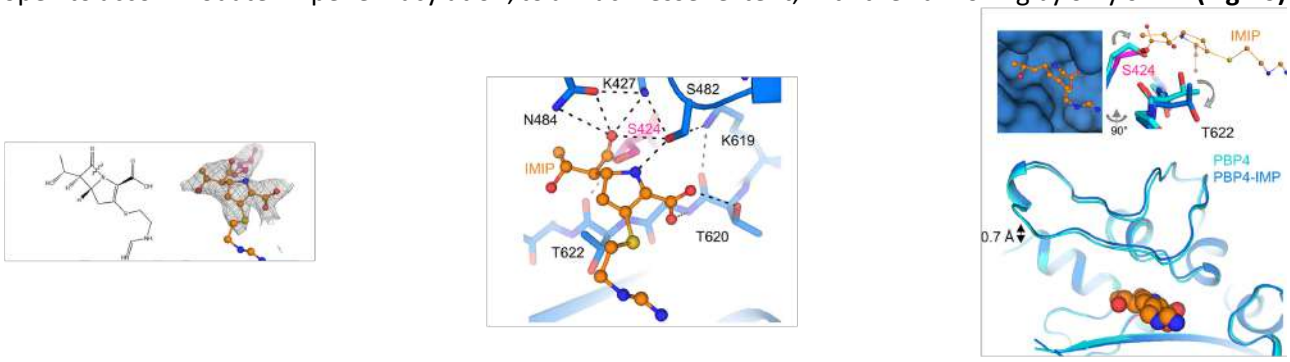

Figure 20 *PBP4 TPase catalytic cleft conformational changes after interaction with Imipenem. Left:Electron density for the imipenem-acylated Ser-424.Middle: active site in the imipenem-acyl-PBP4 structure (imipenem in orange, PBP4 in blue, and Ser-424 in pink). Polar interactions are indicated by dashed line. Right: surface representation of PBP4 (blue) with bound imipenem (orange). overlay of nonacylated PBP4 (cyan) with imipenem-acyl-PBP4 (blue; acylated Ser-424 in pink; view rotated by 90°. Conformational changes in backbone and side-chain atoms are highlighted with arrows. Overlay opening of the lid to accommodate imipenem binding (Moon T. et al. 2018) (Moon T. et al. 2018).*

The ceftaroline carbonyl oxygen points toward the oxyanion hole defined by the backbone nitrogen atoms of Ser-424 and Thr-622. Ceftaroline is further stabilized by multiple polar interactions with the side chains of Ser-482, Asn-484, Lys-619 and Thr-620 and the backbone atoms of Gly541 and Thr-622 and intraprotein polar interactions between Lys-427, Ser-482, Asn-484 and Lys-619. Ceftaroline acylation results in a rotation of the nucleophilic serine upward away from the oxyanion hole. The acylation of PBP4 by ceftaroline displaces the Thr-622 carbonyl out of the oxyanion hole, causing strand β3 to twist outward. This new orientation is stabilized by a hydrogen bond with ceftaroline. An Identical polar interaction is present in the penG-acyl-PBP4 complex between the nitrogen from benzylpenicillin and Thr622 carbonyl, in contrast with Imipenem that lacks a nitrogen in the corresponding position, explaining why the imipenem-acyl PBP complex does not result in a rotation of strand β3.

The adduct formation with ceftaroline results in the greatest opening of the catalytic cleft, with the lid and central β-sheet both moving by 2.7 Å to accommodate ceftaroline binding. **(Fig. 21)**

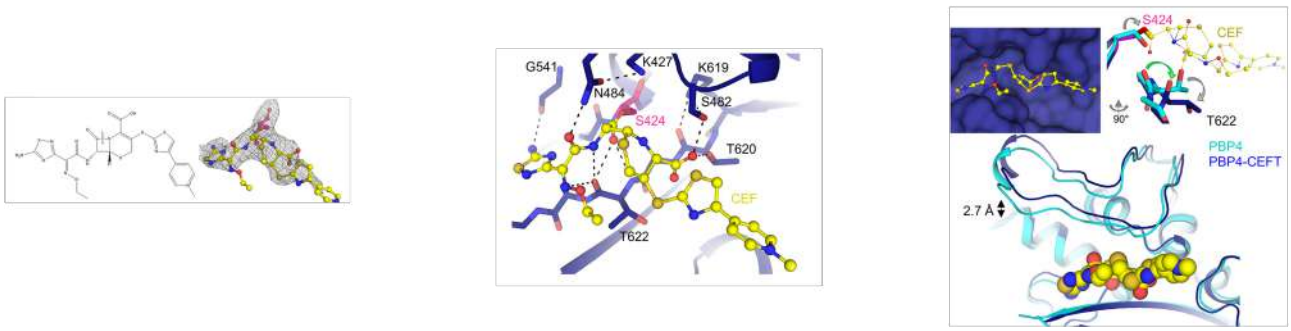

Figure 21 *PBP4 TPase catalytic cleft conformational changes after interaction with ceftaroline. Left: Electron density for the imipenem-acylated Ser-424. Middle: active site in the ceftaroline-acyl-PBP4. structure (ceftaroline in yellow, PBP4 in dark blue, and Ser-424 in pink). Polar interactions are indicated by dashed lines. surface representation of PBP4 (dark blue) with bound ceftaroline (yellow). Overlay of nonacylated PBP4 (cyan) with ceftaroline-acyl-PBP4 (blue; acylated Ser-424 in pink. Conformational changes in backbone and side chain atoms are highlighted with arrows. Overlay opening of the lid to accommodate ceftaroline binding (Moon T. et al. 2018).*

It follows that the low affinity of PBP4 for beta-lactams is due to the formation of inefficient bonds at the acyl-PBP4 intermediate level.

The study of Louis B.Rice et al. (2018) shown the correlation between the decrease susceptibility to penicillin and ampicillin in *E. faecalis* and the presence of aminoacidic substitutions in PBP4 and greater quantities of PBP4 due to increased transcription of *pbp4* associated with a point mutation upstream of the putative *pbp4* promoter region.

Sequence alignment between two strains, one with high MIC values at penicillin/ampicillin, and one reference strain, highlighted the presence of two aminoacid difference, a valine-to-isoleucine change at residue 223 (V223I), located In proximity of the N-terminal domain of PBP4, that contributes negligibly to the reduce affinity of PBP4 for β-lactams antibiotic , and an alanine to threonine change at residue 617 (A617T), close to the PBP4 transpeptidase domain, two aminoacids N-terminal to the KTG motif, facilitating the β-lactams binding **(Ligozzi M. et al.,1996).**

This last mutation destabilizes the PBP4 fold, increasing the melting temperature of PBP4 mutated, and decrease its affinity for penicillin confirmed by the reduction in affinity for BOCILLIN FL (penicillin homologue). Ala617 is located on the same β-strand as active-site motif III, which includes Thr620, a conserved residue in PBPs that facilitates substrate binding and defines the active-site oxyanion hole. Ala 617 defines the centre of an extended hydrophobic pocket that is adjacent to the PBP4 active site.

Other studies have shown that strains with high MIC ampicillin values (8-16 ug/ml) presented some amino acid changes in PBP4 (H605Y and P520S) and (D573E), and that these changes are between the active site defining SDN and KTG motifs, suggesting that these variations are the main responsible for the increased MICs value **(Ono S. et al., 2005; Infante et al., 2016)**.

Analysis of level expression of pbp4 in a mutant strain revealed a single base pair deletion 8 bases upstream of a putative -35 region for the pbp4 gene that consist of the loss of an A residue in a string of seven. This region, which are commonly A-T rich, can have an impact on the expression of downstream gene, supporting the involvement of this adenine deletion in the increased expression of PBP4. It was confirmed that the adenine deletion is involved in higher expression of PBP4, leading to a 4000-fold reduction in the MIC of any antibiotics, like ceftriaxone, whereas the MIC of ampicillin was only reduced 4-fold **(Arbeloa et al.,2004).** The subsequent cloning of *pbp4* gene under the control of strength promoter, restored wild-type beta-lactam resistant. This fact confirms how the adenine deletion alone may not sufficiently increase the β-lactams MIC value, suggesting that the insurgence of resistant strain is the results of cumulative impact between adenine deletion in promoter region and amino acid change within the transpeptidase domain.

2. AIM of the work

During my second and third PhD years, I focused my research project on the study of the ceftobiprole activity, a new generation cephalosporin, against a selected sample of *Enterococcus faecalis* clinical isolates, belonging to different resistance phenotypes, and deepening the knowledge on the molecular factors influencing the decrease of susceptibility to this molecule.

This project was faced by different but complementary approaches: phenotypic, molecular, and protein/enzymatic, the ability to produce beta-lactamases under antibiotic induction was further evaluated.

Therefore, the main goals of this project were to: i) analyze the susceptibility profiles of a larger collection of *E. faecalis* clinical isolates belonging to severe infections, in order to select a sample of significative strains; ii) investigate the activity of diverse β-lactams, focusing on the ceftobiprole *in vitro* antibacterial and bactericidal activity, by Time-kill curve assay; iii) analyze the *pbp4* gene sequence and its expression levels compare the *pbp*4 expression levels with the reduced susceptibility to β-lactams and, specifically, ceftobiprole; v) study the interactions between ceftobiprole and high-molecular-mass (HMM) low-reactive PBPs, with a particular *focus* on PBP4, to look for a possible role of PBP4 alterations in influencing the binding to ceftobiprole.

This project can be schematically subdivided into two parts **(Tab 2):**

Part I: Assessment of the ceftobiprol –*cidal* activity and Impact of PBP4 Alterations on beta-Lactam Resistance and Ceftobiprole Non-Susceptibility among *Enterococcus faecalis* Clinical Isolates	Part II: Study of Ceftobiprole/PBP's interactions and ability to produce beta-lactamases.
Antimicrobial-susceptibility testing	Competition assay
Gradient-test	
Time-kill curve assay	
*pbp*4 gene sequencing	Nitrocefin test
Real-time-quantitative PCR	

Table 2 *The results of the first part of the project were successfully published (Lazzaro LM et al., 2022).*

3. MATERIALS AND METHODS

3.1. Strains in study

Twenty-two non-duplicate *E. faecalis* clinical strains isolated from blood-stream-infections (BSIs) and collected from hospitals in different Italian cities were phenotypically characterized for their ability to hydrolyze esculin in esculetin by culture in Bile Esculin Azyde (BEA) agar; their metabolic and biochemical characteristics were identified by Api®Strep gallery (Bio-Mèrieux-l'Etoile, France); their antibiotic-susceptibility values were obtained by gradient-test (MIC test strip - MTS) and broth-microdilution method.

Among this larger collection, seven strains were further selected for their antibiotic-resistance behaviors, belonging to the major multi-drug-resistance phenotypes.

The bactericidal activity of ceftobiprole and all the molecular and enzymatic assays were only evaluated against the selected sample.

Below, a schematic representation of the β-lactam multidrug-resistant profiles of the study sample:
Efs1 – PRAS; BPR-NS; HLAR.
Efs2 – PSAS; BPR-S and fully susceptible to all antimicrobials tested.
Efs7 – PRAS; BPR-NS; HLAR.
Efs8 – PRAS; BPR-NS; HLGR; VRE/VanA.
Efs11 – PRAS; BPR-S; HLAR; VRE/VanA.
Efs18 – PRAS; BPR-NS; HLAR.
Efs20 – PSAS; BPR-S; HLSR.
*Penicillin-resistant ampicillin-susceptible (PRAS); ceftobiprole non susceptible (BPR-NS); penicillin-susceptible ampicillin-susceptible (PSAS); ceftobiprole susceptible (BPR-S); vancomycin resistant (VRE); high level aminoglycosides resistant (HLAR).

Two beta-lactam-susceptible *E. faecalis* strains were also included as control: *E. faecalis* ATCC 29212, used as control for antibiotic susceptibility tests **(EUCAST, 2022**) and *E. faecalis* OG1RF, deposited in the American Type Culture Collection (ATCC) under ATCC 47077, deriving from *E. faecalis* OG1 by selection for resistance to rifampin and fusidic acid **(Bourgogne et al., 2008)**, used as control in the molecular studies.

3.2. Antimicrobial susceptibility testing

The *in vitro* antimicrobial activity of the 22 *E. faecalis* strains were performed under standardized conditions to ensure the reproducibility and accuracy of the results.

The antibiotic-susceptibility values were obtained for ceftobiprole, provided by Basilea Pharmaceutica international Ltd. (Basel; Switzerland); ceftaroline, linezolid and tigecycline, by Pfizer Inc. (New York, NY, USA); daptomycin, by Novartis (Basel, Switzerland). Penicillin, ampicillin, amoxicillin, imipenem, vancomycin, teicoplanin, gentamicin, streptomycin, piperacillin-tazobactam were purchased commercially (Sigma Chemical Co., ST. Louis, MO, USA).

The Minimal Inhibitory Concentration (MIC), the lowest concentration of antibiotic capable to inhibit the bacterial growth, was obtained by gradient-test (GT) using MIC Test Strips (MTS; Liofilchem, Roseto degli Abruzzi, Italy) and broth microdilution assay (BMD), following standard criteria. Briefly, the gradient test was carried out using bacterial suspensions of 0.5 McFarland, corresponding to 1.5 x 10^8 CFU/ml. The surface of Mueller Hinton agar plates (Oxoid™, Thermo Scientific™, Basingstoke, UK) were swab inoculated with the suspension and the MTS containing a stable and predefined antibiotic gradient, were then placed on the agar surface. After o/n incubation at 37°C, the MIC value correspond to the area of intersection between the lower margins of the inhibition zone and the graduate strip.

The BMD method, the gold standard assay to determine the MIC value was carried out in 96-well microtiter plates using Cation-Adjusted Mueller Hinton Broth (CA-MHB) (BBL ™). MICs values were determined by broth microdiluition and interpreted according to the European Committee on Antimicrobial Susceptibility testing (EUCAST) clinical breakpoints (http://www.eucast.org/clinical_breakpoints/) (**EUCAST,2021**). In the absence

of EUCAST clinical breakpoint, those of the Clinical and Laboratory Standards Institute were applied **(Clinical and Laboratory Standards Institute, 2021)**.

The results were interpretated according to the European Committee on Antimicrobial Susceptibility Testing (EUCAST) clinical breakpoints (http://www.eucast.org/clinical_breakpoints/) **(EUCAST 2022).** In the absence of EUCAST clinical breakpoints, those of the Clinical and Laboratory Standards Institute were applied **(CLSI, 2021)**. There are no CLSI and EUCAST official breakpoints regarding Ceftobiprole and Ceftaroline, eCOFFs not determined.

3.3. Time-kill curve assays

The main advantage of this technique is that provide a dynamic picture of the antimicrobial action and interaction over time (based on serial colony counts). For this reason, the time-kill curve assay represents the gold standard to determine the potential bactericidal activity.

In vitro time-kill experiments were performed in duplicate in 20 mL tubes containing CA-MHB (Difco, Detroit, MI) using a starting *inoculum* of 10^5-10^6 CFU/mL with ceftobiprole (1X, 2X and 4X MIC).

Briefly, the pre-*inoculum* was aseptically withdrawn for optical density (OD) measurement at 450 nm, in order to perform a correct dilution to obtain a starting *inoculum* concentration of $5x10^5$ -$5x10^6$CFU/ml. At predetermined time points, representing the antibiotic time exposure, in hours (T0-T2-T4-T8-T24), each sample was measured at 450 nm and 100 μl of appropriate dilutions were spread onto Mueller Hinton Agar plates (Oxoid™, Thermo Scientific™, Basingstoke, UK) and incubated at 37°C o/n. Time kill curves were then constructed as a function of time and the results were represented as a difference in $\log_{10}$ between the CFU/ml at 0 and 24 h. All experiments were repeated at least three times; data points are averages from duplicate CFU/mL determinations within an experiment. Bactericidal activity was defined as a ≥3 $\log_{10}$ decrease in bacterial count at 24h **(White et al, 1996).**

3.4. Molecular characterization

3.4.1. DNA extraction

The DNA genomic extraction was performed following a protocol for low GC% content. Briefly, 1 ml of o/n broth-cultures were centrifugated at 15,000 rcf for 5 minutes at RT. The harvested cells were resuspended in 1 ml of saline solution (0.9% NaCl) and washed for two times. β 1-4 glycosidic peptidoglycan linkage was lysed by adding 10 mg/ml lysozyme and incubated at 37°C for 1 hour. A second lysis step was performed by heat-cold shift from -20°C to +37°C to break the cell wall. The suspensions were treated with a mix solution of sodium-dodecyl-sulfate (SDS 10%), to separate nucleic acids from proteins and inhibit the nucleases activity, and proteinase K for the protein digestion, and incubated at 65°C for 10 minutes.

A RNase treatment was also performed by adding the enzyme at the final concentration of 10 mg/ml and incubate the cells for 1h at RT. The treatment with cetyl-triethyl-ammonium bromide (CTAB/Nacl), a preheated (65°C) anionic detergent allowed to separate the polysaccharides from phenols and other impurities often associated with DNA. Finally, the DNA was extracted with phenol-chloroform-isoamyl alcohol (25:24:1) solution, precipitated o/n in 750 μl of ice-cold isopropyl alcohol, centrifugated and resuspended in nuclease-free water. Verification of the extraction was conducted by electrophoresis on 1% agarose gel, stained with 4 μl Syber-safe (10,000 X), at 120 V in TBE 0.5 X (0.5 mm Tris-Borate, 1 mm EDTA pH 8.0).

3.4.2. Gene amplification and sequence analysis

All isolates were molecularly characterized for the *pbp*4 gene sequence in order to analyze possible mutations and verify their role in influencing BPR activity. *pbp*4 was amplified by PCR and the entire gene was double strand sequenced using oligonucleotides specifically designed for this study.
The PCR reaction was performed in a final volume of 25 ul, as follows: Multiplex PCR Master MIX 1X (Biotechrabbit GmbH, Berlin, Germany); 0.5 pmol/μl primer forward; 0.5 pmol/μl primer reverse; H_2O. The amplification was conducted in a termocycler Biometra Personal Cycler, according to the following program:

Predenaturation at 94°C (5 min); 30 cycles of annealing at 56°C (1 min), extension at 72°C (3 min) and denaturation at 94°C (1 min); a final step of elongation at 72°C (10 min); maintenance at 4°C.

The primer oligonucleotides used in this study were appropriately designed on the sequences of the *E. faecalis* ATCC 47077 *pbp*4 using Vector NTI version 11.5.4 software **(Tab 3).**

Primer	Sequence (5-3)	PCR product size	Tm
pbp4-up	GTGTCCCCCATATTATCAGGTTC	2429bp	60.6 °C
pbp4-dw	CGCTTCATTGTAGCACACTTTCC		60.6 °C
pbp4-up	GTGTCCCCCATATTATCAGGTTC	822bp	60.6 °C
pbp4.1-dw	GTTTGGCATTATCTACTTGAATCG		57.6°C
pbp4.1-up	GTCTTATCAATCAAGTATCGCCAA	747bp	57.6°C
pbp4.2-dw	CTAACCGTTGCTAATAAATCGCC		58.9°C
pbp4.3-up	AAATTAACGATTGACAGTGGCGT	511bp	57.1 °C
pbp4.3-dw	TTGGTAAATCTAGTTCCTCACCGA		59.3°C
pbp4.2-up	CAAGTCCAGTCAATCTGCGTACC	722bp	62.4 °C
pbp4-dw	CGCTTCATTGTAGCACACTTTCC		60.6°C

Table 3 *Oligonucleotides designed in this study for pbp4 gene sequencing*

The resulting amplimers were tested on 1.5% agarose gel, stained with 2.5 µl of Syber-safe (10,000 X) at 100 V, using as running Buffer TBE 0.5 X (0.5 mm Tris-Borate, 1 mm EDTA pH 8.0) and analyzed using UVITEC transilluminator.

The amplimers were purified using the QIAquick Purification PCR kit (Qiagen, Milan, Italy) following the manufacturer's instructions. Briefly, 5 volumes of Buffer PB (containing guanidine hydrochloride and isopropanol) were added to 1 volume of the PCR reaction, placed in a QIAquick column and centrifugated to 18,000 rcf for 1 min. After a QIAquick column double washing in 750 µl of PE Buffer and centrifugation for 30-60 s, the DNA was eluted in 30 µl of EB Buffer (10 mM Tris·HCl, pH 8.5) or Nuclease-Free-water by centrifugation at 18,000 rcf for 1 min.

The purified PCR product was quantified using the Qubit® dsDNA Assay Kit, a fluorometric test executed using Qubit 2.0 (Invitrogen-life Technologies, Turin, Italy) and sent to the BMR Genomics, according to the specification provided by the same company, to sequence the entire gene double strand and verify that any changes occurred were not due to reading errors, but really to mutations.

Sequencing was performed using the Dye Terminator DNA sequencing kit V1.1 (Applied Biosystems TM), followed by purification using the DyeEx 2.0 Spin Kit (Quiagen, Hilden, Germany). The sequences obtained were corrected and analyzed using the Chromas Lite 2.1 program and then exported in FASTA format. Sequence alignment and gene and translated protein analysis were performed by using BLAST tool (Basic Local Alignment Search Tool) (https://blast.ncbi.nlm.nih.gov/Blast.cgi), CLC Sequence Viewer 8.0 and UniProt (www.uniprot.org). *E. faecalis* ATCC 47077, whose complete genome sequence is deposited at NCBI under the accession number CP025020.1., was used as reference.

3.4.3. Real-Time Quantitative PCR

Total RNA was extracted using the RNeasy ® Mini kit (Qiagen, Hilden, Germany), starting from a 7 mL of bacterial suspensions (10^5 CFU/mL), incubated at 37°C until late-log phase. Bacterial suspensions were measured at a OD_{600} nm, and the following conversion formula was used to standardize all samples (CFU/ml) (0.1 $OD_{600} \cong 1x10^8$ CFU/mL):

$$7 \times 10^8 \times OD\text{-}3x10^7$$

In details, two volumes of RNA Protect bacteria Buffer were added to one volume of bacterial culture, vortexed and incubated at RT (25°C) for 5 min. After centrifugation for 10 min at 3,000 rcf, pellets were resuspended in 100 µl of TE buffer (30 mM Tris-Cl, 1 mM EDTA pH8), containing lysozyme (150 mg/ml), 10 ng/ml and proteinase K (10 mg/ml) and incubated at RT for 20-30 min with shaking. 700 µl of RLT Buffer

(containing guanidine isothiocycanate and β-mercaptoethanol) were added and the samples were vortexed and mixed with 500 μl of absolute ethanol. The volume mixture (> 700 μl) was, then, transferred to the RNeasy mini spin columns and centrifuged for 30 sec at 11,000 rcf. After discarding the residual liquid, 350 μl of RW1 Buffer were added to the RNeasy columns and centrifuged at 11,000 rcf for 30 sec to wash the column membrane.

On-column DNA digestion was carried out by adding 10 μl of DI stock-solution and 70 μl of RDD buffer, and incubating at 30°C for 15 min.

Removal of carbohydrates, proteins and fatty acids was conducted by incubation for 5 min in 350 μl RW1 stringent washing buffer, containing guanidine salt and ethanol, and centrifugation for 30 sec at 11,000 rcf. The column was transferred to a new collection tube and a mild washing buffer to remove traces of salts, was carried out in 500 μl of RPE buffer and centrifugation for 30 sec at 11,000 rcf. A second wash to eliminate all ethanol residues was conducted in 500 μl of RPE buffer. Final RNA elution was carried out in new collection tubes by adding 30 μl of RNAse-free water and centrifugating for 1 min at 10,621 rcf.

The RNA extracted was quantified using the Qubit® RNA Assay Kit, a fluorometric test executed using Qubit 2.0 (Invitrogen-life Technologies, Turin, Italy).

The RNA extracted was further purified from potential contaminating genomic DNA (gDNA) and retro-transcripted (RT) in cDNA using the QuantiNova ™ Reverse Transcription kit (Quiagen, Hilden, Germany), according to the manufacturer's instructions.

Briefly, 2μl of gDNA Removal Mix, 2μl of RNA template (> 5 μg) and 11 μl of RNase-free water, were brought to a final volume of 15μl, incubated for 2 min at 45°C and placed in ice. Reverse-transcription reaction was carried out by adding 1μl Reverse Transcription (RT) Enzyme and 4μl RT mix to 15μl RNA template. The RT reaction was conducted in a termocycler Biometra Personal Cycler, according to the following program: annealing at 25°C for 3 min; Reverse Transcription at 45°C for 10 min, and inactivation step at 85°C for 5 min. To exclude the presence of cDNA, a quantification assay was done by using the Qubit® ssDNA Assay Kit, in Qubit 2.0 (Invitrogen-life Technologies, Turin, Italy).

Real-time qPCR was performed in a Rotor-Gene Q (Quiagen, Hilden, Germany) instrument, using the QuantiNova™SYBR®GreenPCR kit (Qiagen, Hilden, Germany), according to the manufacturer's instructions.

QuantiNova DNA polymerase is in an inactive state and has no enzyme activity at RT, preventing the formation and extension of primers that bind in a non-specific way during the preparation and the first denaturation step. Polymerase is inactivated by QuantiNova Antibody and QuantiNova guard, which stabilizes the complex **(Fig 22).**

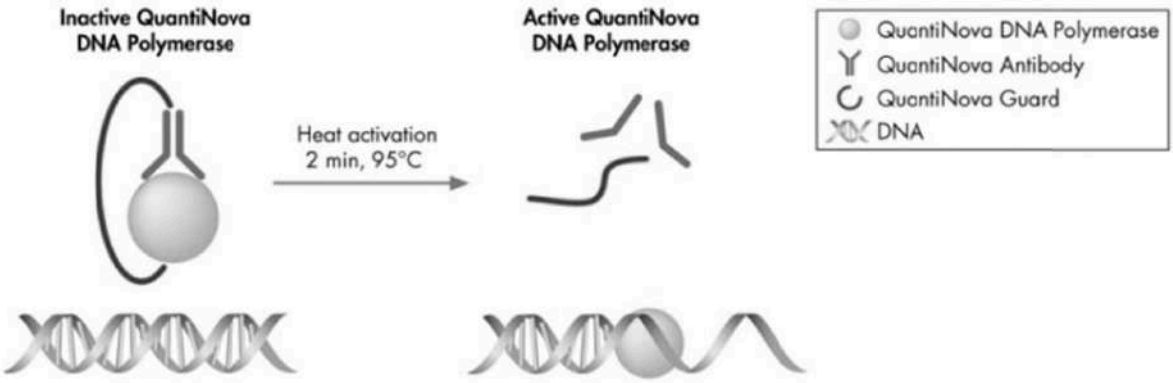

***Figure 22**. Principle of the novel QuantiNova hot-start mechanism. QuantiNova DNA polymerase is kept in an active state by QuantiNova Antibody and QuantiNova Guard until the initial heat activation step. (QuantiNova ™SYBR® Green PCR Handbook, Quiagen).*

PBP4 (5RT) and 16S rRNA qPCR oligonucleotides were specifically designed for this study. **(Tab 4)**

Primer	Sequence (5-3)	PCR product size	Tm
E.fs 16S UP	CGTCAAATCATCATGCCCC	299 bp	50.1 °C
E.fs 16S DW	CCCCAATCATCTATCCCACC		51.2 °C
E.fs 5RT pbp4 UP	TTTGACGAAGTGGGCGTAG	132 bp	52.1 °C
E.fs 5RT pbp4 DW	GGACCCATCCTTGGCTTAAC		52.4 °C

Table 4 *Oligonucleotides designed in this study to evaluate gene expression by RT-qPCR.*

The RT qPCR reaction was performed in a total volume of 20 μl, as follows: 1X SYBR Green PCR Master Mix; 0.7 μM Primer UP; 0.7 μM Primer DW; 100 ng/reaction cDNA template (less than 10% of the total volume); RNAse Free water (up to volume).

The amplification was conducted, according to the following program: PCR initial activation at 95°C (2 min); 40 cycles of denaturation at 95°C (5 s) and annealing/extension at 60°C (10 s).

Data acquisition should be carried out during the annealing/extension step. Once this is done, the melting curve analysis of PCR products is performed. For each sample, three biological replicates were prepared. In this study, relative gene expression levels of transcription were calculated by the quantification cycle (Cq) method, normalized to the 16S rRNA expression and calculated using the $^{2\text{-}\Delta\Delta Ct}$ method **(Livak and Schmittgen, 2001).**

$\Delta\Delta$Ct represents the difference between the ΔCt values of the treated (experimental sample) and the untreated/control; while ΔCt refers to the difference between the Ct of the gene of interest, and the Ct of the housekeeping gene for a given sample. When performing the qPCR in duplicate or triplicate, these values need to be averaged first. Finally, to work out the fold change in gene expression (ratio between two values) the $2^{-\Delta\Delta Ct}$ method is applied.

The data obtained were expressed as the fold-change in expression compared to that of the *E. faecalis* ATCC 47077 reference.

Comparison of the expression levels of transcription of all strains and statistical analysis were conducted using the Relative Expression Software Tool "REST 2009" (Quiagen Hilden, Germany) and Graphpad Prism (Version 8.4.0).

3.4.4. Study of PBP4/BPR affinity and competition assay

The fluorescent β-lactam BOCILLIN FL (Invitrogen) is the most common fluorophore-conjugated penicillin V derivative, in which penicillin V is linked to BODIPY (fluorochrome) by a modification of the β-lactam phenyl side chain, developed to detect and study the expression and folding of PBPs, as all PBPs are simultaneously detected.

To evaluate the affinity of ceftobiprole for PBPs and determine if PBP4 significant aminoacidic substitutions could affect and alter the binding and stability of the BPR/PBP4 complex, a competition assay was carried out by using the Bocillin FL able to detect bacterial PBPs in an activity-dependent fashion, in living cells **(Fig. 23).** In this study, the BOCILLIN FL was used to detect the formation of the β-lactam/PBPs complex and evaluate the potential rate of inhibition of PBPs acylation in PRAS and BPR-NS strains. The unlabeled competitor competes for binding to the same site with the labeled molecule. This assay yields the IC50, the antibiotic concentration that displaces 50% of the labeled molecule from the binding site. The affinity of the non-labeled ligand for the protein can then be calculated.

In detail, the relative binding of ceftobiprole was evaluated at different concentration (1/2X; 1X; 2X and 4X MIC).

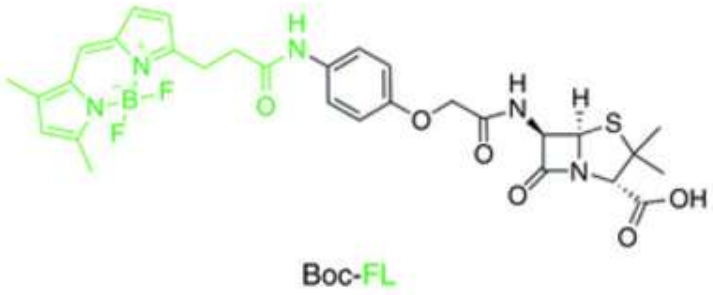

***Figure 23**. Molecular structure of Bocillin FL*

Initially, a bacterial colony from fresh culture plate was inoculated into 5 ml BHI broth and incubated o/n at 37°C. Then, the strain culture was measured to an OD_{450} to obtain a starting *inoculum* of 10^5-10^6 CFU/ml. The cells are therefore incubated for two hours at 37°C, until reaching an OD_{620} ~0.20, corresponding to the exponential phase. Bacteria were harvested by centrifugation for 2 min at RT and washed in PBS (10 mM, pH 7,4). Different BPR concentrations were added, and the samples were incubated at 37°C for 30 minutes, centrifugated at 16,000 rcf for 2 min at RT and resuspend in 50 μl of PBS containing 5 μg/ml of Bocillin™ FL (7,6 μM); after incubation at RT for 10 minutes, the bacterial suspensions were twice centrifuged at 16,000 rcf for 2 min at RT and resuspended in PBS (10 mM, pH 7.4).

After incubation with lysozyme (10 mg/ml) for 30 min at 37°C, cells were lysed by 5 cycles of sonication in a Bandelin Sonifier (30 seconds, 30% duty cycle for 6 intervals). Therefore, the membrane proteome was isolated by centrifugation at 21,000 rcf for 15 minutes at 4°C, resuspended in 100 μl of PBS and homogenized by further sonication (power setting 1, 10% duty cycle for one second).

The protein concentration was determined by using the Qubit® protein Assay Kit, a fluorometric test executed using Qubit 2.0 (Invitrogen-life Technologies, Turin, Italy) and normalized. 51 μl of each sample was added with 17 μl of 4X Laemli buffer plus β-mercaptoethanol, as a reducing reagent, boiled for 5 min at 90°C for protein denaturation, and cooled at RT. Electrophoresis was carried out in a SDS-PAGE on a Criterion™ TGX™ (Tris-Glycine extended) 8-16% polyacrylamide gel, for 2h at a constant voltage of 100V.

To predict the molecular weight of each PBPs, two different commercial pre-stained standards, SeeBlue® Plus2 Prestained Standard (Invitrogen by Thermo Fisher Scientific) and Thermo Scientific Spectra Multicolor High Range Protein Ladder, were used.

The fluorescent Bocillin covalently bound to the PBPs was detected with excitation at 488 nm and emission at 520 nm (Typhoon FLA 9500; filter Alexa 488; PMT 1000; pixel 50 μm).

To detect the PBP profile and identify their molecular weight, the SDS-PAGE Criterion™ TGX™ (Tris-Glycine extended) 8-16% polyacrylamide gel was stained for 1h in a Coomassie brilliant blue R-250 buffer (40% methanol; 10% glacial acetic acid; 0,1% Coomassie Brilliant Blue R-250), and destained for 1h (40% methanol; 10% glacial acetic acid).

The fluorescence was analyzed using the ImageJ software. The brightness and contrast on the image should be adjusted to optimize the signal-to noise ratio. The background signal should be subtracted. Normalization was obtained correlating labeled PBPs with Coomassie stained PBPs.

Our study was completed by the determination of the relative binding (IC_{50}), i.e. the 50% inhibitory concentration values [concentration of ceftobiprole (μg/ml) needed to reduce by 50% the binding of Bocillin FL to individual PBPs], determined by plotting the PBP band volumes *versus* compound concentrations. The 100% binding of Bocillin FL was represented by the PBPs labeled with Bocillin FL but with no drug. IC_{50} values were calculated and statistically analyzed using the GraphPad Prism 8 software.

We calculated the exact molecular weight of each PBPs by the online bioinformatic database “Quest Calculate™ Peptide and Protein Molecular Weight Calculator” (AAT Bioquest, Inc.)

(https://www.aatbio.com/tools/calculate-peptide-and-protein-molecular-weight-mw) and the amino acid and nucleotide sequences listed in GenBank (https://www.ncbi.nlm.nih.gov/nuccore/CP025020.1).

3.4.5. β-lactamases assay

Nitrocefin is a chromogenic cephalosporin that does not have antimicrobial properties. As a cephalosporin, nitrocefin contains a β-lactam ring which is susceptible to beta-lactamase mediate hydrolysis. Once hydrolyzed, the degraded nitrocefin compound rapidly changes color from yellow to red. Beta-lactamase activity was evaluated by Nitrocefin assay (Oxoid™, Thermo Scientific™, Basingstoke, UK) with and without induction with oxacillin (8 mg/L) after 24h incubation on whole cells, starting from a high inoculum, simulating *in vivo* infections (10^9 CFU/ml). The detection of the hydrolysis activity on enzyme preparations (supernatant) and pellets (cellular debris) was performed following a protocol previously published **(Tomayko JF, et al. 1996. Sarti M et al., 2012).** Both assays were performed in duplicate and reconfirmed. *Staphylococcus aureus* ATCC 29213 was used as a Bla+ control strain.

Chromosomal extraction of whole genomic DNA was performed as previously described **(Pitcher DG et al., 1989)**. The sequence of the bla operon *bla*Z-*bla*I-*bla*R1, carried on Tn*552* by S. aureus (available in GenBank, under accession no. X52734), was used to design the primers by the VectorNTI program (Invitrogen). **(Tab 5)**

Primers	Corresponding gene	Sequences	Fragment size (bp)	Source
blaZup	*bla*Z	TGCTCATATTGGTGTTTATGCTT	725	Sarti et al., 2012
blaZdw		CACTCTTGGCGGTTTCACTTATC		

***Table 5**. Primers used to detect bla-operon (blaI/R1/Z), designated on the sequence of S. aureus Tn552 (GenBank accession number X52734).*

4. RESULTS

4.1. Strain selection and *in vitro* antibacterial activity

The sample in study consists of 22 *E. faecalis* clinical strains belonging from different Italian centers and isolated from blood stream infections.

The antimicrobial susceptibility profile was first tested against the principal β-lactam antibiotics: penicillin G, ampicillin, amoxicillin, imipenem and ceftobiprole. The results revealed that 5 isolates (22.7%) were resistant to penicillin G (MIC $\geq$ 16 mg/L) with MIC values ranging from 16-64 mg/L. All strains showed susceptibility to ampicillin (MIC range 0.50-8 mg/L), amoxicillin (MIC range 0.25-4), imipenem (MIC range 0.125-4). Overall, ceftobiprole exhibited a good *in vitro* antibacterial activity against the *E. faecalis* strain tested, lower than 4 mg/L. MIC values ranged from 0.125 to 16 mg/L. Only one isolate (E.fs 1) showed a MIC value of 16 mg/L.

The antibacterial activity in terms of MIC range (mg/L), MIC_{50} e MIC_{90} values and resistance rates, against the main β-lactam antibiotics was shown in **Tab 6**.

	Compound	Range (mg/L)	MIC50	MIC90	% R (N)
E.faecalis N=22	Penicillin	2-64	8	16	22.7 (5)
	Ampicillin	0.5-8	2	4	0
	Amoxicillin	0.25-4	0.5	1	0
	Imipenem	0.125-4	1	2	0
	Ceftobiprole	0.12-16	1	4	/

***Table 6**: Activity of ceftobiprole and beta-lactam comparators tested by broth-microdilution method (BMD) against N. 22 E. faecalis.*

A complete antibiotic susceptibility profile of the main anti-Gram-positive drugs was further evaluated by gradient-tests; the β-lactam values previously obtained by BMD, and E-test showed comparable results. All samples showed susceptibility to the β-lactam ampicillin, ampicillin-sulbactam, amoxicillin, amoxicillin-clavulanic acid and imipenem, and susceptibility to tigecycline (MIC > 0.25 mg/L) with a range of 0.023-0.125 mg/L. 16.67% showed resistance to both glycopeptides. A deep analysis showed that E.fs 5, E.fs 8 and E.fs 11 strains with higher MIC values to vancomycin and teicoplanin (MIC > 64 mg/L) possessed the *van*A gene. 50% of the strains showed high-resistance-level to gentamicin (HLGR) (MIC value > 256-2048 mg/L) and 29.1% high-resistance-level to streptomycin (HLSR) (MIC value > 1024 mg/L). Ceftaroline and ceftobiprole showed a good activity, (ranging from 0.19-256 mg/L and 0.094-32 mg/L, respectively, except for some strain with MIC value > 32 mg/L. **(Tab 7)**

Compound	Range (mg/L)	MIC_{50}	MIC_{90}
Ampicillin	0.38-8	1	3
Ampicillin-sulbactam	0.75-6	2	6
Amoxicillin	0.25-1	0.38	1
Amoxicillina-clavulanic acid	0.19-1	0.50	0.75
Imipenem	0.50-6	2	4
Piperacillin-tazobactam	1.5-32	4	8
Ceftaroline	0.19-256	1	32
Ceftobiprole	0.094-32	0.25	3
Gentamycin	8-2048	64	>1024
Streptomycin	32-1024	128	>1024
Linezolid	2-6	4	4
Tigecycline	0.023-0.125	0.094	0.25
Vancomycin	0.38-256	0.075	12
Teicoplanin	0.50-256	1.50	2

***Table 7** Range, MIC50/MIC90 values*

4.2. *In vitro* antibacterial activity

Table 8 shows the detailed susceptibility values of the 7 *E. faecalis* strains in study to β-lactams and comparator drugs. Five strains were found to be penicillin-resistant ampicillin-susceptible (PRAS) and ceftaroline non-susceptible (CPT-NS) (32 - >256 mg/L). Four out of 5 strains were ceftobiprole non-susceptible (BPR-NS) (4 -16 mg/L). All isolates were also susceptible to the other β-lactams tested (amoxicillin and imipenem), and susceptible to daptomycin, linezolid and tigecycline. High-level resistance to gentamicin (HLGR) (n=1), streptomycin (HLSR) (n=1) and both aminoglycosides (HLAR) (n=4) was detected. Vancomycin and teicoplanin resistance (VRE) were detected in 2 isolates and further found to be associated with the presence of the *vanA* gene.

Below, a schematic representation of the antibiotic-resistance profiles of the study sample:
Efs1 – PRAS; BPR-NS (16mg/L); HLAR.
Efs2 – PSAS; BPR-S and fully susceptible to all antimicrobials tested.
Efs7 – PRAS; BPR-NS (8mg/L); HLAR.
Efs8 – PRAS; BPR-NS (4mg/L); HLGR; VRE/*van*A.
Efs11 – PRAS; BPR-S; HLAR; VRE/*van*A.
Efs18 – PRAS; BPR-NS (4mg/L); HLAR.
Efs20 – PSAS; BPR-S; HLSR.

Penicillin-resistance/ampicillin-susceptible (PRAS); penicillin-susceptible/ampicillin-susceptible; ceftobiprole non susceptible (BPR-NS); Ceftobiprole-susceptible (BPR-S); High level amynoglicoside resistance (HLAR); Higl-level gentamicin resistance (HLGR); High level streptomycin resistance (HLSR); Vancomycin resistant Enterococci (VRE).

E. faecalis code	*MIC values (mg/L)*												
	P[1]	**AMP**	**AML**	**IMI**	**BPR**[2]	**CPT**[2]	**VA**	**TEC**	**CN**	**S**	**LNZ**	**TGC**	**DAP**[1]
E.fs1	16	1	0.5	4	16	>256	0.5	2	>1024	>1024	4	0.25	0.5
E.fs2	4	0.5	0.5	4	2	1	4	2	32	256	4	0.125	0.5
E.fs7	64	4	4	4	8	>256	1	2	>1024	>1024	4	0.06	0.5
E.fs8	16	4	1	2	4	32	>256	>256	>1024	128	4	0.125	0.5
E.fs11	16	4	1	4	2	32	>256	128	>1024	>1024	2	0.25	0.5
E.fs18	16	2	1	2	4	4	1	2	>2048	>1024	2	0.125	0.5
E.fs20	4	2	0.5	1	0.25	0.5	1	0.5	32	>1024	2	0.06	1

Table 8 *β-lactams and comparator antimicrobial MIC values against E. faecalis clinical isolate*

[1] Penicillin and Daptomycin susceptibility values were established according to CLSI breakpoints (EUCAST breakpoints absent). [2] Ceftobiprole and Ceftaroline: No EUCAST an official breakpoints; eCOFFs not determined.
P: Penicillin; **AMP**: Ampicillin; **AML**: Amoxicillin; **IMI**: Imipenem; **BPR**: Ceftobiprole; **CPT**: Ceftaroline; **VA**: Vancomycin; **TEC**: Teicoplanin; **CN**: Gentamicin; **S:** Streptomycin; **LNZ** Linezolid; **TGC**: Tigecyclin; **DAP**: Daptomycin.

4.3. Bactericidal activity of ceftobiprole

As shown in time-kill curve analysis, among BPR-NS strains a single-drug exposure to BPR resulted in a potent bactericidal activity at 4X MIC, after 24 h (E.fs 1-E.fs 7), while BPR-S strains showed a greater log reduction (3 to 5 log_{10}) even at lower concentrations (i.e. 1X-2X MIC) (E.fs 2; E.fs 11; E.fs 20). Enhanced killing activity was also observed at 8h (E.fs 8; E.fs 18), and in rare case after 4h (E.fs. 2)

These data confirmed that ceftobiprole alone exerts a great bactericidal activity against *E. faecalis* clinical isolates, despite their MDR phenotypes **(Fig 24)**

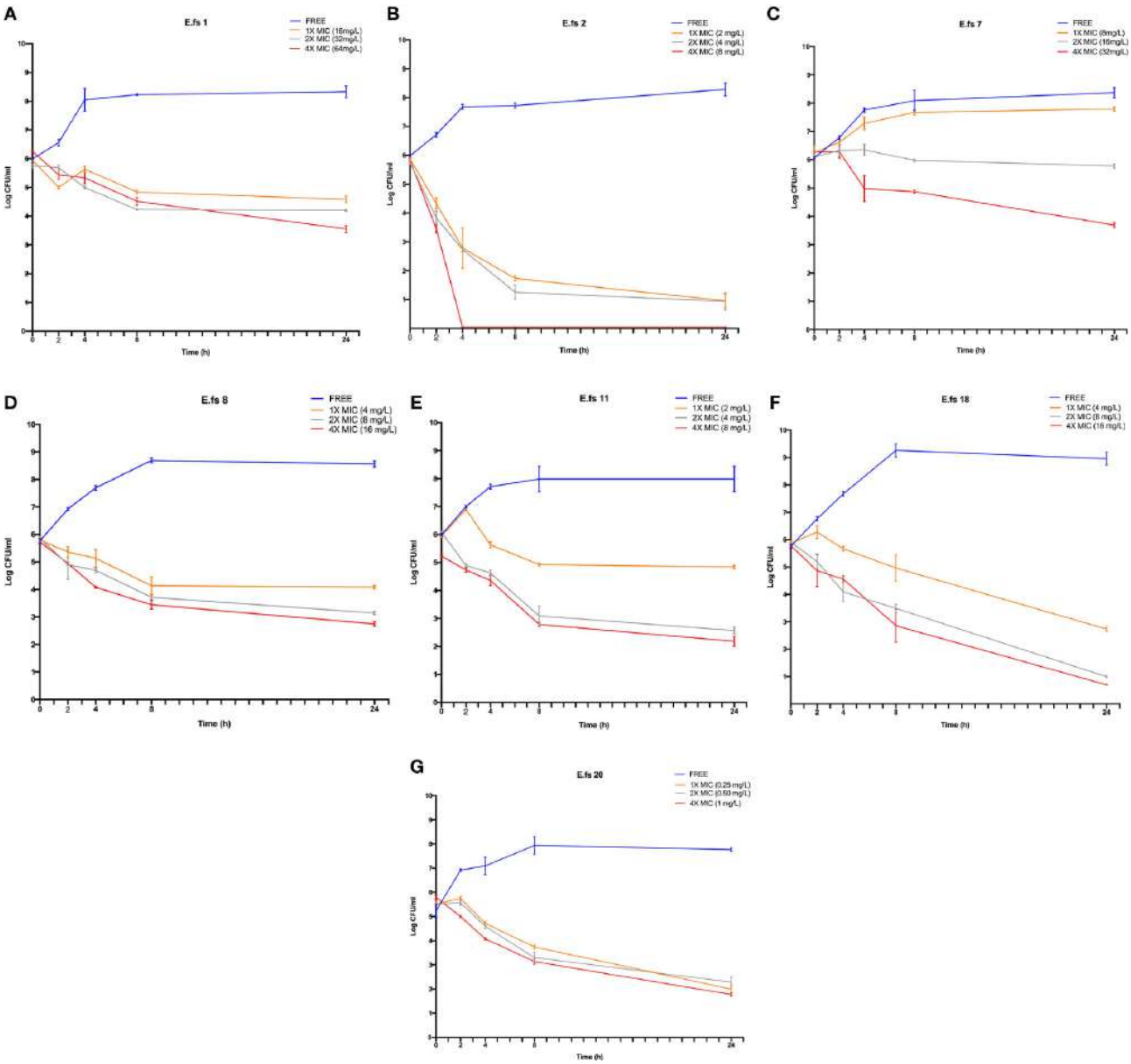

***Figure 24**| Time-kill assays of ceftobiprole (BPR) against the seven E. faecalis clinical isolates in study. Cell count was reported as log10 (CFU/ml) at 0, 2, 4, 8 and 24h Time-points (T0, T2, T4, T24); Ceftobiprole (BPR) exposure was tested at 1X, 2X and 4X MICs. Error bars represent standard deviations (±SD) of the mean of triplicate experiments (A–G).*

4.4. Evaluation of β-lactamases (Bla) production

All the 7 *E. faecalis* clinical strains were phenotypically confirmed by the modified nitrocefin test. For this reason, the hydrolytic activity was detected in the cell-debrid pellets (cellular membranes), after growth under induction with oxacillin 8 mg/L, in presence of a high inoculum (10^8 CFU/ml).

As shown in **Fig 25,** *S. aureus* ATCC 29213, used as Bla-positive control, rapidly developed a more intense red color demonstrating abundant enzyme release. On the contrary, *E. faecalis* ATCC 29212, used as Bla-negative control, remained yellow, synonymous of the absence of hydrolytic activity. These results were confirmed by the *bla*Z gene amplification.

The crude extracts of E.fs1, E.fs7, E.fs11 and E.fs18 isolates developed a moderate red color 24 h post-exposure to NITROCEFIN, demonstrating the enzyme production and the hydrolytic activity. These results were further confirmed through the detection of blaZ gene, encoding the β-lactamase enzyme, only in E.fs1, E.fs7 and E.fs18 (PRAS; BPR-NS). In E.fs 11 isolate (PRAS; BPR-S; VRE *van*A), after 24 h of treatment with Nitrocefin, the pellet developed a red color, although there was no correlation with the PCR amplification (blaZ negative).

We considered beta-lactamase producers only E.fs 1, E.fs 7 and E.fs18, as reported positive by both assays. Beta-lactamase production of these strains should be potentially in line with their resistant phenotype, with higher MIC values to penicillin (**Tab.9**).

SAMPLE	NITROCEFIN ASSAY	PCR BLA GENE	RESULTS
ATCC 29213 (POSITIVE CONTROL)	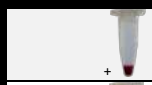	+	β-lactamase producer
ATCC 29212 (NEGATIVE CONTROL)		-	β-lactamase non-producer
E.fs1		+	β-lactamase producer
E.fs2		-	β-lactamase non producer
E.fs7		+	β-lactamase producer
E.fs8		-	β-lactamase non producer
E.fs11		-	β-lactamase non producer
E.fs18		+	β-lactamase producer
E.fs20		-	β-lactamase non producer

Figure 25*. Visual estimation of the beta-lactamase activity in E. faecalis strains. Nitrocefin test in cellular debrids (pellets) obtained after incubation with 8 mg/L oxacillin induction after 24 h of incubation. S. aureus 29213 positive control strain; E .faecalis 29212 negative control strain.*

4.5. *pbp4* sequence analysis and significant protein alterations

PCR and sequence analysis of the *pbp4* gene revealed some mutations that may account for the changes in PBP4 affinity and MIC increase to cephalosporins and penicillin G. The adenine deletion (*delA*) in the promoter region, 8bp upstream of the -35 consensus site, was carried by all 4 BPR-NS strains showing non-susceptibility to BPR (MICs 4-16 mg/L) and high-level resistance to penicillin (MIC between 16-64 mg/L). **(Table 9; Fig 26 and Fig. 27)**

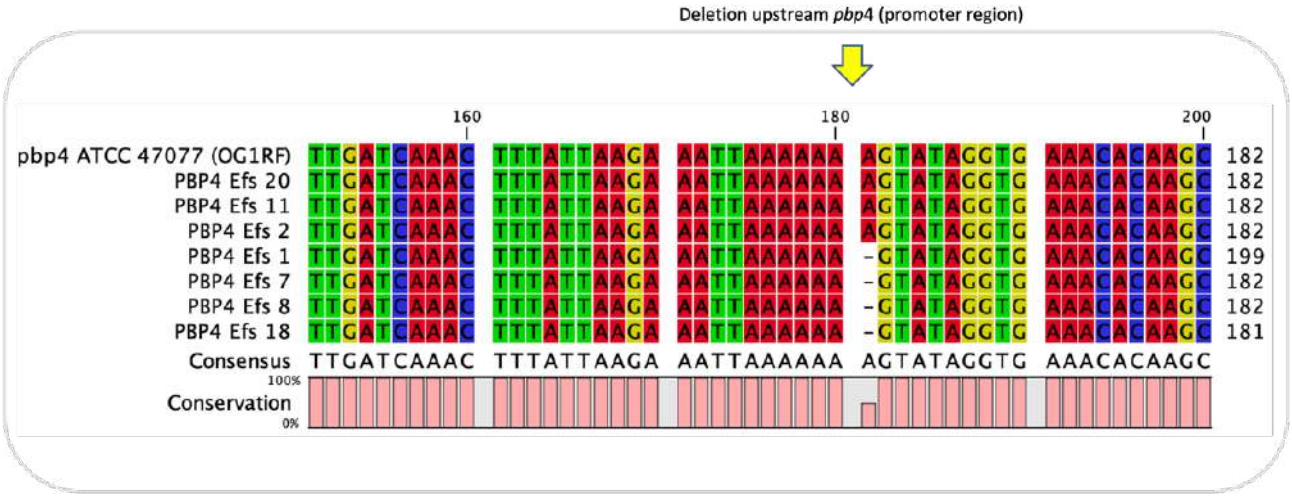

Figure 26 *Blast alignments and translated sequence analysis of pbp4 gene analyzed by CLC Sequence Viewer 8.0 software package (QIAGEN CLC Genomics). Focus on the adenin deletion (delA) in the promoter region, located 8bp upstream of the -35 consensus site.*

Sequence analysis of the translated PBP4 identified 12 different missense mutations, 7 of which were next to the PBP catalytic sites (region of the protein where catalytic residues of the site interact with the substrate to lower the activation energy of a reaction and thereby make it proceed faster)**.**

These mutations, all located near to the PBP active-site, could be involved in the possible binding alteration between beta-lactams antibiotic and PBP4, influencing their resistance phenotype **(Table 9; Figure 26).**

Notably;

- T418A mutation in Efs1 was located 6 amino acids (aa) upstream of the catalytic serine included in the $_{424}$STFK$_{427}$ *motif* I, that affect the MIC value (16 mg/L) to ceftobiprole.
- A536T substitutions, always shown Efs1, located in the region between $_{482}$SDN$_{484}$ and $_{619}$KTGT$_{622}$
- D573E, also located in the region between $_{482}$SDN$_{484}$ and $_{619}$KTGT$_{622}$ of Efs11, which potentially affects the MIC values of penicillin and ceftaroline (16 and 32 mg/L, respectively), but not those of ceftobiprole (2 mg/L).
- L475Q in Efs8, located 7 aa upstream of the $_{482}$SDN$_{484}$ motif II, involved in β-lactam leaving group protonation.
- Y605H, a novel mutation carried by Efs18, and the already described V606A detected in Efs7, 13/14 aa upstream of the $_{619}$KTGT$_{622}$ motif III, which facilitates substrate binding.

Other mutations were found far from the PBP catalytic site, thus not altering the binding affinity, and consequently not affecting MICs to beta-lactams.

- T50I, quite common in our sample (3/7), and I223V, only present in a fully susceptible strain (Efs20) in which it does not affect MICs to β-lactams, both located in proximity of the non-penicillin binding module (nPB module), near the N-terminal end.
- L639F, T665I and T678A (all in Efs7), and D666P (Efs1), located in the C-terminal end.

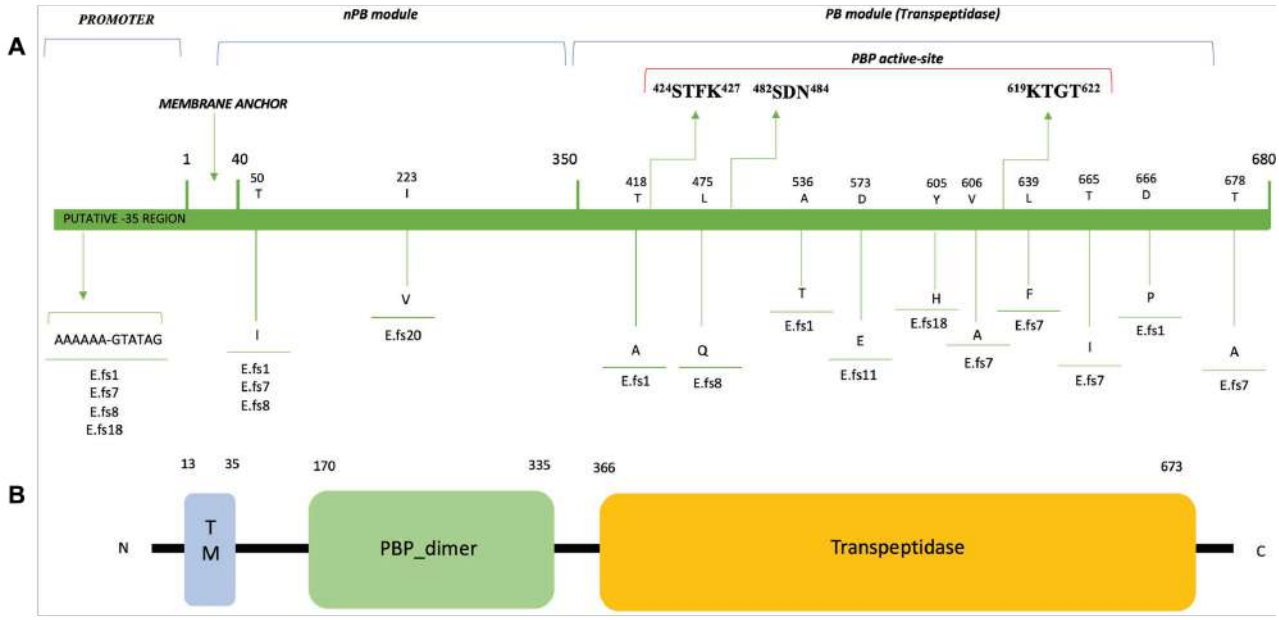

Figure 27 *Amino acid substitutions and domain architecture of PBP4 of E faecalis clinical isolates. GenBank accession no. from OM032878 to OM032884. The numbers above the diagrams indicate residue numbers of the domain boundaries in the proteins. (A) Non-Penicillin Binding module (nPB); Penicillin Binding module (PB); TM, transmembrane helix region. 424STFK427, 482SDN484 and 619KTGT622: catalytic-site motifs (STFK424 includes the catalytic serine S424). (B) The domain architecture of PBP4 of E faecalis ATCC 47077 (OG1RF) was analyzed using SMART (Simple Modular Architecture Research Tool; http://smart.embl-heidelberg.de/) and reported in a simplified version.*

4.6. Correlation between ceftobiprole bactericidal activity and PBP4 alterations

Even if ceftobiprole alone exerts a great bactericidal activity at 24h, against all *E. faecalis* clinical isolates, despite their MDR phenotypes, differences were shown among the strains in study.

In the BPR-NS strains, several significative PBP4 substitutions within the transpeptidase domain (T418A mutation in Efs1; L475Q in Efs8; Y605H in Efs18; V606A in Efs7) greatly affect the MIC values to ceftobiprole (4-16 mg/L), but presumably also to ceftaroline (4- >256 mg/L) and penicillin (16-64 mg/L), retaining however ceftobiprole bactericidal activity at 4-fold the MIC value.

In the BPR-S strains E.fs2 (MIC 2 mg/L) and E.fs20 (MIC 0.25 mg/L), ceftobiprole exerts bactericidal activity 8h after exposure and, starting from 4h in E.fs2; these strains are susceptible to penicillin (MIC 4 mg/L). Sequence analysis revealed neither adenine deletion in the promoter region nor mutations near the catalytic sites. The only mutation detected was the I223V, only present in the fully susceptible E.fs20 strain, located far from PBP active site, in the nPB module, that not alters the PBP4 catalytic activity. In fact, this region is known to have no enzymatic function.

E.fs 11 isolate is a special case, being susceptibility to ceftobiprole (MIC 2 mg/L), but showing a penicillin and ceftaroline-resistance (MIC 16 and 32 mg/L, respectively). Sequence analysis did not show adenine deletion in the promoter region; only the D573E mutation, located in the PBP active site, between $_{482}$SDN$_{484}$ and $_{619}$KTGT$_{622}$ motifs was detected. This PBP4 substitution is probably responsible for the higher MIC values to penicillin and ceftaroline, although it does not affect the ceftobiprole MIC value.

4.7. Increase in the level of *pbp*4 expression

Gene expression studies were performed to evaluate a possible correlation between *pbp*4 mutations (upstream or within the coding sequence) and increase in the expression level of *pbp*4.

The evaluation of *pbp*4 gene expression was analyzed by real-time quantitative PCR, relative to that of the ATCC47077 (OG1RF) reference strain and showed varying level of upregulation in all seven strains tested, in relation to their beta-lactam MIC values.

The data obtained showed that PRAS/BPR-S E.fs2 and E. fs20 strains exhibited lower expression levels ($\leq 10^2$ fold-change increase), unlike PRAS BPR-NS strains, that displayed PBP4 overexpression with greater fold-change increase (0.5-4 x 10^3), due to adenine deletion (*del*A) in the PBP4 promoter region and to different mutations in the PBP catalytic sites **(Fig 28)**

Noteworthy, the *pbp*4 gene expression was more evident in the Vancomycin Resistant Enterococci/VanA type (VRE/*van*A) strains (E.fs8 and E.fs 11), regardless of the presence of the *del*A in the promoter region **(Fig 28, pattern-filled bars).**

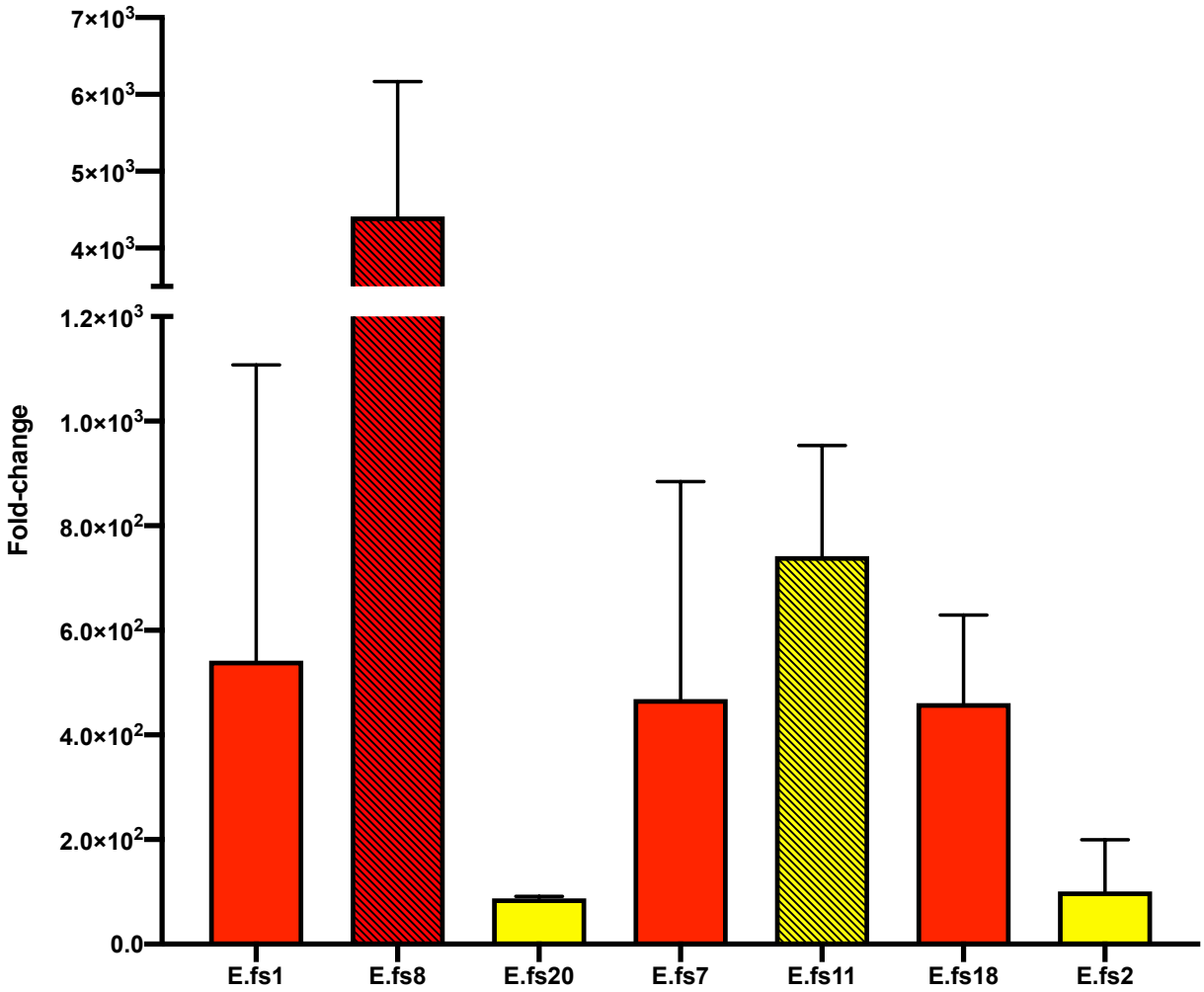

Figure 28 *pbp4 gene expression analysis of the E. faecalis isolates in study, compared to that of the ATCC 47077 (OG1RF) reference. Evaluation of pbp4 relative mRNA expression expressed as fold-change (linear). 16S rRNA gene expression levels were used as calibrator. ATCC 47077 (OG1RF) was used as reference. Error bars indicate the average of three biological replicates in three RT-qPCR assays ± SD; PSAS, white; PRAS, gray. VRE/ vanA, pattern-filled bars.*

4.8. Correlation between sequence alterations and increase in the level of *pbp*4 expression

Different missense mutations are common in the coding region of *pbp*4, both in BPR-NS and fully susceptible strains. This leads to hypothesize that the reduced susceptibility to ceftobiprole resides on the strong association between the increase in the level of *pbp*4 expression and the adenine deletion in the promoter region, upstream the coding sequence. In fact, all BPR-NS strains that carried the adenine deletion (*del*A) showed a 3 $\log_{10}$ increase expression compared to that of the ATCC47077 (OG1RF) reference, demonstrating its role in establishing *in vitro* non-susceptibility to BPR, although it does not influence bactericidal activity.

The only apparent exception to this is represented by E.fs11 (PRAS;CPT-NS;BPR-S), which does not carried the adenine deletion, but still shows a high *pbp*4 increase expression especially if compared to the other strains without *del*A. The only mutation carried by this strain is D573E substitution. We were not able to demonstrate whether this mutation within the SDN/KTG catalytic sites alone may potentially interfere with the expression of pbp4 transcription, or if the higher upregulation may be related to the VRE/vanA phenotype, as stated above. Further experiments are needed to confirm its role **(Tab 9).**

Code	Phenotype characteristics	Bla	BPR MIC (mg/L)[a]	§Fold-change mean	Deletion in promoter region[b]	Amino acid substitutions in PBP4[d]										
								PBP active-sites								
						50 T	223 I	418 T	475 L	536 A	573 D	605 Y	606 V	639 L	665 T	666 D	678 T
Efs20	PSAS; BPR-S; HLSR	+	0.25	88. 80	-	-	V	-	-	-	-	-	-	-	-	-	-
Efs2	PSAS; BPR-S; fully susceptible	-	2	77.36	-	-	-	-	-	-	-	-	-	-	-	-	-
Efs11	PRAS; BPR-S; VRE/*van*A; HLAR	-	2	695.413	-	-	-	-	-	-	E	-	-	-	-	-	-
Efs8	PRAS; BPR-NS; VRE/*van*A; HLGR	-	4	4851.96	2013028_2013029 *del*A[c]	I	-	-	Q	-	-	-	-	-	-	-	-
Efs18	PRAS; BPR-NS; HLAR	+	4	422.88	2013028_2013029 *del*A[c]	-	-	-	-	-	-	H	-	-	-	-	-
Efs7	PRAS; BPR-NS; HLAR	+	8	571.068	2013028_2013029 *del*A[c]	I	-	-	-	-	-	-	A	F	I	-	A
Efs1	PRAS; BPR-NS; HLAR	+	16	698.895	2013028_2013029 *del*A[c]	I	-	A	-	T	-	-	-	-	-	P	-

Table 9 *Ceftobiprole MIC values (mg/L) and expression levels for E. faecalis clinical isolates, compared to sequence alterations.*

[a]BPR, Ceftobiprole; [b]single base pair deletion 8 bases upstream of the putative -35 region; [c]Accession number GenBank: CP025020.1 (ATCC47077); [d]Protein ID GenBank: AEA94594.1 (ATCC47077); §Fold-change expression levels relative to that of ATCC47077. Average of three independent experiments. HLSR, High Level Streptomycin Resistance; VRE,Vancomycin Resistant E. faecalis; HLAR, High Level Aminoglycosides Resistance; PRAS, Penicillin-Resistant Ampicillin-Susceptible; BPR-NS, Ceftobiprole Non-Susceptible; PSAS,Penicillin-Susceptible Ampicillin-Susceptible; BPR-S, Ceftobiprole Susceptible; HLGR, High Level Gentamicin Resistance; β-lactamase producer (Bla). GenBank accession no. from OM032878 to OM032884.

4.9. Binding profiles of all PBPs

Purified membrane proteins of ATCC 47077 (OG1RF) control strain and beta-lactam-resistant and susceptible strains were labelled with fluorescent penicillin (Bocillin FL) and analyzed after electrophoresis in SDS-PAGE gel. Based on the mobility on the gel, we were able to detect 6 High-Molecular-mass (HMM) and 2 Low-Molecular-mass (LMM) PBPs (DD, carboxypeptidase). The putative function of each protein was also inferred by the NCTC database (**Tab. 10**).

Analysis of HMM-PBPs of class A and B was performed for all *E. faecalis* isolates in study. The PBP binding profiles of each strain were compared with that of the ATCC control, in treated (1/2- 1- 2- 4-fold the MIC value) and untreated conditions. Our study was completed by the determination of the 50% inhibitory concentration (IC_{50}) values for ceftobiprole, to evaluate the intensity of fluorescence as indicator of BPR inhibition concentration (IC_{50}) (decrease of fluorescence).

Treatment of the ATCC 47077 control strain with ceftobiprole (MIC 0.5mg/L; range tested 0.25-2 mg/L) resulted in a variable acylation of all PBPs, at diverse concentrations, except for PonA (PBP1a), PBP1b and PBP4.

Similar results were observed in all strains, regardless their ceftobiprole (and penicillin) susceptibility or resistance. BPR had lower affinity for PBP4 in all isolates, demonstrating its leading role in beta-lactam resistance. Similar unresponsiveness was detected for PonA (PBP1a) in almost all strains, demonstrating a necessary cooperation between class B and class A PBPs in establishing beta-lactam resistance, to carry out PG cross-linking in the presence of cephalosporins and promote growth. PBP1b was also acylated in 3 strains, similar to the ATCC control. Unexpectedly, Efs7 did not show PBP1b. Sensitivity of the other PBPs to ceftobiprole was variable: treatment with ceftobiprole decreased the binding of almost all PBPs, at variable concentrations (IC_{50} ½X MIC - 4X MIC). In only one strains (Efs 20), no PBP was significantly acylated by BPR. Of note, in Efs 1 and Efs 2 strains, all PBPs were strongly inhibited already at ½-fold the MIC concentration, except for PBP4 that remains the only PBP able to confer resistance to ceftobiprole **(Tab 11**; **Fig. 29).**

More specifically, among the BPR susceptible strains: in Efs2, ceftobiprole (MIC 2mg/L; range tested 1- 8 mg/L) completely saturated all PBPs at every concentration, with the only exception of PBP4 and PBP1a; In Efs11, (VRE, *van*A), ceftobiprole (MIC 2 mg/L; range tested 1-8 mg/L) completely saturated all PBPs at any concentrations, except for PonA (PBP1a) and PBP4; in Efs20, ceftobiprole (MIC 0.25mg/L; range tested 0.12 - 1 mg/L) did not acylate any PBPs, though the IC_{50} value was close to 50% for PBP2 and PBP2a.

Among BPR non-susceptible strains: in Efs 1, ceftobiprole (MIC 16mg/L; range tested 8-64 mg/L) variably acylated all PBPs, at different concentrations, except for PBP4 and PBP1a, that remained the only PBP able to confer resistance to BPR (and penicillin), due to its over-expression levels, for the delA in the promoter region; in Efs7, ceftobiprole (MIC 8 mg/L; range tested 4-32 mg/L) strongly acylated all PBPs at different concentrations, except for PonA (PBP1a) and PBP4. This strain lacks PBP1b; in Efs8, (VRE, *van*A), ceftobiprole (MIC 4 mg/L; range tested 2-16 mg/L) completely saturated all PBPs at the different concentrations tested, except for PonA (PBP1a) and PBP4; in Efs18, ceftobiprole (MIC 4 mg/L; range tested 2-16 mg/L) moderately saturated all PBPs at the different concentrations tested, except for PonA (PBP1a) and PBP4.

PBP	PBP (other name)	PBP class	Locus_Tag	N. aminoacids (aa)	[b]Molecular weight (kDa)	[c]Enzymatic activity	Gene	GenBank CP025020.1 (genome pos.)	N. nucleotides (bp)
PBP2b	PBPA	class B	***CVT43_02290***	728	79.56664	TPase	*pbp2b*	***966441-968777***	*2187*
PBP2	PBPB	class B	***CVT43_03860***	742	81.71274	TPase - Cell division protein FtsI	*pbp2*	***747766-749994***	*2229*
PBP1b	PBPZ	class A	***CVT43_04970***	778	85.35237	TPase/Gtase	*pbp1b*	***431566-433752***	*2331*
PBP1a	PONA	class A	**CVT43_07655**	803	88.40413	TPase/Gtase	*pbp1a*	**1509774-1512185**	2412
PBP4	PBP4(5)	class B	**CVT43_10030**	680	74.01754	TPase	*pbp4*	**2010904-2012946**	2043
PBP2a	PBPF	class A	**CVT43_11360**	711	77.85899	TPase/Gtase	*pbp2a*	**2276447-2278582**	2136
PBP	PBP	class C	**CVT43_05000**	498	57.71227	D,D-Carboxypeptidase M32	*pbp M32*	**972441-973937**	1497
VanY	PBP	class C	***CVT43_11375***	236	27.04	D-Ala-D-Ala carboxypeptidase VanY	*pbp vanY*	***2281379-2282089***	*711*

Table 10 *PBP genes of E. faecalis OG1RF (ATCC 47077) chromosome, corresponding proteins and putative molecular weights (kDa).*
**Bocillin/PBPs competition assay of OG1 RF in free conditions (left) and corresponding Comassie blue staining gel (SDS-PAGE).*

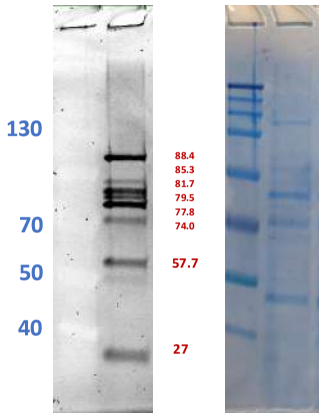

[a] *https://www.ncbi.nlm.nih.gov/nuccore/CP025020.1*
[b] *PBP Molecular weights were calculated with the online bioinformatic software AAT Bioquest, Inc. (2023, February 1). Quest Calculate™ Peptide and Protein Molecular Weight Calculator. AAT Bioques*
[c] *Transpeptidase (TPase); Transpeptidase/GlycosylTransferase (Tpase/Gtase).*

Figure 29a. Relative affinities of ceftobiprole and PBP/Bocillin-labelled profiles for (A) ATCC 47077 and (B) E.fs1.

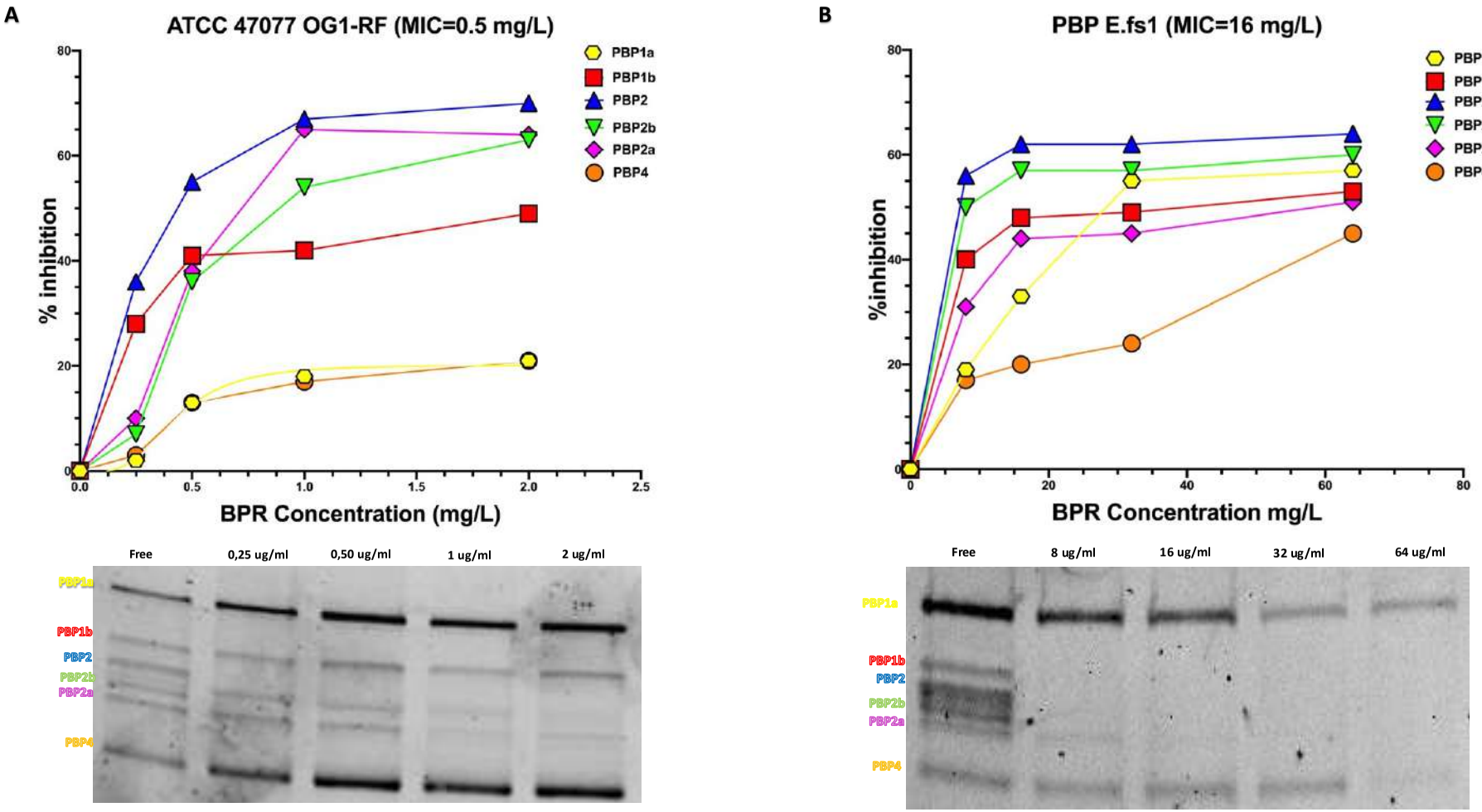

The affinity of ceftobiprole for PBPs was analyzed by a competition assay using fluorescent penicillin. Membrane proteins were prepared from BPR-S and -NS. Nonlabelled ceftobiprole was incubated with membrane proteins, followed by the addition of fluorescent penicillin (Bocillin FL). The membrane fractions were subjected to SDS-PAGE and fluorography.

Figure 29b. Relative affinities of ceftobiprole and PBP/Bocillin-labelled profiles for (C) E.fs2 and (D) E.fs7.

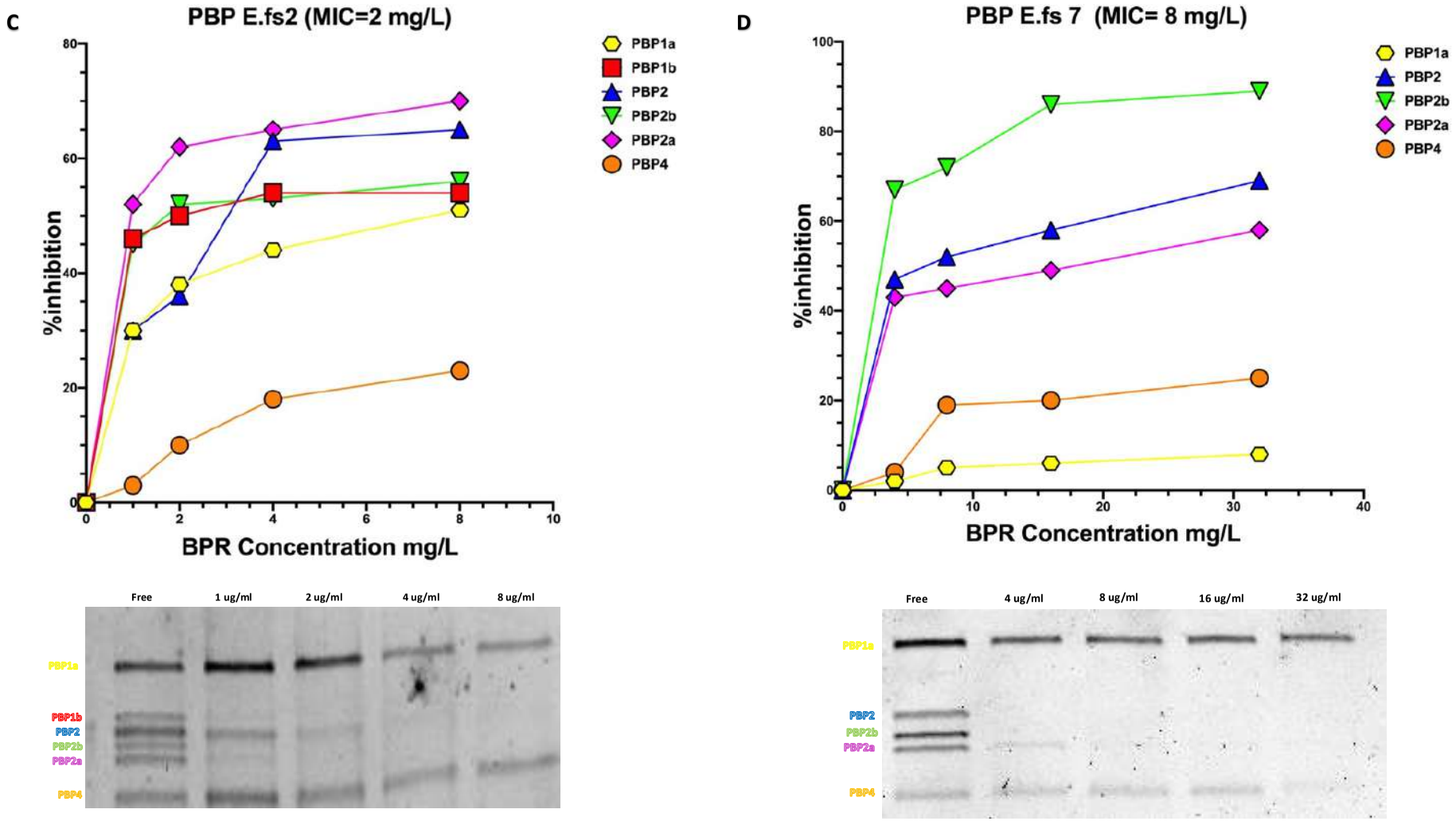

The affinity of ceftobiprole for PBPs was analyzed by a competition assay using fluorescent penicillin. Membrane proteins were prepared from BPR-S and -NS. Nonlabelled ceftobiprole was incubated with membrane proteins, followed by the addition of fluorescent penicillin (Bocillin FL). The membrane fractions were subjected to SDS-PAGE and fluorography.

Figure 29c. Relative affinities of ceftobiprole and PBP/Bocillin-labelled profiles for (E) E.fs 8 and (F) E.fs11.

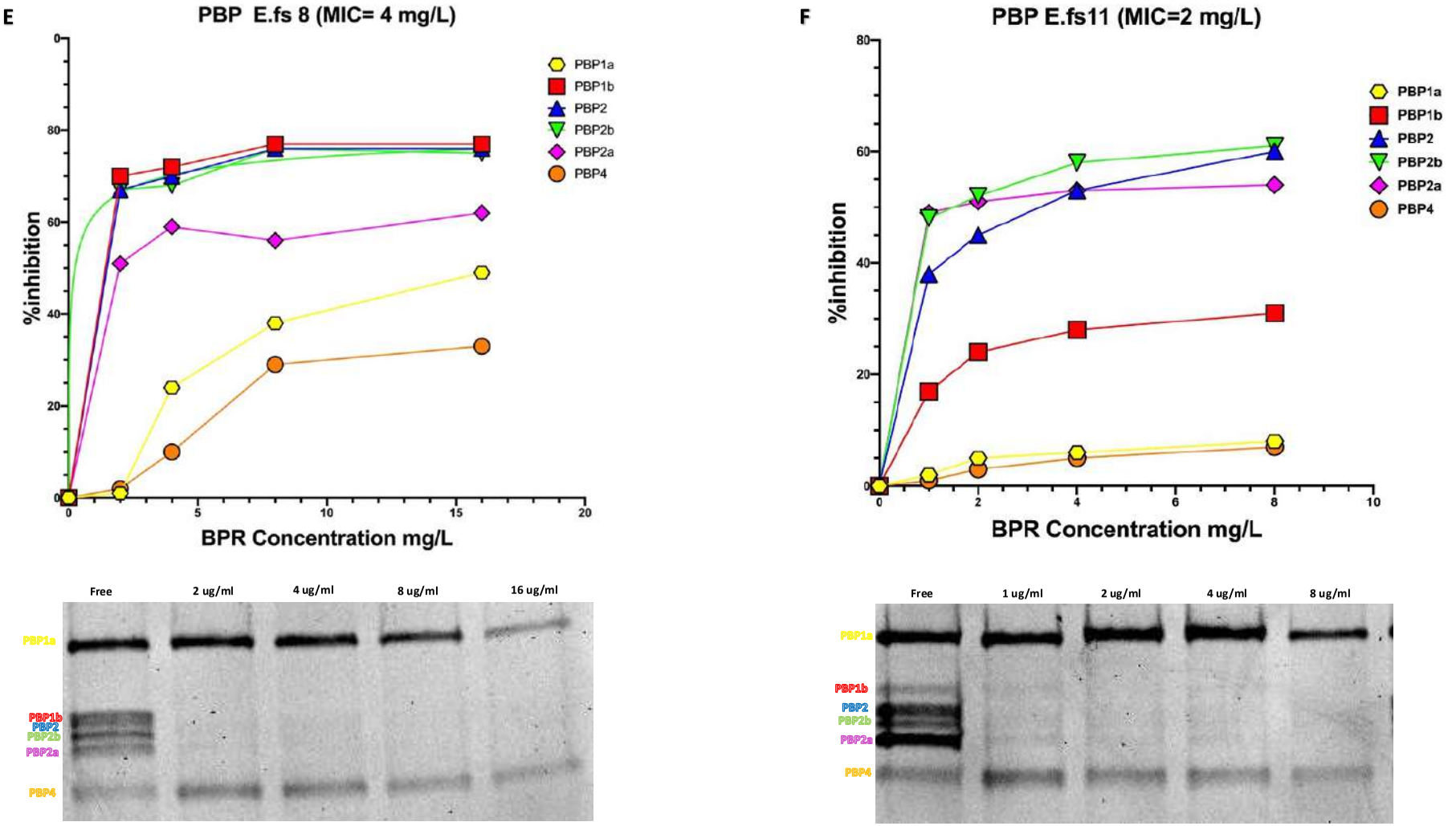

The affinity of ceftobiprole for PBPs was analyzed by a competition assay using fluorescent penicillin. Membrane proteins were prepared from BPR-S and -NS. Nonlabelled ceftobiprole was incubated with membrane proteins, followed by the addition of fluorescent penicillin (Bocillin FL). The membrane fractions were subjected to SDS-PAGE and fluorography.

Figure 29d. Relative affinities of ceftobiprole and PBP/Bocillin-labelled profiles for (G) E.fs 18 and (H) E.fs20.

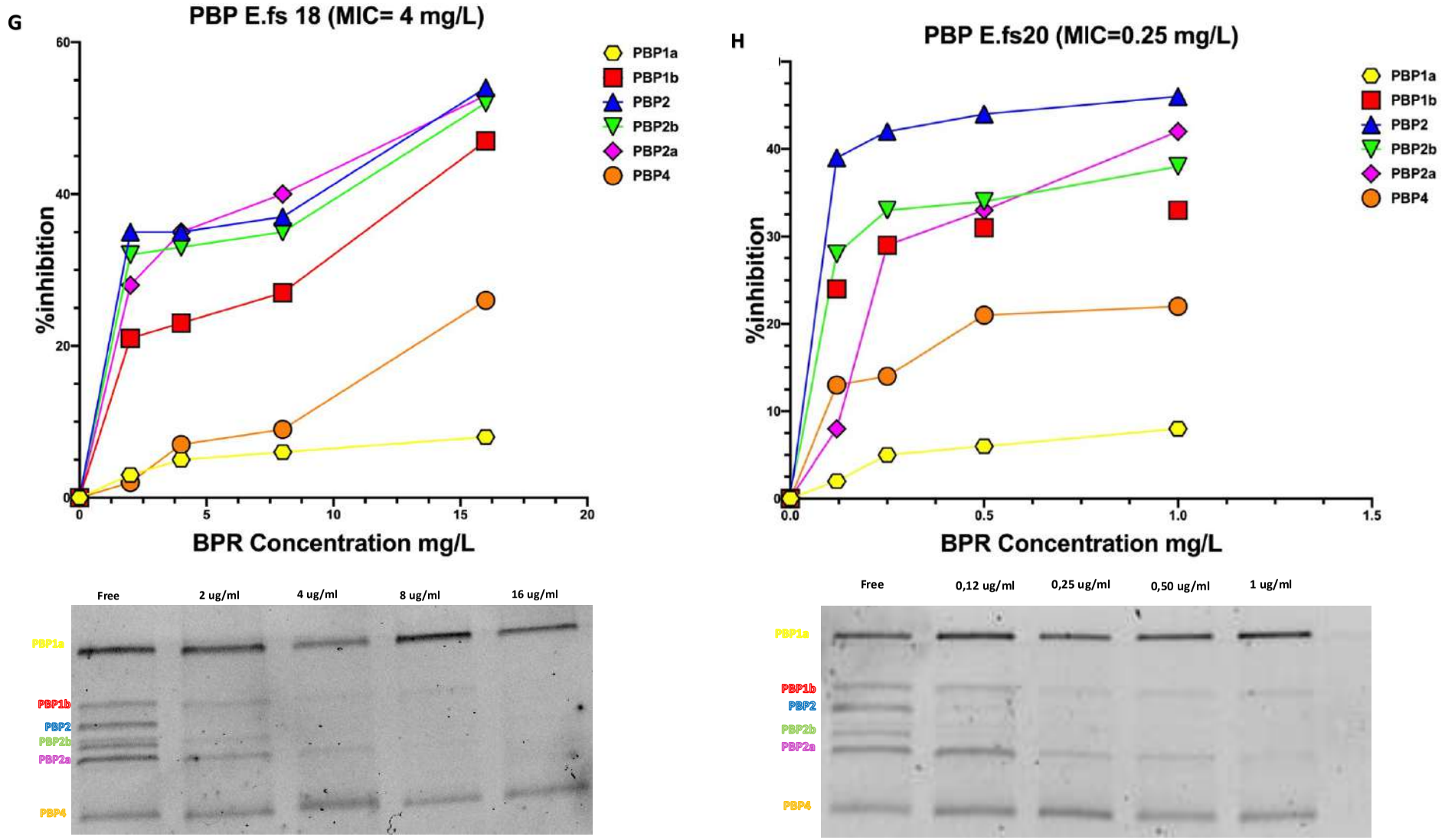

The affinity of ceftobiprole for PBPs was analyzed by a competition assay using fluorescent penicillin. Membrane proteins were prepared from BPR-S and -NS. Nonlabelled ceftobiprole was incubated with membrane proteins, followed by the addition of fluorescent penicillin (Bocillin FL). The membrane fractions were subjected to SDS-PAGE and fluorography.

Strain	IC_{50} (µg/ml) PBP						BPR MIC (µg/ml)
	1a	1b	2	2b	2a	4	
ATCC 47077 OG1RF	N.A.	N.A.	0.45	0.89	0.74	N.A.	0.5
E.fs1	28.59	38.45	7.30	8.42	57.64	N.A.	16
E.fs2	7.27	2.17	3.11	1.70	1	N.A.	2
E.fs7	N.A.	N.A.	7	3.07	16.3	N.A.	8
E.fs8	N.A.	1.53	1.53	0.31	2.2	N.A.	4
E.fs11	N.A.	N.A.	3.35	1.52	1.52	N.A.	2
E.fs18	N.A.	N.A.	14.2	15.19	14.2	N.A.	4
E.fs20	N.A.	N.A.	N.A.	N.A.	N.A.	N.A.	0.25

Table 11 *Inhibition of expressed as IC_{50} of ceftobiprole (BPR) concentration versus PSAS/BPR-S and PRAS/BPR-NS E. faecalis* ***strains.***

IC_{50}=Concentration of ceftobiprole that inhibits 50% of the fluorescent penicillin (BOCILLIN FL) in comparison with the level of the free-control, containing no drug. NA= not available values.

5. DISCUSSION

High resistance to penicillins in *E. faecalis* strains is rare, it can emerge after prolonged β-lactam therapy treatments **(Rice et al., 2018**). Nevertheless, the PRAS phenotype was described in several countries (**Conceição et al., 2014**; **Guardabassi et al., 2010**; **Metzidie et al., 2006**), but its epidemiological and clinical impact remains ambiguous, as ampicillin is the treatment of choice for enterococcal infections **(Kristich, Rice and Arias, 2014)** and penicillin MIC values were never reported **(Mendes et al., 2016)**. The evolution of nosocomial *E. faecalis* clones is driven by the acquisition of resistance genes, and the spread of PBP4 variants, responsible for resistance to all beta-lactams, may potentially compromise the clinical efficacy of *E. faecalis* therapy in hospital settings. Ceftobiprole, a novel cephalosporin that inhibits the PG cross-linking reaction by acylating the catalytic serine of the PBP active sites, maintains a certain affinity for PBP4 being the best candidate as a valid therapeutic option for remarkable *E. faecalis* MDR-phenotypes such as PRAS and VRE.

PBPs perform the penultimate steps of bacterial cell wall synthesis through their glycosyltransferase (GTase) and/or transpeptidase (TPase) domains, also being targets of the β-lactams. They are classified into two groups, the high-molecular-mass (HMM) and low-molecular-mass (LMM), based on their molecular weights, amino acid sequences, and enzymatic and cellular functions. *E. faecalis* membranes carry three class A PBPs [PonA(1a); PBPZ(1b); PBPF(2a)], with TPase and GTase activity, and three monofunctional class B [PBPA(2b), PPBB(2); Pbp4], mainly with transpeptidase activity, elongase activity, or divisome. Two further class C LMM PBPs (D,D-carboxypeptidases and/or endopeptidases), involved in cell separation or peptidoglycan maturation or recycling, are also carried **(Sauvage et al., 2008.)**. Class B PBPs hold a key role in establishing cephalosporin resistance.

Monofunctional PBP4, which allows the cross-linking of the peptidoglycan (PG), works in concert with a bifunctional class A PBP (such as PBP2b) for effective cell wall synthesis and surviving upon cephalosporin occurrence. Due to its low responsiveness, PBP4 is considered the key for intrinsic resistance to cephalosporins in *E. faecalis* **(Arbeloa et al., 2004).** More recently, PBP2b and PBP2 poor reactivity toward cephalosporins, has been demonstrated **(Dijoric et al AAC 2020)**. PBP2, encoded by a gene cluster together with *ftsQ, ftsA, ftsZ,* and *divIVA* genes, is considered potentially essential for the cell viability, due to its involvement in septal PG biosynthesis, during cell division. PBP2b and PonA (PBP1a) of class A are implicated to function in concert with PBP4, although a direct interaction between them has not been experimentally verified **(Sauvage et al., 2008**). PBP4 could carry missense mutations or altered expression level that amplify their involvement in resistance **(Lazzaro LM, et al, 2022)**. Ceftobiprole, a new generation cephalosporin, has been reported to moderately retain their ability to target low-affinity PBPs, specifically PBP4. The inhibition of PBPs activity occurs via competition with the peptidoglycan-pentapeptide precursor for binding to the active-site serine of the transpeptidase domain. Alterations in this enzyme cause conformational changes that impact the structure of the catalytic *motifs,* resulting in a lack of bonding and evident *in vitro* antibacterial activity **(Moon at al., 2018).**

In this study, we addressed the molecular mechanism of non-susceptibility to ceftobiprole, the involvement of alteration in the expression of *pbp*4 and/or significant substitutions in the PBP4 transpeptidase domain, and the resulting interactions with PBPs of *E. faecalis* clinical strains, all isolated from bloodstream infections. Our study also demonstrates an unforeseen complexity in the mechanism of beta-lactam resistance. It implies that the susceptibility of PBP4-mediated peptidoglycan cross-linking to diverse beta-lactams differs as a function of the class A (glycosyltransferase) PBP partner produced by the host.

A link between benzyl-penicillin resistance and 5th generation cephalosporins non-susceptibility was observed. Our data suggest that this common insensitivity in PRAS isolates results from the involvement of *pbp*4 mutations (*del*A) which increased gene expression levels and altered the penicillin binding domain that could remodel the PBP/β-lactam complex.

Our *in vitro* dynamic data by time-kill curve assays showed that BPR exerts a bactericidal activity against *E. faecalis* isolates despite their MDR phenotypes (VRE, PRAS and BPR-NS), and PBP4 alterations, even after 8h, consistently with other studies (**Werth and Abbott, 2015**; **Arias et al., 2007**). After 24 hours, the bactericidal activity against all isolates - with or without significative PBP4 changes - was similar, suggesting that

ceftobiprole could maintain high affinity also for other PBPs. Besides, we can assume that the bactericidal effect after 24h of antibiotic treatment may reasonably result of succeeding acylation and deacylation cycles, in presence of increasing concentrations of active ceftobiprole (above the MIC value), and PBP4 alterations unable to maintain the binding with the molecule.

A rare mechanism of β-lactams resistance in *E. faecalis* strains is due to the β-lactamases production. **(Rice, L. B. and Murray, B. E. 1995**; **Schell et al., 2020).** In staphylococci, beta-lactamases production is inducible, whereas BlaZ is costitutively expressed in enterococci, at a much lower level (clinically significant *inoculum* effect). Enterococci produce much less enzyme than staphylococci, which likely explains the lack of phenotypic resistance of beta-lactamases-producing (Bla +) enterococci. Moreover, Bla + enterococci showed an *inoculum* effect: standard *inoculum* (1×10^5 used for routine susceptibility testing) produces little amount of enzyme, and strains were tested as susceptible. Another important difference in Enterococci is that the enzyme remains embedded in the cell wall, *Staphylococcus* strains release their enzyme into the extracellular medium and it can be recovered from cell-free supernatants, in enterococci, the enzyme have not found in cell-free supernatants, but the enzyme remained cell associated **(Sarti et al., 2012)**.

Our data reinforce the nature of beta-lactam resistance in Enterococci as a multifactorial phenomenon. Among the 7 *E. faecalis* clinical strains in study, 3 strains were beta-lactamases producers, but this was not so relevant in terms of beta-lactam resistance. As reported in the literature, it is likely that the appearance of the PRAS phenotype is also facilitated by the production of beta-lactamase **(Schell et al., 2020)** and that the activity of beta-lactamases could enhance the resistance to penicillin and, potentially, to 5th generation cephalosporins, leading to a phenotype in which the increase in resistance against the two beta-lactams occurs in parallel.

The majority of the PBP4 mutations found in this study were already reported in the literature, frequently related to PRAS strains (**Conceição et al., 2014**; **Gawryszewska et al., 2021**; **Infante et al., 2016**), but the mechanisms underlying this relationship were not elucidated.

This adenine deletion has been already described in the literature. The presence of a deletion in this site, commonly rich in A-T, is thought to have a strong impact on the regulation of downstream gene expression, resulting in PBP4 overexpression, thus affecting penicillin G and ceftobiprole (both 5th generation cephalosporins) antibacterial activity. **(Estrem et al., 1998).** In *E. faecalis*, the involvement of an adenine deletion (*del*A) upstream of the -35 region of the *pbp*4 promoter was recently analyzed in a single strain **(Rice et al., 2018)**.

Supported by these observations, we provided a comprehensive analysis on a larger sample of clinical strains belonging to different antibiotic-resistance profiles. In all BPR-NS, we observed that the *del*A upstream of the coding sequence results in *pbp*4 overexpression, hypothetically altering the binding of regulatory proteins. Elevated expression levels may cause increased transpeptidation, resulting in a highly cross-linked peptidoglycan. This demonstrates its role in establishing *in vitro* non-susceptibility to BPR without affecting its *cidal* activity. The combination of *del*A with additional significant amino acid changes within the PBP4 active sites might result in a destabilization and formation of a less competent β-lactam binding-complex. In one PRAS/BPR-NS strain (Efs1), the T418A mutation located 6 amino acids upstream of the catalytic serine included in the ^{424}STFK^{427} *motif* I affects the MIC value of BPR (BPR 16 mg/L), which only remains bactericidal at the highest BPR concentration tested (4X MIC). On the contrary, the I223V mutation located in the N-terminal end, carried by a PSAS/BPR-S strain (Efs20), does not affect the MIC of β-lactams. This region is known to have no enzymatic function **(Djorić et al., 2020; Rice et al., 2018; Infante et al., 2016)**, and this corroborates the excellent *in vitro* antibacterial and bactericidal activity of BPR against this strain, exerted at 1X, 2X and 4X MICs.

We observed that *pbp*4 was more overexpressed in the VRE/*van*A strains regardless of *del*A in the promoter region (Efs8 and Efs11) **(Figure 27, pattern-filled bars)**; these strains also reported lower BPR MIC values (2-4 mg/L). This phenomenon was difficult to explain. In VRE/*van*A isolates, the DAla-DLac PG precursor is not processed by PBP4, as previously reported in *E. faecium* for PBP5 (**al-Obeid et al., 1992**). We could hypothesize that PBP4 may not work with the modified precursor ending in DLac as it may not be able to

identify the target, and this may result in overexpression and subsequent buildup. Besides, production of precursors ending in DAla or in DLac alternatively responsible for resistance to cephalosporins or glycopeptides, could promote enhanced cephalosporin susceptibility in the presence of vancomycin/beta-lactam association **(Kristich et al., 2014**).

Our study was completed by the determination of the 50% inhibitory concentration (IC_{50}) values for ceftobiprole by using purified membrane preparations and fluorescent penicillin (Bocillin FL). The results of ceftobiprole/PBP affinity and its enzymatic activity highlighted the major role of PBP4 as sufficient and necessary for high-level β-lactam resistance. PBPs were alternatively acylated by ceftobiprole or Bocillin FL at their active-site serine, thereby preventing PBP transpeptidase/glycosyltransferase activity. Three PBPs were essentially not acylated by BPR, enabling subsequent acylation by Bocillin FL: two class A PonA (PBP1a) and PBP2b, and one class B PBP4. This pattern was maintained in almost all *E. faecalis* strains we examined. Together, these results reveal that other bifunctional PBPs with GTase and TPase properties, are required for enterococcal cephalosporin resistance, enabling PBP4 to carry out PG cross-linking in the presence of ceftobiprole increasing concentrations - perceived as “cell-wall stress”- to promote growth. Our results did not provide evidence that other class B PBP (i.e. PBP2b) are similarly involved in BPR resistance, as reported in the literature (**Dijoric et al AAC 2020**).

Analysis of *PBP Binding profiles demonstrated that t*here is no direct correlation among MIC values, PBP4 expression levels and/or aminoacidic substitutions in the catalytic sites, and the percentages of BPR inhibition concentration against the low-affinity PBP4, even at increasing concentrations of ceftobiprole.

PBP4 binding to ceftobiprole is BPR-concentration related and not MIC-concentration related (related to the respective MIC value for each strain).

Neither PBP4 from ATCC47077 nor those of susceptible and resistant strains strongly reacted with BPR.

Surprisingly, PBPs of BPR-NS strains were more prone to be saturated by ceftobiprole, independently from the MICs of these strains; the function of the only low-reactivity overexpressed PBP4, together with the PonA, is sufficient to establish reduced susceptibility to BPR. PBP4 up-regulation leads to increased cell wall cross-linking, as a plausible consequence of its increased TPase activity. A similar association of PBP4 overproduction leading to increased cell wall cross-linking and β-lactam resistance has been described previously **(Rice and Moon, 2018; Duez, 2001)**. In susceptible strains, PBP4 alone is not sufficient to counteract increasing concentration of cephalosporin over the MIC value, enrolling all other PBPs. Almost all BPR-S showed the same profile of labeled PBPs: poorly expressed PBP4 needs to cooperate with all other class A and B PBPs, to sustain the effect of a BPR treatment with increasing concentrations. After BPR treatment, in some strains the reduction in the band intensity of the fluorescence of PBP4 to Bocillin FL varied at higher drug concentration (2X- 4X-fold the MIC concentrations).

From the comparative analysis of our graphs, it could be hypothesized that, immediately after treatment with ceftobiprole, the known low reactivity of PBP4 acts on the *in vitro* antibacterial activity, preventing its binding which, however, occurs only at high concentrations and after prolonged exposure times (**Fig. 24**). After binding, the mutations could spatially and temporally interfere on the PBP4/BPR bond, which is not retained but released: it could be hypothesize alternation of cycles of acylation and diacylation, especially when higher concentrations of active BPR are still present (**Fig. 30**).

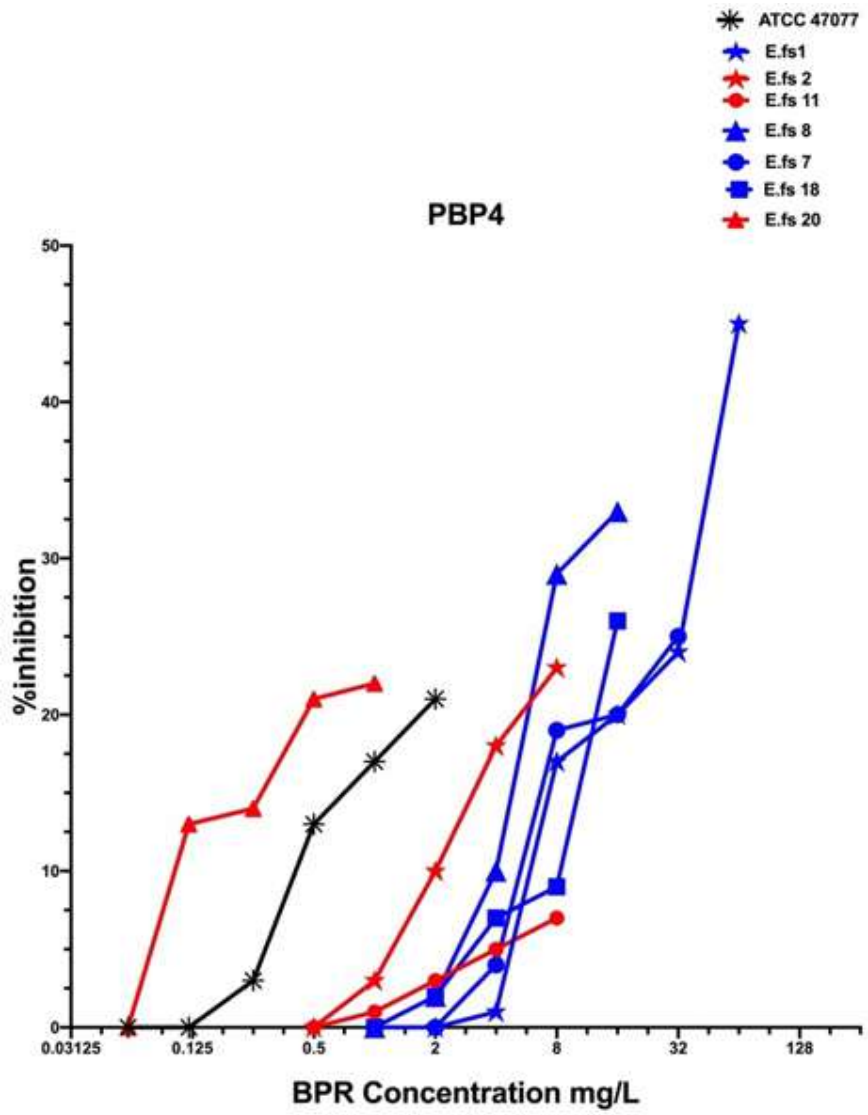

***Figure 30**. Comparison of PBP4 percentages of inhibition concentrations of BPR of all strains. Black line: ATCC 47077 reference sample; Red line: BPR-S strains; Blue line: BPR-NS strains.*

6. CONCLUSION

Here we found that benzyl-penicillin and 5th generation cephalosporins interact with PBP4 in similar ways. In PRAS/BPR-NS *E. faecalis* clinical isolates, the interaction between increased *pbp*4 gene expression, due to the *del*A in the upstream region *consensus* sequence, and the supposed remodeling of the penicillin-binding domain, due to alterations in the PBP4 amino acid sequence, influence their β-lactams and ceftobiprole susceptibility profiles, explicating an *in vitro* antibacterial effect, without affecting BPR *cidal* activity. Enhanced PBP4 expression did not alter the bactericidal activity of ceftobiprole, but was only responsible for increased MIC values in PRAS/BPR-NS strains carrying delA in the regulatory promoter region. Alterations in the cathalitic-site are not involved in the low-reactivity of PBP4, that is a common characteristic for all *E. faecalis* strains. Other PBPs showed low-reactivity upon exposure to cell-wall stress, due to BPR-treatment, demonstrating their critical role in intrisic cephalosporin resistance of *E. faecalis.*

Investigations on the genetic mechanisms involved in cephalosporin resistance, and alterations of the main molecular targets used by enterococci to subvert beta-lactam/PBPs affinity, are imperative for preventing and treating life-threatening infections. Our results shift the paradigm for enterococcal cephalosporin resistance, by demonstrating that the PBP4 is necessary and sufficient for BPR resistance. Ceftobiprole exposure involves the cooperation between low-affinity class B PBP4 and at least one (PonA/PBP1a) or two (PBPF/2a) bifunctional class A PBPs. Class B low-affinity PBP4 acts in concert with either the PonA or PBP2a to synthesize peptidoglycan in presence of concentration of BPR sufficient to inhibit all the other PBPs except for the PBP4. Our data are also corroborated by a recently published paper (**Dijoric et al., 2020**).

Molecular analysis of all PBPs is ongoing, to evaluate their involvement in ceftobiprole non-susceptibility, due to mutations and/or altered gene expression levels. Further experimental approaches should be attempted to confirm the genetic basis of altered ceftobiprole/PBP complexes, to clarify: i) the functional role of *del*A and amino acid substitutions in PBP4, by site-directed mutagenesis; ii) the expression levels of *pbp*4 and iii) the *in vivo* analysis of labelled PBPs, after different exposition times to ceftobiprole treatment.

7. REFERENCES

- **Adediran SA**, Zhang Z, Nukaga M, Palzkill T & Pratt RF (2005) The D-methyl group in beta-lactamase evolution: evidence from the Y221G and GC1 mutants of the class C beta-lactamase of Enterobacter cloacae P99. Biochemistry 44: 7543–7552.
- **Alborn WE**, Jr., Allen NE, Preston DA. (1991). Daptomycin disrupts membrane potential in growing Staphylococcus aureus. Antimicrob Agents Chemother; 35:2282-7.
- **al-Obeid S**, Billot-Klein D, van Heijenoort J, Collatz E, Gutmann L. (1992). Replacement of the essential penicillin-binding protein 5 by high-molecular mass PBPs may explain vancomycin-beta-lactam synergy in low-level vancomycin-resistant Enterococcus faecium D366. FEMS Microbiol Lett. 1992 Feb 1;70(1):79-84.
- **Antonelli A**, D'Andrea MM, Brenciani A, Galeotti CL, Morroni G, Pollini S, Varaldo PE, Rossolini GM.(2018) Characterization of poxtA, a novel phenicol-oxazolidinone-tetracycline resistance gene from an MRSA of clinical origin. J Antimicrob Chemother. 1763-1769.
- **Arbeloa A**, Segal H, Hugonnet J-E, Josseaume N, Dubost L, Brouard J-P, Gutmann L, Mengin-Lecreulx D, Arthur M. (2004). Role of class A penicillin-binding proteins in PBP5-mediated b-lactam resistance inEnterococcus faecalis. J Bacteriol 186:1221–1228.
- **Arias CA**, Singh KV, Panesso D, Murray BE. (2007).Evaluation of ceftobiprole medocaril against Enterococcus faecalis in a mouse peritonitis model. J Antimicrob Chemother;60(3):594-8.
- **Arias CA**, Singh KV, Panesso D, Murray BE. (2007).Time-kill and synergism studies of ceftobiprole against Enterococcus faecalis, including beta-lactamase-producing and vancomycin-resistant isolates. Antimicrob Agents Chemother; 51:2043-7.
- **Arias CA**, Murray BE. The rise of the Enterococcus: beyond vancomycin resistance. (2012).Nat Rev Microbiol.;10(4):266-78.
- **Arthur M**, Depardieu F, Snaith HA, Reynolds PE & Courvalin P (1994) Contribution of VanY D,D-carboxypeptidase to glycopeptide resistance in Enterococcus faecalis by hydrolysis of peptidoglycan precursors. Antimicrob Agents Chemother 38: 1899–1903.
- **Arthur M**, Depardieu F, Molinas C, Reynolds P, Courvalin P. (1995). The vanZ gene of Tn1546 from Enterococcus faecium BM4147 confers resistance to teicoplanin. Gene 154:87–92.
- **Arthur M**, Depardieu F, Gerbaud G, Galimand M, Leclercq R, Courvalin P. (1997). The VanS sensor negatively controls VanR-mediated transcriptional activation of glycopeptide resistance genes of Tn1546 and related elements in the absence of induction. J Bacteriol 179:97–106.
- **Bentorcha F**, De Cespédès G, Horaud T. (1991).Tetracycline resistance heterogeneity in Enterococcus faecium. Antimicrob Agents Chemother.; 35:808–12.
- **Bizzini A**, Zhao C, Auffray Y, Hartke A. (2009).The Enterococcus faecalis superoxide dismutase is essential for its tolerance to vancomycin and penicillin. J Antimicrob Chemother; 64:1196-202.
- **Born P**, Breukink E & Vollmer W (2006). In vitro synthesis of cross-linked murein and its attachment to sacculi by PBP1A from Escherichia coli. J Biol Chem 281: 26985–26993.
- **Bourgogne A**, Garsin DA, Qin X, Singh KV, Sillanpaa J, Yerrapragada S, Ding Y, Dugan-Rocha S, Buhay C, Shen H, Chen G, Williams G, Muzny D, Maadani A, Fox KA, Gioia J, Chen L, Shang Y, Arias CA, Nallapareddy SR, Zhao M, Prakash VP, Chowdhury S, Jiang H, Gibbs RA, Murray BE, Highlander SK, Weinstock GM. (2008)Large scale variation in Enterococcus faecalis illustrated by the genome analysis of strain OG1RF. Genome Biol.R110.
- **Brenciani A**, Morroni G, Schwarz S, Giovanetti E. (2022). Oxazolidinones: mechanisms of resistance and mobile genetic elements involved. J Antimicrob Chemother. 2596-2621.
- **Bushby S.R**., Hitchings G.H. (1968).Trimethoprim, a sulphonamide potentiator. British Journal of Clinical Pharmacology,; 33:72-90.

- **Cabrera, N.L.,**Malek,A.E., Aitken, S.L., andArias,C.A. (2020).Outcomes of Patients With Bloodstream Infections Caused by Ampicillin-Susceptible But Penicillin- Resistant Enterococcus Faecalis: Caution in Interpreting the Results. Antimicrob. Agents Chemother. 64 (4), e02387–e02319.
- **Carlier C**, Courvalin P. (1990). Emergence of 4',4''-aminoglycoside nucleotidyltransferase in enterococci. Antimicrob Agents Chemother; 34:1565-9.
- **Casadewall B**, Reynolds PE & Courvalin P (2001). Regulation of expression of the vanD glycopeptide resistance gene cluster from Enterococcus faecium BM4339. J Bacteriol 183: 3436–3446.
- **Chen H**, Wu W, Ni M, Liu Y, Zhang J, Xia F, He W, Wang Q, Wang Z, Cao B, Wang H.(2013) Linezolid-resistant clinical isolates of enterococci and Staphylococcus cohnii from a multicentre study in China: molecular epidemiology and resistance mechanisms. Int J Antimicrob Agents. Oct;42(4):317-21.
- **Chopra I**, Roberts M. (2001). Tetracycline antibiotics: mode of action, applications, molecular biology, and epidemiology of bacterial resistance. Microbiol Mol Biol Rev.; 65:232–60.
- Clinical & Laboratory Standard Institute: CLSI Guidelines. 2020;30th edition.
- **Chow JW**. (2000). Aminoglycoside resistance in enterococci. Clin Infect Dis; 31:586-9.
- **Coburn B,** Low DE, Patel SN, Poutanen SM, Shahinas D, Eshaghi A, Willey BM, McGeer A. (2014).Vancomycin-variable Enterococcus faecium: in vivo emergence of vancomycin resistance in a vancomycin-susceptible isolate. J Clin Microbiol. 1766-7.
- **Coburn PS**, Gilmore MS. (2003). The Enterococcus faecalis cytolysin: a novel toxin active against eukaryotic and prokaryotic cells. Cell Microbiol 5:661– 669.
- **Comenge Y**, Quintiliani R Jr, Li L, Dubost L, Brouard JP, Hugonnet JE, Arthur M. (2003).The CroRS two-component regulatory system is required for intrinsic beta-lactam resistance in Enterococcus faecalis. J Bacteriol. 185(24):7184-92.
- **Conceição, N**., da Silva, L. E., Darini, A. L., Pitondo-Silva, A., and de Oliveira, A. G. (2014). Penicillin Resistant, Ampicillin-Susceptible Enterococcus Faecalis of Hospital Origin: Pbp4 Gene Polymorphism and Genetic Diversity. Infect. Genet. Evol. 28, 289–295.
- **Courvalin P**, Carlier C, Collatz E. (1980). Plasmid-mediated resistance to aminocyclitol antibiotics in group D streptococci. J Bacteriol; 143:541-51.
- **Cremniter J**, Mainardi JL, Josseaume N, Quincampoix JC, Dubost L, Hugonnet JE, Marie A, Gutmann L, Rice LB, Arthur M. (2006). Novel mechanism of resistance to glycopeptide antibiotics in Enterococcus faecium. J Biol Chem. Oct 27;281(43):32254-62.
- **Crowe-McAuliffe C.**, Murina V., Turnbull K.J., Huch S., Kasari M., Takada H., Nersisyan L., Sundsfjord A., Hegstad K., Atkinson G.C., Pelechano V., Wilson D.N., Hauryliuk V. (2022). Structural basis for PoxtA-mediated resistance to phenicol and oxazolidinone antibiotics.;13(1):1860.
- **Daniel RA**, Harry EJ & Errington J (2000). Role of penicillinbinding protein PBP 2B in assembly and functioning of the division machinery of Bacillus subtilis. Mol Microbiol 35: 299–311.
- **den Blaauwen T**, de Pedro M, Nguyen-Diste`che M & Ayala J (2008) Morphogenesis of rod-shaped sacculi. FEMS Microbiol Rev 32: 321–344.
- **Denome SA**, Elf PK, Henderson TA, Nelson DE & Young KD (1999) Escherichia coli mutants lacking all possible combinations of eight penicillin binding proteins: viability, characteristics, and implications for peptidoglycan synthesis. J Bacteriol 181: 3981–3993.
- **Deshpande, L. M**., and R. N. Jones. (2003). Bactericidal activity and synergy studies of BAL9141, a novel pyrrolidinone-3-ylidenemethyl cephem, tested against streptococci, enterococci and methicillin-resistant staphylococci. Clin. Microbiol. Infect. 9:1120–1124.
- **Djorić D**, Little JL, Kristich CJ. (2020). Multiple Low-Reactivity Class B Penicillin-Binding Proteins Are Required for Cephalosporin Resistance in Enterococci. Antimicrob Agents Chemother. Mar 24;64(4):e02273-19.

- **Dowson CG**, Jephcott AE, Gough KR & Spratt BG (1989) Penicillin-binding protein 2 genes of non-beta-lactamaseproducing, penicillin-resistant strains of Neisseria gonorrhoeae. Mol Microbiol 3: 35–41.
- **Duez C**, Zorzi W, Sapunaric F, Amoroso A, Thamm I, Coyette J.(2001). The penicillin resistance of Enterococcus faecalis JH2-2R results from an overproduction of the low-affinity penicillin-binding protein PBP4 and does not involve a psr-like gene. Microbiology 147:2561–2569.
- **el Kharroubi A**, Piras G, Jacques P, Szabo I, Van Beeumen J, Coyette J & Ghuysen JM (1989) Active-site and membrane topology of the DD-peptidase/penicillin-binding protein no. 6 of Enterococcus hirae (Streptococcus faecium) A.T.C.C. 9790. Biochem J 262: 457–462.
- European Committe on Antimicrobial Susceptibility Testing (EUCAST). 2022.European Centre for Disease Prevention and Control. 2013. Point prevalence survey of healthcare-associated infections and antimicrobial use in European acute care hospitals 2011–2012. European Centre for Disease Prevention and Control, Solna, Sweden. https://www.eucast.org.
- **Estrem, S. T.,** Gaal, T., Ross, W., and Gourse, R. L. (1998). Identification of an UP Element Consensus Sequence for Bacterial Promoters. Proc. Natl. Acad. Sci. U.S.A. 18, 95(17):9761–6.
- **Evers S**, Sahm DF, Courvalin P. (1993). The vanB gene of vancomycinresistant Enterococcus faecalis V583 is structurally related to genes encoding D-ala:D-ala ligases and glycopeptide-resistance proteins VanA and VanC. Gene 124:143–144.
- **Farrell DJ**, Mendes RE, Ross JE, Sader HS, Jones RN. (2011). LEADER Program results for 2009: an activity and spectrum analysis of linezolid using 6,414 clinical isolates from 56 medical centers in the United States. Antimicrob Agents Chemother.55(8):3684-90.
- **Ferretti JJ**, Gilmore KS, Courvalin P. (1986). Nucleotide sequence analysis of the gene specifying the bifunctional 6'-aminoglycoside acetyltransferase 2''-aminoglycoside phosphotransferase enzyme in Streptococcus faecalis and identification and cloning of gene regions specifying the two activities. J Bacteriol; 167: 631-8.
- **Fines M**, Perichon B, Reynolds P, Sahm DF, Courvalin P. (1999). VanE, a new type of acquired glycopeptide resistance in Enterococcus faecalis BM4405. Antimicrob Agents Chemother 43:2161–2164.
- **Fioriti S**, Coccitto SN, Cedraro N, Simoni S, Morroni G, Brenciani A, Mangiaterra G, Vignaroli C, Vezzulli L, Biavasco F, Giovanetti E.(2021) Linezolid Resistance Genes in Enterococci Isolated from Sediment and Zooplankton in Two Italian Coastal Areas. Appl Environ Microbiol.;87(9);
- **Fontana R**, Cerini R, Longoni P, Grossato A, Canepari P. (1983). Identification of a streptococcal penicillin binding protein that reacts very slowly with penicillin. J Bacteriol 155:1343–1350.
- **Fontana R**, Aldegheri M, Ligozzi M, Lopez H, Sucari A, Satta G. (1994). Overproduction of a low-affinity penicillin-binding protein and high-level ampicillin resistance in Enterococcus faecium. Antimicrob Agents Chemother.38(9):1980-3.
- **Fontana R**, Aldegheri M, Ligozzi M, Lopez H, Sucari A, Satta G. (1994). Overproduction of a low-affinity penicillin-binding protein and high-level ampicillin resistance in Enterococcus faecium. Antimicrob Agents Chemother.;38(9):1980-3.
- **Fonz´e E,** Vermeire M, Nguyen-Diste`che M, Brasseur R & Charlier P (1999) The crystal structure of a penicilloyl-serine transferase of intermediate penicillin sensitivity. The DD-transpeptidase of Streptomyces K15. J Biol Chem 274: 21853–21860.
- **Galimand M**, Schmitt E, Panvert M, Desmolaize B, Douthwaite S, Mechulam Y, Courvalin P. (2011)Intrinsic resistance to aminoglycosides in Enterococcus faecium is conferred by the 16S rRNA m5C1404-specific methyltransferase EfmM. RNA. 17(2):251-62.
- **Gallant CV**, Daniels C, Leung JM, Ghosh AS, Young KD, Kotra LP & Burrows LL (2005) Common beta-lactamases inhibit bacterial biofilm formation. Mol Microbiol 58: 1012–1024.

- **García-Solache M**, Rice LB. (2019) The Enterococcus: a Model of Adaptability to Its Environment. Clin Microbiol Rev.;32(2)
- **Gawryszewska,** I., Żabicka, ,. D., Hryniewicz, W., and Sadowy, E. (2021). Penicillin-Resistant, Ampicillin-Susceptible Enterococcus Faecalis in Polish Hospitals. Microb. Drug Resist. 27 (3), 291–300.
- **Georgopapadakou NH**, Smith SA & Sykes RB (1982) Mode of action of azthreonam. Antimicrob Agents Chemother 21: 950–956.
- **Ghuysen JM** (1968) Use of bacteriolytic enzymes in determination of wall structure and their role in cell metabolism. Bacteriol Rev 32: 425–464.
- **Ghuysen JM**. (1991)Serine beta-lactamases and penicillin-binding proteins. Annu Rev Microbiol.;45:37-67.
- **Gittins JR**, Phoenix DA & Pratt JM (1994) Multiple mechanisms of membrane anchoring of Escherichia coli penicillin-binding proteins. FEMS Microbiol Rev 13: 1–12.
- **Goffin C & Ghuysen JM** (1998) Multimodular penicillin-binding proteins: an enigmatic family of orthologs and paralogs. Microbiol Mol Biol Rev 62: 1079–1093.
- **Gonzales R. D.**, Schrekenberger P. C., Graham M. B., Kelkar S., DenBesten K., Quinn J. P.(2001) Infections due to vancomycin-resistant Enterococcus faecium resistant to linezolid. Lancet.;357(9263):1179.
- **Grayson ML**, Eliopoulos GM, Wennersten CB, Ruoff KL, De Girolami PC, Ferraro MJ, Moellering RC Jr.(1991) Increasing resistance to beta-lactam antibiotics among clinical isolates of Enterococcus faecium: a 22-year review atone institution. Antimicrob Agents Chemother; 35:2180-4.
- **Guardabassi, L.,** Larsen, J., Skov, R., and Schonheyder, H. C. (2010). Gentamicin- Resistant Enterococcus Faecalis Sequence Type 6 With Reduced Penicillin Susceptibility: Diagnostic and Therapeutic Implications. J. Clin. Microbiol. 48, 3820–3821.
- **Guinane CM**, Cotter PD, Ross RP & Hill C (2006) Contribution of penicillin-binding protein homologs to antibiotic resistance, cell morphology, and virulence of Listeria monocytogenes EGDe. Antimicrob Agents Chemother 50: 2824–2828.
- **Guzman Prieto AM**, van Schaik W, Rogers MRC, Coque TM, Baquero F,Corander J, Willems RJL. (2016). Global emergence and dissemination of enterococci as nosocomial pathogens: attack of the clones? Front Microbiol 7:788.
- **H¨oltje JV** (1998) Growth of the stress-bearing and shapemaintaining murein sacculus of Escherichia coli. Microbiol Mol Biol Rev 62: 181–203.
- **Handwerger S**, Tomasz A. (1985). Antibiotic tolerance among clinical isolates of bacteria. Rev Infect Dis; 7: 368–86.
- **Harris F**, Brandenburg K, Seydel U & Phoenix D (2002) Investigations into the mechanisms used by the C-terminal anchors of Escherichia coli penicillin-binding proteins 4, 5, 6 and 6b for membrane interaction. Eur J Biochem 269: 5821–5829.
- **Hartmann C**., Peter C., Hermann E., Ure B., Sedlacek L., Hansen G., Bohnhorst B. (2010). Successful treatment of vancomycin-resistant Enterococcus faecium ventriculitis with combined intravenous and intraventricular chloramphenicol in a newborn. Journal of Medical Microbiology.;59(Pt 11):1371–1374.
- **Hebeisen, P**., I. Heinze-Krauss, P. Angehrn, P. Hohl, M. G. Page, and R. L. Then. (2001). In vitro and in vivo properties of Ro 63–9141, a novel broadspectrum cephalosporin with activity against methicillin-resistant staphylococci. Antimicrob. Agents Chemother. 45:825–836.
- **Heep M**, Geier B, Hofer B. (2005) Induction of AmpC beta-lactamases in Enter- ceftobiprole against staphylococci displaying normal and small-colony variant Enterobacter cloacae triggers resistance to extended spectrum cephalosporins, but phenotypes. Antimicrob Agents Chemother; 49 (10):

4372-4 not to cefepime and ceftobiprole. 45th Interscience Conference on Anti- microbial Agents and Chemotherapy; 2005 Dec 16-19; Washington, DC

- **Hegstad K**, Mikalsen T, Coque TM, Werner G, Sundsfjord A. (2010). Mobile genetic elements and their contribution to the emergence of antimicrobial resistant Enterococcus faecalis and Enterococcus faecium. Clin microbiol infect; 16:541-54;
- **Henderson TA**, Young KD, Denome SA & Elf PK (1997) AmpC and AmpH, proteins related to the class C beta-lactamases, bind penicillin and contribute to the normal morphology of Escherichia coli. J Bacteriol 179: 6112–6121.
- **Hennig S**, Ziebuhr W. (2010)Characterization of the transposase encoded by IS256, the prototype of a major family of bacterial insertion sequence elements. J Bacteriol; 192:4153–63. [PubMed: 20543074].
- **Henry X**, Amoroso A, Coyette J, Joris B. (2010). Interaction of ceftobiprole with the low-affinity PBP 5 of Enterococcus faecium. Antimicrob Agents Chemother; 54:953-5.
- **Hodges TL**, Zighelboim-Daum S, Eliopoulos GM, Wennersten C, Moellering RC, Jr. (1992) Antimicrobial susceptibility changes in Enterococcus faecalis following various penicillin exposure regimens. Antimicrob Agents Chemother; 36:121-5.
- **Hollenbeck B.L**., Rice L.B. (2012). Intrinsic and acquired resistance mechanisms in enterococcus, Virulence. Landes Bioscience,; 3:5, 421–433.
- **Hollingshead S**, Vapnek D. (1985). Nucleotide sequence analysis of a gene encoding a streptomycin/spectinomycin adenylyltransferase. Plasmid; 13:17-30.
- **Höltje, J. V.** (1998) Growth of the stress-bearing and shape-maintaining murein sacculus of Escherichia coli. Microbiol. Mol. Biol. Rev. 62, 181–203
- **Hoskins J**, Matsushima P, Mullen DL et al. (1999) Gene disruption studies of penicillin-binding proteins 1a, 1b, and 2a in Streptococcus pneumoniae. J Bacteriol 181: 6552–6555.
- **Infante V.H.P**., Conceic N., Goncalves de Oliveira A., Costa Darini A.L., (2016).Evaluation of polymorphisms in pbp4 gene and genetic diversity in penicillin-resistant, ampicillin-susceptible Enterococcus faecalis from hospitals in different states in Brazil. FEMS Microbiology Letters,; 363.
- **Ingerman M**, Pitsakis PG, Rosenberg A, Hessen MT, Abrutyn E, Murray BE, Levison ME. (1987). -Lactamase production in experimental endocarditis due aminoglycoside-resistant Streptococcus faecalis. J Infect Dis 155:1226 –1232.
- **Ke D**, Picard FJ, Martineau F, Menard C, Roy PH, Ouellette M, Bergeron MG. (1999). Development of a PCR assay for rapid detection of enterococci. J Clin Microbiol 37:3497–3503.
- **Kehrenberg C**, Schwarz S, Jacobsen L, Hansen LH, Vester B. (2005). A new mechanism for chloramphenicol, florfenicol and clindamycin resistance: methylation of 23S ribosomal RNA at A2503. Mol Microbiol 57:1064 –1073.
- **Kohanski MA**, Dwyer DJ, Hayete B, Lawrence CA, Collins JJ.(2007). A common mechanism of cellular death induced by bactericidal antibiotics. Cell; 130: 797-810.
- **Kohler P**, Eshaghi A, Kim HC, Plevneshi A, Green K, Willey BM, McGeer A, Patel SN; Toronto Invasive Bacterial Diseases Network (TIBDN). (2018) Prevalence of vancomycin-variable Enterococcus faecium (VVE) among vanA-positive sterile site isolates and patient factors associated with VVE bacteremia. PLoS One.;13(3);
- **Kresken M,** Brauers J, Korber-Irrgang B, Läuffer J, Decker-Burgard S, Davies T. (2007) In vitro activity of ceftobiprole combined with amikacin or levofloxacin against Pseudomonas aeruginosa by time-kill methodology. 47th Interscience Conference on Antimicrobial Agents and Chemotherapy; 16-19; Chicago (IL)
- **Kristich CJ**, Rice LB, Arias CA. (2014) Enterococcal Infection—Treatment and Antibiotic Resistance. In: Gilmore MS, Clewell DB, Ike Y, Shankar N, editors. Enterococci: From Commensals to Leading Causes of Drug Resistant Infection [Internet]. Boston: Massachusetts Eye and Ear Infirmary; 2014–.

- **Krogstad DJ,** Pargwette AR. (1980). Defective killing of enterococci: a common property of antimicrobial agents acting on the cell wall. Antimicrob Agents Chemother; 17:965-8.
- **Kuch A**, Willems RJ, Werner G, Coque TM, Hammerum AM, Sundsfjord A, Klare I, Ruiz-Garbajosa P, Simonsen GS, van Luit-Asbroek M, Hryniewicz W, Sadowy E. (2012). Insight into antimicrobial susceptibility and population structure of contemporary human Enterococcus faecalis isolates from Europe. J Antimicrob Chemother.;67(3):551-8.
- **Lakey JH**, Ptak M. Fluorescence indicates a calciumdependent interaction between the lipopeptide antibiotic LY146032 and phospholipid membranes. Biochemistry 1988; 27:4639-45.
- **Lazzaro LM**, Cassisi M, Stefani S, Campanile F. (2022) Impact of PBP4 Alterations on β-Lactam Resistance and Ceftobiprole Non-Susceptibility Among Enterococcus faecalis Clinical Isolates. Front Cell Infect Microbiol. 20;11:816657.
- **Lebreton F,** Depardieu F, Bourdon N, Fines-Guyon M, Berger P, Camiade S, Leclercq R, Courvalin P, Cattoir V. (2011). D-Ala-D-Ser VanN-type transferable vancomycin resistance in Enterococcus faecium. Antimicrob Agents Chemother 55:4606 – 4612.
- **Le Breton Y**, Muller C, Auffray Y, Rincé A.(2007). New insights into the Enterococcus faecalis CroRS two-component system obtained using a differential-display random arbitrarily primed PCR approach. Appl Environ Microbiol.; 73:3738-41.
- Leach K, Swaney S, Colca J, McDonald WG, Blinn JR, Thomasco LM, Gadwood RC, Shinabarger D, Xiong L, Mankin AS. (2007). The site of action of oxazolidinone antibiotics in living bacteria and in human mitochondria. Mol Cell.; 26:393-402.
- **Lee ZM**, Bussema C, 3rd, Schmidt TM.(2009). rrnDB: documenting the number of rRNA and tRNA genes in bacteria and archaea. Nucleic Acids Res; 37 (Database issue):D489-93.
- **Leimanis S**, Hoyez N, Hubert S, Laschet M, Sauvage E, Brasseur R & Coyette J (2006) PBP5 complementation of a PBP3 deficiency in Enterococcus hirae. J Bacteriol 188: 6298–6307.
- **Leski TA** &Tomasz A (2005) Role of penicillin-binding protein 2 (PBP2) in the antibiotic susceptibility and cell wall crosslinking of Staphylococcus aureus: evidence for the cooperative functioning of PBP2, PBP4, and PBP2A. J Bacteriol 187: 1815–1824.
- **Ligozzi M,** Pittaluga F, Fontana R. (1996). Modification of penicillin-binding protein 5 associated with high-level ampicillin resistance in Enterococcus faecium. Antimicrob Agents Chemother 40:354 –357.
- **Lim D** & Strynadka NC (2002) Structural basis for the beta lactam resistance of PBP2a from methicillin-resistant Staphylococcus aureus. Nat Struct Biol 9: 870–876.
- **Livak KJ**, Schmittgen TD.(2001) Analysis of relative gene expression data using real-time quantitative PCR and the 2(-Delta Delta C(T)) Method. Methods. 402-8.
- **Llarrull LI**, Prorok M, Mobashery S. (2010) Binding of the gene repressor BlaI to the bla operon in methicillin-resistant Staphylococcus aureus. Biochemistry.;49(37):7975-7.
- **Locke JB**, Hilgers M, Shaw KJ. (2009). Mutations in ribosomal protein L3 are associated with oxazolidinone resistance in staphylococci of clinical origin. Antimicrob Agents Chemother.; 53:5275–8.
- **Lovering AL**, de Castro LH, Lim D & Strynadka NC (2007) Structural insight into the transglycosylation step of bacterial cell-wall biosynthesis. Science 315: 1402–1405.
- **Macheboeuf P**, Contreras-Martel C, Job V, Dideberg O & Dessen A (2006) Penicillin binding proteins: key players in bacterial cell cycle and drug resistance processes. FEMS Microbiol Rev 30: 673–691.
- **Mainardi JL**, Legrand R, Arthur M, Schoot B, van Heijenoort J, Gutmann L. Novel mechanism of beta-lactam resistance due to bypass of DD-transpeptidation in Enterococcus faecium. J Biol Chem. 2000 Jun 2;275(22):16490-6.

- **Marshall SH**, Donskey CJ, Hutton-Thomas R, Salata RA, Rice LB. (2002). Gene dosage and linezolid resistance in Enterococcus faecium and Enterococcus faecalis. Antimicrob Agents Chemother 46:3334 –3336.
- **Martínez-Martínez L.,** Pascual A., Jacoby G. A. (1998) Quinolone resistance from a transferable plasmid. Lancet.;351(9105):797–799.
- **Matsuhashi M**, Tamaki S, Curtis SJ & Strominger JL (1979) Mutational evidence for identity of penicillin-binding protein 5 in Escherichia coli with the major D-alanine carboxypeptidase IA activity. J Bacteriol 137: 644–647.
- **McKessar SJ**, Berry AM, Bell JM, Turnidge JD, Paton JC. (2000). Genetic characterization of vanG, a novel vancomycin resistance locus of Enterococcus faecalis. Antimicrob Agents Chemother; 44:3224-8;
- **Meberg BM**, Paulson AL, Priyadarshini R & Young KD (2004) Endopeptidase penicillin-binding proteins 4 and 7 play auxiliary roles in determining uniform morphology of Escherichia coli. J Bacteriol 186: 8326–8336.
- **Mederski-Samoraj BD**, Murray BE. (1983). High-level resistance to gentamicin in clinical isolates of enterococci. J Infect Dis.;147(4):751-7.
- **Mendes, R. E.,** Castanheira, M., Farrell, D. J., Flamm, R. K., Sader, H. S., and Jones, R. N. (2016). Longitudina-14) Analysis of Enterococci and VRE Causing Invasive Infections in European and US Hospitals, Including a Contemporar-13) Analysis of Oritavancin In Vitro Potency. J. Antimicrob. Chemother. 71 (12), 3453–3458.
- **Metzidie, E.,** Manolis, E. N., Pournaras, S., Sofianou, D., and Tsakris, A. (2006). Spread of an Unusual Penicillin- and Imipenem-Resistant But Ampicillin-Susceptible Phenotype Among Enterococcus Faecalis Clinical Isolates. J. Antimicrob. Chemother. 57 (1), 158–160.
- **Miller W.R**., Munita J.M., Arias C.A. (2014). Mechanisms of antibiotic resistance in enterococci. Expert Review of Anti-Infect Therapy.; 12(10): 1221–1236.
- **Mohr J.F.,** Friedrich L.V., Yankelev S., Lamp K.C., (2009). Daptomycin for the treatment of enterococcal bacteraemia: results from the Cubicin Outcomes Registry and Experience (CORE). International Journal of Antimicrobial Agents,; 33(6):543–548.
- **Moon TM**, D'Andréa ÉD, Lee CW, Soares A, Jakoncic J, Desbonnet C, Garcia-Solache M, Rice LB, Page R, Peti W. (2018). The structures of penicillin-binding protein 4 (PBP4) and PBP5 from Enterococci provide structural insights into β-lactam resistance. J Biol Chem. 30;293(48):18574-18584.
- **Morlot C**, Pernot L, Le Gouellec A, Di Guilmi AM, Vernet T, Dideberg O & Dessen A (2005) Crystal structure of a peptidoglycan synthesis regulatory factor (PBP3) from Streptococcus pneumoniae. J Biol Chem 280: 15984–15991.
- **Morosini M.I**., Díez-Aguilar M. Cantón R. (2019). Mechanisms of action and antimicrobial activity of ceftobiprole. Official journal of the Spanish Society of Chemoterapy;32: 03-10.
- **Muller C,** Le Breton Y, Morin T, Benachour A, Auffray Y, Rincé A. (2006). The response regulator CroR modulates expression of the secreted stress-induced SalB protein in Enterococcus faecalis. J Bacteriol. 188:2636-45.
- **Munita J.M.,** Tran T.T., Diaz L., (2013). A liaF codon deletion abolishes daptomycin bactericidal activity against vancomycin-resistant Enterococcus faecalis. Antimicrobial Agents and Chemotherapy,; 57:2831–3.
- **Murray BE**, Mederski-Samaroj B. (1983). Transferable betalactamase. A new mechanism for in vitro penicillin resistance in Streptococcus faecalis. J Clin Invest; 72:1168-71.
- **Murray, B. E.,** B. Mederski-Samoraj, S. K Foster, J. L. Brunton, and P. Harford. (1986). In vitro studies of plasmidmediated penicillinase from Streptococcus faecalis suggest a staphylococcal origin. J. Clin. Invest. 77:289-293.

- **Murray BE**.(1992) Beta-lactamase-producing enterococci. Antimicrob Agents Chemother; 36:2355-9.
- **Na S.H.**, Moon D.C., Kim M.H., Kang H.Y., Kim S.J., Choi J.H., Mechesso A.F., Yoon S.S., Lim S.K. (2020). Detection of the Phenicol-Oxazolidinone Resistance Gene *poxtA* in *Enterococcus faecium* and *Enterococcus faecalis* from Food-Producing Animals during 2008-2018 in Korea. Microorganisms.8(11):1839.
- **Nath, A.P.,** Balasubramanian, A., & Ramalingam, K. (2020). Cephalosporins : An imperative antibiotic over the generations. International Journal of Research in Pharmaceutical Sciences, 11, 623-629.
- **Nelson DE** & Young KD (2001) Contributions of PBP 5 and DDcarboxypeptidase penicillin binding proteins to maintenance of cell shape in Escherichia coli. J Bacteriol 183: 3055–3064.
- **Nicola G**, Peddi S, Stefanova M, Nicholas RA, Gutheil WG & Davies C (2005) Crystal structure of Escherichia coli penicillinbinding protein 5 bound to a tripeptide boronic acid inhibitor: a role for Ser-110 in deacylation. Biochemistry 44: 8207–8217.
- **Ono S**, Muratani T, Matsumoto T. (2005). Mechanisms of resistance to imipenem and ampicillin in Enterococcus faecalis. Antimicrob Agents Chemother 49:2954 –2958.
- **Page MG.(** 2006) Anti-MRSA beta-lactams in development. Curr Opin Pharmacol 6 (5): 480-5
- Palmer KL, Kos VN, GilmoreMS.Horizontal gene transfer and the genomics of enterococcal antibiotic resistance. Curr Opin Microbiol 2010; 13:632-9.
- **Pares S,** Mouz N, Petillot Y, Hakenbeck R & Dideberg O (1996) X-ray structure of Streptococcus pneumoniae PBP2x, a primary penicillin target enzyme. Nat Struct Biol 3: 284–289.
- **Pepper K,** Horaud T, Le Bouguénec C, de Cespédès G. Location of antibiotic resistance markers in clinical isolates of Enterococcus faecalis with similar antibiotypes. Antimicrob Agents Chemother. 1987 Sep;31(9):1394-402. doi: 10.1128/AAC.31.9.1394. PMID: 3118797; PMCID: PMC174949.
- **Pereira SF**, Henriques AO, Pinho MG, de Lencastre H & Tomasz A (2007) Role of PBP1 in cell division of Staphylococcus aureus. J Bacteriol 189: 3525–3531.
- **Périchon B**, Courvalin P. (2009)VanA-type vancomycinresistant Staphylococcus aureus. Antimicrob Agents Chemother; 53:4580-7.
- **Perichon B**, Reynolds P, Courvalin P. (1997). VanD-type glycopeptideresistant Enterococcus faecium BM4339. Antimicrob Agents Chemother 41:2016 –2018.
- **Pinho MG**, de Lencastre H & Tomasz A (2000) Cloning, characterization, and inactivation of the gene pbpC, encoding penicillin-binding protein 3 of Staphylococcus aureus. J Bacteriol 182: 1074–1079.
- **Pitcher DG**, Saunders NA, Owen RJ. 1989. Rapid extraction of bacterial genomic DNA with guanidium thiocyanate. Lett. Appl. Microbiol.8:155–156.
- **Popham DL** & Setlow P (1993) Cloning, nucleotide sequence, and regulation of the Bacillus subtilis pbpE operon, which codes for penicillin-binding protein 4 and an apparent amino acid racemase. J Bacteriol 175: 2917–2925.
- **Popham DL**, Illades-Aguiar B & Setlow P (1995) The Bacillus subtilis dacB gene, encoding penicillin-binding protein 5 is part of a three-gene operon required for proper spore cortex synthesis and spore core dehydration. J Bacteriol 177: 4721–4729.
- **Priyadarshini R**, Popham DL & Young KD (2006) Daughter cell separation by penicillin-binding proteins and peptidoglycan amidases in Escherichia coli. J Bacteriol 188: 5345–5355.
- **Queenan A**, Bush K. Ceftobiprole: effect on AmpC beta-lactamase induction and 35. Rouse MS, Steckelberg JM, Patel R. In vitro activity of ceftobiprole, daptomycin, resistance frequency in Gram-negative bacteria [abstract no. C1-55]. 45th linezolid, and vancomycin against methicillin-resistant staphylococci asso- Interscience Conference on Antimicrobial Agents and Chemotherapy; 2005.

- **Queenan AM**, Shang W, Kania M, Page MG, Bush K. (2007) Interactions of ceftobiprole with beta-lactamases from molecular classes A to D. Antimicrob Agents Chemother.;51(9):3089-95.
- **Reynolds PE**, Depardieu F, Dutka-Malen S, Arthur M, Courvalin P. (1994). Glycopeptide resistance mediated by enterococcal transposon Tn1546 requires production of VanX for hydrolysis of D-alanyl-Dalanine. Mol Microbiol 13:1065–1070.
- **Reynolds PE**, Ambur OH, Casadewall B & Courvalin P (2001) The VanY(D) DD-carboxypeptidase of Enterococcus faecium BM4339 is a penicillin-binding protein. Microbiology 147: 2571–2578.
- **Rice LB**, Marshall SH. (1992). Evidence of incorporation of the chromosomal b-lactamase gene of Enterococcus faecalis CH19 into a transposon derived from staphylococci. Antimicrob Agents Chemother 36: 1843–1846.
- **Rice LB**, Murray BE. (1995). b-Lactamase-producing enterococci, p 107–114. In Brown F, Ferretti JJ (ed), Genetics of streptococci, enterococci and lactococci, vol 85. Developmental and biological standards. Karger, Basel, Switzerland.
- **Rice LB**. (1998). Tn916 family conjugative transposons and dissemination of antimicrobial resistance determinants. Antimicrob Agents Chemother; 42:1871-7;
- **Rice LB**, Carias LL, Hutton-Thomas R, Sifaoui F, Gutmann L, Rudin SD. (2001). Penicillin-Binding Protein 5 and Expression of Ampicillin Resistance in Enterococcus faecium. Antimicrob Agents Chemother.; 45:1480-6.
- **Rice LB**, Bellais S, Carias LL, Hutton-Thomas R, Bonomo RA, Caspers P, Page MGP, Gutmann L. (2004). Impact of specific pbp5 mutations on expression of b-lactam resistance in Enterococcus faecium. Antimicrob.Agents Chemother 48:3028 –3032.
- **Rice LB**, Carias LL, Rudin S, Lakticová V, Wood A, Hutton-Thomas R.(2005). Enterococcus faecium low-affinity pbp5 is a transferable determinant. Antimicrob Agents Chemother; 49:5007-12; PMID:16304165;
- **Rice LB**, Desbonnet C, Tait-Kamradt A, Garcia-Solache M, Lonks J, Moon TM, D'Andr.a .D, Page R, Peti W. (2018). Structural and regulatory changes in PBP4 trigger decreased -lactam susceptibility in Enterococcus faecalis. mBio 9:e00361-18.
- **Ropp PA**, Hu M, Olesky M & Nicholas RA (2002) Mutations in ponA, the gene encoding penicillin-binding protein 1, and a novel locus, penC, are required for high-level chromosomally mediated penicillin resistance in Neisseria gonorrhoeae. Antimicrob Agents Chemother 46: 769–777.
- **Rybkine T**, Mainardi J-L, Sougakoff W, Collatz E, Gutmann L. (1998). Penicillin-binding protein 5 sequence alterations in clinical isolates of Enterococcus faecium with different levels of -lactam resistance. J Infect Dis 178:159 –163.
- **Sacco E**, Hugonnet JE, Josseaume N, Cremniter J, Dubost L, Marie A, Patin D, Blanot D, Rice LB, Mainardi JL, Arthur M. (2010)Activation of the L,D-transpeptidation peptidoglycan cross-linking pathway by a metallo-D,D-carboxypeptidase in Enterococcus faecium. Mol Microbiol.;75(4):874-85.
- **Sadowy E**., (2018). Linezolid resistance genes and genetic elements enhancing their dissemination in enterococci and streptococci. Plasmid; 89–98.
- **Sarti M**, Campanile F, Sabia C, Santagati M, Gargiulo R, Stefani S. (2012)Polyclonal diffusion of beta-lactamase-producing Enterococcus faecium. J Clin Microbiol. 169-72.
- **Sassi M**, Guerin F, Lesec L, Isnard C, Fines-Guyon M, Cattoir V, Giard JC. (2018). Genetic characterization of a VanG-type vancomycin-resistant Enterococcus faecium clinical isolate. J Antimicrob Chemother 73: 852–855.
- **Sauvage E**, Kerff F, Fonz´e E et al. (2002) The 2.4-A crystal structure of the penicillin-resistant penicillin-binding protein PBP5fm from Enterococcus faecium in complex with benzylpenicillin. Cell Mol Life Sci 59: 1223–1232.

- **Sauvage E**, Herman R, Petrella S, Duez C, Bouillenne F, Fre`re JM & Charlier P (2005) Crystal structure of the Actinomadura R39 DD-peptidase reveals new domains in penicillin-binding proteins. J Biol Chem 280: 31249–31256.
- **Sauvage E**, Duez C, Herman R et al. (2007) Crystal structure of the Bacillus subtilis penicillin-binding protein 4a, and its complex with a peptidoglycan mimetic peptide. J Mol Biol 371: 528–539.
- **Sauvage E**, Kerff F, Terrak M, Ayala JA, Charlier P. (2008). The penicillin-binding proteins: structure and role in peptidoglycan biosynthesis. FEMS Microbiol Rev. Mar;32(2):234-58.
- **Sauvageot N**, Mokhtari A, Joyet P, Budin-Verneuil A, Blancato VS, Repizo GD, Henry C, Pikis A, Thompson J, Magni C, Hartke A, Deutscher J. (2017). Enterococcus faecalis uses a phosphotransferase system permease and a host colonization-related ABC transporter for maltodextrin uptake. J Bacteriol 199:e00878-16.
- **Scheffers DJ** & Errington J (2004) PBP1 is a component of the Bacillus subtilis cell division machinery. J Bacteriol 186: 5153–5156.
- **Scheffers DJ**, Jones LJ & Errington J (2004) Several distinct localization patterns for penicillin-binding proteins in Bacillus subtilis. Mol Microbiol 51: 749–764.
- **Scheffers DJ** (2005) Dynamic localization of penicillin-binding proteins during spore development in Bacillus subtilis. Microbiology 151: 999–1012.
- **Schell CM**, Tedim AP, Rodríguez-Baños M, Sparo MD, Lissarrague S, Basualdo JA, Coque TM. (2020). Detection of β-Lactamase-Producing Enterococcus faecalis and Vancomycin-Resistant Enterococcus faecium Isolates in Human Invasive Infections in the Public Hospital of Tandil, Argentina. Pathogens. 9(2):142.
- **Schleifer KH** & Kandler O (1972) Peptidoglycan types of bacterial cell walls and their taxonomic implications. Bacteriol Rev 36: 407–477.
- **Schnappinger D**, Hillen W. (1996) Tetracyclines: antibiotic action, uptake, and resistance mechanisms. Arch Microbiol.; 165:359–69.
- **Schwarz S**, Cardoso M, Wegener HC. (1992). Nucleotide sequence and phylogeny of the tet(L) tetracycline resistance determinant encoded by plasmid pSTE1 from Staphylococcus hyicus. Antimicrob Agents Chemother.; 36:580–8.
- **Schwartz B,** Markwalder JA, Seitz SP,Wang Y & Stein RL (2002) A kinetic characterization of the glycosyltransferase activity of Escherichia coli PBP1b and development of a continuous fluorescence assay. Biochemistry 41: 12552–12561.
- **Sharkey L.K**., Edwards T.A., O'Neill A.J.,(2016). ABC-F proteins mediate antibiotic resistance through ribosomal protection. MBio,
- **Shaw KJ**, Rather PN, Hare RS, Miller GH. (1993). Molecular genetics of aminoglycoside resistance genes and familial relationships of the aminoglycoside-modifying enzymes. Microbiol Rev 57:138 – 163.
- **Shepard B. D**., Gilmore M. S. (2002). Antibiotic-resistant enterococci: the mechanisms and dynamics of drug introduction and resistance. Microbes and Infection.;4(2):215–224.
- **Shinabarger DL**, Marotti KR, Murray RW, Lin AH, Melchior EP, Swaney SM, Dunyak DS, Demyan WF, Buysse JM.(1997) Mechanism of action of oxazolidinones: effects of linezolid and eperezolid on translation reactions. Antimicrob Agents Chemother.;41(10):2132-6.
- **Sifaoui F**, Arthur M, Rice L, Gutmann L, (2001) Role of penicillin-binding protein 5 in expression of ampicillin resistance and peptidoglycan structure in Enterococcus faecium. Antimicrob Agents Chemother.;45(9):2594-7.
- **Signoretto C**, Boaretti M, Canepari P. (1994). Cloning, sequencing and expression in Escherichia coli of the low-affinity penicillin binding protein of Enterococcus faecalis. FEMS Microbiol Lett.; 123:99–106.

- **Silverman JA**, Perlmutter NG, Shapiro HM.(2003). Correlation of daptomycin bactericidal activity and membrane depolarization in Staphylococcus aureus. Antimicrob Agents Chemother; 47:2538-44.
- **Smith, M. C.,** and B. E. Murray. (1992). Comparison of enterococcal and staphylococcal b-lactamase-encoding fragments. Antimicrob. Agents Chemother. 36:273-276.
- **Spratt BG** & Strominger JL (1976) Identification of the major penicillin-binding proteins of Escherichia coli as D-alanine carboxypeptidase IA. J Bacteriol 127: 660–663.
- **Spratt BG** (1977) Temperature-sensitive cell division mutants of Escherichia coli with thermolabile penicillin-binding proteins. J Bacteriol 131: 293–305.
- **Stefanova ME**, Tomberg J, Olesky M, Holtje JV, Gutheil WG & Nicholas RA (2003) Neisseria gonorrhoeae penicillin-binding protein 3 exhibits exceptionally high carboxypeptidase and beta-lactam binding activities. Biochemistry 42: 14614–14625;
- **Stefanova ME**, Tomberg J, Davies C, Nicholas RA & Gutheil WG (2004) Overexpression and enzymatic characterization of Neisseria gonorrhoeae penicillin-binding protein 4. Eur J Biochem 271: 23–32.
- **Thaker MN**, Kalan L, Waglechner N, Eshaghi A, Patel SN, Poutanen S, Willey B, Coburn B, McGeer A, Low DE, Wright GD. (2015). Vancomycin-variable enterococci can give rise to constitutive resistance during antibiotic therapy. Antimicrob Agents Chemother. 1405-10.
- **Thiercelin ME**. (1899). Sur un diplocoque saprophyte de l'intestin susceptible de devenir pathog.ne. C R Seances Soc Biol 50:269 –271.
- **Thurlow LR**, Thomas VC, Narayanan S, Olson S, Fleming SD, Hancock LE. 2010. Gelatinase contributes to the pathogenesis of endocarditis caused by Enterococcus faecalis. Infect Immun 78:4936–4943.
- **Tipper DJ** & Strominger JL (1965) Mechanism of action of penicillins: a proposal based on their structural similarity to acyl-D-alanyl-D-alanine. Proc Natl Acad Sci USA 54: 1133–1141.
- **Tomayko JF**, Zscheck KK, Singh KV, Murray BE.(1996). Comparison of the beta-lactamase gene cluster in clonally distinct strains of Enterococcus faecalis. Antimicrob Agents Chemother. May;40(5):1170-4.
- **Tran JH**, Jacoby GA, Hooper DC.(2005) Interaction of the plasmid-encoded quinolone resistance protein Qnr with Escherichia coli DNA gyrase. Antimicrob Agents Chemother.;49(1):118-25.
- **Trieu-Cuot P**, Courvalin P. (1983). Nucleotide sequence of the Streptococcus faecalis plasmid gene encoding the 3'5''-aminoglycoside phosphotransferase type III. Gene; 23:331-41.
- **Vega D** & Ayala JA (2006) The DD-carboxypeptidase activity encoded by pbp4B is not essential for the cell growth of Escherichia coli. Arch Microbiol 185: 23–27.
- **Vesić D**, Kristich CJ. (2012).MurAA is required for intrinsic cephalosporin resistance of Enterococcus faecalis. Antimicrob Agents Chemother. 56:2443–51.
- **Vester B**. (2018). The cfr and cfr-like multiple resistance genes. Res Microbiol 169:61– 66.
- **Vollmer W,** Blanot D & de Pedro M (2008a) Peptidoglycan structure and architecture. FEMS Microbiol Rev 32: 149–167.
- **Wang Y**, Lv Y, Cai J, Schwarz S, Cui L, Hu Z, Zhang R, Li J, Zhao Q, He T, Wang D, Wang Z, Shen Y, Li Y, Feßler AT, Wu C, Yu H, Deng X, Xia X, Shen J. (2015). A novel gene, optrA, that confers transferable resistance to oxazolidinones and phenicols and its presence in Enterococcus faecalis and Enterococcus faecium of human and animal origin. J Antimicrob Chemother 70:2182–2190.
- **Wei Y**, Havasy T,McPherson DC & Popham DL (2003) Rod shape determination by the Bacillus subtilis class B penicillin-binding proteins encoded by pbpA and pbpH. J Bacteriol 185: 4717–4726.
- **Werth BJ,** Abbott AN. (2015). The combination of ampicillin plus ceftaroline is synergistic against Enterococcus faecalis. J Antimicrob Chemother. 2414-7.

- **Williamson R**, Le Bougu.nec C, Gutmann L, Horaud T. (1985). One or two low affinity penicillin-binding proteins may be responsible for the range of susceptibility of Enterococcus faecium to benzylpenicillin. JGen Microbiol. 131(8):1933-40.
- **Williamson R,** Gutmann L, Horaud T, Delbos F, Acar JF.(1986). Use of penicillin-binding proteins for the identification of enterococci. J Gen Microbiol. Jul;132(7):1929-37.
- **Wilson DN,** Hauryliuk V, Atkinson GC, O'Neill AJ. (2020).Target protection as a key antibiotic resistance mechanism. Nat Rev Microbiol. 18(11):637-648.
- **Wyke AW**, Ward JB, Hayes MV & Curtis NA (1981) A role in vivo for penicillin-binding protein-4 of Staphylococcus aureus. Eur J Biochem 119: 389–393.
- **Xavier BB**, Coppens J, De Koster S, Rajakani SG, Van Goethem S, Mzougui S, Anantharajah A, Lammens C, Loens K, Glupczynski Y, Goossens H, Matheeussen V. (2021) Novel vancomycin resistance gene cluster in *Enterococcus faecium* ST1486, Belgium,. 26(36):2100767.
- **Xu X,** Lin D, Yan G, Ye X, Wu S, Guo Y, Zhu D, Hu F, Zhang Y, Wang F, Jacoby GA, Wang M. (2010). vanM, a new glycopeptide resistance gene cluster found in Enterococcus faecium. Antimicrob Agents Chemother 54:4643– 4647.
- **Yeats C**, Finn RD & Bateman A (2002) The PASTA domain: a beta-lactam-binding domain. Trends Biochem Sci 27: 438.
- **Zapun A**., Contreras-Martel C., Vernet T., (2008). Penicillin binding proteins and beta-lactam resistance. FEMS Microbiology Reviews,; 32:361-85.
- **Zapun A**, Vernet T & Pinho M (2008a) The different shapes of cocci. FEMS Microbiol Rev 32: 345–360.
- **Zawadzka-Skomial J**, Markiewicz Z, Nguyen-Disteche M, Devreese B, Frere JM & Terrak M (2006) Characterization of the bifunctional glycosyltransferase/acyltransferase penicillinbinding protein 4 of Listeria monocytogenes. J Bacteriol 188: 1875–1881.
- **Zhanel GG**, Lam A, Schweizer F, Thomson K, Walkty A, Rubinstein E, Gin AS, Hoban DJ, Noreddin AM, Karlowsky JA. (2008). Ceftobiprole: a review of a broad-spectrum and anti-MRSA cephalosporin. Am J Clin Dermatol.;9(4):245-54.
- **Zhong Z,** Zhang W, Song Y, Liu W, Xu H, Xi X, Menghe B, Zhang H, Sun Z. (2017). Comparative genomic analysis of the genus Enterococcus. Microbiol Res 196:95–105.
- **Zscheck K**, and B. E. Murray. (1991). Nucleotide sequence of the P-lactamase gene from Enterococcus faecalis HH22 and its similarity to staphylococcal ,B-lactamase genes. Antimicrob. Agents Chemother. 35:1736-1740.
- **Zscheck, K KL**, M. C. Smith, and B. E. Murray. (1992). Elements involved in the regulation of beta-lactamase production in enterococci and staphylococci. Program Abstr. 32nd Intersci. Conf. Antimicrob. Agents Chemother. American Society for Microbiology, Washington, D.C.
- **Zscheck KK**, Murray BE.(1993). Genes involved in the regulation of beta-lactamase production in enterococci and staphylococci. Antimicrob Agents Chemother. Sep;37(9):1966-70.

PUBLISHED WORK

Lazzaro LM, Cassisi M, Stefani S, Campanile F. (2022) Impact of PBP4 Alterations on β-Lactam Resistance and Ceftobiprole Non-Susceptibility Among Enterococcus faecalis Clinical Isolates. Front Cell Infect Microbiol. 20;11:816657.

frontiers in Cellular and Infection Microbiology

ORIGINAL RESEARCH
published: 20 January 2022
doi: 10.3389/fcimb.2021.816657

Impact of PBP4 Alterations on β-Lactam Resistance and Ceftobiprole Non-Susceptibility Among *Enterococcus faecalis* Clinical Isolates

Lorenzo M. Lazzaro[†], *Marta Cassisi*[†], *Stefania Stefani and Floriana Campanile*[*]

Section of Microbiology, Department of Biomedical and Biotechnological Sciences (BIOMETEC), Microbiologia Medica Molecolare e Antibiotico Resistenza (MMARLab), University of Catania, Catania, Italy

OPEN ACCESS

Edited by:
Max Maurin, Université Grenoble Alpes, France

Reviewed by:
Heer Mehta, Rice University, United States
Vincent Cattoir, University of Rennes 1, France

***Correspondence:**
Floriana Campanile
f.campanile@unict.it

[†]*These authors have contributed equally to this work and share first authorship*

Specialty section:
This article was submitted to Clinical Microbiology, a section of the journal Frontiers in Cellular and Infection Microbiology

Received: *17 November 2021*
Accepted: *23 December 2021*
Published: *20 January 2022*

Citation:
Lazzaro LM, Cassisi M, Stefani S and Campanile F (2022) Impact of PBP4 Alterations on β-Lactam Resistance and Ceftobiprole Non-Susceptibility Among Enterococcus faecalis Clinical Isolates. Front. Cell. Infect. Microbiol. 11:816657. doi: 10.3389/fcimb.2021.816657

Penicillin-resistance among *Enterococcus faecalis* clinical isolates has been recently associated with overexpression or aminoacidic substitutions in low-affinity PBP4. Ceftobiprole (BPR), a new-generation cephalosporin, is a therapeutic option against *E. faecalis.* Here, we present evidence that *pbp*4 gene sequence alterations may influence the expression level of the gene and ceftobiprole binding to PBP4 in *E. faecalis* clinical isolates showing remarkable MDR-phenotypes, and how this could interfere with BPR *in vitro* antibacterial and bactericidal activity. Seven *E. faecalis* strains from bloodstream infections were analyzed for their antibiotic and β-lactam resistance. BPR bactericidal activity was assessed by time-kill analysis; *pbp*4 genes were sequenced and *pbp*4 relative expression levels of transcription were performed by RT-qPCR. Five penicillin-resistant ampicillin-susceptible (PRAS) isolates were detected, 4 of which were also BPR non-susceptible (BPR-NS). In the time-kill experiments, BPR exposure resulted in a potent bactericidal activity (3-5 $\log_{10}$ reduction) at the different concentrations tested. *pbp*4 gene sequence analysis revealed some mutations that may account for the changes in PBP4 affinity and MIC increase in the 4 BPR-NS strains (MICs 4-16 mg/L): the deletion of an adenine (*del*A) in the promoter region in all PRAS/BPR-NS strains; 12 different amino acid substitutions, 7 of which were next to the PBP catalytic-sites. The most significant were: T418A, located 6 amino acids (aa) upstream of the catalytic-serine included in the ^{424}STFK^{427} *motif* I; L475Q, 7 aa upstream of the ^{482}SDN^{484} *motif* II; V606A and the novel Y605H, 13/14 aa upstream of the ^{619}KTGT^{622} *motif* III. Taken together, our data showed that elevated BPR MICs were attributable to increased transcription of *pbp*4 - associated with a single upstream adenine deletion and PBP4 alterations in the catalytic-site *motifs* – which might interfere with the formation of the BPR/PBP4 complex. *pbp*4 molecular alterations may account for the changes in PBP4 affinity and MIC increase,

without affecting BPR *cidal* activity. Indeed, our *in vitro* dynamic analysis by time-kill assays showed that BPR exerted a bactericidal activity against *E. faecalis* clinical isolates, despite their MDR phenotypes.

Keywords: *Enterococcus faecalis*, time-kill curve assays, PBP4, ceftobiprole, *pbp*4 gene expression

INTRODUCTION

Enterococci are the third most commonly isolated nosocomial pathogens, accounting for 12% of all hospital infections (Hollenbeck and Rice, 2012). The clinical importance of the genus *Enterococcus* is closely related to antibiotic resistance, which contributes to the risk of infection.

Enterococci have high-level resistance to most cephalosporins and all semi-synthetic penicillins.

Among the species of greatest clinical interest, *E. faecalis* is intrinsically resistant to most β-lactams and only susceptible to a limited group of penicillins, such as ampicillin, penicillin and piperacillin (Arias and Murray, 2012; Kristich et al., 2014a).

Ampicillin resistance has been rarely reported in *E. faecalis*, as this did not represent a clinical and therapeutic challenge. Until recently, it was assumed that ampicillin- susceptible *E. faecalis* was also susceptible to penicillin, but *E. faecalis* clinical isolates have been exhibiting increasing levels of resistance to penicillin, due to the emergence of Penicillin-Resistant Ampicillin-Susceptible (PRAS) isolates, eliminating β-lactams as a treatment option. This uncommon phenotype has been reported in various hospitals worldwide but its real epidemiological impact is still unknown (Metzidie et al., 2006; Guardabassi et al., 2010; Tan et al., 2014; Cabrera et al., 2020; Conceição et al., 2020; Gawryszewska et al., 2021).

Reduced susceptibility to β-lactams in *E. faecalis* is attributable to two main mechanisms: the first is the production of β-lactamases, rarely described among *E. faecalis* strains (Rice and Murray, 1995; Sarti et al., 2012; Schell et al., 2020), while the second is the over-production of a single low-affinity class B penicillin-binding protein (PBP), named PBP4. The PBP4 active site in the Trans-Peptidase (TPase) domain encompasses three conserved *motifs*: the ^{424}STFK^{427} *motif* I, containing the catalytic serine; the ^{482}SDN^{484} *motif* II, involved in the protonation of the β-lactam leaving group; and the ^{619}KTGT^{622} *motif* III, which facilitates substrate binding and defines the oxyanion hole (Ghuysen, 1991; Djorić et al., 2020). Accumulation of point mutations in the penicillin-binding module of PBP4 has been associated with a decreased affinity for β-lactams (Ono et al., 2005; Zapun et al., 2008; Infante et al., 2016; Moon et al., 2018; Rice et al., 2018; Gawryszewska et al., 2021).

The pandemic led to an alarming increase of *E. faecalis* isolated from patients with COVID-19 under mechanical ventilation and ICU-acquired enterococcals BSI (Giacobbe et al., 2021; Posteraro et al., 2021), also worsened by their increasing multi-resistance to all therapeutic options. *E. faecalis* pathogens play a crucial role in determining the severity of the clinical conditions, critically influencing the patients' outcome, and represent a serious threat in infection therapy (Kim et al., 2019).

Among 5th generation cephalosporins, ceftobiprole exerts superior *in vitro* antibacterial and bactericidal activity also against vancomycin-resistant and β-lactamase producing strains, due to its high affinity for PBPs (Mendes et al., 2016; Hamilton et al., 2017; Campanile et al., 2019).

The aims of this study were: 1) to investigate the *in vitro* antibacterial and bactericidal activity of BPR alone against *E. faecalis* clinical isolates belonging to selected antibiotic-resistance classes; 2) to analyze the occurrence of *pbp*4 mutations and verify their role in influencing the activity of β-lactams and, specifically, of BPR; 3) to compare the *pbp*4 expression levels in all *E. faecalis* clinical isolates with reduced susceptibility to beta-lactams and PBP4 alterations, with the aim of evaluating which of these alterations may be involved in non-susceptibility and BPR *cidal* activity, and how.

MATERIALS AND METHODS

Strains

Seven *E. faecalis* clinical strains, isolated from bloodstream infections (BSI) in Italian hospitals, were selected for their antibiotic-resistance behaviors from a larger collection of twenty-two isolates already characterized (Campanile, et al. 31st ECCMID 2021, P 2004). They belonged to the major MDR phenotypes (PRAS, BPR-NS, VRE, HLAR); two beta-lactam-susceptible *E. faecalis* isolates were also selected for comparison.

E. faecalis OG1RF, deposited in the American Type Culture Collection (ATCC) under ATCC 47077, deriving from *E. faecalis* OG1 by selection for resistance to rifampin and fusidic acid (Bourgogne et al., 2008), was used as control in molecular studies. *E. faecalis* ATCC 29212 was used as control for antibiotic-susceptibility tests (EUCAST, 2021).

Antimicrobial Susceptibility Testing

Ceftobiprole was provided by Basilea Pharmaceutica International Ltd. (Basel, Switzerland); ceftaroline, linezolid and tigecycline by Pfizer Inc. (New York, NY, USA); daptomycin by Novartis (Basel, Switzerland). Penicillin, ampicillin, amoxicillin, imipenem, vancomycin, teicoplanin, gentamicin and streptomycin were purchased commercially (Sigma Chemical Co., ST. Louis, MO, USA). MICs were determined by broth microdilution and interpreted according to the European Committee on Antimicrobial Susceptibility Testing (EUCAST) clinical breakpoints (http://www.eucast.org/clinical_breakpoints/) (EUCAST, 2021). In the absence of EUCAST clinical breakpoints, those of the Clinical and Laboratory Standards Institute were applied (Clinical and Laboratory Standards Institute, 2021).

Bactericidal Assays

In vitro time-kill experiments were performed in duplicate in 20 mL tubes containing Cation Adjusted Mueller-Hinton broth (CA-MHB)

(Difco, Detroit, MI) using a starting *inoculum* of 10^5-10^6 CFU/mL with ceftobiprole (1X, 2X and 4X MIC). Bactericidal activity was defined as a ≥3 $\log_{10}$ decrease in bacterial count at 24h (White et al., 1996). Statistical analysis was performed using GraphPad Prism (Version 8.4.0). All experiments were performed in triplicate. Data were represented as mean ±SD of triplicate experiments.

Gene Amplification and Sequence Analysis

All isolates were molecularly characterized for the *pbp*4 gene sequence in order to analyze possible mutations and verify their role in influencing BPR activity. *pbp*4 was amplified by PCR and the entire gene was double-strand sequenced using oligonucleotides specifically designed for this study (**Supplemental Table 1**). Sequencing was performed using the Dye Terminator DNA sequencing kit V1.1 (Applied Biosystems TM), followed by purification using the DyeEx 2.0 Spin Kit (Quiagen, Hilden, Germany). The sequences obtained were corrected and analyzed using the Chromas Lite 2.1 program and then exported in FASTA format. Sequence alignment and gene and translated protein analysis were performed by using BLAST tool (Basic Local Alignment Search Tool) (https://blast.ncbi.nlm.nih.gov/Blast.cgi), CLC Sequence Viewer 8.0 and UniProt (www.uniprot.org). *E. faecalis* ATCC 47077, whose complete genome sequence is deposited at NCBI under the accession number CP025020.1., was used as reference.

Real-Time Quantitative PCR

For real-time quantitative PCR (RT-qPCR) studies, 7 mL of bacterial suspensions (10^5 CFU/mL) were incubated at 37°C until late-log-phase (0.1 OD_{600} ≅ $1x10^8$ CFU/mL); total RNA was extracted using the RNeasy® Mini kit (Qiagen, Hilden, Germany), purified from contaminating DNA genomics and retro-transcripted in cDNA using the QuantiNova™ Reverse Transcription Kit (Qiagen, Hilden, Germany), according to the manufacturer's instructions. cDNA was quantified using the Qubit™ 4 fluorometer.

RT-qPCR was performed in a Rotor-Gene Q (Qiagen, Hilden, Germany) instrument, using the QuantiNova™ SYBR® Green PCR kit (Qiagen, Hilden, Germany), according to the manufacturer's instructions. *pbp*4 (5RT) and 16S rRNA qPCR oligonucleotides were specifically designed for this study (**Supplemental Table 1**). For each sample, three biological replicates were prepared. Relative gene expression levels of transcription were calculated by the quantification cycle (Cq) method and normalized to the expression of 16S rRNA. Relative expression was calculated using the $2^{-\Delta\Delta Ct}$ method (Livak and Schmittgen, 2001). The data obtained were expressed as the fold-change in expression compared to that of the ATCC 47077 reference. Comparison of the expression levels of transcription of all strains and statistical analysis were conducted using the Relative Expression Software Tool "REST 2009" (Qiagen, Hilden, Germany) and GraphPad Prism (Version 8.4.0).

RESULTS

In Vitro Antibacterial Activity

Table 1 shows the susceptibility values of the 7 *E. faecalis* strains in study to β-lactams and comparator drugs. Five strains were found to be penicillin-resistant ampicillin-susceptible (PRAS), besides showing reduced susceptibility to ceftaroline (MICs ≥4 mg/L). Four out of 5 strains showed higher ceftobiprole MIC values (≥4 mg/L) and were reported as ceftobiprole non-susceptible (BPR-NS). All isolates were also susceptible to the other β-lactams tested (amoxicillin and imipenem), and susceptible to daptomycin, linezolid and tigecycline. High-level resistance to gentamicin (HLGR) (n=1), streptomycin (HLSR) (n=1) and both aminoglycosides (HLAR) (n=4) was detected. Vancomycin and teicoplanin resistance (VRE) was detected in 2 isolates and further found to be associated with the presence of the *van*A gene.

Bactericidal Activity of Ceftobiprole

In BPR-NS, BPR exposure resulted in a potent bactericidal activity (3 to 5 $\log_{10}$) at 4X MIC after 24h. BPR-S strains showed a greater log reduction (3 to 5 $\log_{10}$) even at lower concentrations (i.e., 1X and/or 2X MIC). Enhanced killing activity was also observed at 8 h (**Figure 1**).

pbp4 Sequence Analysis and Significant Protein Alterations

PCR and sequence analysis of the *pbp*4 gene revealed some mutations that may account for the changes in PBP4 affinity and MIC increase in the 4 BPR-NS strains (MICs 4-16 mg/L). The adenine deletion (*del*A) in the promoter region, 8bp upstream of the -35 *consensus* site, was the carried by all 4 strains showing non-susceptibility to BPR and high-level resistance to penicillin (**Tables 1**, **2**). Sequence analysis of translated PBP4 identified 12 different missense mutations, 7 of which were next to the PBP catalytic sites (**Table 2**; **Figure 2**). Notably, the T418A mutation (Efs1) was located 6 amino acids (aa) upstream of the catalytic serine included in the ^{424}STFK^{427} *motif* I; L475Q (Efs8), 7 aa upstream of the ^{482}SDN^{484} *motif* II, involved in β-lactam leaving group protonation; the novel Y605H (Efs18) and V606A (Efs7), 13/14 aa upstream of the ^{619}KTGT^{622} *motif* III, which facilitates substrate binding. Other mutations were found far from the PBP catalytic site: i) T50I, quite common in our sample (3/7), and I223V, only present in a fully susceptible strain (Efs20) in which it does not affect MICs to β-lactams, both located in the N-terminal end; ii) L639F, T665I and T678A (all in Efs7), and D666P (Efs1), located in the C-terminal end.

Two further mutations in the region between the ^{482}SDN^{484} and ^{619}KTGT^{622} catalytic sites were detected (A536T; D573E) in Efs1 and Efs11, respectively; in Efs11, the D573E substitution potentially affects the MIC values of penicillin and ceftaroline (16 and 32 mg/L, respectively), but not those of ceftobiprole (2 mg/L).

Nucleotide Sequence Accession Numbers. The complete sequences of the pbp4 gene variants have been deposited in GenBank under accession numbers from OM032878 to OM032884.

Increase in the Level of *pbp*4 Expression

The evaluation of *pbp*4 gene expression relative to that of the ATCC47077 (OG1RF) reference strain showed varying levels of upregulation in all strains, linked to their β-lactam MIC values. The PRAS/BPR-S Efs2 and Efs20 strains exhibited lower expression levels (≤10^2 fold-change increase). All PRAS-BPR-NS

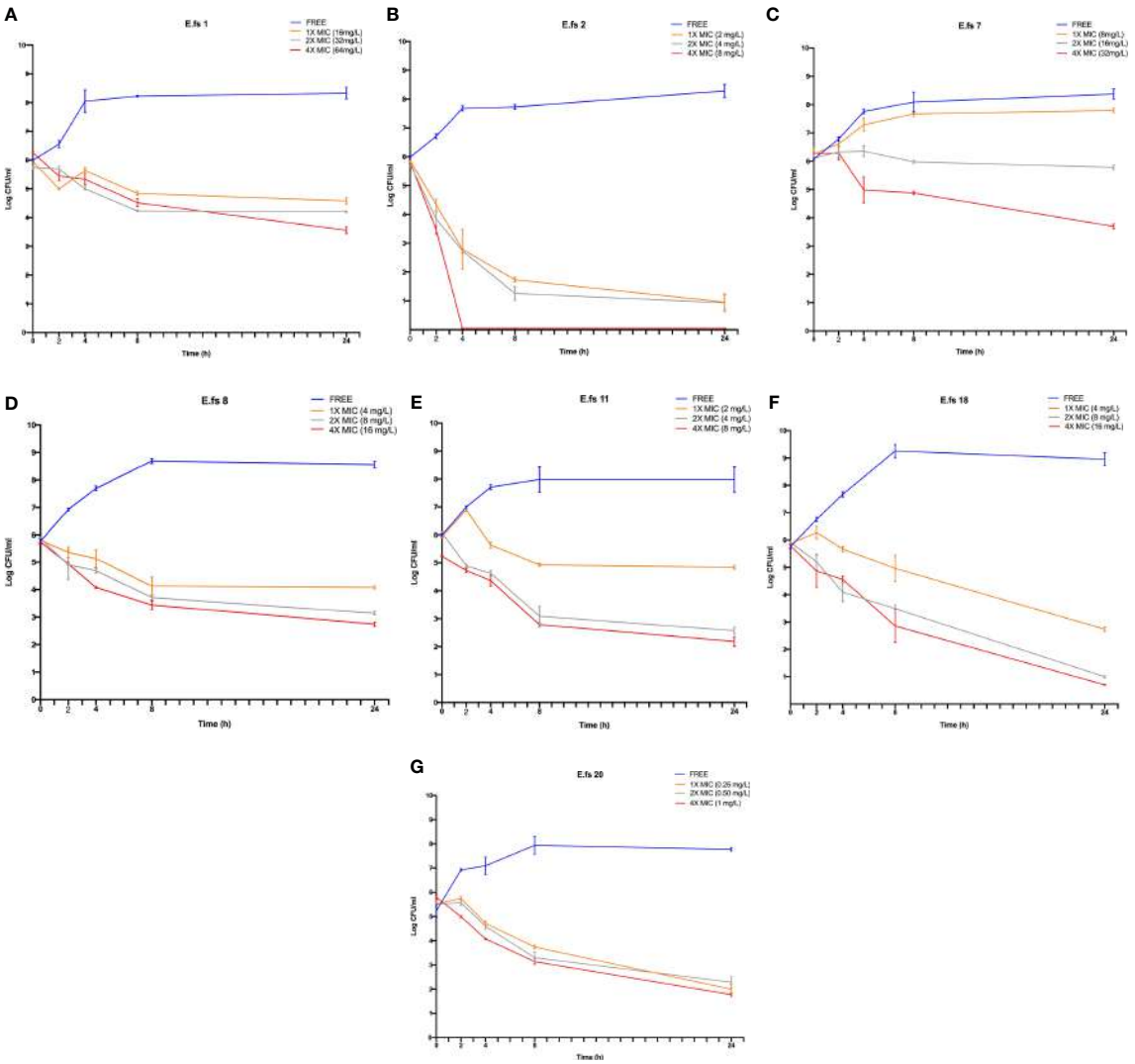

FIGURE 1 | Time-kill assays of ceftobiprole (BPR) against the seven *E. faecalis* clinical isolates in study. Cell count was reported as $\log_{10}$ (CFU/ml) at 0, 2, 4, 8 and 24h Time-points (T0, T2, T4, T24); Ceftobiprole (BPR) exposure was tested at 1X, 2X and 4X MICs. Error bars represent standard deviations (±SD) of the mean of triplicate experiments **(A–G)**.

TABLE 1 | Beta-lactams and comparator antimicrobial MIC values against *E. faecalis* clinical isolates.

Code	MIC values (mg/L)												
	P[1]	AMP	AML	IMI	BPR[2]	CPT[2]	VA	TEC	CN	S	LNZ	TGC	DAP[1]
Efs1	16	1	0.5	4	16	>256	0.5	2	>1024	>1024	4	0.25	0.5
Efs2	4	0.5	0.5	4	2	1	4	2	32	256	4	0.125	0.5
Efs7	64	4	4	4	8	>256	1	2	>1024	>1024	4	0.06	0.5
Efs8	16	4	1	2	4	32	>256	>256	>1024	128	4	0.125	0.5
Efs11	16	4	1	4	2	32	>256	128	>1024	>1024	2	0.25	0.5
Efs18	16	2	1	2	4	4	1	2	>2048	>1024	2	0.125	0.5
Efs20	4	2	0.5	1	0.25	0.5	1	0.5	32	>1024	2	0.06	1

[1]Penicillin and Daptomycin susceptibility values were established according to CLSI breakpoints (EUCAST breakpoints absent). [2]Ceftobiprole and Ceftaroline: No EUCAST and CLSI official breakpoints; eCOFFs not determined.

P, Penicillin; AMP, Ampicillin; AML, Amoxicillin; IMI, Imipenem; BPR, Ceftobiprole; CPT, Ceftaroline; VA, Vancomycin; TEC, Teicoplanin; CN, Gentamicin; S, Streptomycin; LNZ, Linezolid; TGC, Tigecyclin; DAP, Daptomycin.

TABLE 2 | Ceftobiprole MIC values (mg/L) and expression levels for *E. faecalis* clinical isolates, compared to sequence alterations.

Code	Phenotype characteristics	BPR MIC (mg/L)[a]	[§]Fold-change mean	Deletion in promoter region[b]	Amino acid substitutions in PBP4[d]											
					PBP active-sites											
					$_{50}$T	$_{223}$I	$_{418}$T	$_{475}$L	$_{536}$A	$_{573}$D	$_{605}$Y	$_{606}$V	$_{639}$L	$_{665}$T	$_{666}$D	$_{678}$T
Efs20	**PSAS; BPR-S; HLSR**	0.25	88. 80	–	-	**V**	-	-	-	-	-	-	-	-	-	-
Efs2	**PSAS; BPR-S; fully susceptible**	2	77.36	–	-	-	-	-	-	-	-	-	-	-	-	-
Efs11	**PRAS; BPR-S; VRE/*van*A; HLAR**	2	695.413	–	-	-	-	-	-	**E**	-	-	-	-	-	-
Efs8	**PRAS; BPR-NS; VRE/*van*A; HLGR**	4	4851.96	2013028_2013029 *del*A[c]	**I**	-	-	**Q**	-	-	-	-	-	-	-	-
Efs18	**PRAS; BPR-NS; HLAR**	4	422.88	2013028_2013029 *del*A[c]	-	-	-	-	-	-	**H**	-	-	-	-	-
Efs7	**PRAS; BPR-NS; HLAR**	8	571.068	2013028_2013029 *del*A[c]	**I**	-	-	-	-	-	-	**A**	**F**	**I**	-	**A**
Efs1	**PRAS; BPR-NS; HLAR**	16	698.895	2013028_2013029 *del*A[c]	**I**	-	**A**	-	**T**	-	-	-	-	-	**P**	-

[a]*BPR, Ceftobiprole;* [b]*a single base pair deletion 8 bases upstream of the putative -35 region;* [c]*Accession number GenBank: CP025020.1 (ATCC47077);* [d]*Protein ID GenBank: AEA94594.1 (ATCC47077);* [§]*Fold-change expression levels relative to that of ATCC47077. Average of three independent experiments. HLSR, High Level Streptomycin Resistance; VRE, Vancomycin Resistant E. faecalis; HLAR, High Level Aminoglycosides Resistance; PRAS, Penicillin-Resistant Ampicillin-Susceptible; BPR-NS, Ceftobiprole Non-Susceptible; PSAS, Penicillin-Susceptible Ampicillin-Susceptible; BPR-S, Ceftobiprole Susceptible; HLGR, High Level Gentamicin Resistance. GenBank accession no. from OM032878 to OM032884.*

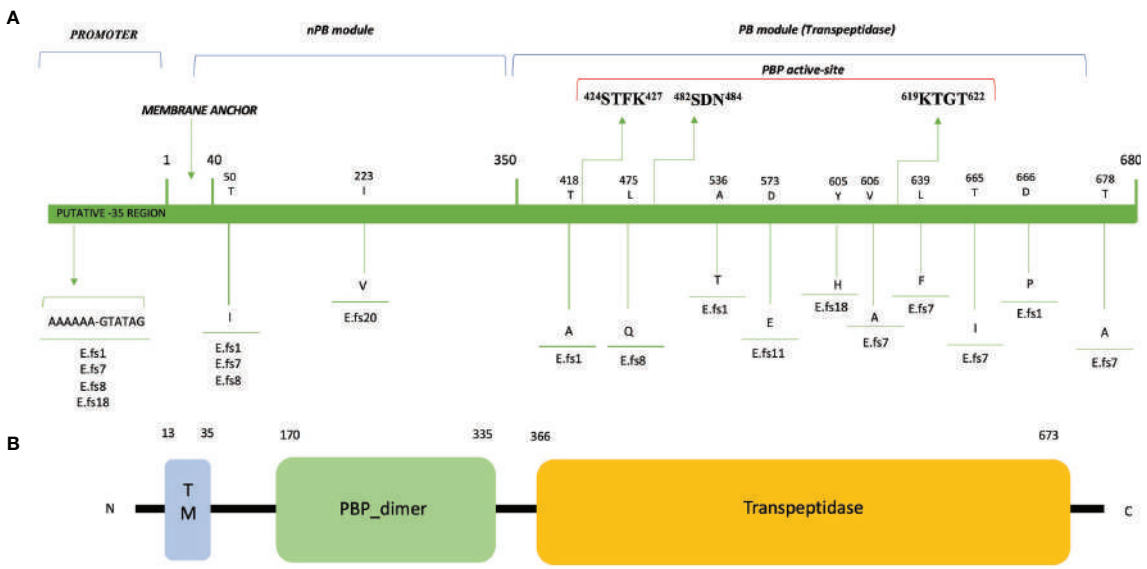

FIGURE 2 | Amino acid substitutions and domain architecture of PBP4 of *E faecalis* clinical isolates. GenBank accession no. from OM032878 to OM032884. The numbers above the diagrams indicate residue numbers of the domain boundaries in the proteins. **(A)** Non-Penicillin Binding module (nPB); Penicillin Binding module (PB); TM, transmembrane helix region. ^{424}STFK^{427}, ^{482}SDN^{484} and ^{619}KTGT^{622}: catalytic-site motifs (STFK$_{424}$ includes the catalytic serine S$_{424}$). **(B)** The domain architecture of PBP4 of *E faecalis* ATCC 47077 (OG1RF) was analyzed using SMART (Simple Modular Architecture Research Tool; http://smart.embl-heidelberg.de/) and reported in a simplified version.

strains carrying the *del*A in the *pbp*4 promotor region and mutations in the PBP catalytic sites displayed *pbp*4 overexpression with greater fold-change increases (0.5-4 x10^3).

We observed that *pbp*4 gene expression was more evident in the VRE/*van*A strains (PRAS/BPR-NS Efs8 and PRSA/BPR-S Efs11), with or without *del*A in the promoter region (**Figure 3**, pattern-filled bars).

Correlation Between Sequence Alterations and Expression Level Increase

Missense mutations in the *pbp*4 sequence were common in BPR-NS and fully susceptible strains.

We observed a strong association between the increase in the level of *pbp*4 expression and the adenine deletion in the promoter region, upstream of the coding sequence. *del*A leads to a 3 $\log_{10}$

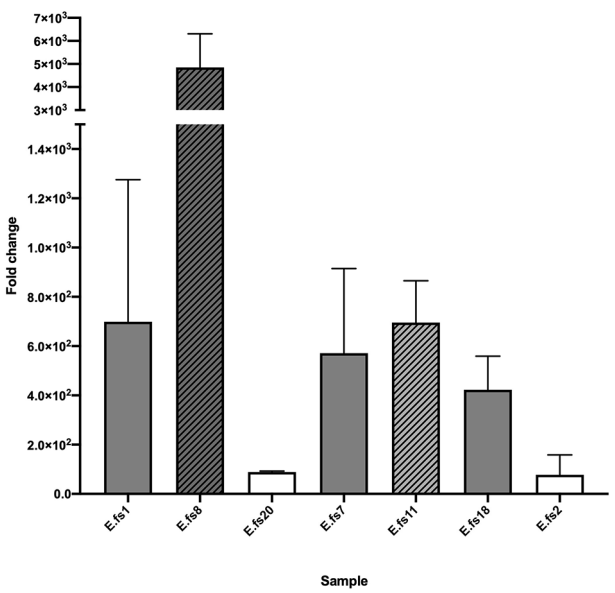

FIGURE 3 | *pbp*4 gene expression analysis of the *E. faecalis* isolates in study, compared to that of the ATCC 47077 (OG1RF) reference. Evaluation of *pbp*4 relative mRNA expression expressed as fold-change (linear). 16S rRNA gene expression levels were used as calibrator. ATCC 47077 (OG1RF) was used as reference. Error bars indicate the average of three biological replicates in three RT-qPCR assays ± SD; PSAS, white; PRAS, gray. VRE/*van*A, pattern-filled bars.

increase compared to that of the ATCC47077 (OG1RF) reference in all BPR-NS strains, demonstrating its role in establishing *in vitro* non-susceptibility to BPR, although it does not influence bactericidal activity (**Figure 3**).

The only exception was Efs11 (PRAS; CPT-NS; BPR-S), carrying only the D573E substitution. We were not able to demonstrate whether this mutation within the SDN/KTG catalytic sites alone may potentially interfere with the expression of *pbp*4 transcription, or if the higher upregulation may be related to the VRE/*van*A phenotype, as stated above. Further experiments are needed to confirm its role.

DISCUSSION

High resistance to penicillins in *E. faecalis* strains is rare, it can emerge after prolonged β-lactam therapy treatments (Rice et al., 2018). Nevertheless, the PRAS phenotype was described in several countries (Metzidie et al., 2006; Guardabassi et al., 2010; Conceição et al., 2014), but its epidemiological and clinical impact remains ambiguous, as ampicillin is the treatment of choice for enterococcal infections (Kristich et al., 2014a) and penicillin MIC values were never reported (Mendes et al., 2016). Recently, Kim et al. reported significative differences in mortality rates in patients with a PRAS *E. faecalis* BSI, likely due to the treatment failures of ampicillin and/or piperacillin (Kim et al., 2019).

PBP4, like other PBPs of the same class B (i.e., PBP2a of methicillin-resistant *S. aureus*) performs the cross-linking reaction of the peptidoglycan (PG) biosynthesis, but retains low responsiveness to beta-lactams. Due to its low-reactivity, PBP4 is considered the key basis for intrinsic resistance to cephalosporins in *E. faecalis* (Arbeloa et al., 2004).

Ceftobiprole, a novel cephalosporin that inhibits the PG cross-linking reaction by acylating the active-site serine of PBPs, maintains a higher affinity for PBP4. Due to its unique ability to target low-affinity PBP4, ceftobiprole is the best candidate as a valid therapeutic option for remarkable *E. faecalis* MDR-phenotypes such as PRAS and VRE. Alterations in this enzyme cause conformational changes that impact the structure of the catalytic *motifs* (Moon et al., 2018).

This study addressed the mechanism of non-susceptibility to ceftobiprole and the resulting interactions with *E. faecalis* clinical strains, all isolated from bloodstream infections.

A link between benzyl-penicillin resistance and 5th generation cephalosporins non-susceptibility was observed. Our data suggest that this common insensitivity in PRAS isolates results from the involvement of *pbp*4 mutations in increased gene expression levels and alteration of the penicillin binding domain that could remodel the PBP/β-lactam complex.

Our *in vitro* dynamic data by time-kill curve assays showed that BPR exerts a bactericidal activity against *E. faecalis* isolates despite their MDR phenotypes (VRE, PRAS and BPR-NS), and PBP4 alterations, even after 8h, consistently with other studies (Werth and Abbott, 2015; Arias et al., 2007). After 24 hours, the bactericidal activity against all isolates - with or without significative PBP4 changes - was similar, suggesting that ceftobiprole maintains high affinity also for other PBPs.

The majority of the PBP4 mutations found in this study were already reported in the literature, frequently related to PRAS strains (Conceição et al., 2014; Infante et al., 2016; Gawryszewska et al., 2021), but the mechanisms underlying this relationship were not elucidated.

It is well known that the upstream region *consensus* sequence, in the bacterial promoters, can have an impact on the expression of downstream coding genes (Estrem et al., 1998). In *E. faecalis*, the involvement of an adenine deletion (*del*A) upstream of the -35 region of the *pbp*4 promoter was recently analyzed in a single strain (Rice et al., 2018). Supported by these observations, we provided a comprehensive analysis on a larger sample of clinical strains belonging to different antibiotic-resistance profiles.

In all BPR-NS, we observed that the *del*A upstream of the coding sequence results in *pbp*4 overexpression, hypothetically altering the binding of regulatory proteins. Elevated expression levels may cause increased transpeptidation, resulting in a highly cross-linked peptidoglycan. This demonstrates its role in establishing *in vitro* non-susceptibility to BPR without affecting its *cidal* activity.

The combination of *del*A with additional significant amino acid changes within the PBP4 active sites might result in destabilization and formation of a less competent β-lactam binding-complex. In one PRAS/BPR-NS strain (Efs1), the

T418A mutation located 6 amino acids upstream of the catalytic serine included in the ^{424}STFK^{427} *motif* I affects the MIC value of BPR (BPR 16 mg/L), which only remains bactericidal at the highest BPR concentration tested (4X MIC). On the contrary, the I223V mutation located in the N-terminal end, carried by a PSAS/BPR-S strain (Efs20), does not affect the MIC of β-lactams. This region is known to have no enzymatic function (Infante et al., 2016; Rice et al., 2018; Djorić et al., 2020), and this corroborates the excellent *in vitro* antibacterial and bactericidal activity of BPR against this strain, exerted at 1X, 2X and 4X MICs.

We observed that *pbp*4 was more overexpressed in the VRE/*van*A strains regardless of *del*A in the promoter region (Efs8 and Efs11) (**Figure 3**, pattern-filled bars); these strains also reported lower BPR MIC values (2-4 mg/L). This phenomenon was difficult to explain. In VRE/*van*A isolates, the DAla-DLac PG precursor is not processed by PBP4, as previously reported in *E. faecium* for PBP5 (al-Obeid et al., 1992). We could hypothesize that PBP4 may not work with the modified precursor ending in DLac as it may not be able to identify the target, and this may result in overexpression and subsequent buildup. Besides, production of precursors ending in DAla or in DLac alternatively responsible for resistance to cephalosporins or glycopeptides may promote enhanced cephalosporin susceptibility in the presence of vancomycin/beta-lactam association (Kristich et al., 2014b).

Even though the aim of this study was not to trace *E. faecalis* epidemiology, we detected three strains carrying PBP4 variants already reported in hospital-associated PRAS strains, epidemiologically related to the High-Risk Enterococcal Clonal Complex (HiRECC) CC87 (Kuch et al., 2012; Gawryszewska et al., 2021). In particular, Efs7 exhibited 4 combined mutations in PBP4 (designating the F3 variant), hypothetically responsible for its indifference to 1X MIC ceftobiprole concentration, in time-kill assays; Efs1, 3 combined mutations (E1 variant); and Efs8, a single mutation (C4 variant). This observation has a clinical and epidemiological impact: the evolution of nosocomial CCs is driven by the acquisition of resistance genes, and the spread of PBP4 variants, responsible for resistance to all beta-lactams, may potentially compromise the clinical efficacy of *E. faecalis* therapy in hospital settings.

In conclusion, in this study we revealed that benzyl-penicillin and 5th generation cephalosporins interact with PBP4 in similar ways. In PRAS/BPR-NS *E. faecalis* clinical isolates, the interaction between increased *pbp*4 gene expression, due to the *del*A in the upstream region *consensus* sequence, and the supposed remodeling of the penicillin-binding domain, due to alterations in the PBP4 amino acid sequence, influence their β-lactams susceptibility profiles without affecting BPR *cidal* activity.

In the light of the above, we recommend penicillin MICs determination not just for clinical, but also and foremost for epidemiological purposes, to evaluate the spread of isolates belonging this difficult-to-treat epidemic PRAS phenotype as well as to address the proper antimicrobial treatment options for these infections.

The major limitation of this study is the lack of a functional evaluation of *del*A and amino acid substitutions in PBP4. Further experimental approaches such as whole genome sequence analysis and site-directed mutagenesis, should be attempted to confirm the genetic basis of altered beta-lactams/PBP4 complexes induced by sequence substitutions.

DATA AVAILABILITY STATEMENT

The data presented in the study are deposited in the GenBank repository (https://www.ncbi.nlm.nih.gov/genbank), under accession numbers from OM032878 to OM032884.

AUTHOR CONTRIBUTIONS

FC designed the research and directed the project. LL, MC, and FC conducted the research. LL, MC and FC analyzed the data. LL, MC, SS, and FC wrote the manuscript. FC and SS, edited and reviewed the manuscript. All authors read and approved the manuscript.

FUNDING

This study was partially supported by ADVANZ PHARMA and Programma PIACERI [CovDock]-Linea di intervento 2', University of Catania, Dept. of Biomedical and Biotechnological Sciences (BIOMETEC).

ACKNOWLEDGMENTS

We would like to thank PharmaTranslated (http://www.pharmatranslated.com/), in particular Dr Silvia Montanari for the language revision. We are grateful to Prof. Daniela Ferrarello and Dr Gino Mongelli for their valuable scientific advice, and the BRIT (Bio-nanotech Research and Innovation Tower) service center of the University of Catania, for the technical support.

SUPPLEMENTARY MATERIAL

The Supplementary Material for this article can be found online at: https://www.frontiersin.org/articles/10.3389/fcimb.2021.816657/full#supplementary-material

REFERENCES

al-Obeid, S., Billot-Klein, D., van Heijenoort, J., Collatz, E., and Gutmann, L. (1992). Replacement of the Essential Penicillin-Binding Protein 5 by High-Molecular Mass PBPs may Explain Vancomycin-Beta-Lactam Synergy in Low-Level Vancomycin-Resistant *Enterococcus Faecium* D366. *FEMS Microbiol. Lett.* 70 (1), 79–84. doi: 10.1016/0378-1097(92)90566-7

Arias, C. A., and Murray, B. E. (2012). The Rise of the Enterococcus: Beyond Vancomycin Resistance. *Nat Rev Microbiol* 10 (3), 256–78. doi: 10.1038/nrmicro2761.

Arias, C. A., Singh, K. V., Panesso, D., and Murray, B. E. (2007). Evaluation of Ceftobiprole Medocaril Against Enterococcus Faecalis in a Mouse Peritonitis Model. *J. Antimicrob. Chemother.* 60 (3), 594–8. doi: 10.1093/jac/dkm237

Arbeloa, A., Segal, H., Hugonnet, J. E., Josseaume, N., Dubost, L., Brouard, J. P., et al. (2004). Role of Class A Penicillin-Binding Proteins in PBP5-Mediated

Beta-Lactam Resistance in *Enterococcus Faecalis*. *J. Bacteriol* 186 (5), 1221–1228. doi: 10.1128/JB.186.5.1221-1228.2004

Bourgogne, A., Garsin, D. A., Qin, X., Singh, K. V., Sillanpaa, J., Yerrapragada, S., et al. (2008). Large Scale Variation in Enterococcus Faecalis Illustrated by the Genome Analysis of Strain OG1RF. *Genome Biol.* 9, R110. doi: 10.1186/gb-2008-9-7-r110

Cabrera, N. L., Malek, A. E., Aitken, S. L., and Arias, C. A. (2020). Outcomes of Patients With Bloodstream Infections Caused by Ampicillin-Susceptible But Penicillin-Resistant Enterococcus Faecalis: Caution in Interpreting the Results. Antimicrob. *Agents Chemother.* 64 (4), e02387–e02319. doi: 10.1128/AAC.02387-19

Campanile, F., Bongiorno, D., Mongelli, G., Zanghì, G., and Stefani, S. (2019). Bactericidal Activity of Ceftobiprole Combined With Different Antibiotics Against Selected Gram-Positive Isolates. *Diagn Microbiol. Infect. Dis.* 93 (1), 77–81. doi: 10.1016/j.diagmicrobio.2018.07.015

Campanile, F., Cassisi, M., Lazzaro, L. M., and Stefani, S. *Ceftobiprole Exerts Synergism Against Enterococcus Faecalis Clinical Isolates Despite Their β-Lactam Resistance. 31st ECCMID, Online 9-12 July 2021*. Available at: https://markterfolg.de/ESCMID/Final_Programme_2021/#page=192.

Clinical and Laboratory Standards Institute (2021). *Performance Standards for Antimicrobial Susceptibility Testing, 31th ed*. CLSI supplement M100 (ISBN 978-1-68440-104-8 print; ISBN 978-1-68440-105-5 electronic). USA: Clinical and Laboratory Standards Institute.

Conceição, N., da Silva, L. E., Darini, A. L., Pitondo-Silva, A., and de Oliveira, A. G. (2014). Penicillin-Resistant, Ampicillin-Susceptible Enterococcus Faecalis of Hospital Origin: *Pbp*4 Gene Polymorphism and Genetic Diversity. *Infect. Genet. Evol.* 28, 289–295. doi: 10.1016/j.meegid.2014.10.018

Conceição, N., Rodrigues, W. F., de Oliveira, K. L. P., da Silva, L. E. P., de Souza, L. R. C., da de Cunha Hueb Barata, Oliveira, C., et al. (2020). Beta-Lactams Susceptibility Testing of Penicillin-Resistant, Ampicillin-Susceptible *Enterococcus Faecalis* Isolates: A Comparative Assessment of Etest and Disk Diffusion Methods Against Broth Dilution. *Ann. Clin. Microbiol. Antimicrob.* 19 (1), 43. doi: 10.1186/s12941-020-00386-8

Djorić, D., Little, J. L., and Kristich, C. J. (2020). Multiple Low-Reactivity Class B Penicillin-Binding Proteins Are Required for Cephalosporin Resistance in Enterococci. *Antimicrob. Agents Chemother.* 64 (4), e02273–e02219. doi: 10.1128/AAC.02273-19

Estrem, S. T., Gaal, T., Ross, W., and Gourse, R. L. (1998). Identification of an UP Element Consensus Sequence for Bacterial Promoters. *Proc. Natl. Acad. Sci. U.S.A.* 18, 95(17):9761–6. doi: 10.1073/pnas.95.17.9761

Gawryszewska, I., Żabicka, ,. D., Hryniewicz, W., and Sadowy, E. (2021). Penicillin-Resistant, Ampicillin-Susceptible Enterococcus Faecalis in Polish Hospitals. *Microb. Drug Resist.* 27 (3), 291–300. doi: 10.1089/mdr.2019.0504

Ghuysen, J. M. (1991). Serine Beta-Lactamases and Penicillin-Binding Proteins. *Annu.Rev Microbiol.* 45, 37–67. doi: 10.1146/annurev.mi.45.100191.000345

Giacobbe, D. R., Labate, L., Tutino, S., Baldi, F., Russo, C., Robba, C., et al. (2021). Enterococcal Bloodstream Infections in Critically Ill Patients With COVID-19: A Case Series. *Ann. Med.* 53 (1), 1779–1786. doi: 10.1080/07853890.2021.1988695

Guardabassi, L., Larsen, J., Skov, R., and Schonheyder, H. C. (2010). Gentamicin-Resistant *Enterococcus Faecalis Sequence* Type 6 With Reduced Penicillin Susceptibility: Diagnostic and Therapeutic Implications. *J. Clin. Microbiol.* 48, 3820–3821. doi: 10.1128/JCM.01252-10

Hamilton, S. M., Alexander, J. A. N., Choo, E. J., Basuino, L., da Costa, T. M., Severin, A., et al. (2017). High-Level Resistance of Staphylococcus Aureus to β-Lactam Antibiotics Mediated by Penicillin-Binding Protein 4 (Pbp4). *Antimicrob. Agents Chemother.* 61 (6), e02727–e02716. doi: 10.1128/AAC.02727-16

Hollenbeck, B. L., and Rice, L. B. (2012). Intrinsic and Acquired Resistance Mechanisms in Enterococcus. *Virulence* 5, 421–433. doi: 10.4161/viru.21282

Infante, V. H., Conceição, N., de Oliveira, A. G., and Darini, A. L. (2016). Evaluation of Polymorphisms in Pbp4 Gene and Genetic Diversity in Penicillin-Resistant, Ampicillin-Susceptible *Enterococcus Faecalis* From Hospitals in Different States in Brazil. *FEMS Microbiol. Lett.* 363 (7):fnw044. doi: 10.1093/femsle/fnw044

Kim, D., Lee, H., Yoon, E. J., Hong, J. S., Shin, J. H., Uh, Y., et al. (2019). Prospective Observational Study of the Clinical Prognoses of Patients With Bloodstream Infections Caused by Ampicillin-Susceptible But Penicillin-Resistant Enterococcus Faecalis. *Antimicrob. Agents Chemother.* 63 (7), e00291–e00219. doi: 10.1128/AAC.00291-19

Kristich, C. J., Djorić, D., and Little, J. L. (2014b). Genetic Basis for Vancomycin-Enhanced Cephalosporin Susceptibility in Vancomycin-Resistant Enterococci Revealed Using Counterselection With Dominant-Negative Thymidylate Synthase. *Antimicrob. Agents Chemother.* 58 (3), 1556–1564. doi: 10.1128/AAC.02001-13

Kristich, C. J., Rice, L. B., and Arias, C. A. (2014a). "Enterococcal Infection - Treatment and Antibiotic Resistance," in *Enterococci: From Commensals to Leading Causes of Drug Resistant Infection*. Eds. M. S. Gilmore, D. B. Clewell, Y. Ike and N. Shankar (Boston: Massachusetts Eye and Ear Infirmary).

Kuch, A., Willems, R. J., Werner, G., Coque, T. M., Hammerum, A. M., Sundsfjord, A., et al. (2012). Insight Into Antimicrobial Susceptibility and Population Structure of Contemporary Human Enterococcus Faecalis Isolates From Europe. *J. Antimicrob. Chemother.* 67 (3), 551–558. doi: 10.1093/jac/dkr544

Livak, K. J., and Schmittgen, T. D. (2001). Analysis of Relative Gene Expression Data Using Real-Time Quantitative PCR and the $2^{-\Delta\Delta\ Ct}$ Method. *Methods* 25 (4), 402–408. doi: 10.1006/meth.2001.1262

Mendes, R. E., Castanheira, M., Farrell, D. J., Flamm, R. K., Sader, H. S., and Jones, R. N. (2016). Longitudina-14) Analysis of Enterococci and VRE Causing Invasive Infections in European and US Hospitals, Including a Contemporar-13) Analysis of Oritavancin In Vitro Potency. *J. Antimicrob. Chemother.* 71 (12), 3453–3458. doi: 10.1093/jac/dkw319

Metzidie, E., Manolis, E. N., Pournaras, S., Sofianou, D., and Tsakris, A. (2006). Spread of an Unusual Penicillin- and Imipenem-Resistant But Ampicillin-Susceptible Phenotype Among Enterococcus Faecalis Clinical Isolates. *J. Antimicrob. Chemother.* 57 (1), 158–160. doi: 10.1093/jac/dki427

Moon, T. M., D'Andréa, É.D., Lee, C. W., Soares, A., Jakoncic, J., Desbonnet, C., et al. (2018). The Structures of Penicillin-Binding Protein 4 (PBP4) and PBP5 From Enterococci Provide Structural Insights Into β-Lactam Resistance. *J. Biol. Chem.* 293, 18574–18584. doi: 10.1074/jbc.RA118.006052

Ono, S., Muratani, T., and Matsumoto, T. (2005). Mechanisms of Resistance to Imipenem and Ampicillin in Enterococcus Faecalis. *Antimicrob. Agents Chemother.* 49 (7), 2954–2958. doi: 10.1128/AAC.49.7.2954-2958.2005

Posteraro, B., De Angelis, G., Menchinelli, G., D'Inzeo, T., Fiori, B., De Maio, F., et al. (2021). Risk Factors for Mortality in Adult COVID-19 Patients Who Develop Bloodstream Infections Mostly Caused by Antimicrobial-Resistant Organisms: Analysis at a Large Teaching Hospital in Italy. *J. Clin. Med.* 10 (8):1752. doi: 10.3390/jcm10081752

Rice, L. B., Desbonnet, C., Tait-Kamradt, A., Garcia-Solache, M., Lonks, J., Moon, T. M., et al. (2018). Structural and Regulatory Changes in PBP4 Trigger Decreased β-Lactam Susceptibility in. *Enterococcus faecalis mBio* 3, 9 (2). doi: 10.1128/mBio.00361-18

Rice, L. B., and Murray, B. E. (1995). Beta-Lactamase-Producing Enterococci. In Genetics of *Streptococci, Enterococci and Lactococci.*: Review of the Six International Conference. *Dev. Biol. Stand* 85, 107–114.

Sarti, M., Campanile, F., Sabia, C., Santagati, M., Gargiulo, R., and Stefani, S. (2012). Polyclonal Diffusion of Beta-Lactamase-Producing *Enterococcus Faecium*. *J. Clin. Microbio* 50 (1), 169–172. doi: 10.1128/JCM.05640-11

Schell, C. M., Tedim, A. P., Rodríguez-Baños, M., Sparo, M. D., Lissarrague, S., Basualdo, J. A., et al. (2020). Detection of β-Lactamase-Producing *Enterococcus Faecalis* and Vancomycin-Resistant *Enterococcus Faecium* Isolates in Human Invasive Infections in the Public Hospital of Tandil, Argentina. *Pathogens* 9 (2):142. doi: 10.3390/pathogens9020142

Tan, Y. E., Ng, L. S., and Tan, T. Y. (2014). Evaluation of Enterococcus Faecalis Clinical Isolates With 'Penicillin-Resistant, Ampicillin-Susceptible' Phenotype as Reported by Vitek-2 Compact System. *Pathol.* 46 (6), 544–550. doi: 10.1097/PAT.0000000000000146

The European Committee on Antimicrobial Susceptibility Testing – EUCAST *(Valid From 2021-01-01). Version 11.0*. Available at: www.eucast.org.

Werth, B. J., and Abbott, A. N. (2015). The Combination of Ampicillin Plus Ceftaroline is Synergistic against Enterococcus faecalis. *J. Antimicrob Chemother.* 70 (8), 2414–2417. doi: 10.1093/jac/dkv125

White, L. R., Burgess, D. S., Manduru, M., and Bosso, A. J. (1996). Comparison of Three Different In Vitro Methods of Detecting Synergy: Time-Kill, Checkerboard, and E Test. *Antimicrob. Agents Chemother.* 40 (8), 1914–1918. doi: 10.1128/AAC.40.8.1914

Zapun, A., Contreras-Martel, C., and Vernet, T. (2008). Penicillin Binding Proteins and Beta-Lactam Resistance. *FEMS Microbiol. Rev.* 32 (2), 361–385. doi: 10.1111/j.1574-6976.2007.00095.x

Conflict of Interest: The authors declare that the research was conducted in the absence of any commercial or financial relationships that could be construed as a potential conflict of interest.

Publisher's Note: All claims expressed in this article are solely those of the authors and do not necessarily represent those of their affiliated organizations, or those of the publisher, the editors and the reviewers. Any product that may be evaluated in this article, or claim that may be made by its manufacturer, is not guaranteed or endorsed by the publisher.